

**ELECTROCHEMICAL STUDIES  
ON  
METAL PHTHALOCYANINES**

Thesis submitted to  
the Cochin University of Science and Technology  
in partial fulfilment of the requirements  
for the degree of  
**DOCTOR OF PHILOSOPHY**

*by*

**HARIKUMAR P. S.**

DEPARTMENT OF APPLIED CHEMISTRY  
COCHIN UNIVERSITY OF SCIENCE AND TECHNOLOGY  
COCHIN - 682 022

JANUARY 1990

## **DECLARATION**

I hereby declare that the work presented in this thesis is based on the original work done by me under the guidance of Dr. V.N. Sivasankara Pillai, Professor, Department of Applied Chemistry, Cochin University of Science and Technology and that no part of this thesis has been included in any other thesis submitted previously for the award of any degree.

Cochin - 22  
17<sup>th</sup> January 1990

  
**HARIKUMAR P S**

## **CERTIFICATE**

Certified that the work presented in this thesis is based on the bonafide work done by Mr. Harimumar, P.S. under my guidance in the Department of Applied Chemistry, Cochin University of Science and Technology and that no part thereof has been included in any other thesis submitted previously for the award of any degree.



**DR. V.N. SIVASANKARA PILLAI**  
**Professor**

,  
Department of Applied Chemistry  
Cochin University of Science and Technology

Cochin - 22,  
17<sup>th</sup> January 1990

## **ACKNOWLEDGEMENT**

I wish to express my sincere gratitude and obligation to Prof. V.N. Sivasankara Pillai, for his kind and patient guidance and encouragement given all through the period of my research.

The help extended by Prof. Paul A. Vatakencherry, Head of the Department of Applied Chemistry is gratefully acknowledged. I am extremely thankful to all the faculty members of this department for their co-operation and encouragement.

I am very much indebted to Dr. Syed Akheel Ahamed, Department of P.G. Studies and Research in Chemistry, University of Mysore and Dr.K. Ravindran, Head, Crafts and Gears Division, CIFT, Cochin for their valuable suggestions.

I am thankful to the administrative and technical staff of the Department of Applied Chemistry and the staff of the University Science Instrumentation Centre for their timely help and co-operation.

The endless support, affection and timely help extended by my friends are remembered with great appreciation and a deep sense of gratitude.

The financial assistance extended to me in the form of Research Fellowship, by the university Grants Commission, Government of India is gratefully acknowledged.

Finally I would like to extend my gratitude to Mrs. Bharathi, P.A. and M/s. TC Computeck Pte Ltd. South Kalamassery for their excellent work at typing this thesis.

**HARIKUMAR P.S**

# P R E F A C E

The work embodied in this thesis was carried out by the author in the Department of Applied Chemistry during 1985 - '89. The primary aim of these investigations was to probe the electrochemical and material science aspects of some selected metal phthalocyanines(MPCs).

Metal phthalocyanines are characterised by a unique planar molecular structure. As a single class of compounds they have been the subject of ever increasing number of physicochemical and technological investigations. During the last two decades the literature on these compounds was flooded by an outpour of original publications and patents. Almost every branch of materials science has benefited by their application-surface coating, printing, electrophotography, photoelectrochemistry, electronics and medicine to name a few.

The present study was confined to the electrical and electrochemical properties of cobalt, nickel, zinc, iron and copper phthalocyanines. The use of soluble Pcs as corrosion inhibitor for aluminium was also investigated.

In the introductory section of the thesis, the work done so far on MPCs is reviewed. In this review emphasis is given to their general methods of synthesis and the physicochemical properties.

In phthalocyanine chemistry one of the formidable tasks is the isolation of singular species. In the second chapter the methods of synthesis and purification are presented with necessary experimental details.

The studies on plasma modified films of CoPc, FePc, ZnPc, NiPc and CuPc are presented in the third chapter. Modification of electron transfer process by such films for reversible redox systems is taken as the criterion to establish enhanced electrocatalytic activity.

Metal phthalocyanines are p- type semiconductors and the conductivity is enhanced by doping with iodine. The effect of doping on the activation energy of the conduction process is evaluated by measuring the temperature dependent variation of conductivity. Effect of thermal treatment on iodine doped CoPc is investigated by DSC, magnetic susceptibility, IR, ESR and electronic spectra. The electrocatalytic activity of such doped materials was probed by cyclic voltammetry. The results are presented in the fourth chapter.

The electron transfer mediation characteristics of MPC films depend on the film thickness. The influence of reducing the effective thickness of the MPC film by dispersing it into a conductive polymeric matrix was investigated. Tetrasulphonated cobalt phthalocyanine (CoTSP) was electrostatically immobilised into polyaniline and poly(o-toluidine) under varied conditions. Such chemically modified electrodes were studied and the results are presented in the fifth chapter.

Chapter six contains the studies on corrosion inhibition of aluminium by CoTSP and CuTSP. By virtue of their anionic character they are soluble in water and are strongly adsorbed on aluminium. Hence they can act as corrosion inhibitors. CoTSP is also known to catalyze the reduction of dioxygen. This reaction can accelerate the anodic dissolution of metal as a complementary reaction. The influence of these conflicting properties of CoTSP on the corrosion of aluminium was studied and compared with those of CuTSP.

In the concluding chapter the salient features of the results obtained are summarised.

In the course of these investigations a number of gadgets like cell for measuring the electrical conductivity of solids under non-isothermal conditions, low power rf oscillator and a rotating disc electrode were fabricated. These are mentioned in appropriate sections.

# CONTENTS

	PAGE NO.
<b>CHAPTER 1. A BRIEF SURVEY OF THE WORK ON METAL PHTHALOCYANINES</b>	
1.1 Structure of Phthalocyanine	1
1.2 General Methods for the Synthesis of Phthalocyanines	2
1.2.1 Monomeric Phthalocyanine	2
1.2.2 Lanthanide and Actinide Phthalocyanines	8
1.2.3 Miscellaneous MPcs	8
1.3 Purification of Metal Phthalocyanines	10
1.4 Physicochemical Characteristics of Metal Phthalocyanines	10
1.4.1 Crystal Structure and Polymorphism	10
1.4.2 Spectral Characteristics	12
1.4.3 Magnetic Propertis	12
1.4.4 Electrical Characteristics of MPcs	13
1.4.5 Aggregation of MPcs	13
1.5 Technological Application of Phthalocyanines	14
<b>CHAPTER II SYNTHESIS AND CHARACTERISATION OF METAL PHTHALOCYANINES</b>	
2.1 Synthesis of Metal Phthalocyanines	18
2.1.2 Characterisation of Metal Phthalocyanines	19
<b>CHAPTER III ELECTROCHEMICAL STUDIES</b>	
3.1 Introduction	24
3.1.1 Plasma Treatment of MPc Layers	25
3.1.3 Experimental Techniques for Plasma Treatment	26
3.1.5 Application of Plasma	27
3.2 Cyclic Voltammetry in the Study of Electrode Process	28
3.3 Experimental Procedure	31
<b>CHAPTER IV ELECTRICAL CONDUCTIVITY OF METAL PHTHALOCYANINES</b>	
4.1 Introduction	41
4.2 Experimental	42
4.2.2 Characterisation of MPcI	42
4.2.3 Measurment of Conductivity	42
4.2.4 Cyclic Voltammetry	43
4.3 Results and Discussion	43
4.3.6 Electrochemical Studies on CoPcI	44
4.4 Iron Phthalocyanine	45
4.5 Zinc Phthalocyanine	45

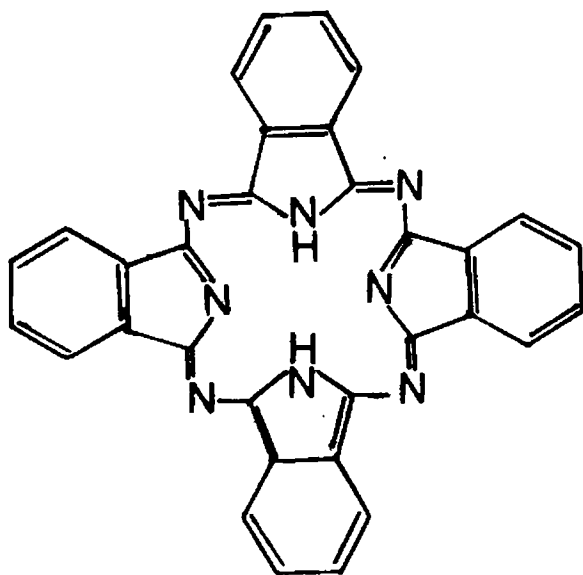
<b>CHAPTER V CHEMICALLY MODIFIED ELECTRODES</b>	<b>PAGE NO.</b>
5.1 Introduction	46
5.3 Electrochemical Behaviour of Cobalt Tetrasulphophthalocyanine ion Doped into Polyaniline and poly( <i>o</i> -Toluidine)	50
5.3.1 Introduction	50
5.3.2 Experimental	51
5.4 Preparation and Characterisation of Polyaniline Films	51
5.5 Results and Discussion	52
5.6 Electrochemical Characterisation of Chemically Prepared Polyaniline	53
5.7 Electrochemical Preparation of CoTSP - PA electrodes	53
5.8 Electrochemical Behaviour of CoTSP - PA electrodes	54
5.9 Dioxygen Reduction	55
5.10 Conclusions	56
5.11 Mediation of Electron Transfer by CoTSP Incorporated into Poly ( <i>o</i> -Toluidine)	56
5.12 Experimental	56
<b>CHAPTER VI METAL TETRASULPHOPHTHALOCYANINE AS CORROSION INHIBITORS</b>	
6.1 Introduction	60
6.2 Inhibition of Corrosion of Aluminium in Hydrochloric Acid by Metal Tetrasulphophthalocyanines	64
6.2.2 Experimental	65
6.3.3 Results and Discussion	66
<b>CHAPTER VII SUMMARY AND CONCLUSION</b>	<b>69</b>
<b>REFERENCES</b>	<b>72</b>

# A BRIEF SURVEY OF THE WORK ON METAL PHTHALOCYANINES

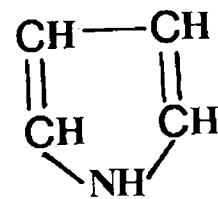
## 1.0 INTRODUCTION

### 1.1 Structure of Phthalocyanines

Phthalocyanines are macrocyclic compounds containing four pyrrole units and structurally similar to porphyrins and tetraazaporphins. More generally, they include tetraazaporphins in which the four pyrrole units are fused to an aromatic structure (Fig. 1). In addition to the structural similarity of phthalocyanines to porphyrins, they are closely related in many other respects. Both are stable to alkalis, less so to acids, both are highly colored, and form complex metallic compounds, both are degraded by oxidation to the imides of dibasic acids. The order of stability of the metallic derivatives of the two classes are also similar.



**PHTHALOCYANINE**

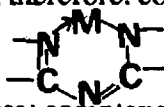


**PYRROLE**

**Fig. 1**

The compounds usually referred to under the phthalocyanine class consist of metal derivatives of phthalocyanine. The two hydrogen atoms attached to the two isoindole group can be replaced by metal atoms from every group the periodic table to form the metal phthalocyanines. Also, each of the sixteen peripheral hydrogen atoms on the four benzene rings can be substituted by a variety of atoms and groups. The phthalocyanine can be considered as a weak dibasic acid and the metal derivatives as its salts. In metal phthalocyanines, for example, the metal atom supplies one electron

each to the nitrogen atoms of the isoindole groups and these isoindole nitrogen atoms in turn supplies an electron to the metal atom, forming a covalent bond. The unshared pairs of electrons in the remaining two isoindole nitrogen atoms presumably form coordinate covalent bonds with the metal atom. A metal phthalocyanine molecule, therefore, contains four six membered chelate rings of the type:



The unusual stability of these metal complexes can be explained by the coordination of the central metal atom.

## 1.2.0 General Methods for the Synthesis of Phthalocyanines

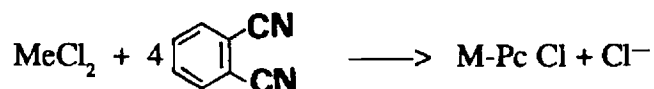
The technological importance of phthalocyanine pigments has generated renewed interest in their synthesis, purification and characterization. The methods available for the synthesis of phthalocyanines can be classified into four groups:

- 1) Reaction of phthalonitrile with a metal or metal salt in a high boiling liquid like nitrobenzene or quinoline.
  - 2) Reaction of phthalic acid or phthalic anhydride with urea and metal salts in presence of a catalyst or phthalimide with a metal salt in presence of catalyst.
  - 3) Reaction of *o*-cyanobenzamide with a metal
- and
- 4) Reaction of phthalocyanine or labile metal phthalocyanine with a metal forming a more stable phthalocyanine.

### 1.2.1 Monomeric phthalocyanines

#### Method 1

In this method phthalonitrile and metal chloride with mole ratio . 4:1 is heated to 180-190°C for two hours in quinoline or in a mixture of quinoline and trichlorobenzene. Cobalt, nickel chromium, iron, vanadyl, chloroaluminium, lead and titanium phthalocyanines have been synthesised by this method.<sup>2,3</sup> The reaction may be written as:

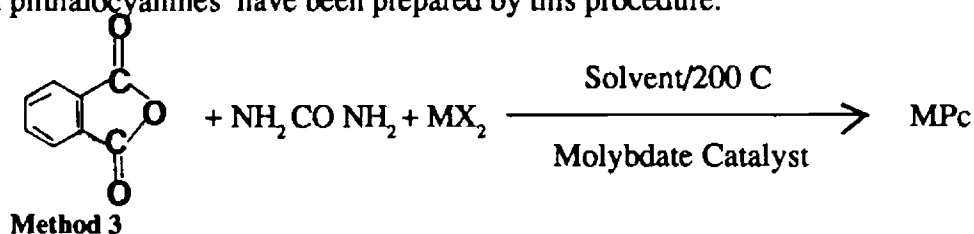


This reaction takes place in the presence of urea, or quinoline. The decomposition products of urea and quinoline act as acceptors for the halogen atoms which enter the phthalocyanine molecule to an appreciable extent when the acceptors are not present.

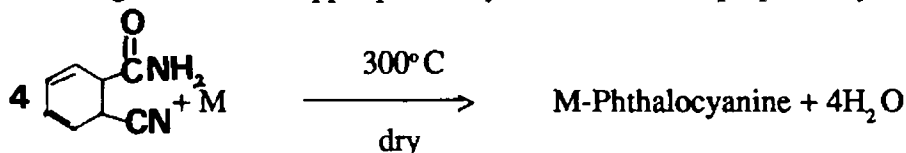
#### Method 2

A stoichiometric mixture of phthalic anhydride, a metal salt, urea and catalyst is heated at 170-200° C for 4 h in a medium such as nitrobenzene or chlorobenzene. Copper, cobalt, nickel, iron

and tin phthalocyanines have been prepared by this procedure.

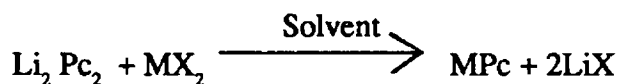


*o*-Cyanobenzamide and a metal or metal salt are heated to 250 C for 4 to 6 h. The product is freed of phthalamide and *O*-cyanobenzamide by heating with concentrated sodium hydroxide. After filtration, washing, drying and grinding, the product is freed of excess metal by mechanically removing the metal and floatation of the pigment in a suitable solvent, or chemical means. Iron, nickel, cobalt, magnesium and copper phthalocyanine have been prepared by this method.



**Method 4**

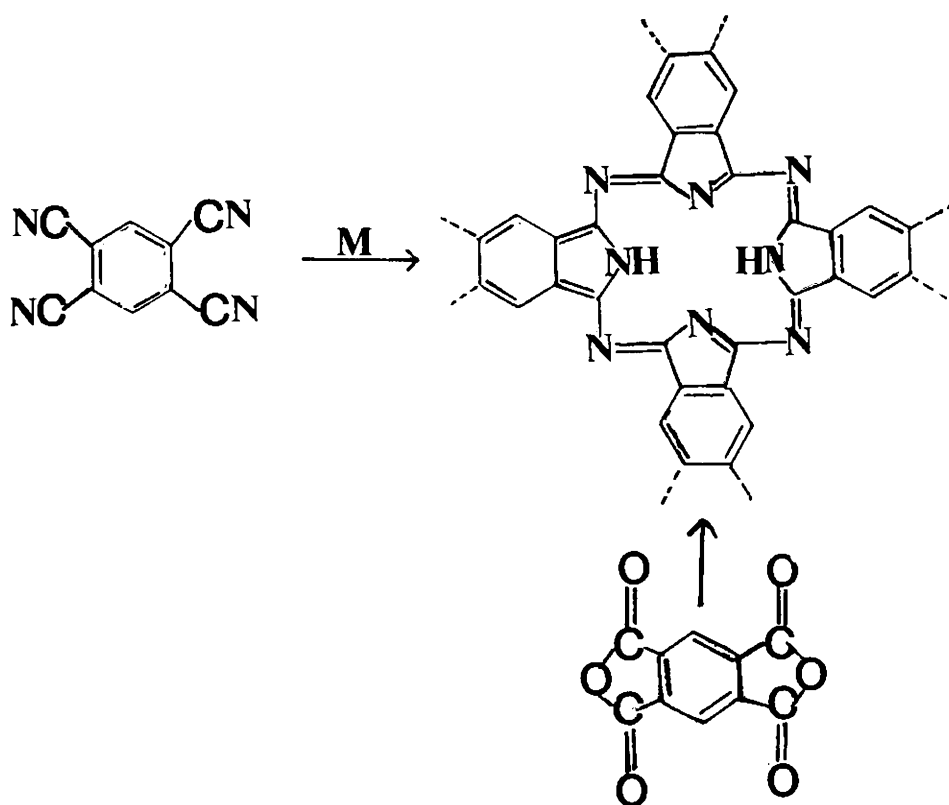
This method involves boiling phthalocyanine and a metal in quinoline or benzophenone and is to prepare more stable metal derivatives from dilithium phthalocyanine. This complex is particularly useful because of its solubility in alcohol. Copper phthalocyanine is immediately precipitated when alcoholic solutions of dilithium phthalocyanine and anhydrous cupric chloride are mixed. Phthalocyanine derivatives of silver, mercury, calcium, zinc, lead, manganese and cobalt have been prepared by this procedure. A number of rare earth metal phthalocyanines have been synthesised from dilithium phthalocyanine by double decomposition in liquid Lewis-base type organic compounds such as dimethyl formamide or methyl sulfoxide as the reaction medium. The method is especially suited for the preparation of phthalocyanine complexes of uranium, lead, thorium, lanthanum, neodymium, gadolinium, dysprosium, samarium, holmium, erbium, europium, thulium, lutetium, ytterbium and hafnium.



In place of lithium phthalocyanine, phthalocyanines, phthalocyanine of sodium, potassium, magnesium or beryllium may be used.

## 1.2.2 Polymeric Phthalocyanines

Polymeric phthalocyanines are synthesised by starting with a tetrafunctional benzene like 1,2,4,5-tetracyanobenzene (TCB) or pyromellitic dianhydride (PMDA).



The various methods available for the synthesis of nontransition metal phthalocyanines are given in table - I and the transition metal phthalocyanines in table - II.

**Table - I.**

**METHODS FOR THE SYNTHESIS OF PHTHALOCYANINES OF NONTRANSITION ELEMENTS**

GROUP	COMPLEX	METHOD	MATERIAL PROPERTIES	REF.
IA	Li <sub>2</sub> Pc	3(LiOAm)*	Sol. in acetone and alcohols	4
	Na <sub>2</sub> Pc	3(NaOAm) 3(KOAm)	Hydrolyzed with AcOH or mineral acids	5
IIA	BePc	3(etched Be)	Hygroscopic	5
	MgPc	3(Mg)	Hydrate	5
	CaPc	3(CaO)	—	5
	BaPc	3(BaO)	—	5
IIB	ZnPc	3(Zn)	—	5
		2(Zn/TiCl <sub>4</sub> )	—	6
	CdPc	3(Cd)	—	5
	HgPc	4(HgCl <sub>2</sub> + Li <sub>2</sub> Pc)	—	4
IIIB	AlClPc	3(AlCl <sub>3</sub> )	Hydrolysed to Al(OH)Pc	4,7
	GaClPc	3(GaCl <sub>3</sub> )	(From <i>o</i> -cyanobenzamide)	8
	InClPc	3(InCl <sub>3</sub> )	(From <i>o</i> -cyanobenzamide)	8
IVB	SiCl <sub>2</sub> Pc	1(SiCl <sub>4</sub> )	Hydrolysed to Si(OH) <sub>2</sub> Pc	9
		1(SiCl <sub>4</sub> )	—	10
	GeCl <sub>2</sub> Pc	3(GeCl <sub>4</sub> )	—	11
	SnPc	3(Sn)	—	5,12
	SnCl <sub>2</sub> Pc	3(SnCl <sub>2</sub> )	—	9,12
	PbPc	3(PbO)	—	5,12
	AsClPc	4(AsCl <sub>3</sub> / DMF)	—	
	Sb <sub>2</sub> Pc	2(Sb)	structure uncertain	4
	SbClPc	4(SbCl <sub>3</sub> + H <sub>2</sub> Pc)	—	4

\*Lithium amyloxyde

Table II

## METHODS FOR THE SYNTHESIS OF PHTHALOCYANINES OF THE TRANSITION METALS

GROUP	COMPLEX	METHOD	PROPERTIES	REF.
IVA	TiClPc	4(TiCl <sub>3</sub> )	Oxidized to TiOPc	14
	TiCl <sub>2</sub> Pc	2(TiCl <sub>3</sub> )	Hydrolyzed to TiOPc	15
	TiOPc	From Chloroderivative	Probably Polymeric	14,15
	Zr(OH) <sub>2</sub> Pc	3(ZrCl <sub>4</sub> )	May alternatively be Formulated	16
	Hf(OH) <sub>2</sub> Pc VoPc	3(HfCl <sub>4</sub> ) 3(V <sub>2</sub> O <sub>5</sub> )	(MoPc) hydrate	16 5,17
V A	NbCl <sub>x</sub> (OH) <sub>y</sub> Pc	3(NbCl <sub>3</sub> +Nb(Cl <sub>5</sub> ))	Mixed product, partially hydrolyzed	18
	TaCl <sub>x</sub> (OH) <sub>y</sub> Pc	3(TaCl <sub>5</sub> )	Mixed product, partially hydrolyzed	18
	CrPc	3Cr(CO) <sub>6</sub>	Oxidized to Cr (OH) Pc	19
VI A	Cr(OH)Pc	3Cr(OCOCH <sub>3</sub> ) <sub>3</sub>		20
	MoOPc	3(MoO <sub>2</sub> Cl <sub>2</sub> / DMF)	(Low yield of characterizable Product)	21
VIIA	MnPc	3(Mn)	Demetallized with H <sub>2</sub> SO <sub>4</sub> readily oxidized and absorbs O <sub>2</sub>	5,13
	MnOPc	(MnPc)	Polymeric	22
	(ReClPc) <sub>2</sub> .2PhNH <sub>2</sub>	3(K ReOCl <sub>4</sub> + OCB)	Complex Oxide Product broken down with aniline	22a
VIII	FePc	3(Fe + OCB)	Further coordinates with bases like CN <sup>-</sup>	5
	FeClPc	From FePc	—	4
	RuPc	3(RuCl <sub>3</sub> + OCB)	—	23
	Os(SO <sub>4</sub> )Pc	3(OsO <sub>4</sub> )	Product from H <sub>2</sub> SO <sub>4</sub> Probably Polymeric	24
	CoPc	4Co	—	5
	Rh (HSO <sub>4</sub> ) Pc	3(RHCl <sub>3</sub> )	Product ppt. from H <sub>2</sub> SO <sub>4</sub>	25
	Ir(HSO <sub>4</sub> )Pc	3(IrCl <sub>3</sub> )	some chlorination of Pc ring	26
	NiPc	2(NiCl <sub>2</sub> )	—	27
	PdPc	4(PdCl <sub>2</sub> )	—	4
	PtPc	2(PtCl <sub>2</sub> )	—	5

GROUP	COMPLEX	METHOD	PROPERTIES	REF
I B	CuPc	2 and 3		
	AgPc	4(AgNO <sub>3</sub> )		4
	AuPc	1(AuBr)		28
Lanthanides	MPc	3(MCl <sub>3</sub> + OCB)	M = Eu, Gd, Yb; Solvent Soluble	29
		3 M(OCOCH <sub>3</sub> ) <sub>3</sub>	M = Pr, Nd, Er, Lu; uncharacterized Mixture	30
Actinides	ThCl <sub>2</sub> Pc	3(ThCl <sub>4</sub> )		31
	UO <sub>2</sub> Pc	4(UO <sub>2</sub> (NO <sub>3</sub> ) <sub>2</sub> / DMF) 3(UO <sub>2</sub> Cl <sub>2</sub> / DMF)	—	33

## 1.2.2 LANTHANIDE AND ACTINIDE PHTHALOCYANINES

The rare earth phthalocyanines are easily prepared by the method described by Moskalev and Kirin.<sup>36,37</sup> Praseodymium, neodymium, erbium and lutetium phthalocyanines have been prepared by heating a mixture of rare earth acetate and phthalonitrile in 1:3 mole ratio at 280° to 290° C. Completion of the reaction is indicated by the solidification of the melt which takes longer period for the yttrium subgroup (~90min.) than for the cerium subgroup (~50 min). The solid mass obtained is dissolved in DMF and chromatographed on alumina. Methanol is used as eluent for neodymium diphthalocyanine and a saturated solution of NH<sub>4</sub>Cl in 1:2 benzene/methanol is used to elute neodymium monophthalocyanine.

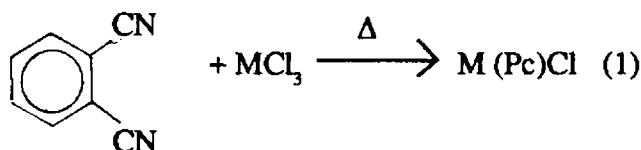
Europium, gadolinium and ytterbium phthalocyanines have also been prepared from 1,2-dicyanobenzene and the corresponding rare earth acetate at 250° C.<sup>38</sup>

Thorium phthalocyanine is prepared by the action of thorium tetrachloride with phthalonitrile at 260° C. Uranyl phthalocyanine (UO<sub>2</sub>Pc) is formed by the reaction of bis (dimethyl formamide) Uranyl acetate with dilithium phthalocyanine.<sup>39</sup> the reaction of uranyl acetate with phthalic anhydride and urea also gives the same product.<sup>40</sup>

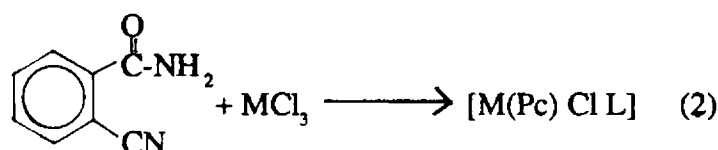
Bloor et al<sup>41</sup> have reported the formation of uranyl phthalocyanine by the reaction between uranyl chloride and phthalonitrile in dimethyl formide at 180° C. This product gives an infrared absorption spectrum different from that originally reported and on the basis of IR absorption spectra they conclude that the uranyl phthalocyanine obtained by previous workers was essentially a mixture of metal-free phthalocyanine and salts of uranium.

## 1.2.3 Miscellaneous MPcs

Procedures have been developed for the synthesis of metal derivatives especially those with metals in higher oxidation states. For example, a variation of the phthalonitrile condensation route has been used to prepare M(III)complexes of the type M(Pc) Cl where M is Al (III), Sc(III), In(III) or Yb(III).<sup>42</sup>



An analogous condensation reaction with *o*-cyanobenzamide has also been used to prepare other M(III) derivatives.



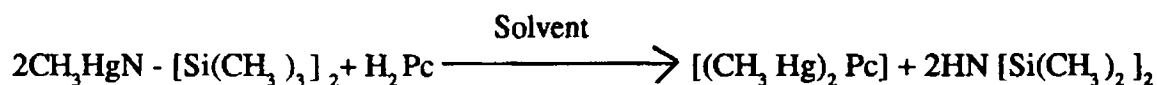
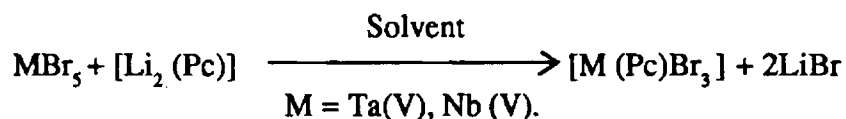
where M is Ru (III) or Rh(III)

Using reaction (1), complexes of the type [M(Pc) ClL]

(Where L = *o*-cyanobenzamide or phthalonitrile and M = Ru(III), Os(III), Ir(III) and Rh(Pc)Cl and Os O (Pc) were prepared.

Reaction (1) was also used to synthesize bivalent rare earth complexes. <sup>43</sup> [Yb(Cl-Pc)Cl].2H<sub>2</sub>O and H [Gd(Pc)<sub>2</sub>]

A cleaner method of preparing selected M(Pc) derivatives involves metal exchange with a preformed Pc complex or acid-base reaction with the metal-free Pc.<sup>44</sup>



Phthalocyanine derivatives that are soluble in aqueous and nonaqueous solvents have also been synthesized. Water soluble phthalocyanine sulfonic acid direct dyes have been obtained by the action of fuming sulfuric acid on phthalocyanine.

Tetrasulfonated phthalocyanines (MTSP) are prepared from monosulphophthalic acid. salts of MTSPs are water soluble. Rosch et al<sup>45</sup> have prepared a group of phthalocyanine sulfonic acids by the reaction of a benzene *o*-dicarboxylic acid, urea and a copper compound at elevated temperatures. Weber and Bush<sup>46</sup> have reported the preparation of transition metal derivatives of 4,4',4'',4''' tetrasulphophthalocyanine and have measured the magnetic moments of these substances both in the solid state and in solution.

The method involves heating a stoichiometric mixture of 4-sulphophthalic acid, urea, ammonium molybdate and the corresponding transition metal salt in nitrobenzene. Recently the synthesis of new R-type CuPc blue pigment with a deeper red tint than the  $\alpha$ -type and which is not converting to the  $\beta$ -type in aromatic solvents is reported.<sup>47</sup>

In addition to polymorphs, other forms of phthalocyanines such as  $\mu$ -oxo and  $\mu$ -nitrido bridged derivatives are also reported.<sup>48-50</sup>

A new solid  $\mu$ -oxo dimer is also synthesized by the interaction of FePc with O in dimethyl formamide and in other solvents.<sup>51</sup>

( $\mu$ -oxo) bis(phthalocyanato) iron(III) was prepared by exposure of a suspension of FePc in DMF to air. the same species was obtained when DMF was replaced by dimethyl acetamide (DMA), tetrahydrofuran (THF) or dioxane. Eager et al<sup>49</sup> have reported the spectroscopic and electrochemical data involving two  $\mu$ -oxo forms of FePc. This study has given a new insight into the physical state of the macrocyclics dispersed in high area carbon supports and their electrocatalytic activity for dioxygen reduction.

$\mu$ -nitrido bridged iron phthalocyanine dimer has been studied by spectroelectrochemistry.<sup>50</sup>

Many techniques are also reported for the preparation of phthalocyanine thin films on conducting substrates. <sup>52-55</sup> The thin films of phthalocyanine is prepared by deposition of a layer containing Pc on a conduction substrate by electrolysis of a nonaqueous solution containing carboxy

phthalocyanine and supporting electrolyte. Another technique used to prepare thin films is by electrolyte micelle disruption method.<sup>56</sup> In this case the film formation consists of the following stages: (1) solubilization (or dispersion) of a water-insoluble chemical by a surfactant with ferrocenyl moiety (2) electrochemical oxidation of the ferrocenyl moiety, followed by break up of the micelle (3) release of molecules (or particles) from the aggregates and then (4) deposition of the water-insoluble substance on the electrode surface. These methods facilitate the preparation of electrodes with controllable layer thickness, uniformity, adhesion and durability.

### 1.3 Purification of Metal Phthalocyanines

A formidable hurdle in phthalocyanine chemistry is the isolation of phthalocyanine in its pure form. Every method of synthesis of phthalocyanines results in the contamination of the product with unreacted materials such as phthalic anhydride, urea, phthalimide or phthalonitrile. The phthalocyanine formed itself is a mixture of oligomers. Classical purification techniques such as acid and alkali washing, solvent washing, solvent extraction, regeneration by concentrated  $H_2SO_4$ , vacuum sublimation and chromatography are used to purify the crude phthalocyanines.

The first step in the purification of phthalocyanine involves washing with 10% caustic soda, 2M HCl, methanol and benzene successively. The solid mass so obtained is slurried in concentrated sulphuric acid and dropped on ice. The precipitate which is essentially a mixture of various polymorphs of metal phthalocyanines is washed with water and dried. Though this method is sufficient for the removal of unreacted materials, the different polymorphs and oligomers cannot be separated.

Linstead et al.<sup>56</sup> have reported that phthalocyanines sublime under vacuum slowly at 550°C and rapidly at 580°C. This method is found suitable to prepare very pure crystals and thin films of MPcs. The vapour is deep blue and the crystals formed have the purple lustre characteristic of the  $\alpha$ -form. These films of MPcs of thickness 1000-4000 Å can be conveniently prepared by sublimation technique.

The phthalocyanines especially rare earth phthalocyanines are found to be mixtures of complexes having different compositions. Neodymium, praseodymium, erbium, lutetium and lanthanum phthalocyanines give two forms, mono and diphthalocyanines. The several forms of Pcs can often be separated only by chromatography.<sup>58,59</sup>

The rare earth phthalocyanine formed is dissolved in DMF and passed through a column of aluminium oxide. Methanol is used as the eluent. Separation is also achieved by eluting with a saturated solution of  $NH_4Cl$  in a 1:2 benzene-methanol mixture. Neodymium phthalocyanine is purified by this method. Lutetium diphthalocyanine is purified by chromatography over neutral alumina with DMF as eluent. It was rechromatographed over silica gel using chloroform as eluent. Walton et al.<sup>60</sup> purified lutetium and ytterbium diphthalocyanines avoiding time consuming chromatographic elution techniques. They have isolated the Pcs from the mixture by extraction into chloroform. The green powder obtained by solvent evaporation was washed with acetic anhydride, methanol and acetone to remove traces of persistent impurities.

### 1.4.0 Physicochemical Characteristics of Metal Phthalocyanines

#### 1.4.1 Crystal Structure and Polymorphism

The X-ray studies of crystals of copper, nickel, platinum, cobalt, iron and manganese phthalocyanines show that the crystals are all monoclinic, having a centre of symmetry.

Linstead et al<sup>61</sup> have given the following X-ray data for the metallic derivatives of phthalocyanines.

Table -1.3		Phthalocyanine							
		Metal free	Be	Mn	Fe	Co	Ni	Cu	Pt
At. No of Metal		—	4	25	26	27	28	29	78
a, Å	19.85	21.2	20.2	20.2	20.2	19.9	19.6	23.9	
b, Å	4.72	4.8	4.75	4.77	4.71	4.71	4.79	3.81	
c, Å	14.8	14.7	15.1	15.0	15.0	14.9	14.6	16.9	
	122.2°	121.0°	121.7°	121.6°	121.3°	121.9°	120.6°	129.6°	
Space Group	P2 <sub>1</sub> /a								
Molecules per cell	2	2	2	2	2	2	2	2	
Mol. symmetry								Centre for all	
Vol. Unit Cell (Å) <sup>3</sup>	1173	1293	1233	1237	1235	1186	1180	1186	
d(calcd)	1.445	1.33	1.52	1.52	1.53	1.59	1.61	1.97	
M	514	521	567	568	571	571	576	707	
Electrons per cell	532	536	578	580	582	584	586	684	

In metal phthalocyanines, the rigid, planar organic portion of the molecule imposes its steric requirements upon the metal and that there is more tolerance in the distribution of valencies about 4-co-ordinate metal atoms. In the case of platinum phthalocyanine, though the molecular structure is similar to that of other MPCs, the crystal structure differs<sup>64</sup> because molecules are inclined to 010 at angles of 26.5° rather than 44.2°. The space group is C<sub>2h</sub><sup>5</sup> - P2<sub>1</sub>/a, a = 23.9 Å, b = 3.81 Å, c = 15.9 Å and  $\beta = 129.6^\circ$  and there are 2 molecules per unit cell.

### Polymorphism

Both H<sub>2</sub>Pc and CuPc are known to exist in at least three polymorphic forms “ $\beta$ -form” is the stable polymorph and the other two forms ‘ $\alpha$ ’ and ‘ $\gamma$ ’ are metastable. X-ray studies are used to distinguish the polymorphs of phthalocyanines.<sup>65</sup> The typical parameters observed for  $\alpha$  and  $\beta$ -CuPcs are given in Table 1.4.<sup>64</sup>

Table -1.4		Cell Dimensions and Constants from X-Ray Analysis of $\alpha$ and $\beta$ -Copper Phthalocyanines	
		$\alpha$ -CuPc	$\beta$ -CuPc
a, Å		17.367	19.6
b, Å		12.790	14.6
c, Å			
Space Group		C <sub>2h</sub> <sup>1</sup> - P4/M	C <sub>2h</sub> <sup>5</sup> P2 <sub>1</sub> /a
Mols. Per Cell		6	2
Density		1.49g cm <sup>-3</sup>	1.61g cm <sup>-3</sup>

The  $\alpha$ -form of metal phthalocyanine is formed in both the solvent and melt methods of synthesis. Heating to 200° C reconverts the  $\alpha$ -form to the  $\beta$ -form. The  $\alpha$  -  $\beta$  transition can be followed from the temperature-conductivity measurements. The sublimation product of copper phthalocyanine at 550° C is the  $\beta$ -form. The  $\beta$ -form can be converted to the  $\alpha$ -form by dissolution in concentrated sulphuric acid followed by precipitation with water. The  $\alpha$ -form is also obtained from the  $\beta$ -form by the permutoid swelling process i.e. by adding the  $\beta$ -form pigment to 68% sulphuric acid, forming a yellowish green sulphate, followed by drowning in water, to hydrolyse the sulphate. The precipitate formed is of the  $\alpha$ -form. The polymorphs can be identified both quantitatively and qualitatively by infrared spectroscopy.<sup>65</sup> The enthalpy difference between  $\alpha$  and  $\beta$  CuPc has been measured by isothermal calorimetry.<sup>66</sup>

The third polymorph  $\gamma$ -CuPc first reported by Estates<sup>67</sup>, is obtained by stirring crude CuPc with sulphuric acid of less than 60% concentration. Salts of CuPc made by slurrying it in nitrobenzene and adding a non-oxidising strong mineral acid, followed by filtration and hydrolysis of the filtered salt by water also produced the  $\gamma$ -type crystal. The solvent unstable forms of  $\alpha$ - and  $\gamma$ -phthalocyanines were converted to stable  $\alpha$  or  $\gamma$  polymorphs by pasting with 50-100% H<sub>2</sub>SO<sub>4</sub> in the presence of an undisclosed stabilizer.<sup>68</sup>

## 1.4.2 Spectral Characteristics

### Absorption Spectra

The absorption maximum of phthalocyanines is calculated by assuming the  $\Pi$ -electrons to be one dimensional free electron gas, resonating between two equivalent limiting structures of the phthalocyanine ring with constant potential energy along its length.<sup>69,70</sup>

In the normal state, the stablest energy states of the electron gas, each contains two electrons in accordance with Pauli's exclusion principle. The remaining states are empty. The existence of the first absorption band is a consequence of the jump of a  $\Pi$  - electron from the highest energy level. The spectrum of the phthalocyanine in the visible region is composed of at least seven bands, the main absorption occurring between 6000 and 7000 Å.

The infrared spectra of metal phthalocyanines are reported in media such as nujol and also the form of solid films formed by sublimation.<sup>71,72</sup> Infrared spectra of the two polymorphic forms of CuPc show distinct difference in the 12.5 to 14.5  $\mu$  m range. IR spectroscopy also helps to study the effect of electron donors on phthalocyanines.<sup>73-75</sup>

### 1.4.3 Magnetic Properties

The magnetic susceptibility measurements on metal phthalocyanines give information relating to their structure and the nature of bonding of the central metal atom with the surrounding isoindole nitrogen atoms. NiPc is paramagnetic has a magnetic moment of 1.73 BMg<sup>-1</sup>.<sup>76</sup> The magnetic susceptibility of cobalt, iron, manganese and vanadyl phthalocyanines are 2.9, 10.5 and 1.6 Bohr magnetons respectively.

#### 1.4.4 Electrical characteristics of MPcs

Phthalocyanines are intrinsic semiconductors and the current carriers are mobile  $\Pi$ -electrons. The temperature dependence of conductivity follows the relation

$$\sigma = \sigma_0 \exp(-E_a/kT)$$

where  $\sigma$  = Specific conductivity at temperature T in ohm<sup>-1</sup> cm<sup>-1</sup>  
 $\sigma_0$  = specific conductivity at infinite temperature  
 $E_a$  = Activation energy and R= Gas constant.

Pressure has only a little effect on the conductivity of MPcs. Replacement of the two central hydrogen atoms by a metal atom has little effect upon the energy gap which lies between 1.5 to 1.7 eV and is sensitive to the atmosphere surrounding the sample. Replacement of the two central hydrogen atoms by a metal atom has little effect upon the energy gap which lies between 1.5 to 1.7 eV and is sensitive to atmosphere surrounding the sample.

#### 1.4.5 Aggregation of MPcs

Many workers<sup>77-80</sup> have studied the dimerization and aggregation of substituted phthalocyanines and metal phthalocyanines. The orientation and packing of the phthalocyanine units can be controlled, using Langmuir-Blodgett technique of monomolecular layer formation and transfer. As monomolecular layer films, phthalocyanine compounds display properties like electrical conductivity, electrical switching between conducting states, photovoltaic effects, oxidative catalytic activity etc. The full utilization of Langmuir-Blodgett technique requires soluble phthalocyanine compounds, the ability to modify them chemically and a knowledge of their solution and solid-state molecular aggregation.<sup>81</sup> The data presented below relates to soluble metal tetrasulphophthalocyanine. The molar absorptivities of the monomer and dimer in 50% ethanol at 697 nm are  $9.98 \times 10^4$  M<sup>-1</sup> cm<sup>-1</sup> and  $3.22 \times 10^4$  M<sup>-1</sup> cm<sup>-1</sup> respectively. The concentration equilibrium constant for dimer formation,  $Q_D$  is given by

$$Q_D = \frac{D}{M^2} = \frac{(2\epsilon_M - \epsilon_D)(\epsilon_M - \epsilon_0)}{C_T(2\epsilon_0 - \epsilon_D)^2} = \frac{d_1 d_2}{C_T d^2}$$

Where (M) and (D) are the molar monomer and dimer concentrations, respectively,  $\epsilon_M$  and  $\epsilon_D$  are the monomer and dimer molar extinction coefficients,  $C_T$  is the total concentration of the phthalocyanine tetrasulfonate anion,  $\epsilon_0$  is equal to the absorbance A for the equilibrium mixture divided by  $C_T$ . The dimer formation constant of phthalocyanine tetrasulfonate anion in its 1M solution in 20 v/v% aqueous ethanol is  $8.1 \times 10^5$  in M HCl. Addition of HCl, HClO<sub>4</sub>, NaCl and LiCl markedly affect the spectrum of aqueous solutions of the dimer. The effect was reported in terms of tetramer formation and tetramer formation constants.<sup>82</sup> The aggregates of copper (II) and vanadyl complexes of tetrasulphophthalocyanine exist in aqueous solution at relatively high concentrations used (0.01-0.04M) and dimeric complexes are formed as dimethylformamide is added.<sup>80</sup> It is also found that small amounts of NaClO<sub>4</sub> stabilize the dimer of the iron tetrasulphophthalocyanine and that large amounts of NaClO<sub>4</sub> cause further aggregation.<sup>83</sup>

The synthesis of a series of tetrakis (amylphenoxy) phthalocyanine, the degree of their association in solution and their monolayer forming properties at the water/air interface were also studied. It is found that the degree of association is dependent on the identity of the ion in the

phthalocyanine cavity. The phthalocyanine aggregate forms stable monomolecular films whose packing densities at the air/water interface relate to the degree of association.

## 1.5.0 Technological Applications of Phthalocyanines

### 1.5.1 Pigments and Dyes

The phthalocyanines are widely used in textile, paint, printing ink and plastic industries. The noncolorant applications include catalysts, lubricating greases, analytical reagents, clinical diagnostic agents and electrical devices.

Although the shade range of the phthalocyanines is rather limited and covers only the blue-green regions of the spectrum, their excellent fastness to light, and high absorptivity render them apt for many applications. The insolubility of phthalocyanines necessitates preparation of soluble derivatives for application as dyes for textile fibres. Phthalocyanine pigments in the form of aqueous dispersions is used in pad-dyeing with resin emulsions. Because of their excellent stability to acids, alkalis and solvents phthalocyanines are particularly useful in spin dyeing. They have also been used in coloring polyvinylchloride fibres, viscose, cuprommonium cellulose, nylon, 'perlon L', etc.

Both phthalocyanine blue (copper phthalocyanine) and phthalocyanine green (copper polychloro phthalocyanine) have found wide use as paint pigments. Metal surfaces can be coated by forming the metal phthalocyanine directly on them.<sup>84</sup> Large metal surfaces can be coated with metal phthalocyanine by dipping in a solution of phthalonitrile in acetone, drying, and subjecting the metal to temperatures of around 350° C in a sealed oven. The coating is very adherent and the shade of color depends on the metal used.

Phthalocyanines have been used to color rubber, poly styrene, poly urethane foams, cellulose acetate sheeting, polysters, polyamides, vinylchloride polymers and other plastic and polymeric materials.<sup>85-88</sup> Copper phthalocyanine-sodium sulfonate have been used in photographic processes to produce colored prints. Copper phthalocyanine is also used as a certified food color.<sup>89</sup>

### 1.5.2 Analytical Reagent

Copper phthalocyanine in concentrated sulphuric acid has been used as a reagent for the detection of oxidizing agents such as  $\text{NO}_2^-$ ,  $\text{NO}_3^-$ ,  $\text{ClO}_3^-$ ,  $\text{BrO}_3^-$ ,  $\text{IO}_3^-$ ,  $\text{Cr}_2\text{O}_7^{2-}$  and  $\text{MnO}_4^-$ . Copper tetrasulphophthalocyanine is used as a redox indicator in the cerimetric determination of iron (II) and ferrocyanide<sup>90</sup>. It was found that copper 4, 4', 4'', 4''' tetrasulphophthalocyanine (CuTSP) is a suitable indicator for the titration of Fe(II) in 0.5 - 2.5M HCl or  $\text{H}_2\text{SO}_4$  or  $\text{Fe}(\text{CN})_6^{4-}$  in 0.5N  $\text{H}_2\text{SO}_4$  with 0.01N to 0.001N  $\text{Ce}^{+4}$ . CuTSP is stable towards HCl,  $\text{H}_2\text{SO}_4$  and  $\text{H}_3\text{PO}_4$ . A 0.1% solution of CuTSP is used as the indicator solution.

### 1.5.3 Catalyst

The first mention of phthalocyanines as catalyst is on the activation of molecular hydrogen<sup>91</sup> and found that crystals of phthalocyanine and copper phthalocyanine catalyse atomic interchange between molecular hydrogen and water vapour, and oxygen.<sup>92</sup> Phthalocyanines catalyse the oxidation of many organic compounds.<sup>93-95</sup> Cobalt, nickel and iron phthalocyanines catalyse the oxidation of  $\alpha$ -pinene to verbenone. Nickel phthalocyanine catalyses the autooxidation of saturated ketones such as 2-octanone, 4-heptanone and cyclo hexanone at 120-130° C to  $\alpha$ -diketones and aldehyde. The aerobic oxidation of unsaturated fatty acids catalysed by iron and cobalt

phthalocyanine has been reported.<sup>96</sup> Iron, cobalt, tin and copper phthalocyanines and their derivatives have been used as rubber emulsification catalysts. When cobalt tetrasulphophthalocyanine is attached to poly (vinylamine) it can catalyse the autooxidation of thiols.<sup>97</sup>

#### 1.5.4 Electrocatalysts

$\alpha$ -Keto acids, eg., pyruvic, phenylpyruvic,  $\alpha$ -ketobutyric,  $\alpha$ -ketoglutaric and  $\alpha$ -keto isocaproic undergo electrocatalysed reduction at carbon past electrode modified with cobalt phthalocyanine.<sup>98</sup> CoPc modified electrodes can catalyse numerous electron transfer processes in addition to those of hydrazine and thiol compounds.<sup>99</sup> Metal phthalocyanines have received much attention in the electrocatalytic reduction of dioxygen.<sup>100-102</sup> The phthalocyanines assume importance in electrocatalysis for two reasons:

- 1) Metal phthalocyanines are structural and electronic analogues of porphyrins whose electrochemistry is important in understanding electron transfer processes in biological systems.
- 2) Electrocatalytic reduction of dioxygen is important in fuel cells. Of the metal complexes of phthalocyanine, iron and cobalt have been examined in detail.<sup>103</sup>

Because of the lower solubility of phthalocyanines, water soluble phthalocyanines such as tetrasulphophthalocyanine<sup>104</sup> and tetracarboxy phthalocyanine<sup>105</sup> have been used as facile catalysts in aqueous medium. The electrocatalytic activity of dioxygen reduction was improved at a glassy carbon electrode when modified with polypyrrole/tetrasulfonatophthalocyaninato cobalt electrode.<sup>106</sup> The glassy carbon/polypyrrole/cobalt tetrasulfophthalocyanine (GC/PPY/CoTSP) electrode was formed by electropolymerization of pyrrole on a glassy carbon electrode in methanol solution containing CoTSP. Oxygen reduction reaction at the GC/PPY/CoTSP electrode in 0.5M H<sub>2</sub>SO<sub>4</sub> showed about 0.5V more anodic onset potential than the value obtained with a GC electrode in the same medium.

The reduction of dioxygen at iron tetrasulfonatophthalocyanine (FeTSP) incorporated into polypyrrole was also studied.<sup>107</sup> It was found that thicker films are stable and mediate four-electron reduction of dioxygen. It was indicated that dimeric FeTSP species are responsible for the marked shift in the reduction onset potential.

Polymeric iron phthalocyanine precipitated on activated carbon, when heated to 200-500° C showed a higher rate of deactivation for the electrochemical reduction of dioxygen.<sup>108</sup>

The iron, cobalt, copper phthalocyanine function as a catalyst layer and oxygen sensor in fuel cells and air battery.<sup>109</sup> A porous electrocatalyst material was prepared by soaking activated carbon in iron phthalocyanine pyridine solution and in perfluorodecalin - CCl<sub>4</sub> solution and then mixing with PTFE. The material in the form of sheet was bonded on a nickel mesh. The electrode was used in a zinc-air battery having a discharge current density of 63 mA/cm<sup>2</sup>.

### 1.5.5 Active Layers on Chemically Modified Electrodes

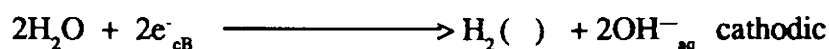
Electrodes derived from different types of phthalocyanines have been fabricated.<sup>101,110-112</sup> powdered carbon or metal is coated with the phthalocyanines by chemical vapour deposition, solvent evaporation or electrophoretic deposition. the powder of the same material has also been pressed with crystalline phthalocyanines in to composite pellets. Various metal and semiconductor substrates demonstrated greatly enhanced activity for the electrolysis of the benzoquinone/hydroquinone redox couple when coated with multimolecular layers of chlorogallium phthalocyanine.<sup>113</sup> Exchange current density on GaPc-Cl/Au electrode irradiated with  $-100\text{mW/cm}^2$  polychromatic light were  $-10^3$  times greater than on plain gold electrode. The role of GaPc-Cl in activating the substrate surface is also reported. The use of chemically modified carbon paste electrodes, which are modified by the incorporation of cobalt phthalocyanine is able to oxidize or reduce solute species which are themselves electrolysed only irreversibly at conventional electrode surfaces.<sup>98</sup> These electrodes decrease the overpotential for the oxidation of thiols<sup>114</sup>, hydrazine<sup>115</sup>,  $\alpha$ -keto acids and oxalic acid. A glassy carbon electrode modified with CoPc can be efficiently used as a liquid chromatographic detector for the clinical assay of oxalic acid and  $\alpha$ -ketoacids in blood and urine. Faulkner et al<sup>116,117</sup> have studied in detail the faradaic processes taking place on Pc modified electrode surfaces. Nearly reversible kinetics and a high degree of selectivity for the electrode process are observed on these films.

Photoreduction of dioxygen takes place on certain phthalocyanines, when they are vacuum deposited to a thickness of 100-1000 Å on polished graphite. Photooxidation of oxalate takes place on 1 m thick films of CuPc deposited on Pt.<sup>118</sup>

### 1.5.6 Photovoltaic and Photogalvanic Devices

Phthalocyanines show photoconductivity. The photoconductive and photovoltaic properties of Pcs have been extensively studied for use in electrophotographic systems, diodes, laser printers, photovoltaic cells, photoelectrochemical devices and vidicon tubes.<sup>119-123</sup>

MnPc can be considered as a model compound for the study of photocatalytic decomposition of water in biochemical processes. Cobalt (II) tetrasulfophthalocyanine (CoTSP) can be covalently bound to the surface of titanium dioxide particles. Upon irradiation with light having energy exceeding the band gap energy of  $\text{TiO}_2$ , Co(II) TSP is reduced to Co(I) TSP. This photochemical reduction is reversible in presence of dioxygen. The photochemical stability and the high quantum yields for  $\text{O}_2$  reduction makes this newly developed material applicable as a potent and stable oxidation catalyst. The interest shown in these systems is due to the simultaneous formation of dihydrogen and dioxygen from water. An overall transfer of conduction band electrons  $e^-_{\text{CB}}$  and valence band holes  $h^+_{\text{VB}}$  is required to achieve this direct storage of solar energy in the form of chemical energy. The reactions taking place are:



Cobalt tetrasulfophthalocyanine covalently bound on the surface of titanium dioxide particles act as efficient electron relays to compete with the  $e^-/h^+$  recombination and thus achieve reasonable but still rather small, quantum yields.

In photocells, with phthalocyanine as the active material under an externally impressed negative bias, the efficiency in energy conversion can reach about 25%.

### **1.5.7 Electrochromic Displays**

Electrochromic (Electrochemichromic EC) effect is the production, by faradaic reaction, of a color change in materials localised at an electrode surface. A thin film of lanthanide diphthalocyanine deposited on optically transparent electrode shows change in absorption spectrum of polarisation in contact with an aqueous electrolyte.<sup>126,127</sup> Rare earth phthalocyanine can be sublimed onto conducting glass and can therefore be used as materials for EC displays. These electrochemichromic materials are also useful for full-colour imaging and graphic and alphanumeric displays.<sup>128</sup> The rapid decay of EC characteristics of rare earth diphthalocyanine film electrodes on potential cycling in neutral aqueous solution has been considerably retarded by using ethyleneglycol as solvent.<sup>129</sup>

### **1.5.8 Batteries**

Phthalocyanines and phthalocyanine derivatives have been used as cathode materials in batteries especially in fuel cells and air cathode batteries. In batteries the porous electroconductive material is loaded with metal phthalocyanine and a perfluoro compound. This composite material is used as the catalyst layer.<sup>130,131</sup>

### **1.5.9 Gas Sensors**

Devices based on metal phthalocyanine such as PbPc show useful response towards NO<sub>2</sub>. A thin film PbPc sensor has successfully been used to monitor NO<sub>x</sub> produced by short firing in coal mines.<sup>132</sup> Pc based devices offer much promise as resistance modulating sensors for toxic gases. They are thus complementary to metal oxide devices which are most useful in the detection of flammable gases. The lanthanide diphthalocyanine complexes have been used as gas detectors for acidic and basic gases.<sup>133</sup>

### **1.5.10 Electrophotography**

Electrically conductive substances are coated with photoconductive layers made up of Pcs dispersed in a binder resin. The plates show high sensitivity, improved durability and excellent imaging characteristics.<sup>134</sup>

# CHAPTER II

## EXPERIMENTAL

### Synthesis and characterisation of metal phthalocyanines Synthesis of copper, cobalt and nickel phthalocyanines

A mixture of phthalic anhydride 5.9g (0.4 mmol), urea 9.6g (1.6 mmol) and 50mg of ammonium molybdate and a speck of ammonium chloride were heated in nitrobenzene at refluxing temperature (205° C) for 2 h. The nitrobenzene was recovered by distillation at reduced pressure. The crude product so obtained was washed several times with methanol until it was free of nitrobenzene. This was again washed with 10% NaOH, 2M HCl to remove any unreacted acid and metal salt, and finally washed with distilled water till the washing were neutral. The solid mass so obtained was slurried in concentrated sulphuric acid and dropped on ice. The precipitate formed was filtered and dried.

The metal phthalocyanines so obtained were further purified by soxhlet extraction with benzene, acetone and DMF. The material was finally purified in a sublimation chamber. The pure phthalocyanine was deposited onto a glass plate at 200° C under about  $10^{-4}$  torr.

#### Phthalonitrile Process

Iron and zinc phthalocyanines were prepared by heating phthalonitrile and the corresponding metal chloride in the molar ratio 4:1 at 180-190° for 2h in quinoline. The metal phthalocyanine so obtained was purified by the procedure described in the previous section. The unreacted phthalonitrile was removed by soxhlet extraction with benzene.

#### Lanthanum phthalocyanine

Rare earth acetates prepared from pure grade oxide were used for the preparation of lanthanide phthalocyanines. Lanthanum acetate was prepared from its oxide by the following procedure.<sup>135</sup>

Lanthanum oxide (Indian Rare Earths Ltd. Udyogamandal) was ignited for 3 h in a silica crucible. This oxide was cooled and refluxed with 200 ml of acetic anhydride for 6 h. After 2 h of refluxing the solid mass was broken up thoroughly and refluxing continued for 4 h. The lanthanum acetate formed was filtered out and dried in vacuum.

A mixture of 1g of lanthanum acetate (0.5 mmol) and 3g of phthalonitrile (2.6 mmol) were heated at 280 - 290° C in a furnace for 2 h. The dark blue solid mass obtained was washed with benzene to remove any unreacted phthalonitrile. This was filtered and the solid dissolved in 200 ml DMF. This solution was then passed through a column of neutral alumina. The pigment was adsorbed on the upper part of the column. Methanol was used to elute the fraction containing the blue pigment. The solution was evaporated to dryness and the residue was dried at 100° C for 1 h.

#### Tetrasodium salt of cobalt(II) 4,4',4'',4''' - tetrasulfophthalocyanine dihydrate.

The procedure is a modification of the method developed by Weber and Busch.<sup>136</sup> The monosodium salt of 4-sulfophthalic acid (4.7g, 0.09mol), urea(58g, 0.97mol), ammonium mo-

lybdate (0.68g, 0.0006 mol), and cobalt(II) sulphate, 7-hydrate (13.6g, 0.048 mol) were ground together to a fine powder. Nitrobenzene (40 ml) was heated to 180° C in a 500 ml two-necked flask fitted with a thermometer and a condenser and a stopper. The solid mixture was added slowly with stirring keeping the temperature between 160° and 190° C.

The mixture was heated for 6 h at 180° C. The crude product was ground and washed with methanol. The washed solid was added to 1L of 1N hydrochloric acid saturated with sodium chloride. This was heated to boiling, cooled and filtered. The resulting solid was dissolved in 700 ml of 0.1N sodium hydroxide. The solution was heated to 90° C and insolubles separated by filtration. Sodium chloride (270g) was added to the solution. At this point the solid product precipitated. This was centrifuged and the solid was washed with 80% aqueous ethanol refluxed for 4 h in 200 ml absolute ethanol and cooled. The product was filtered and dried at 80° C.

Complexes of nickel (II), copper (II) and Fe(III) were prepared by procedures similar to that used for Co(II).

## 2.1.2 CHARACTERISATION OF METAL PHTHALOCYANINES

The various metal phthalocyanines were characterized by the following physical and chemical methods. Nitrogen was estimated by standard Kjeldahl method.<sup>137</sup>

Sulphur content of the compounds was estimated by Schoniger oxygen flask method.<sup>138</sup>

A weighed sample (0.2g) of the material was placed in the sample cup of the Schoniger flask. It was covered with a strip of ashless filter paper having a wick for ignition. Sodium hydroxide solution (40 ml, 10%) was used as absorbent and 5 ml of 30% hydrogen peroxide was used as oxidant. The sample cup was lowered into the flask and the flask was flushed with oxygen. The wick was ignited and the flask was closed by lowering the stopper carrying the cup. After ignition, the contents were thoroughly mixed the solution was acidified with hydrochloric acid and transferred to 250 ml beaker. Sulphate was determined gravimetrically as barium sulphate.

7  
6671-2871-501-12  
11/18

**Table III:****ELEMENTAL ANALYSIS OF VARIOUS METAL PHTHAOCYANINES AND THEIR  
SULPHONIC ACID DERIVATIVES**

Sample	%Nitrogen		%Sulphur		%Metal	
	Experimental	Theoretical	Experimental	Theoretical	Experimental	Theoretical
CoPc	20.81	19.61	—	—	10.92	70.33
CoTSPc	11.95	11.03	11.42	12.62	5.04	5.68
FePc	21.14	19.71	..	..	9.18	9.83
FeTSPc	11.89	11.24	11.68	12.87	4.98	5.32
CuPc	20.76	19.44	..	..	10.07	11.03
CuTSPc	11.85	10.98	11.79	12.56	5.82	6.22
NiPc	21.27	19.61	..	..	9.86	10.27
NiTSPc	11.74	11.44	12.89	13.51	4.98	5.84
LaPc	16.24	17.20	..	..	..	1.33

## Absorption Spectra

The UV-Vis spectra of the metal phthalocyanines were taken in 90% concentrated sulphuric acid and the infrared spectrum were recorded in KBr pellet. The solid state electronic spectrum of the samples were taken by smearing the material with Nujol on a thin strip of filter paper.

The spectral characteristics for different samples are given in Table IV

Sample	Observed $\lambda_{\max}$ , nm				Reported $\lambda_{\max}$ , nm <sup>139</sup>			
CoPc	770,	697,	432,	322,	780,	700,	420,	300
FePc	340,	594,	661,	770	330,	597,	660,	
NiPc		322,	589,	774	300,	595,	700,	774
CuPc	312,	452,	666,	781	305,	440,	704,	794
Lapc (DMF)	462,	604,	665,		461,	602,	670	
ZnPc	314,	442,	708,	788	310,	440,	698,	784

The UV-visible spectra of the sulfonated metal phthalocyanines are markedly depended on the solvent. In water and DMSO the sulfonated phthalocyanines show distinctly different spectra probably due to the association of the phthalocyanines. This also depends on the concentration of MTSPc. In the case of Cu and Ni compounds the shoulders at 665 and 606 nm were observed at low concentrations ( $\sim 10^{-6}$  M), but in the case of CoTSPc the shoulders were observed at still higher concentration ( $\sim 10^{-3}$  M).

**Table V**

VISIBLE SPECTRA OF METAL TETRASULPHOPHTHALOCYANINES					
Material	Solvent	$\lambda_{\max}$ (nm) Observed			$\lambda_{\max}$ (nm) Reported
CoTSPc	Water	668, 629, 605, 350	668, 630, 604, 320		
NiTSPc	Water	668, 622, 351,	668, 630, 604		
FeTSPc	Water	668, 630, 320	669, 338, 630		
CoTSPc	DMSO	661, 601, 357	663, 600, 332		
NiTSPc	DMSO	669, 664, 351	673, 644, 332		
FeTSPc	DMSO	679, 645, 605, 337	679, 645, 608, 342		

### Infrared Spectra

Infrared studies have been used as the main tool for the investigation of metal phthalocyanines because of the characteristic "finger print" of the ligand. Proof of the formation of a new metal phthalocyanine has often been based entirely on a close correlation of the infrared spectrum with that of an authentic phthalocyanine. Table VI compares the infrared data observed and the values reported by Lever et al.

**Table VI**

INFRARED SPECTRA										
Sample	$\lambda_{\max}$ Observed					$\lambda_{\max}$ Reported				
CoPc	435,	518,	575,	645,	756,	435,	518,	575,	644,	756,
	771,	804,	868,	877,	910,	771,	780,	804,	868,	877
	940	948,	957,	1072,	1089,	910,	948,	957,	1072,	1089
	1098	1123,	1165,	1173,	1290,	1098,	1123,	1265,	1173,	1290
	1333,	1422,	1468,	1484,	1516,	1333,	1422,	1468,	1484,	1516
	1592	1611				1592,	1611			
CuPc	580,	630,	740,	788,	881,	580,	630,	740,	780,	860
	907,	949,	1010,			907,	949,	1100		
ZnPc	430,	519,	630,	722,	750	630,	720,	750,	780,	872,
	780,	872,	885,	945,	952,	870,	890,	930,	950,	1115
	1114,	1280,	1338,	1440		1280,	1340,	1440		
LaPc	720,	755,	880,	1052,	1100,	724,	743,	881,	1054,	1112
	1318,	1440,	1600,			1320,	1327,	1448,	1450,	1600

Infrared Spectra of Tetrasulfonated Metal Phthalocyanines	
Sample	$\lambda_{\max}$ (nm)
CoTSPc	875.7, 1033.8, 1192, 1639.5, 1458, 3448, 3691.7
NiTSPc	771, 888, 1053, 1355, 1502, 1610
FeTSPc	777, 876, 1038.7, 1211, 1312, 1354, 1480, 1624

In addition to peaks at 750-770, 890-910, 1010-1020, 1080-1190, which are characteristics of metallophthalocyanines, all these samples show absorption at 130-1300, 1210-1150 and ~ 1500 nm which are characteristic of the absorption of sulfonic acid functional group.<sup>143</sup>

# CHAPTER III

## ELECTROCHEMICAL STUDIES

### Introduction

The surface of an electrode can be characterized by studying the electron transfer across the electrode/electrolyte interface. This also helps in understanding the general rules of electrochemical kinetics and the relation of the electronic structure of the electrode to the electrochemical behaviour. Free charges available for electrical conduction is much lower in semiconductors than in metallic conductors. The electrical field extends deep within the volume of the semiconductor and a space charge region is formed close to its surface. The applied voltage at a semiconductor electrode controls the probability of a surface reaction primarily and not, as at metal electrodes the energy factor.

Depending on whether the semiconductor chosen is n-type or p-type, it can act as electron donor or acceptor, without change in its constitution in an electron transfer reaction. Organic semiconductor electrodes such as phthalocyanines are capable of undergoing faradaic reactions. Faulkner et al <sup>117</sup> have correlated the electrochemical reactivities of several solution species with the relative positions of their energy level and the known band edges and intermediate levels of phthalocyanine thin-film electrodes. They studied the electrochemical properties of thin films of semiconductor electrodes of metal free, zinc and nickel phthalocyanines and found that the facility of charge transfer is determined by the phthalocyanine coverage.

The electrodes modified with layers of electroactive or inactive species is a new tool for the fundamental studies of electron-transfer reactions. Usually the chemical species are attached to the electrode surface and the surface would take on the properties of the attached reagents. Another method is to allow the Faradaic reaction to take place directly on these surfaces. One of the necessary condition for these electrodes is that they should be reasonably conductive. Thin film technology has been utilized for the fabrication of molecular semiconductors with low resistance. A film of thickness of  $\sim 1000 \text{ \AA}$  deposited over a metallic conductor can provide a current path of sufficiently low resistance, even with bulk resistivities in the over layer as high as  $10^8 \text{ ohm cm}$ .

Metal complexes of organic compounds in general and metal phthalocyanines in particular, received much attention since Jasinski <sup>144,145</sup> reported that, they are capable of catalysing the electro-reduction of dioxygen. Subsequently many types of phthalocyanine-modified electrodes have been fabricated. <sup>110,111, 113, 146, 147</sup> Powdered carbon or metal has been coated with the phthalocyanines by chemical vapour deposition, solvent evaporation and electrophoretic deposition. These same powders have also been pressed with crystalline phthalocyanines into composite electrodes. Bulk metal surfaces have been coated by solvent evaporation, by adsorption from solution and also by vacuum deposition. Most of the work based on these electrodes were oriented to study the electrocatalysis of  $\text{O}_2$  reduction by phthalocyanines. It was Faulkner et al <sup>116</sup> who first investigated whether faradaic process is taking place on the phthalocyanine surfaces. They have fabricated electrodes by evaporating chromium, gold and phthalocyanine in sequence onto a glass substrate in vacuo. ZnPc and FePc showed nearly reversible charge transfer reactions on a cyclic voltammetric time scale. ZnPc and FePc could not efficiently mediate electrode reactions (including  $\text{O}_2$  reduction) that occurred on Au at potentials more negative than 0.0 V vs SCE, whereas reactions in the positive region could proceed readily.

## **Plasma treatment of MPC layers**

A gas can exhibit conductivity only when it possesses free charged particles. The concentration of such charged particles will influence the conductivity of the gas. In the presence of charged carriers, a gas, which is a perfect insulator, starts showing the properties of a conductor. Its insulating capability deteriorates owing to the generation and multiplication of charged particles. This characterized behaviour of the gases in the partially or fully ionized state constitutes the plasma. The electron emission from boundary surfaces, especially from electrodes, facilitates generation of charged particles and contributes to a more intense plasma.

The treatment of a material with plasma results in unique surface modification which can be controlled. This property makes it a useful tool for the modification of surface structure and composition of solid materials. The plasma treatment produces chemically active species which results in the surface modification. The thermal treatment of surfaces require temperatures which can either damage or distort the solid being treated, and ultraviolet radiation processes are limited by the spectrum available from UV lamps. The significant advantage of plasma processes is that they can take advantage of both the UV radiation and the active species simultaneously. Thus in the case of a polymer, the UV radiation can produce polymer free radicals which react with free radicals produced in the plasma. A second advantage is that plasma process can be controlled easily through the large number of independent parameters influencing the properties of the plasma. Thermal, chemical and high energy radiation processes usually do not possess equivalent degrees of freedom in their control.

There are three general means by which a plasma and a solid can interact. In the first case, the plasma and the solid are physically in contact, are electrically isolated, and have a steady-state interaction. Physical contact is produced by placing the solid directly in the volume where the plasma is generated or by placing it downstream from this position and allowing the plasma to expand over the solid. Electrical isolation means that there is no net current arriving at the solid boundary and that the potential of the solid floats relative to the plasma. An example of this type of interaction is a sheet of polyethylene placed inside of a rf electrodeless discharge. In the second case, the plasma and solid are both physically and electrically in contact and again have a steady-state interaction. As a result of the electrical contact, current is drawn from the plasma through the solid material. The solid material may be an electrode used in the production of the plasma or it may be independent of the plasma and electrically biased relative to the plasma. A current flow to the solid material can alter the reactions at the surface by producing a change in the plasma and gas composition around the solid. The third case involves a nonsteady-state interaction in which the solid has physical but no electrical contact.

### **3.1.2 Transfer and Dissipation of Plasma Energy**

Energy can be transferred from plasma to a solid through optical radiation, neutral particle fluxes, and through ionic particle fluxes. The energy transferred from the plasma is dissipated within the solid by a variety of chemical and physical processes. These dissipation processes are the origin of the desired surfaces property modifications.

The optical radiation emitted by a plasma contains components in the IR and UV-vis region of the spectrum. For polymers, the visible radiation is weakly absorbed and does not produce interesting chemistry. The UV radiation is strongly absorbed by polymers producing polymer free radicals. The polymer free radicals are active sites which can then react with gas components within

the plasma. The neutral particles in the plasma continually bombard the solid transferring energy from the plasma to the solid. The neutral particle flux contains energy in four forms kinetic, vibrational, dissociation (free radicals), and excitation (metastables). The kinetic and vibrational forms of energy heat the solid. For polymers, the free radical dissociation energy is dissipated through surface chemical reactions such as abstraction, addition, and oxidation as well as through thermal heating caused by free-radical recombination on the surface of the solid. Metastable atoms and molecules are the principal carriers of the energy stored in electronic excitation not released by radiation. These metastable particles release their energy by collisions with the surface. For polymers, the metastable energy in general is larger than the polymer dissociation energy and tends to produce polymer free radicals.

### **3.1.3 Experimental Techniques for Plasma Treatment**

Four different techniques have been used to generate plasmas.

- i Silent discharges
- ii Direct - current and low-frequency low discharges
- iii High-frequency and
- iv Microwave discharges.

#### **(I) Silent Discharges**

In this technique a silent electric discharge is passed through a gaseous medium by applying high voltage ( $>1\text{mV}$ ) Coaxially placed metal electrodes or electrolyte solutions are used as electrodes. Its major disadvantages are the small gap and large surface area are required.

#### **(II) Direct - Current and Low-frequency Glow Discharges**

In this case, two metal electrodes are placed inside a reactor and connected to a variable high voltage source. When this kind of device is used for organic reactions, the electrodes are quickly covered with polymeric material. To prevent this contamination, it is necessary to isolate the electrodes from the organic gases by a shroud of rare gas.

#### **(III) Radio -Frequency Discharges**

At frequencies above 1 MHz direct contact between the electrodes and the plasma is no longer necessary. The energy can be fed to the plasma indirectly by capacitive or inductive coupling. An inductive coupling includes a small percentage of capacitive coupling and vice versa. In the case of capacitive coupling, the electrodes enclose the plasma tube. For inductive coupling, the tube lies on the axis of the coil.

At higher working frequencies the rf circuit elements become very small in both dimension and value.

#### **(IV) Microwave Discharges**

Microwave generators with outputs between a few watts and a kilowatt have frequently been used in plasma experiments. The microwave power is led by coaxial cable or wave guide from the generator to a resonant cavity which encloses the reactor. While microwave discharges have been used successfully with inorganic compounds, it is found that organic substances are almost completely destroyed.

The various kinds of electrical discharges lead to nearly identical results. The choice of equipment is not determined by the chemical problem but by questions of flexibility, ease of availability and cost. For laboratory purposes, radio frequency equipment is best suited because of its great versatility. The frequency range from about 2-60 MHz is particularly convenient because the dimensions of the rf-coupling elements allow easy handling.

### 3.1.4 Applications of Plasmas

Plasma chemistry can be applied to synthesize new compounds, which often leads in a single step to substances which by classical methods can only be synthesized in a number of reaction steps. Treatment of plasma will result in reactions as (a) generation of atoms or radicals (b) isomerization (c) elimination of atoms or small groups (d) dimerization and polymerization (e) reactions involving a complete scrambling or destruction of the starting material.

Plasma technique can be used for the generation and reaction of atomic hydrogen, oxygen and nitrogen.<sup>148-150</sup> The glow discharge technique can be utilized for the cis-trans isomerizations. When the trans stilbene is distilled through a glow discharge, the reaction product is found to be cis-stilbene.<sup>151</sup> Another type of isomerization frequently observed in plasmas is the migration of substituents, especially in aromatic compounds.

Plasma can also be utilized for elimination reactions. At low energies of collision the process eliminates small groups or atoms without altering the rest of the molecule. The remaining species often are reactive intermediates like radicals and carbenes which stabilize through the formation of multiple bonds, through cyclization, ring contraction or dimerization.

### 3.1.5 Application of Plasma - Solid reactions to polymers

The principal changes brought about by exposure of a polymer to a plasma are in the surface wettability, the molecular weight of a surface layer, and the chemical composition of the surface. Plasma processes which lead to an improved wetting have found application in packaging, electronics, construction and clothing industries. Molecular weight changes are another property modification which can be effected by a plasma. Variation in this characteristic affects a number of physical properties of the polymer such as permeability, solubility, melt temperature, and cohesive strength. The cohesive strength is important for adhesion and again is a surface effect.

Exposure of a polymer to a plasma can also be used to create reactive sites on the polymer surface. These changes in the surface composition can be produced by bond rearrangement reactions which lead to unsaturation. The groups are attached through covalent bonds and can act as "hooks" for the addition of new compounds which can further change the surface chemical and electrical properties. The films treated with plasmas are usually amorphous, pinhole-free, and highly crosslinked.

The surface of organic pigments can be modified by low temperature oxygen plasma. Organic pigments of high quality with good sharpness, tinting strength, transparency, fastness etc. can be synthesized by treatment with plasma.<sup>152</sup> The compositions comprising the plasma irradiated pigments showed a newtonian flow, which one of the preferred properties of a coating composition, giving the coating films better gloss and sharpness than original coating films containing untreated pigments.

### 3.2 CYCLIC VOLTAMMETRY IN THE STUDY OF ELECTRODE PROCESS

#### Principles

Cyclic voltammetry on stationary electrode is one of the most effective and versatile electroanalytical technique available for the mechanistic study of electrode reactions.<sup>153-155</sup> An 'electrochemical spectrum' indicating the potentials at which process occur can be rapidly obtained, while from the sweep rate dependence the involvement of coupled homogeneous reactions are readily identified and other complications such as adsorption can be recognised. In view of these capabilities, cyclic voltammetry is nearly always the technique of choice when studying a system for the first time. The repetitive triangular potential excitation signal for CV causes the potential of the working electrode to sweep back and forth between two designated values (the switching potentials). The cyclic voltammogram is obtained by plotting the I-V curve in an unstirred solution.

The fundamental equation for cyclic voltammetry have been developed by Delahay,<sup>156</sup> Shain<sup>157</sup> and others<sup>158-160</sup>. The equation for the cyclic voltammogram known as Randles-Sevick equation is:

$$I_p = \frac{-(2.69 \times 10^5)}{K} n^{3/2} C D^{1/2} v^{1/2}$$

Where  $I_p$  = Peak current density in  $A\ cm^{-2}$   
 $D$  = diffusion coefficient of the electroactive species in  $cm^2\ s^{-1}$   
 $n$  = number of electrons involved in the electrode process  
 $K$  = Randles-Sevick constant  
 $C$  = Concentration of the electroactive species in mM.  
 $v$  = Scan rate  $mVs^{-1}$

For an irreversible process

$$I_p = 2.69 \times 10^5 n (2n_a)^{1/2} A D^{1/2} C v^{1/2}$$

where  $a$  = transfer coefficient and

$n_a$  = number of electrons involved in the rate determining step and other terms have their significance. The value of  $n_a$  can be determined using the relation

$$E_{p/2} - E_p = \frac{0.048}{n_a} \text{ volts}$$

Where  $E_p$  and  $E_{p/2}$  are the peak and half-peak potentials. The forward rate constant can be calculated using the relation.<sup>161</sup>

$$E_p = \frac{-1.14 RT}{n_a F} + \frac{RT}{n_a F} \ln k_m^\circ - \frac{RT}{2 n_a F} \ln(\eta_a V)$$

where,  $k_{fh}^0$  is the heterogeneous forward rate constant and other terms have their usual significance.

The reversibility of a system can be checked from cyclic voltammetry by plotting  $I_p$  as a function of  $v^{1/2}$ . The plot must be both linear and pass through the origin. The other diagnostic tests for reversibility of a process by cyclic voltammetry are:

$$1. E_p = E_p^A/E_p^C = \frac{59}{n} \text{ mV}$$

$$2. E_p - E_{p/2} = \frac{59}{n} \text{ mV}$$

$$3. \left| \frac{I_p^A/I_p^C}{\alpha_c/\alpha_a} \right| = 1$$

$$4. I_p \propto v^{1/2}$$

5.  $E_p$  is independent of  $v$

6. at potentials beyond  $E_p$ ,  $I^2 \propto t$

For an irreversible system the most marked feature is the total absence of a reverse peak.  $E_p^C$  will vary with the sweep rate:

$$E_p^C = K - \frac{2.3 RT}{2 \alpha_c n \alpha_a F}$$

$$\text{Where } K = E_e - \frac{RT}{\alpha_c n \alpha_a F} \left[ \frac{0.78 - 2.3 \log \frac{\alpha_c n \alpha_a F D}{k^2 RT}}{2} \right]$$

ie.,  $E_p^C$  shifts by  $30/\alpha_c n \alpha_a$  mV for each decade change in  $v$ . The shape factor  $|E_p - E_{p/2}|$  is also different for the irreversible case, and is given by:

$$E_p - E_{p/2} = \frac{48}{\alpha_c n} \text{ mV}$$

The diagnostic tests for a quasi-reversible system is given by:

1.  $I_p$  increases with  $v^{1/2}$  but is not proportional to it
2.  $I_p^A/I_p^C = 1$  provided  $\alpha_c = \alpha_a = 0.5$
3.  $\Delta E$  is greater than  $59/n$  mV and increases with increasing  $v$
4.  $E_p^C$  shifts negatively with increasing  $v$ .

Cyclic voltammetry is probably the most powerful tool available for investigating coupled chemical reactions. In the case of a ce mechanism ( $Y \rightleftharpoons O$ ;  $O + ne^- \rightleftharpoons R$ ) if the electron transfer is reversible and the chemical step is very slow, the current will be purely kinetically controlled and therefore no peaks will appear in the cyclic voltammogram. Instead, a simple steady state type wave will be obtained.

The diagnostic tests for CE mechanism are:

1.  $I_p^C / v^{1/2}$  decreases as  $v$  increases
2.  $I_p^A / I_p^E$  increases with  $v$  and is always greater than or equal to unity.

For the ec reaction ( $O + ne^- \rightleftharpoons R$ ;  $R \xrightleftharpoons[k]{k_1} Y$ ) and if the electron transfer is totally irreversible, the following diagnostic tests can be applied to the system.

1.  $I_p^A / I_p^C$  is less than one but tends to unity as  $v$  is increased.
2.  $I_p^C / v^{1/2}$  decreases slightly with increasing  $v$
3.  $E_p^C$  is positive of the value for the reversible case
4.  $E_p^C$  shifts negatively with increasing  $v$ .

Similarly cyclic voltammetry can be utilized for diagnosing catalytic reactions, ece reaction, and also surface process such as adsorption, deposition and passivation. Cyclic voltammetry is the principal technique used to determine the thermodynamic parameters of polymer films formed on an electrode<sup>162</sup> and it is the most extensively used technique to characterize the electroactivity of monomolecular and multimolecular layers of redox species.<sup>163</sup>

### **3.3 EXPERIMENTAL PROCEDURE**

#### **3.3.1. Chemicals**

The metal phthalocyanines used were prepared and purified as described in section 2.1

All chemicals used were of guaranteed purity. The complexes of iron were prepared by mixing stoichiometric amounts of ferrous sulphate with the corresponding ligands. The solutions were prepared in doubly distilled water.

#### **3.3.2 Pretreatment of platinum electrode**

The platinum electrode was immersed in strong dichromate-sulfuric acid 'cleaning solution' for several minutes, then rinsed with tap water and finally with distilled water. It removes grease and oil as well as many of the organic films prevalent in the oxidation of aromatic compounds and oxidizes the platinum surface strongly.<sup>164</sup> The electrode was then dipped in hot nitric acid to oxidatively destroy any further organic materials on the surface. After rinsing with distilled water the electrode was immersed in air-free 0.1M perchloric acid and subjected to strong cathodic pretreatment by holding the potential at -20V vs SCE for 10 minutes, during which time hydrogen was vigorously evolved at the surface. The electrode was then washed with distilled water and applied the cathodic pretreatment by immersing the electrode for 10 min. in an acid solution containing an oxidant (Bromine water). The anodic current occurring between 0.0 and 0.5 V vs SCE was completely eliminated by treating with the oxidant. Finally chemical reduction was done by immersing the electrode in ferrous sulfate solution and then immersing in 12M HCl and washing with distilled water.

A cyclic voltammogram was obtained at the electrode at the beginning of each experiment to check the quality of the electrode and also to determine the cathodic and anodic limits.

#### **3.3.3 Background current and cycling history**

The background current which flows under a set of given experimental conditions in the absence of the electroactive material is determined before the start of a new experiment.

In the electrochemical studies a platinum wire electrode of length 5mm or a platinum button electrode of area  $5(\text{mm})^2$  was used as the working electrode. An auxiliary electrode of a sheet of platinum of area (15mm x 15mm) and a saturated calomel reference electrode were employed. The solution was made air free by flushing with nitrogen for about 20 minutes and keeping a positive nitrogen atmosphere in the cell during the experiment.

A conventional undivided cell (Fig.3.1) was used for the electrochemical experiments. The reference electrode was introduced through a luggin capillary whose tip was positioned close to the working electrode to minimise IR drop.

#### **3.3.4 Procedure For Setting The IR Compensation <sup>165</sup>**

The method involves pulsing the working electrode in potential regions where no faradaic process occurs, while monitoring the current vs time behaviour. The ability of the working electrode to follow an applied square-wave signal is a function of the solution resistance, R between the working and reference electrodes, and of the double-layer capacitance, C of the working electrode.

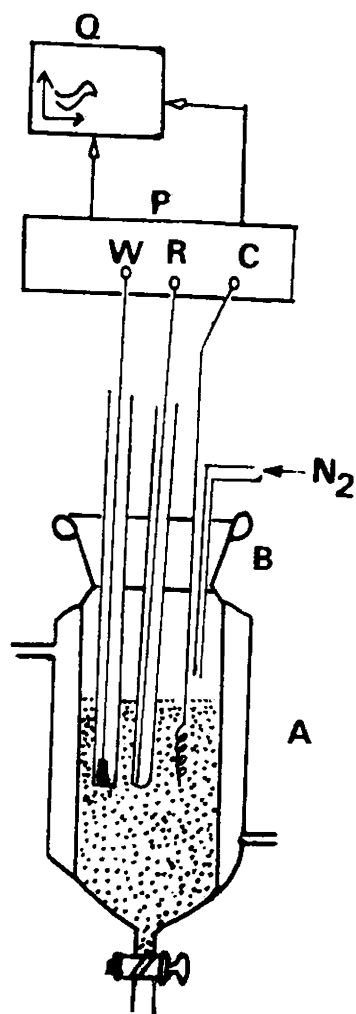


**Fig. 3.1 Schematic of the electrochemical cell and instrumentation for cyclic voltammetry.**

**A — Double walled glass vessel with stop cock , B — 4-Necked glass stopper, C — Counter electrode  
P — Potentiostat, Q — X-Y Recorder. R — Reference electrode, W — Working electrode**

This RC combination shows the response of the working electrode to the applied square wave. Positive feedback IR compensation increases the potential so that the solution RC can be quickly charged. The following procedure was used for setting the IR compensation.

The cell was set up with the electrodes and solution. Initial potential was selected well below the half-wave potential of the reaction. A small amplitude (~20 mV) square wave at 1 kHz was provided from an external square-wave generator and it was superimposed on the potentiostatic output. The oscilloscope was connected to the current monitor terminals of the potentiostat. The oscilloscope was adjusted to display the current vs time trace of the electrode response. The IR compensation dial was turned fully clockwise. After IR compensation was switched on, the dial was rotated clockwise while monitoring the current signal with the oscilloscope. The dial was adjusted for the smoothest fast-charging of the double layer capacitance, as shown in Fig.3.2

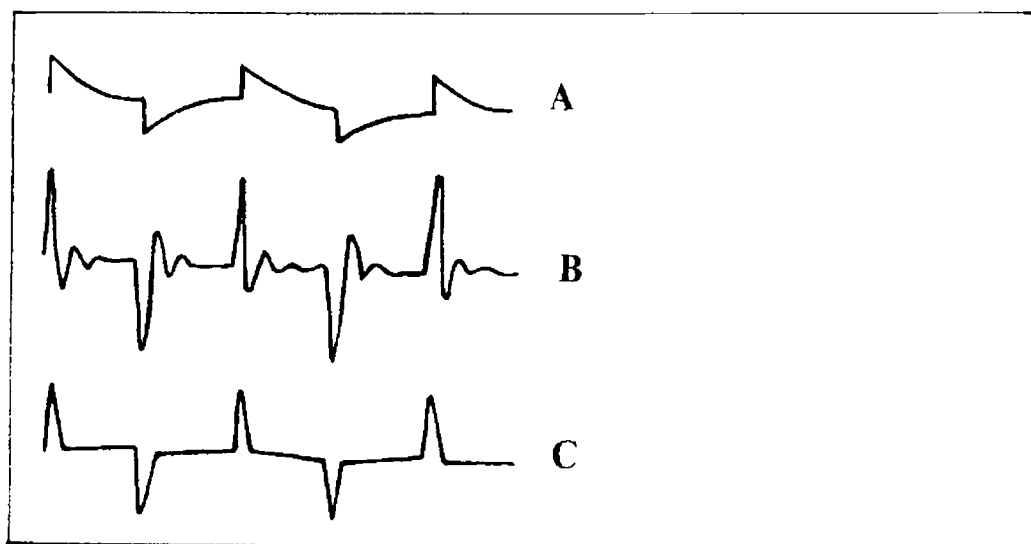


**Fig. 3.2 Current monitor wave forms during IR compensation procedure.**

- A LARGE UNCOMPENSATED RESISTANCE TOO LITTLE IR COMPENSATION SLOW RESPONSE**
- B TOO MUCH IR COMPENSATION HIGH-AMPLITUDE FAST RESPONSE WITH RINGING**
- C CORRECT IR COMPENSATION FAST SMOOTH RESPONSE**

IR compensation adjustments are critical in the sense that any change in the system (sensitivity, cell geometry, supporting electrolyte, etc.) will change the amount of compensation required.

### 3.3.5 Plasma Treatment

The plasma was generated in a glass tube by capacitive coupling as described in section . The electrode was mounted in the closed tube and placed close to the plasma source and rotated periodically to make the treatment uniform. The atmosphere in the tube was air at a pressure of ~30 torr.

### 3.3.6 Results

Electron transfer process mediated by electrodes modified with CoPc, FePc, ZnPc, CuPc and NiPc were carried out by cyclic voltammetry.

The cyclic voltammograms recorded for the supporting electrolyte in bare Pt and MPc coated Pt are shown in Fig.3.3 In deaerated 0.1M KNO<sub>3</sub> solution CoPc, NiPc and ZnPc show a flat background response from 0.0V to -0.8V vs SCE. The cathodic peak onset occurs at -0.8V. A positive scan from 0.0V shows a quasi-reversible process at 0.3V in the case of ZnPc & NiPc and for CoPc a peak is observed at 0.79V. The quasi-reversible nature confirmed nature confirmed from the  $i_p$  vs  $v^{1/2}$  plot The value of  $i_p$  increases with  $v^{1/2}$  but is not directly proportional to it. It is also found that  $\Delta E$  is greater than  $59/n$  mV and increases with increasing scan rate.

The background current is only a small fraction of the faradaic current produced by added electroactive species in the 4-10mM concentration range.

Fig. 3.4 shows the cyclic voltammetric responses of different redox couples at a Pt electrode. The potentials at which electron transfer take place in these compounds lie within the range selected to study the behaviour of phthalocyanine electrodes. All these systems give characteristic well defined redox peaks at a Pt electrode. The cyclic voltammetric characteristics for the oxidation and reduction of these compounds at Pt electrode are summarised in Table.1

Fig.3.4 shows the cyclic voltammograms of the different redox couples at CoPc/Pt electrode. Table II lists the potential at which the redox couples undergone electron transfer. Fig. 3.5 shows the scan rate dependence of the anodic peak current at the CoPc electrode for ferrocyanide in 0.1 M KNO<sub>3</sub> medium. The linear variation of peak current with square root of the scan rate rules out any involvement of the adsorption of electroactive species on the electrode.  $\Delta E_p$  is close to 59 mV and the peak is asymmetric. These results show that diffusion controlled reversible charge transfer of redox species is possible at these electrodes. The electrode process occurring may be on the MPc surface or on the metal surface by the penetration of the solution through pin holes or channels that may be present on the film. Hence it is necessary to confirm the site of the heterogeneous charge transfer.

### Evidences for the occurrence of charge transfer at MPc Surface

1. The diffusion current at CoPc has the same magnitude (within experimental error) as that on a bare electrode (Fig 3.5)
2. Under identical conditions the voltammogram at CuPc (Fig. 3.7 ) is considerably distorted and show only small peak currents. This behaviour is in agreement with the observation of other authors.<sup>166</sup>

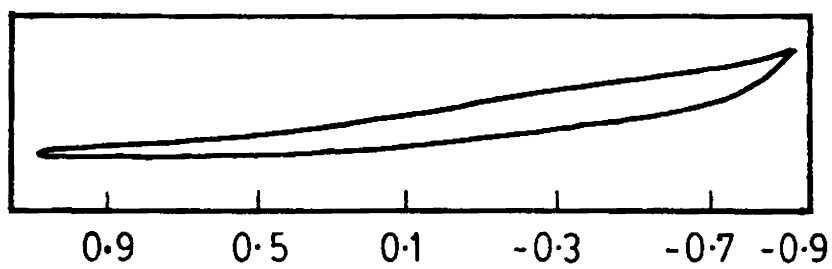


Fig 3.3 Cyclic voltammogram recorded at a bare Pt electrode. Supporting electrolyte 0.1M  $\text{KNO}_3$ , Scan rate 100mV /s

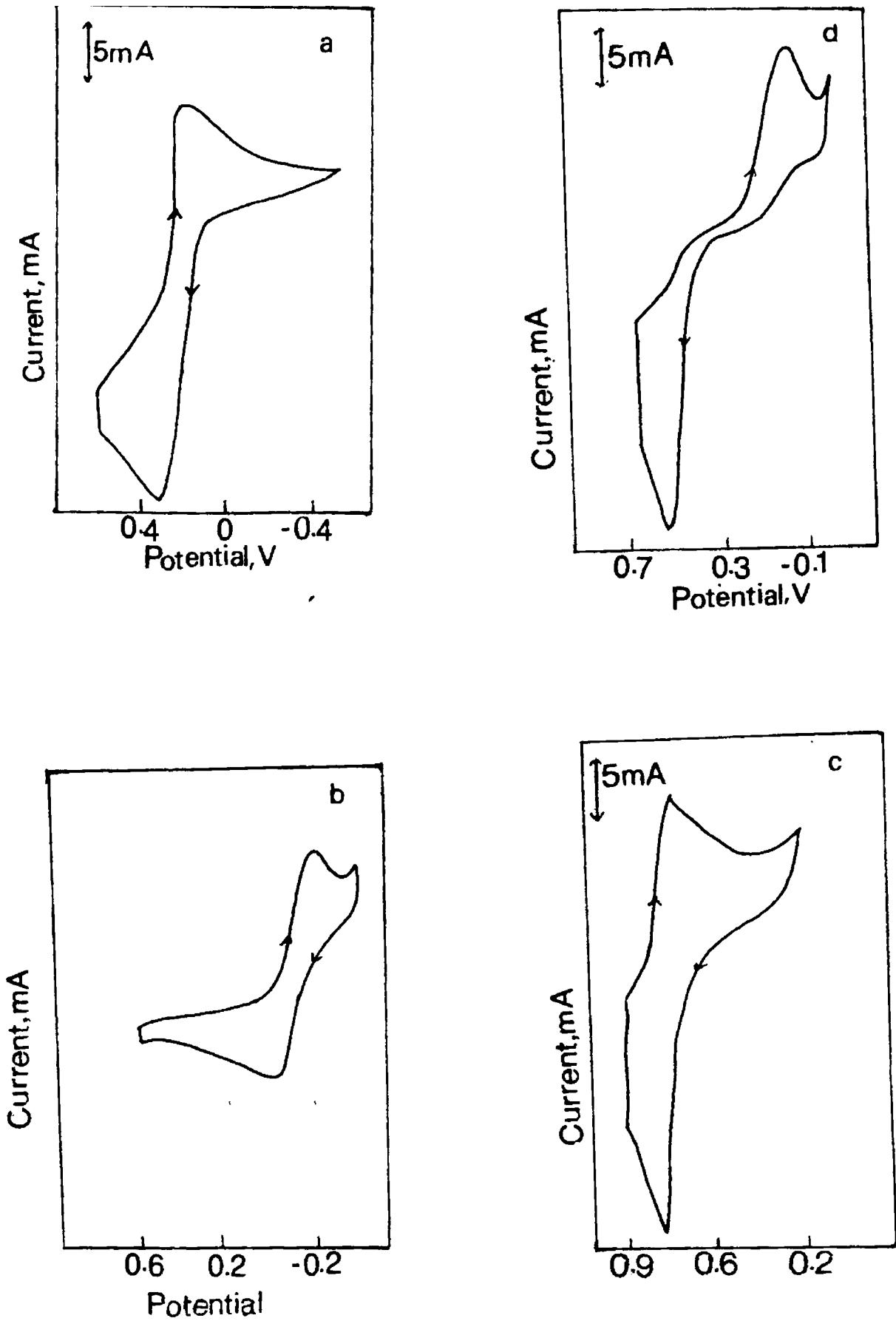


Fig. 3.4 Cyclic voltammetric response of different redox couples at Pt electrode

(a) $\text{Fe}(\text{CN})_6^{4-}$	(b) Fe-EDTA	(c) Fe(o-phenanthroline)	(d) Hydroquinone
Supporting electrolyte		0.1M $\text{KNO}_3$	
Scan Rate		: 100mV/s	

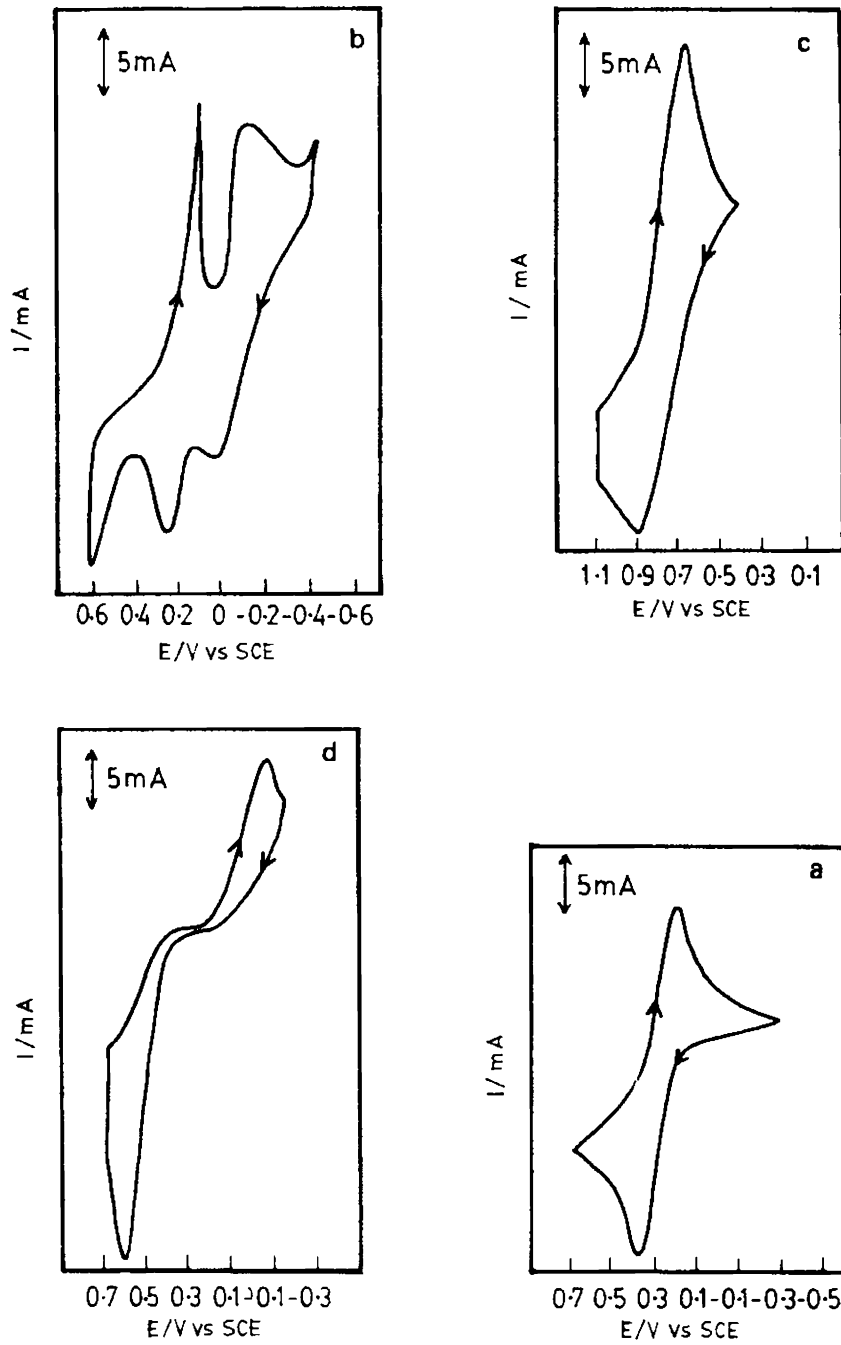


Fig. 3.5 Cyclic voltammograms of different redox species at CoPc/Pt electrode  
 (a)  $\text{Fe}(\text{CN})_6^{4-}$  (b) Fe-EDTA (c) Fe(o-Phenanthroline) (d) Hydroquinone  
 Supporting electrolyte 0.1M  $\text{KNO}_3$   
 Scan Rate : 100mV/s

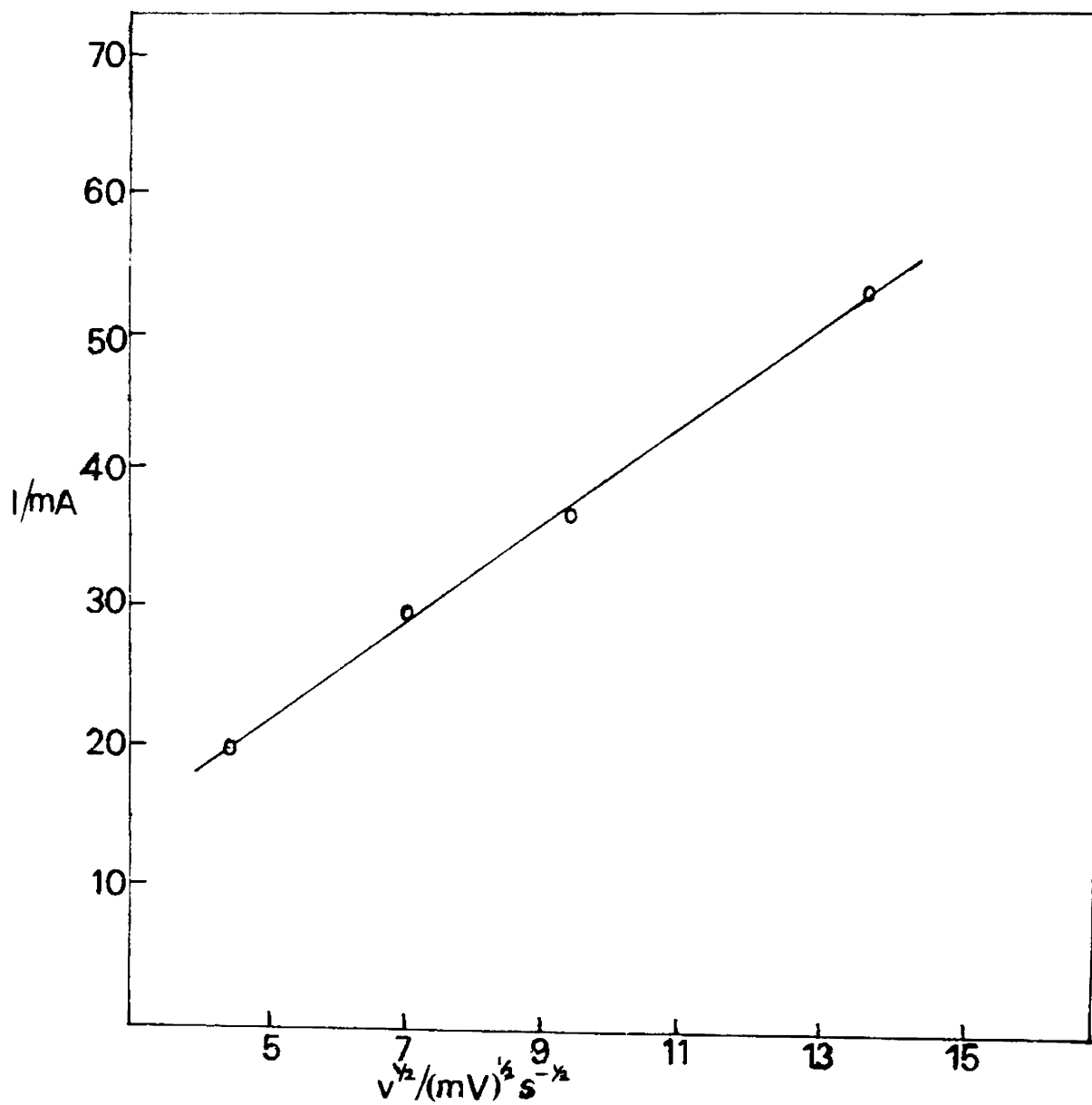


Fig. 3.6 Scan rate dependence of the anodic peak current at CoPc electrode in ferrocyanide/0.1M KNO<sub>3</sub> medium.

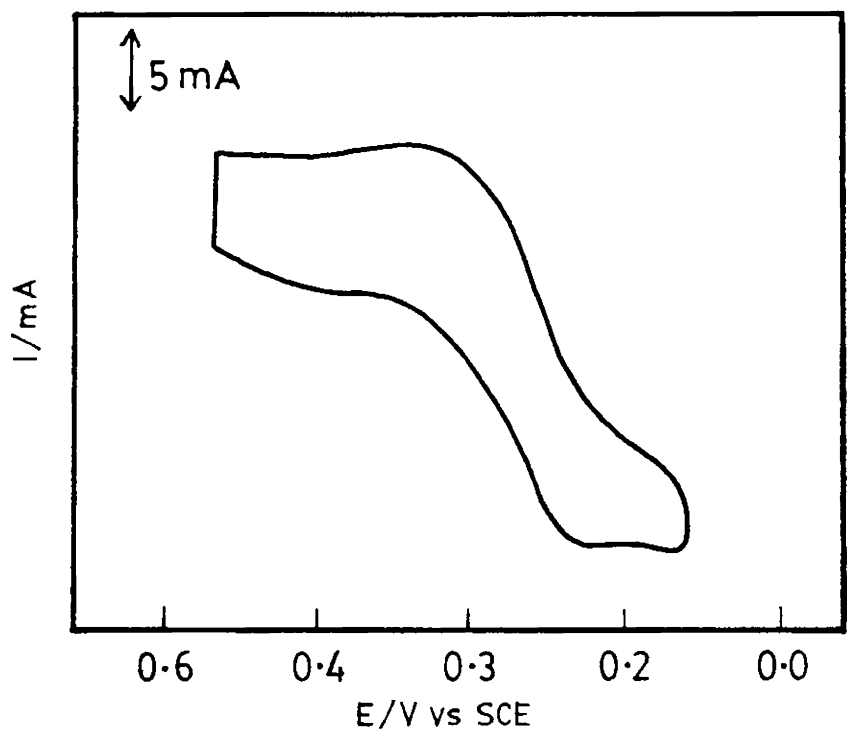


Fig 3.7 Cyclic voltammogram of potassium ferrocyanide at CuPc/Pt electrode.  
Supporting electrolyte : 0.1M KNO<sub>3</sub>  
Scan Rate : 100mV/s

3. The voltammograms at lauryl derivative of tetra-amino phthalocyaninato nickel (II) do not show any faradaic process. i.e., they are of the insulating type <sup>167</sup>. If the charge transfer was through the pinholes or channels distributed over surface of the metal phthalocyanines, then all the phthalocyanines would have given similar electrochemical response irrespective of the nature of the central metal atom. Since the electrochemical response exhibited on the nature of the central metal atom and also on the substitution on the phthalocyanine ring the possibility of charge transfer through the pinholes is ruled out.

These evidences confirm that facile faradaic activity occurs directly on the CoPc layer of the CoPc-modified Pt electrode. The same argument can be extended to other phthalocyanine electrodes also.

When the cyclic voltammograms were recorded on NiPc and ZnPc electrodes for a solution of ferrocyanide in 0.1M KNO<sub>3</sub>, the first two scans show only irreversible response (Fig.8) During subsequent scans the behaviour becomes more reversible with wider peak separations and smaller peak currents than at bare electrodes.

The irreversibility manifested in the initial cycles may be either due to uncompensated  $iR$  losses within the film or due to sluggish electrode kinetics resulting from the depletion of carrier density at the interface<sup>166</sup>. When the electrodes are exposed to water or O<sub>2</sub> the resistance of these films is reduced. The O<sub>2</sub> molecule can act as an acceptor impurity which leads to the formation of holes, which are the majority carriers <sup>168</sup>.

The water molecule may act as an axial ligand for the metal atom of the metal phthalocyanine and thereby enhance the donor strength of a site.

The peak current for the oxidation of ferrocyanide at ZnPc, NiPc, and FePc are also proportional to  $v^{1/2}$ . This shows that the process is diffusion controlled. The Fe(CN)<sub>6</sub><sup>3-4-</sup> couple showed good response even in the initial cycle. This is due to the fact that the carrier densities in the fresh FePc phases are fairly high<sup>166</sup>. This also accounts for the differences in behaviour of FePc and ZnPc.

Fe(II)-EDTA complex also showed reversible charge transfer reaction at CoPc, FePc, NiPc and ZnPc electrodes (Fig.3.7 — 3.11). In addition to the redox potentials of the Fe-EDTA complex, CoPc gave an anodic peak at 0.5V, NiPc at 0.25V and ZnPc at 0.15V. The plot of  $i_p$  vs  $v^{1/2}$  is a straight line and rules out the involvement of any adsorption in the electrode process in this case also.

The same experiment was repeated with Fe (1,10-phenanthroline) and hydroquinone. As shown in Fig.3.9 — 3.11 all the four electrodes CoPc, NiPc, FePc and ZnPc gave reversible charge transfer responses on electrode modified with these compounds. The oxidation-reduction potentials for the different redox species at different Pc coated electrodes are given in Table. II

The facile faradaic activity at MPc/Pt can be explained on the basis of the semiconducting property of MPc. The phthalocyanines are p-type semiconductors with their flat band potentials near 0.0V vs SCE. The systems studied have redox potentials in the positive region and hence facile faradaic activity on the systems take place at these semiconducting electrodes.

The forgoing evidences illustrate the ability of metal phthalocyanines attached on electrode surfaces to mediate electron transfer. Once they are coated on the electrode surface, the electrode shows the electrochemical properties of the metal phthalocyanine species. The MPc- coated

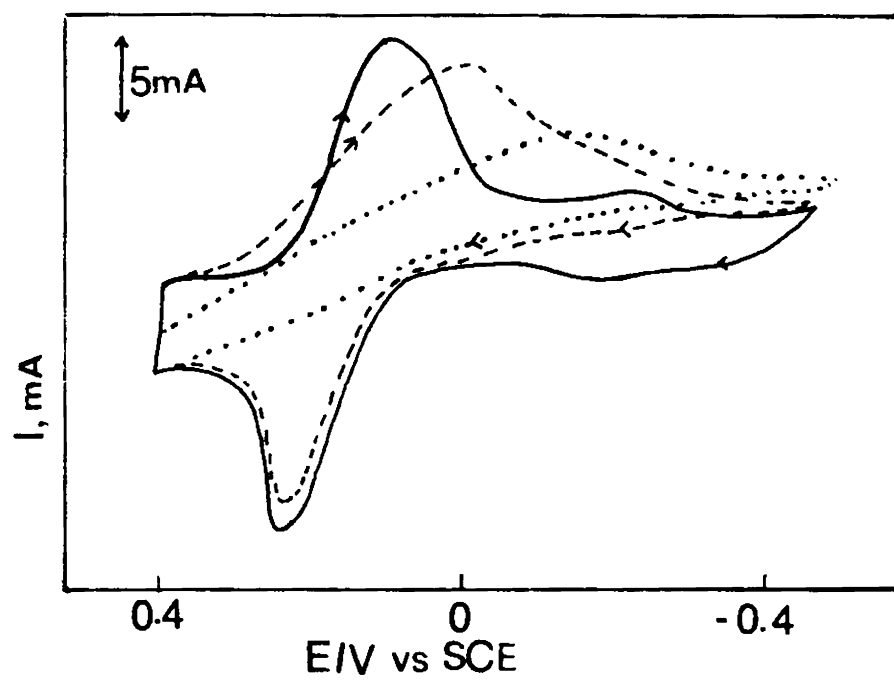


**Fig. 3.8** Continuous cyclic voltammograms at ZnPc electrodes for ferri/ferrocyanide redox couple in 0.1M  $\text{KNO}_3$  medium.

(- -) First cycle

(...) After 4 cycles

(—) After 7 cycles

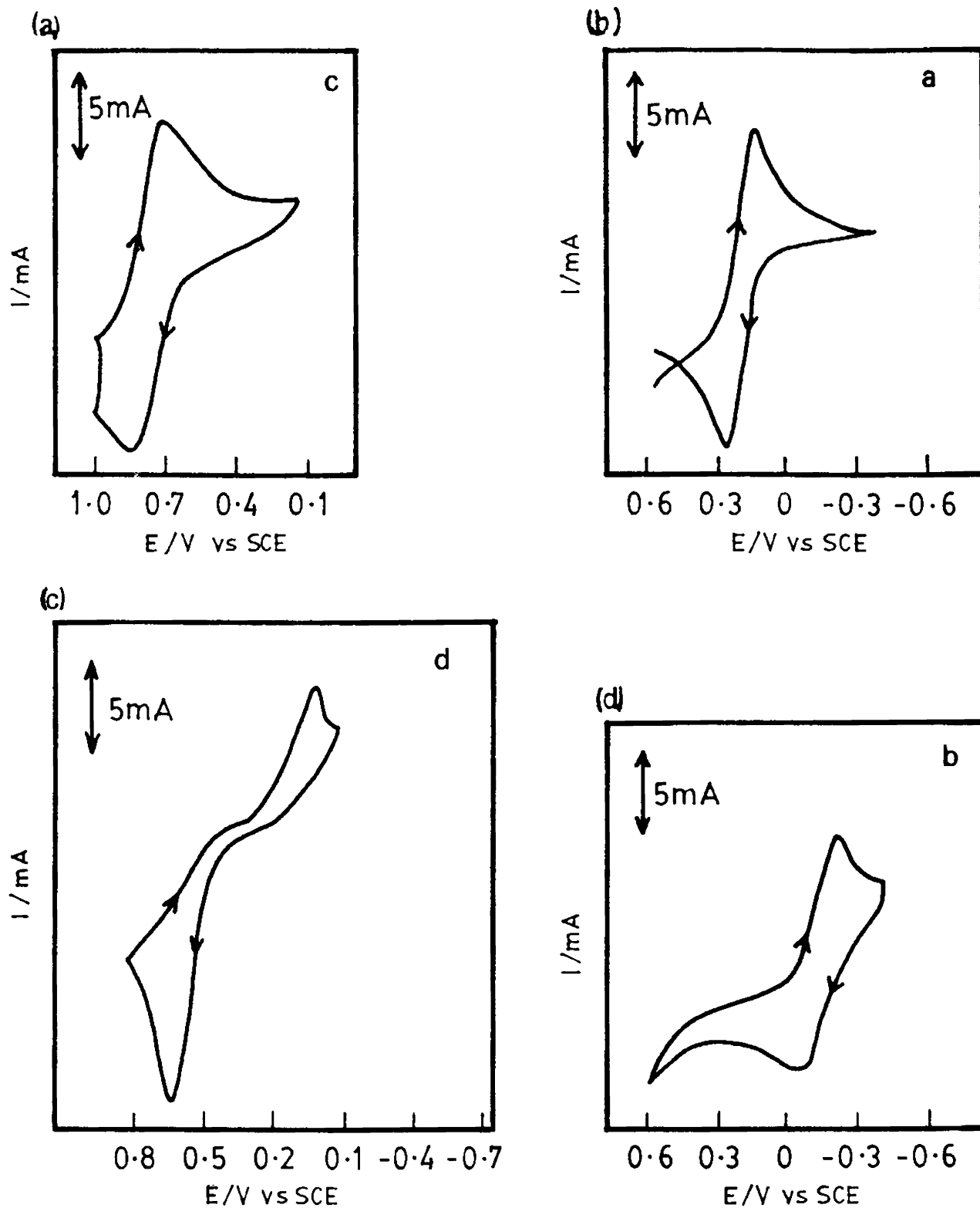
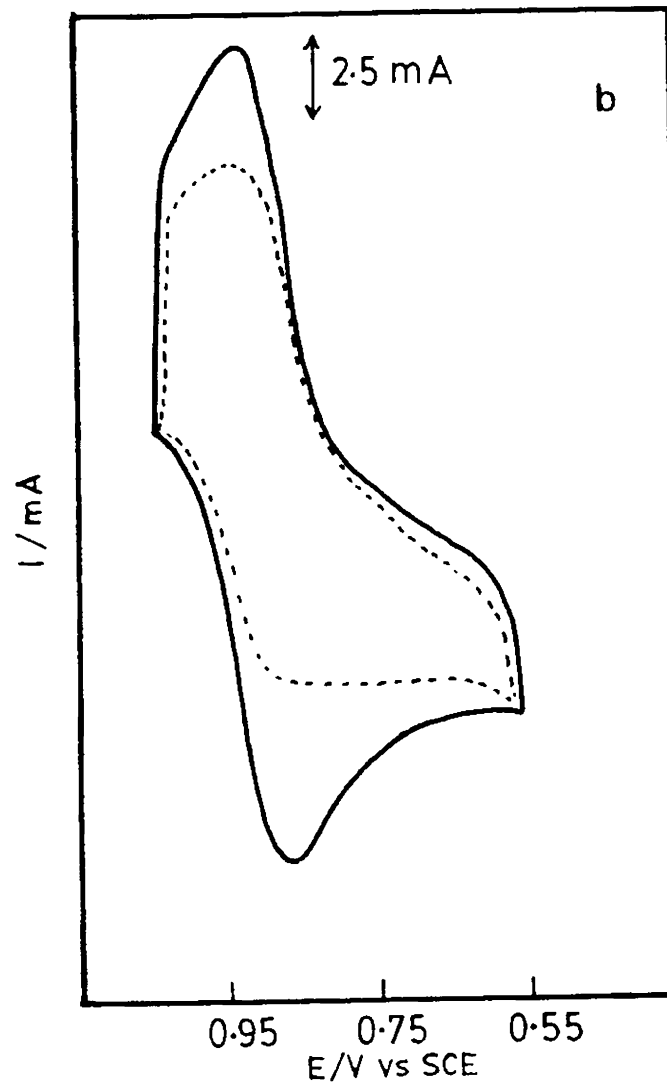
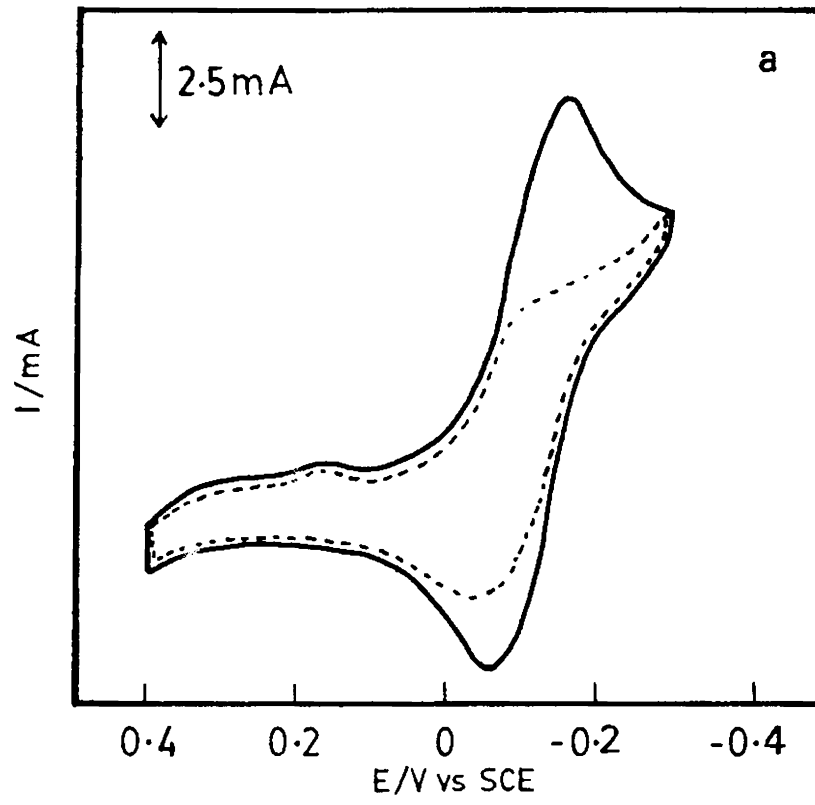


Fig. 3.9 Cyclic voltammograms of different redox species at FePc electrode  
 (a)  $Fe(CN)_6^{4-}$  (b) Fe-EDTA (C) Fe-(*o*-Phenanthroline) (d) hydroquinone  
 Supporting electrolyte : 0.1M  $KNO_3$   
 Scan rate : 100mV/s



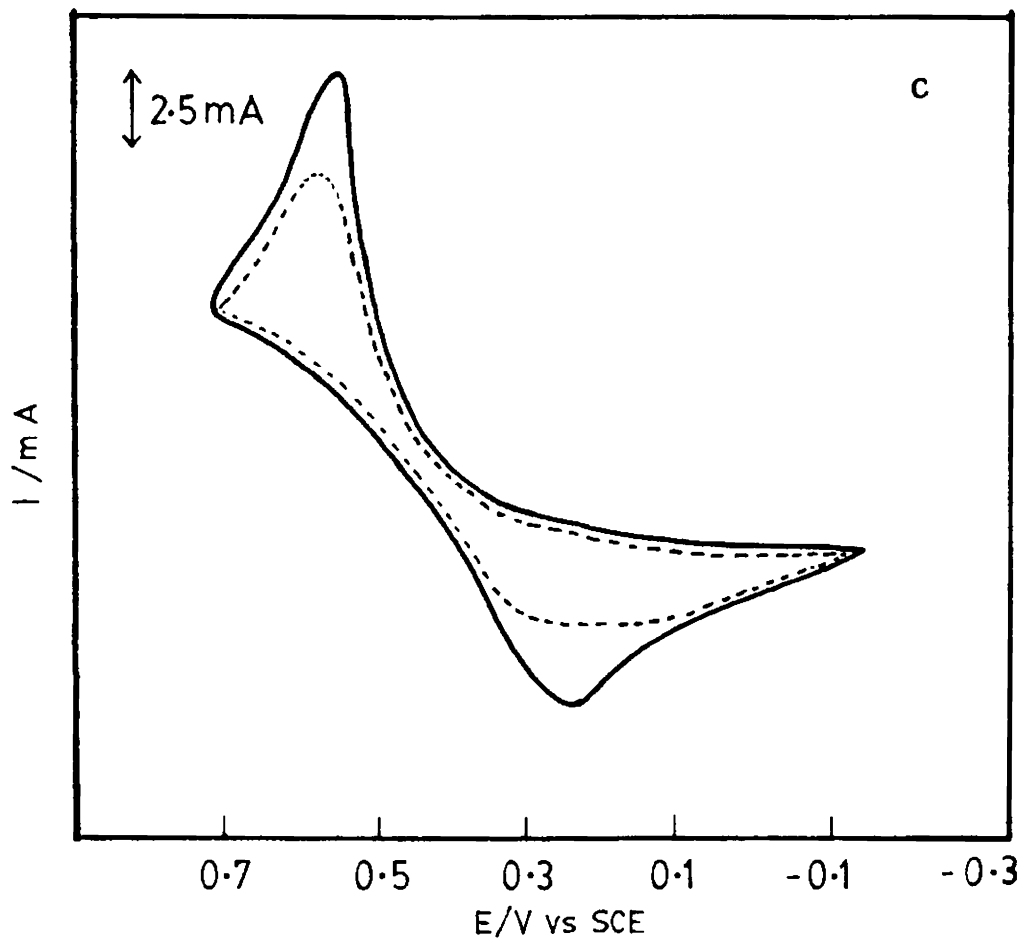
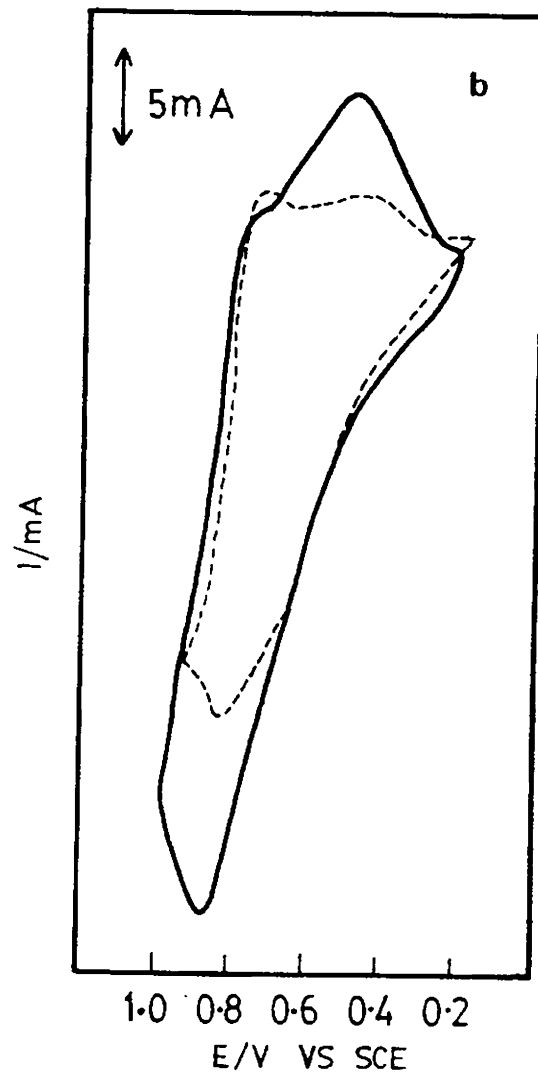
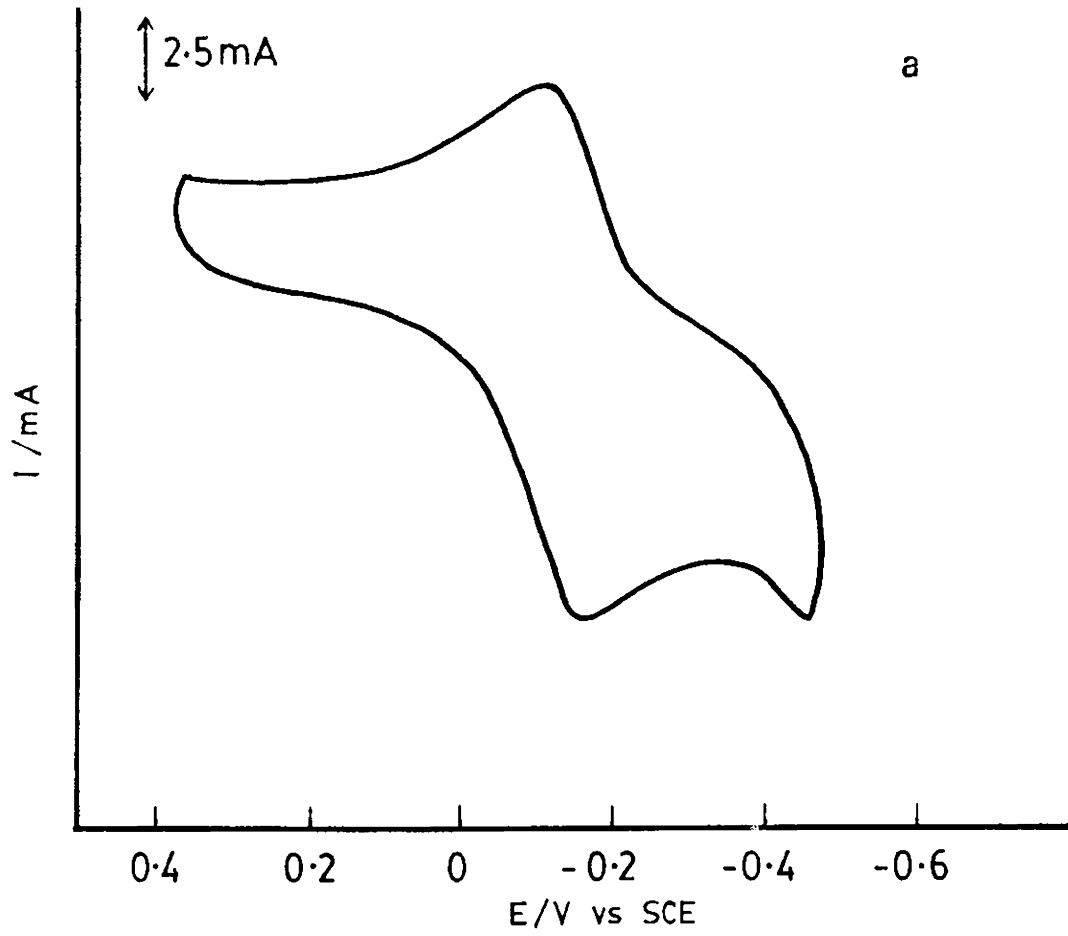


Fig. 3.10 Cyclic voltammograms of different redox species at NiPc electrode  
 (a) Fe-EDTA      (b) Fe(o-phenanthroline)      (c) Hydroquinone



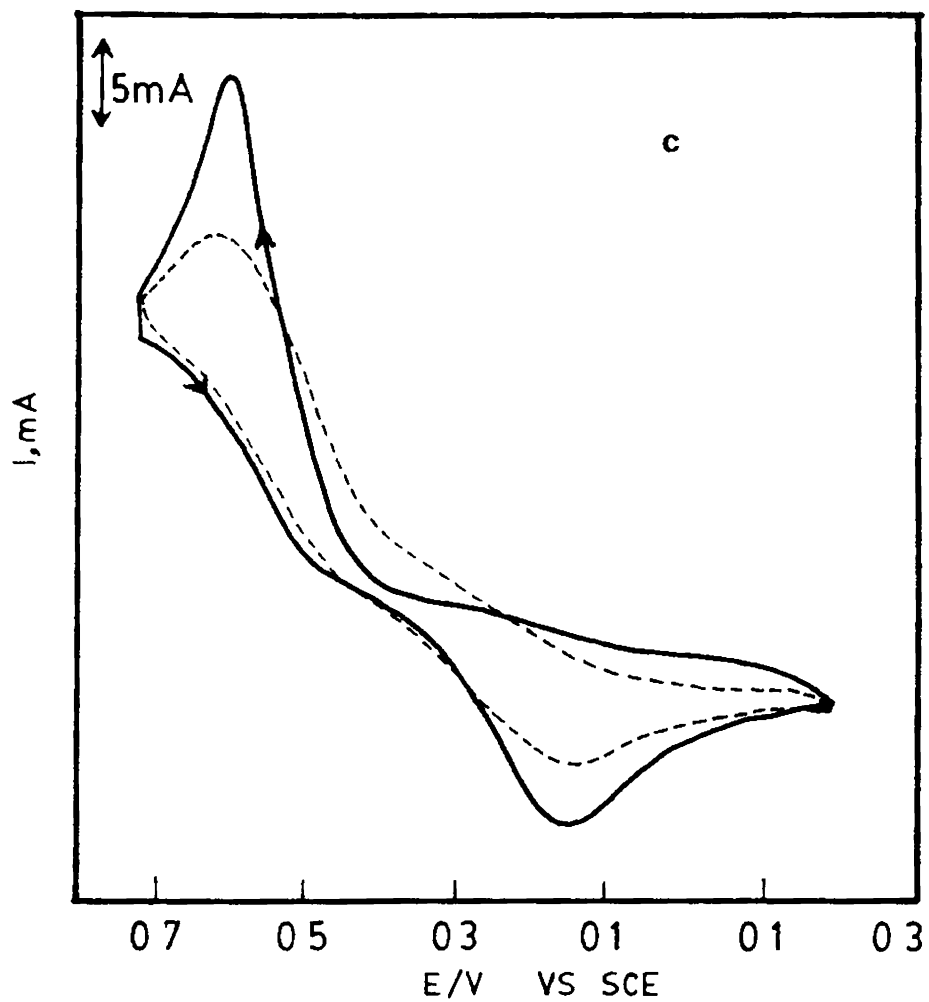


Fig. 3.11 Cyclic voltammetric behaviour of different redox species at ZnPc electrode.  
 (a) Fe-EDTA      (b) Fe(o-phenanthroline)      (c) Hydroquinon

electrodes withstand multiple potential cycling and hence are durable as modified electrodes.

### 3.3.7 Electrochemical behaviour of rf plasma treated metal phthalocyanine electrodes

The metal phthalocyanines are treated with rf-plasma in order to create more active sites on the phthalocyanine surface. Exposure of materials to plasma gives films of increased cohesive strength, adhesion and crosslinking.

Fig. 3.12 shows the cyclic voltammetric behaviour of plasma treated CoPc electrode towards various redox species such as potassium ferrocyanide, hydroquinone, Fe-EDTA, Fe(*o*-Phenanthroline). The treatment of phthalocyanine with plasma evidently lowers the onset potential for the electron transfer process. The peak currents are increased substantially. The diffusional behaviour of the electrode process confirmed by the linear dependence of  $i_p$  on the square root of the scan rate (Fig. 3.13). This also suggests that adsorption does not complicate the electrode process.

The ZnPc electrode which fails to mediate the reversible redox process for ferrocyanide in the initial cycles gives characteristic redox behaviour in the first cycle itself, if it is exposed to rf plasma (Fig. 3.14a) This may be due to the increase in activity and conductivity of ZnPc film as a results of exposure of ZnPc film to plasma.

The CuPc electrode which gives only distorted peaks for the redox process involving ferrocyanide/ferricyanide couple shows better electrochemical response when it is cycled in a 4mM solution of  $\text{Fe}(\text{CN})_6^{4-}$  after treatment with rf plasma (Fig. 3.14.b).

The plasma treatment is thus seen to be an efficient method for increasing the activity of electrodes modified with MPc.

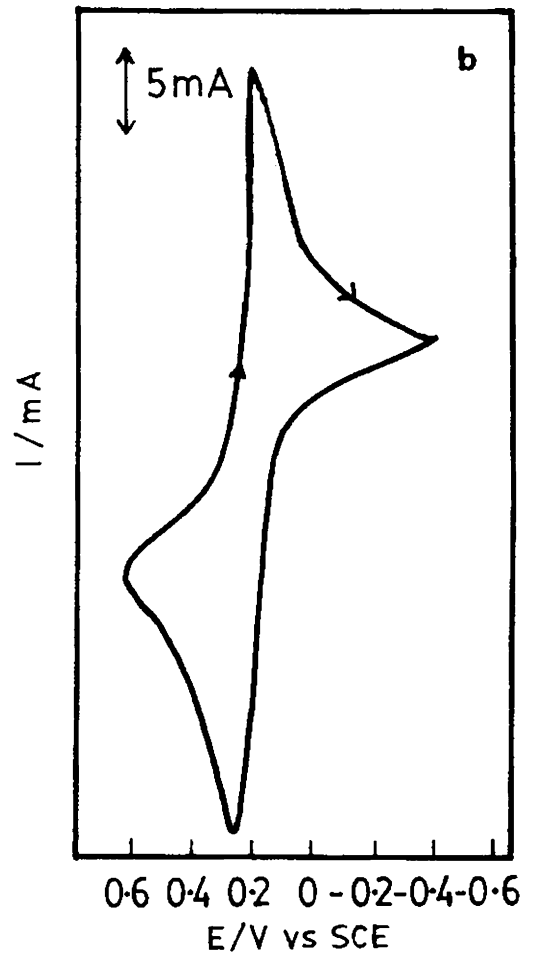
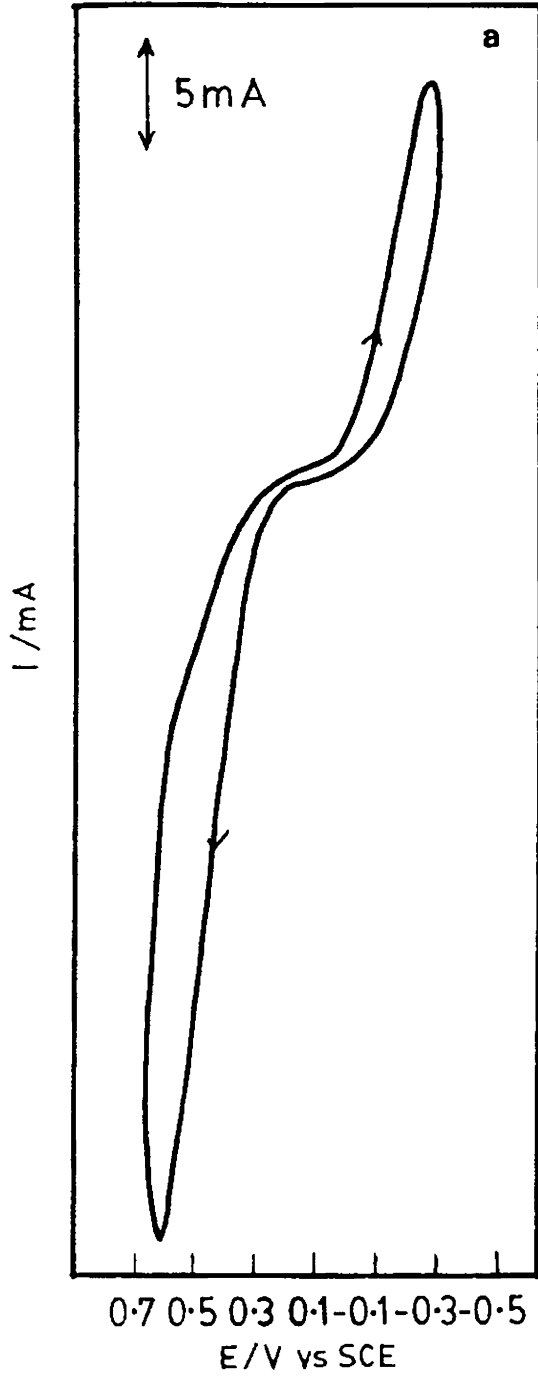
### 3.3.8 Reduction of DiOxygen at MPc Modified Electrodes

A good quantum of research has already been expended on the electrocatalysis of dioxygen reduction because of its use in fuel cells The electrocatalytic behaviour of Mpcs supported on carbon electrodes were studied because of the chemical diversity of carbon electrodes and the possible interaction of extended  $\Pi$ -electron system of phthalocyanine molecule with that of graphite. The type of mechanism for dioxygen reduction at graphite and platinum differ. We have examined the  $\text{O}_2$  reduction at platinum electrode coated with Mpc.

The electrocatalytic activity of MPc coated electrodes are found to be stable in basic media than in neutral or acid media. For a surface to be a good catalyst for the reduction of  $\text{O}_2$  it must not only facilitate the transfer of electrons but also actively decompose  $\text{H}_2\text{O}_2$ <sup>170</sup>. The over voltage for the reduction of  $\text{O}_2$  in alkaline medium is lower because an adsorbed oxygen film may be better maintained in such solutions and the electrode surface may act as a more effective  $\text{H}_2\text{O}_2$  - decomposition catalyst. Hence the electrocatalysis of  $\text{O}_2$  reduction by the MPcs was studied only in alkaline medium.

The  $\text{O}_2$  reduction wave was confirmed from the observation that the intensity of the peak decreases and then completely disappears on displacing  $\text{O}_2$  from the medium using  $\text{N}_2$  gas.

Fig. 3.16a shows the  $\text{O}_2$  reduction wave at a platinum electrode. At this electrode only an irreversible peak of low intensity occurs at  $\sim -0.6\text{V}$ . The response of  $\text{O}_2$  at a CoPc/Pt electrode is shown in Fig.



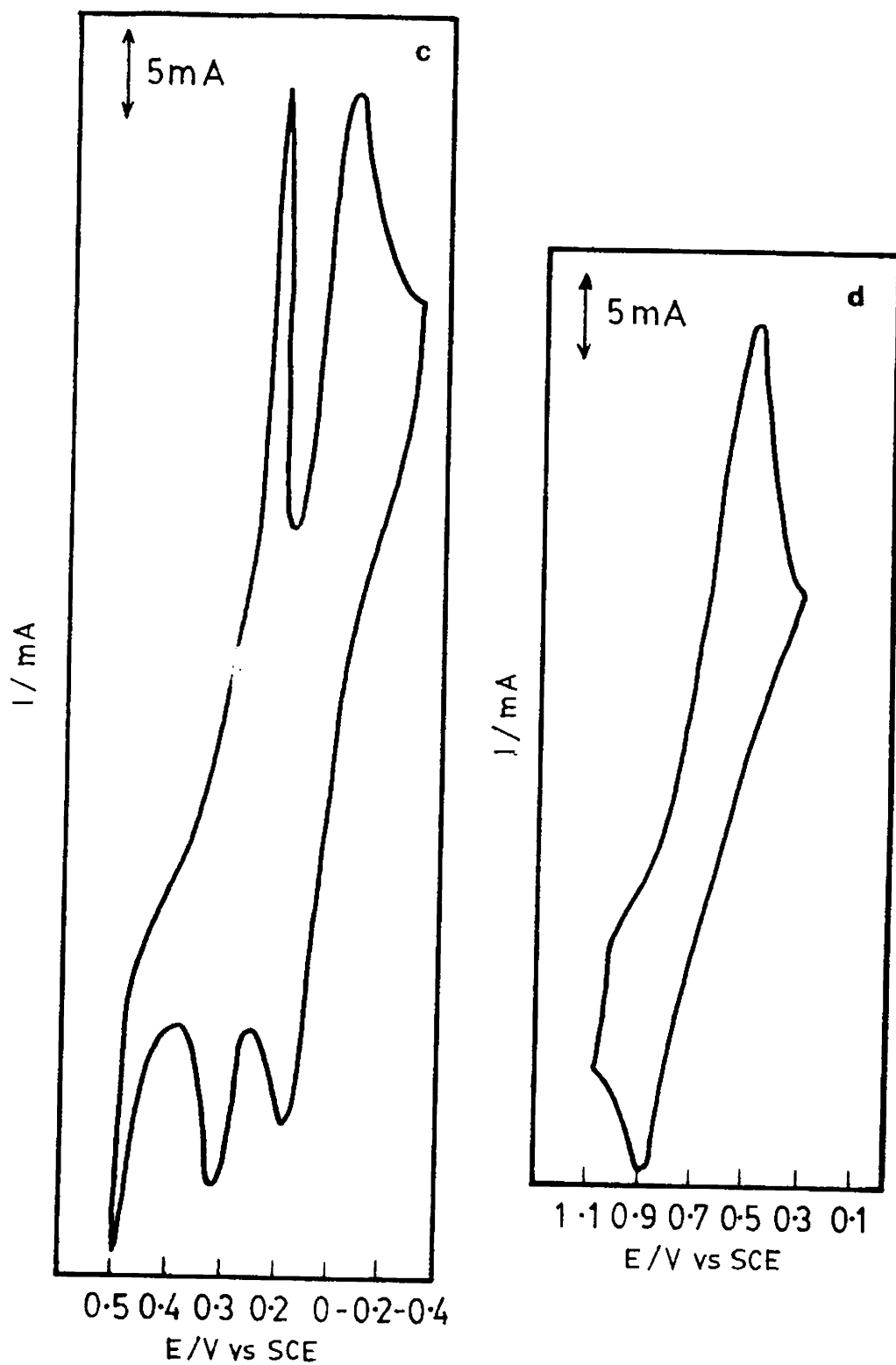


Fig. 3.12 Cyclic voltammetric behaviour of different redox species at plasma treated CoPc electrode

(a) Hydroquinone (b)  $Fe(CN)_6^{4-}$  (c) Fe-EDTA (d) Fe(o-phenanthroline)

Supporting electrolyte : 0.1M  $KNO_3$

Scan rate : 100mV/s

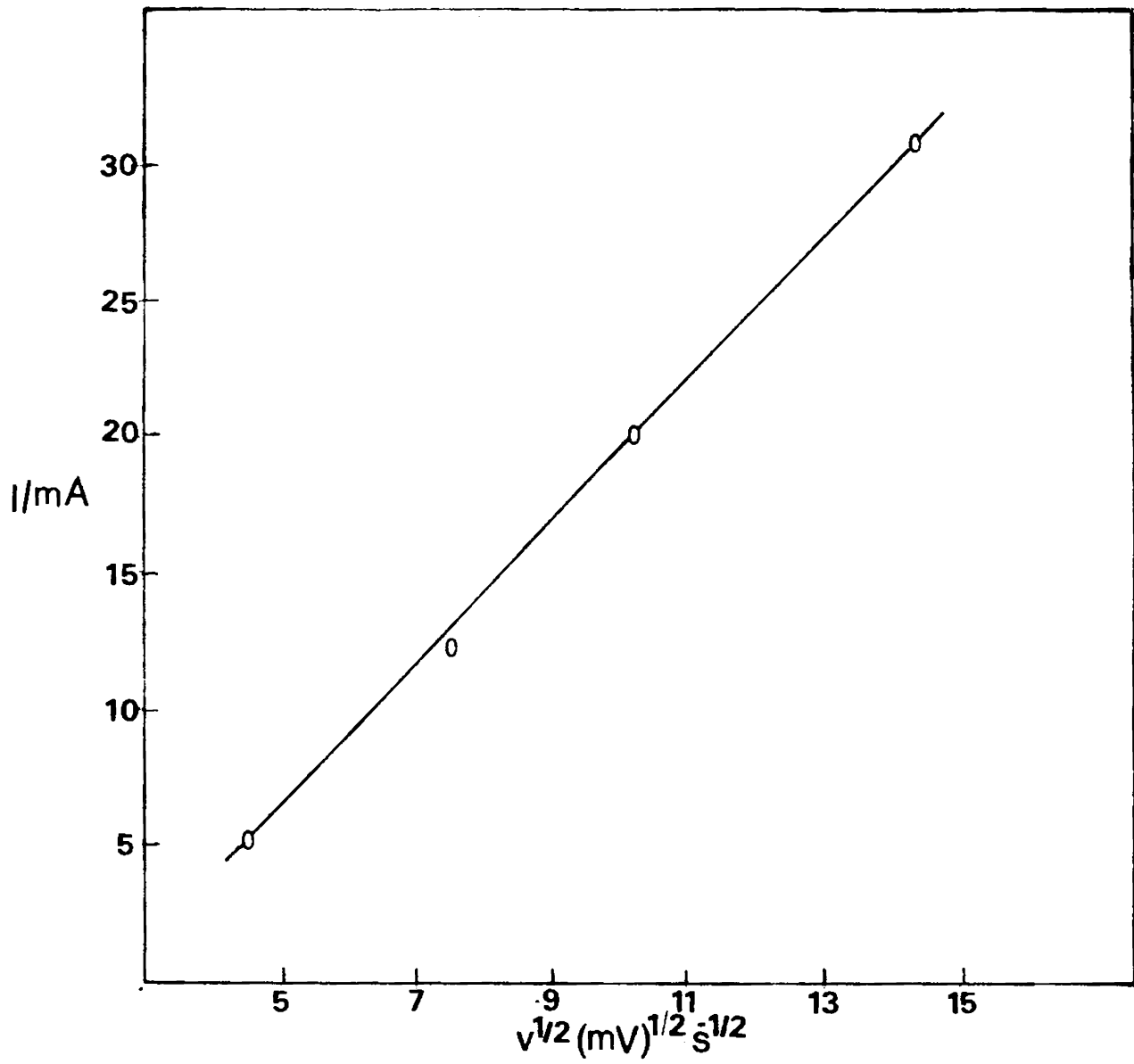


Fig. 3.13 Scan rate dependence of the anodic peak current at plasma treated CoPc electrode for the ferri/ferrocyanide redox couple in 0.1M  $\text{KNO}_3$

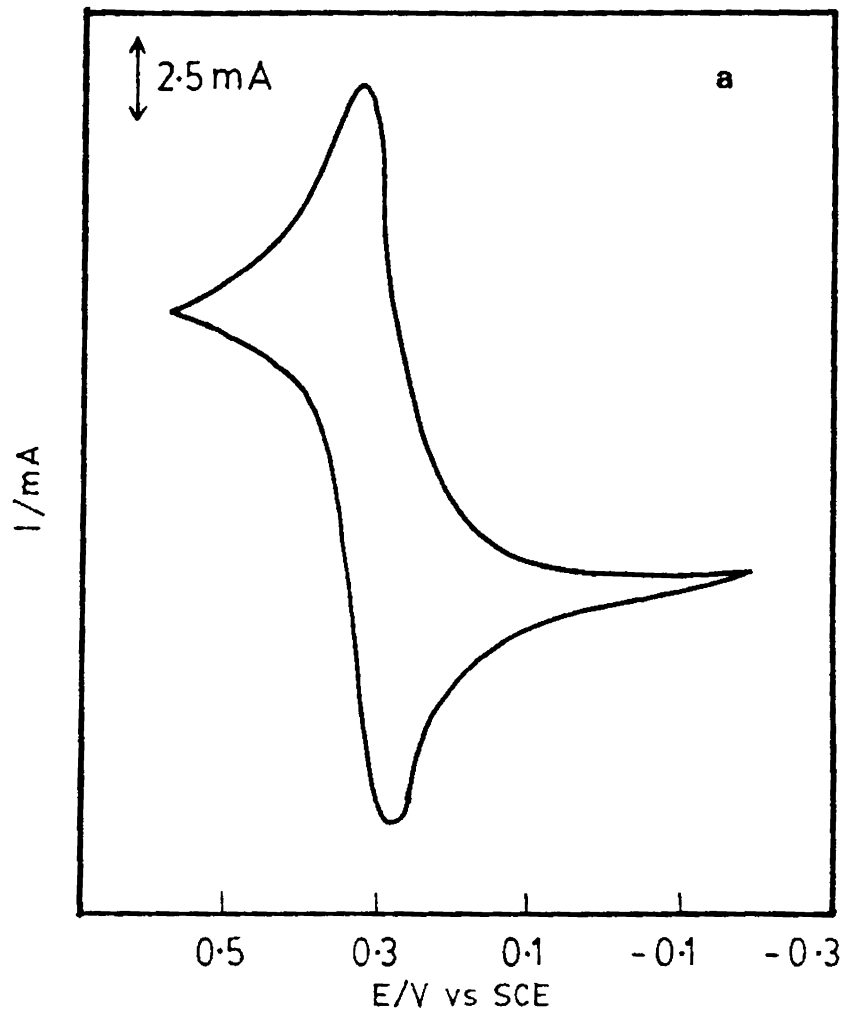
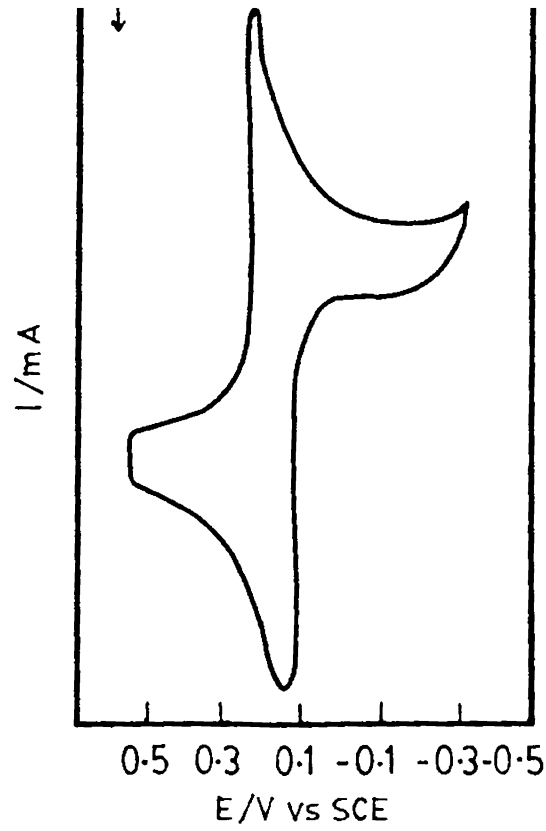
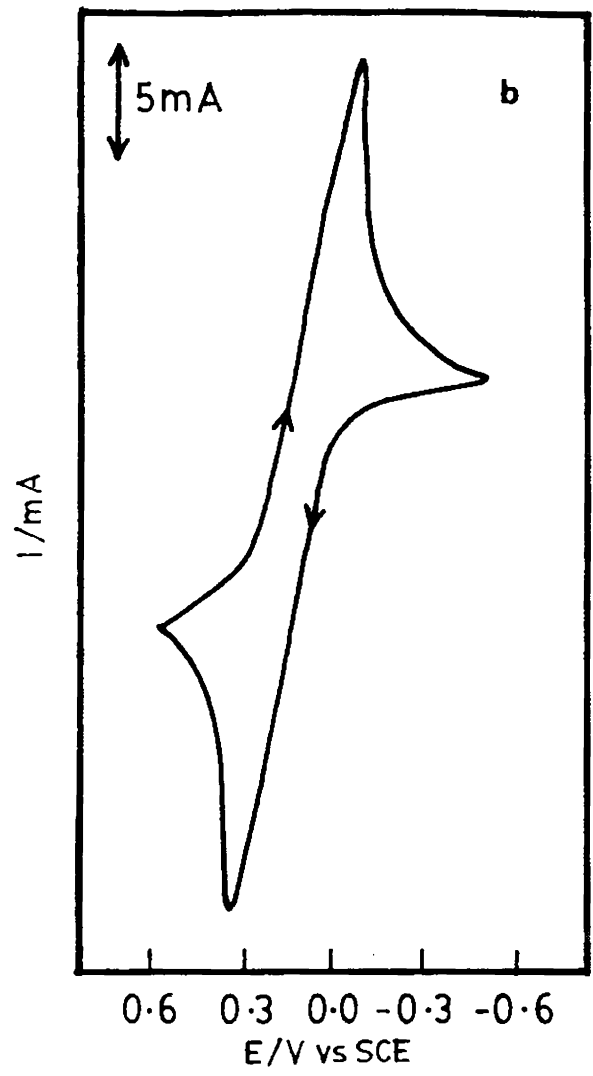
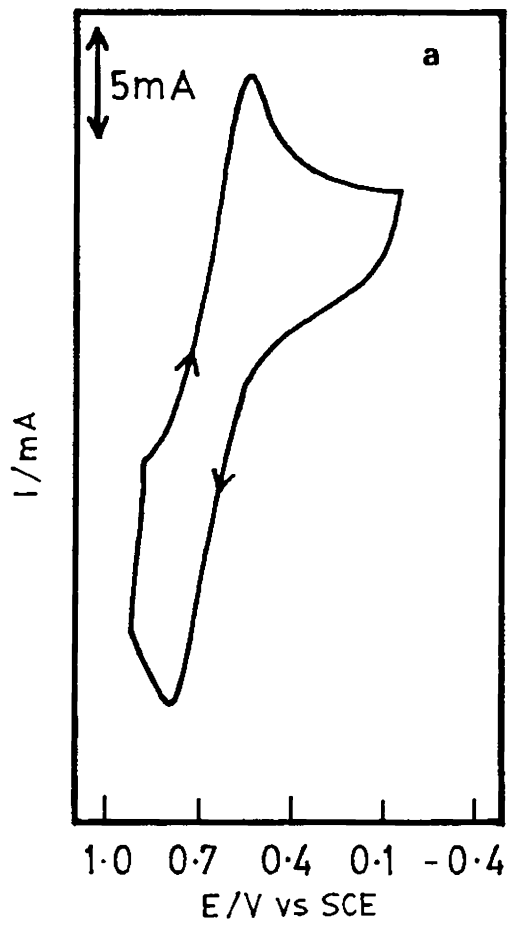


Fig. 3.14. Cyclic voltammogram of the  $\text{Fe}(\text{CN})_6^{4-}$  at  
 (a) Plasma treated ZnPc electrode      (b) Plasma treated CuPc electrode  
 supporting electrolyte : 0.1M  $\text{KNO}_3$   
 Scan rate : 100mV/s



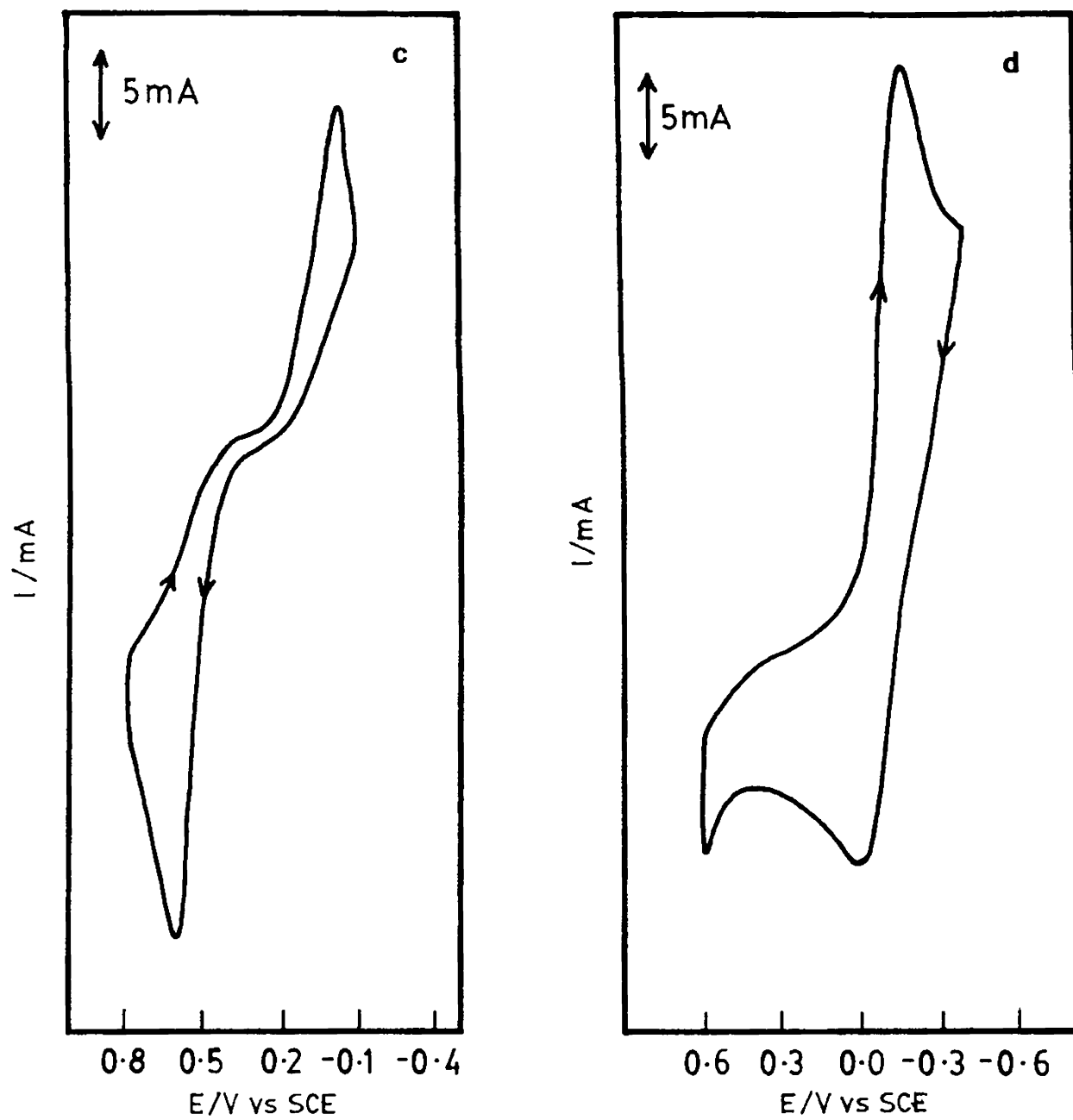


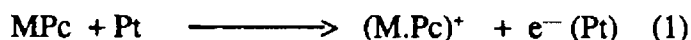
Fig. 3.15 Cyclic voltammograms of different redox species at plasma treated FePc electrode  
 (a) Fe(o-phenanthroline) (b)  $K_4 Fe(CN)_6$  (c) Hydroquinone (d) Fe-EDTA

3.16b  $O_2$  is catalytically reduced at a potential of 0.45V. The well resolved peak with enhanced peak current shows that CoPc exerts electrocatalytic activity for  $O_2$  reduction.

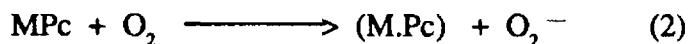
As shown in the Fig. 3.16c FePc reduces dioxygen at a still lower positive potential. The enhanced peak current and the ability of FePc to reduce  $O_2$  at a lower potential suggest that FePc is more effective than CoPc.

Dioxygen is also electrocatalytically reduced at ZnPc and NiPc at 0.45 and 0.40 respectively. (Fig. 3.16c — 3.16d). This is not in agreement with the reports of Faulkner et al <sup>117</sup> They have reported that  $O_2$  reduction was inhibited on ZnPc and FePc thin film (100-4000 Å) when these were deposited on a gold film overlaid on glass substrate.

The catalytic activity of metal phthalocyanine follows the order: FePc>CoPc>CuPc>NiPc>ZnPc. This order can be correlated with the electrooxidation potentials of these metal phthalocyanines as follows. The MPc molecule gets oxidised by donating an electron to the platinum working electrode according to the scheme:



When an  $O_2$  molecule gets reduced at the MPc, the MPc will donate an electron to the oxygen molecule according to the scheme:

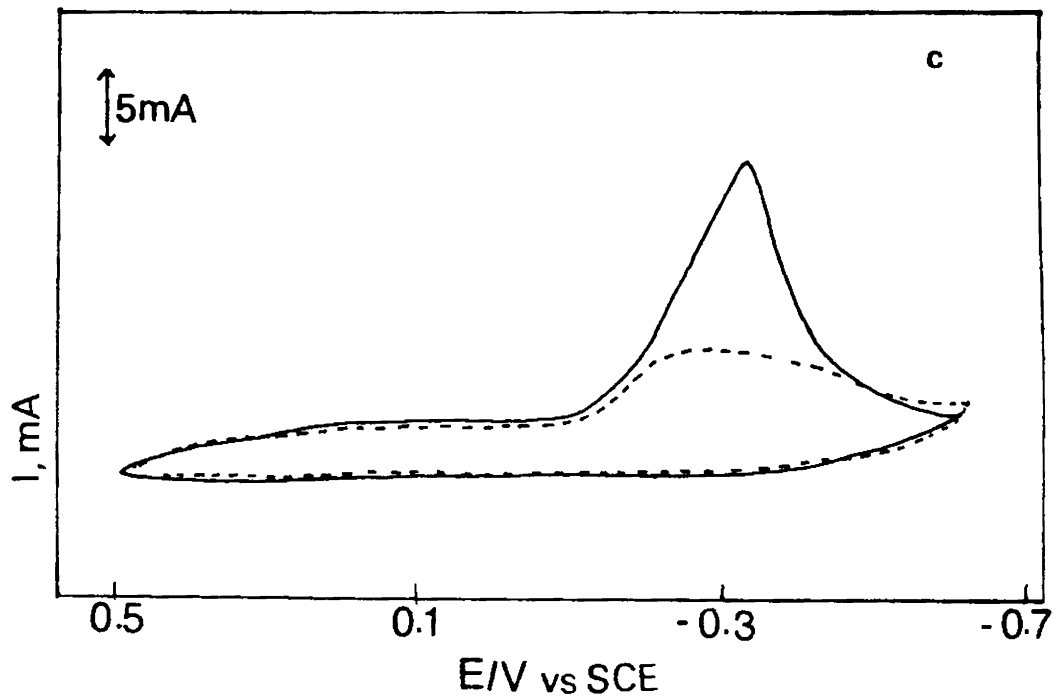
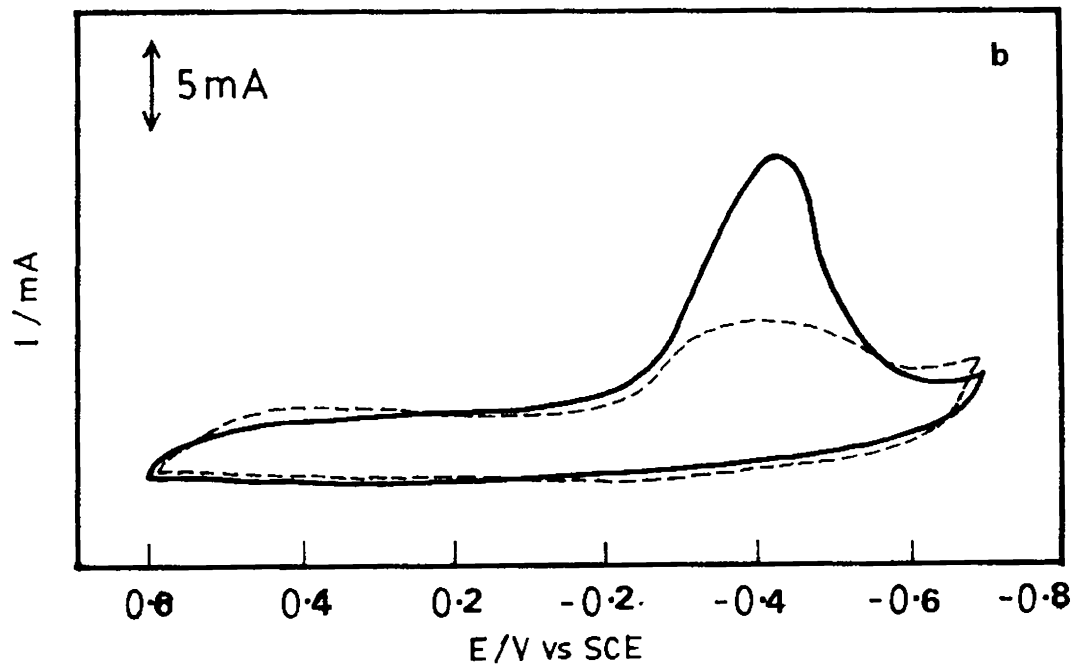
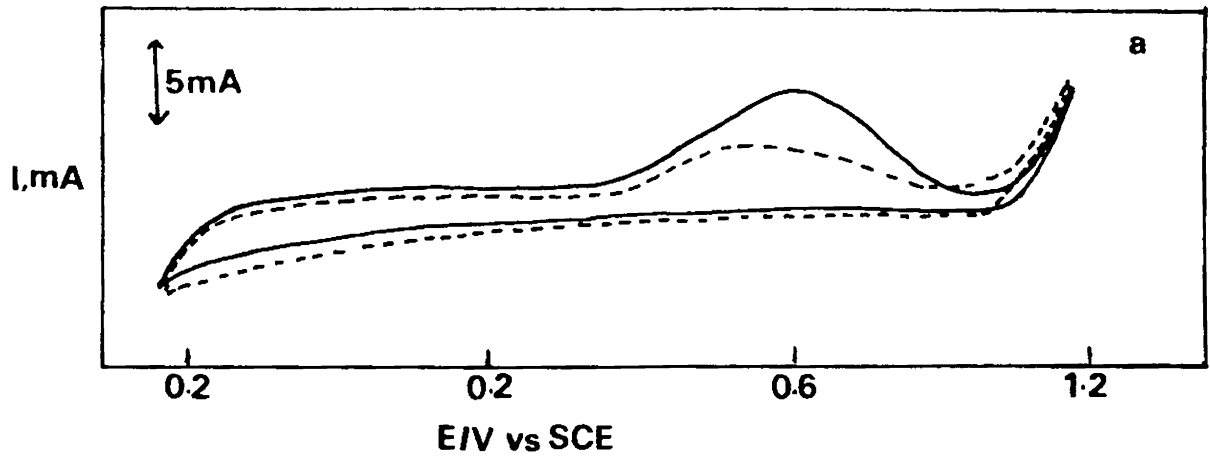


Reduction schemes (1) and (2) are analogous and each involves the donation of an electron by MPc to either Pt or  $O_2$ . It is clear that the first oxidation potential of MPc can be correlated with the catalytic activity for  $O_2$  reduction.

### 3.3.9 Electrocatalytic reduction of dioxygen by plasma-treated cobalt phthalocyanine

As a result of rf-plasma treatment, the electrocatalytic activity of MPc electrodes is increased. Fig. shows that  $O_2$  is reduced at -0.3V on CoPc electrode. The peak current is also enhanced. Other MPcs also show increase in electrocatalytic activity after exposing to plasma.

The heterogenous rate constant for  $O_2$  reduction at MPc electrodes and rf-plasma treated with MPc electrodes are given in Table II



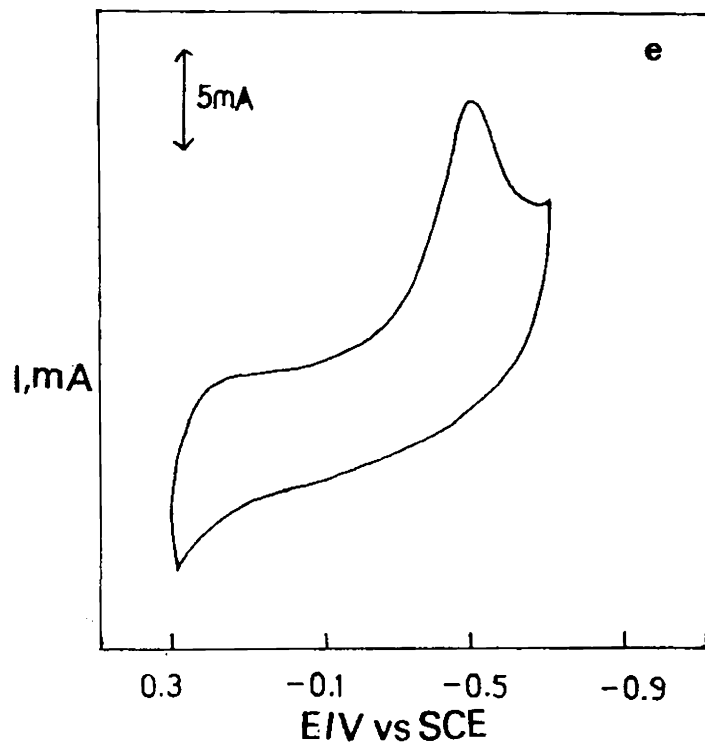
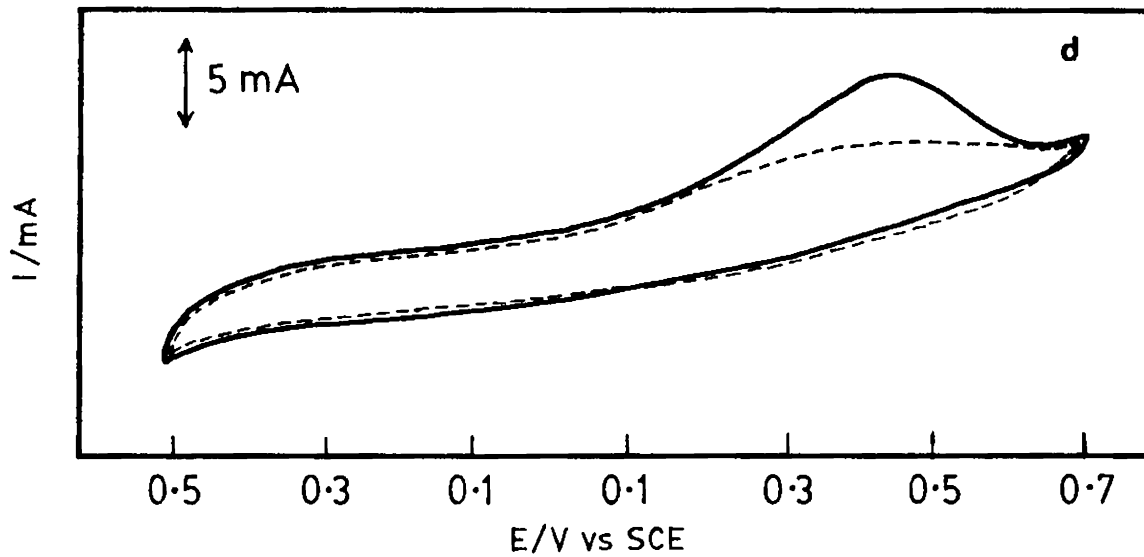


Fig. 3.16 Cyclic voltammogram showing the reduction of  $O_2$  at different electrodes.

(a) Pt (b) CoPc (c) FePc (d) ZnPc (e) NiPc

(—)  $O_2$  saturated (- -)  $N_2$  saturated

Supporting electrolyte : 0.1M  $KNO_3$

Scan Rate : 100mV/s

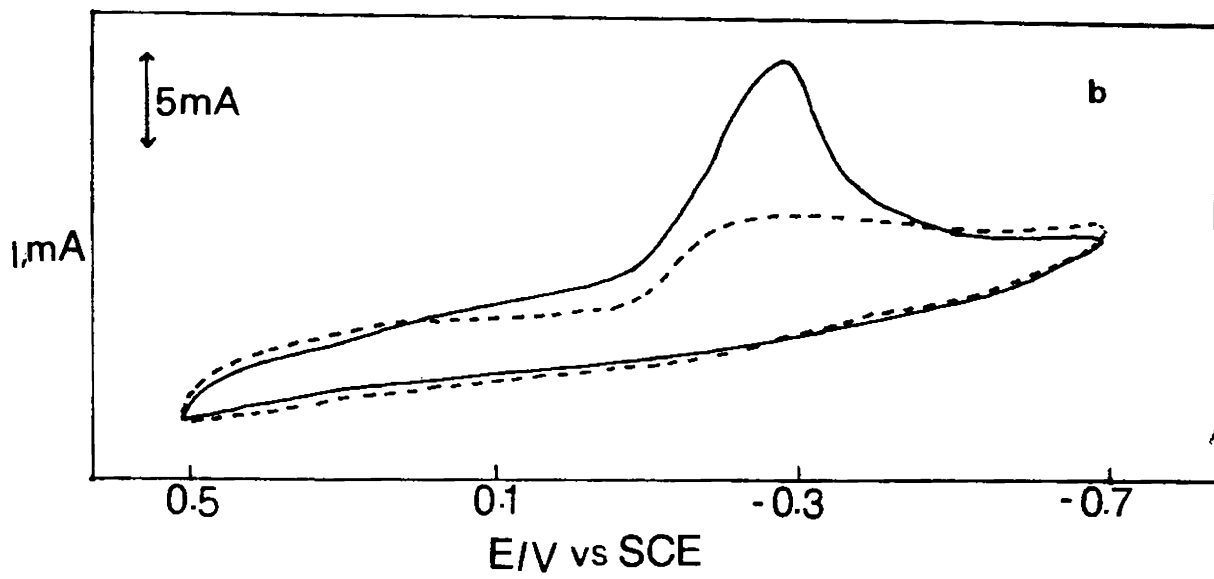
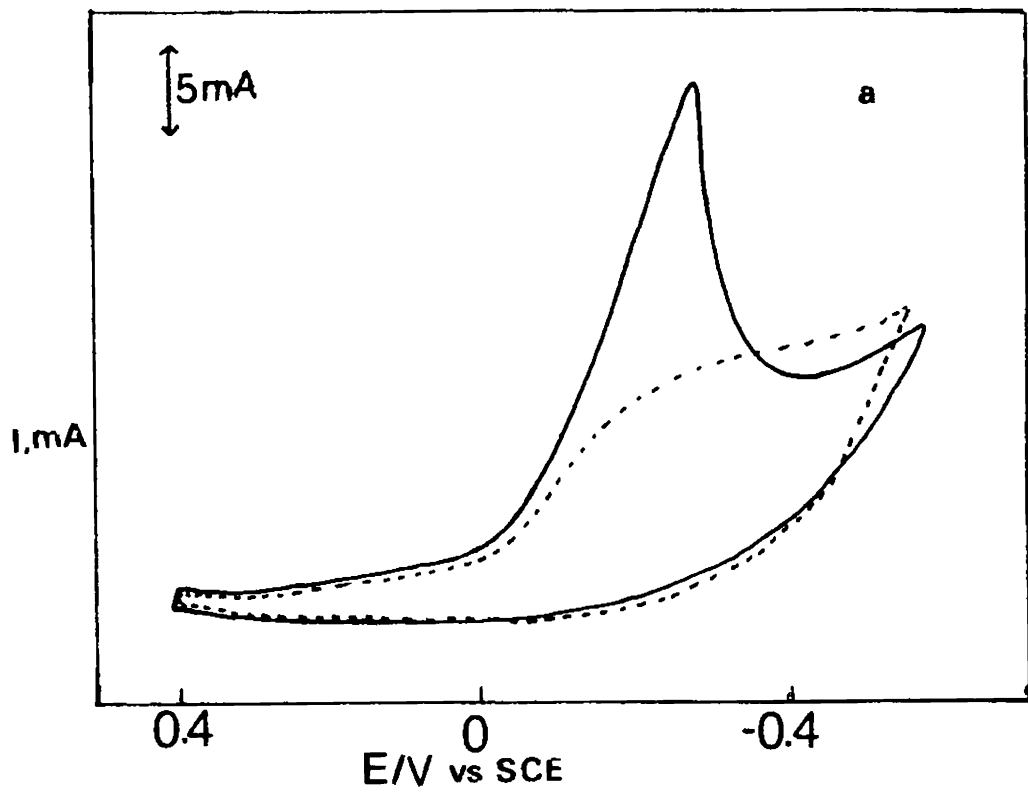
**Table I**  
**Peak Potentials for the reduction and oxidations of different redox species at different electrodes.**

Electrode	Compounds							
	Fe-EDTA		Fe(CN) <sup>3-</sup> <sub>6</sub>		Fe(o-ph) <sup>2+</sup> <sub>3</sub>		H <sub>2</sub> O	
	Ep,a	Ep,c	Ep,a	Ep,c	Ep,a	Ep,c	Ep,a	Ep,c
Platinum	-0.08	0.26	0.23	0.25	0.80	0.82	0.57	0.19
FePc	-0.08	0.18	0.29	0.08	0.82	0.70	0.69	0.11
FePc <sub>rr</sub>	-0.02	-0.32	0.31	0.21	0.78	0.42	0.55	-0.12
CoPc	-0.12	-0.04	0.31	0.22	0.88	0.68	0.59	-0.1
CoPc <sub>rr</sub>	-0.08	0.18	0.24	0.21	0.87	0.49	0.62	-0.31
NiPc	-0.07	0.19	0.24	0.08	0.86	0.88	0.59	-0.28
ZnPc	-0.16	-0.03	0.24	0.09	0.86	0.44	0.58	0.16

Electrode	Compounds							
	FeEDTA		Fe(CN) <sup>3-</sup> <sub>6</sub>		Fe(o-Ph) <sup>2+</sup> <sub>3</sub>		H <sub>2</sub> O	
	$\Delta E_p^c$	$\Delta E_p^f$	$\Delta E_p^c$	$\Delta E_p^f$	$\Delta E_p^c$	$\Delta E_p^f$	$\Delta E_p^c$	$\Delta E_p^f$
FePc	0.34	0	0.02	0.06	0.76	0.02	0.38	0.08
FePc <sub>rr</sub>	0.30	-0.06	0.10	0.08	0.36	0.02	0.67	0.02
CoPc	0.08	0.04	0.09	0.08	0.2	0.08	0.69	0.02
CoPc <sub>rr</sub>	0.26	0	0.04	0.01	0.47	0.07	0.94	0.05
NiPc	0.26	0.01	0.16	0.01	0.02	0.06	0.87	0.02
ZnPc	0.13	0.08	0.15	0.01	0.42	0.06	0.42	0.01

$\Delta E_p^c$  Difference between anodic and cathodic peak potentials

$\Delta E_p^f$  Difference in anodic peak potentials on Pt and the MPc electrode



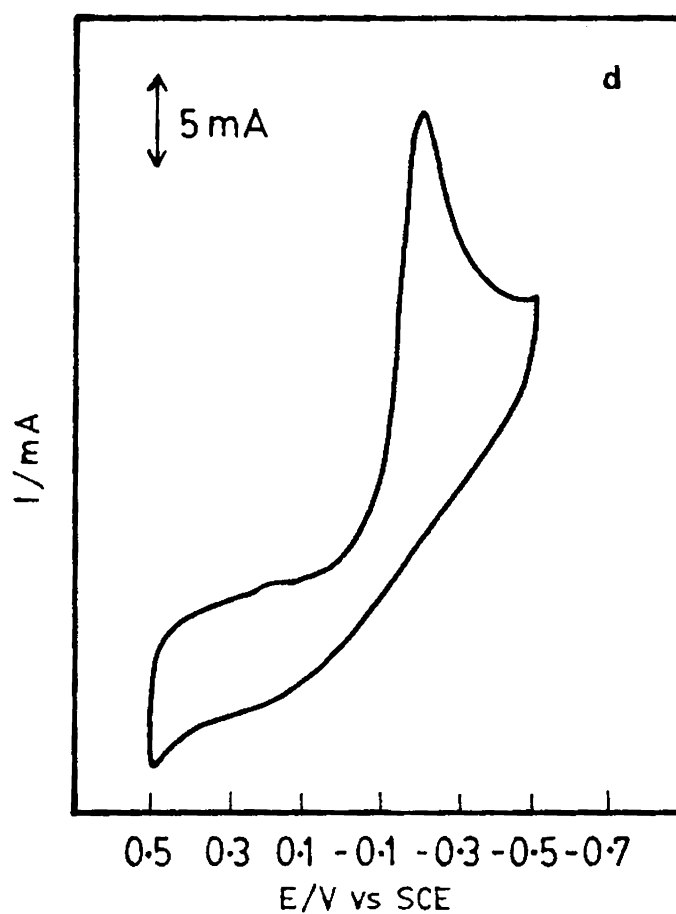
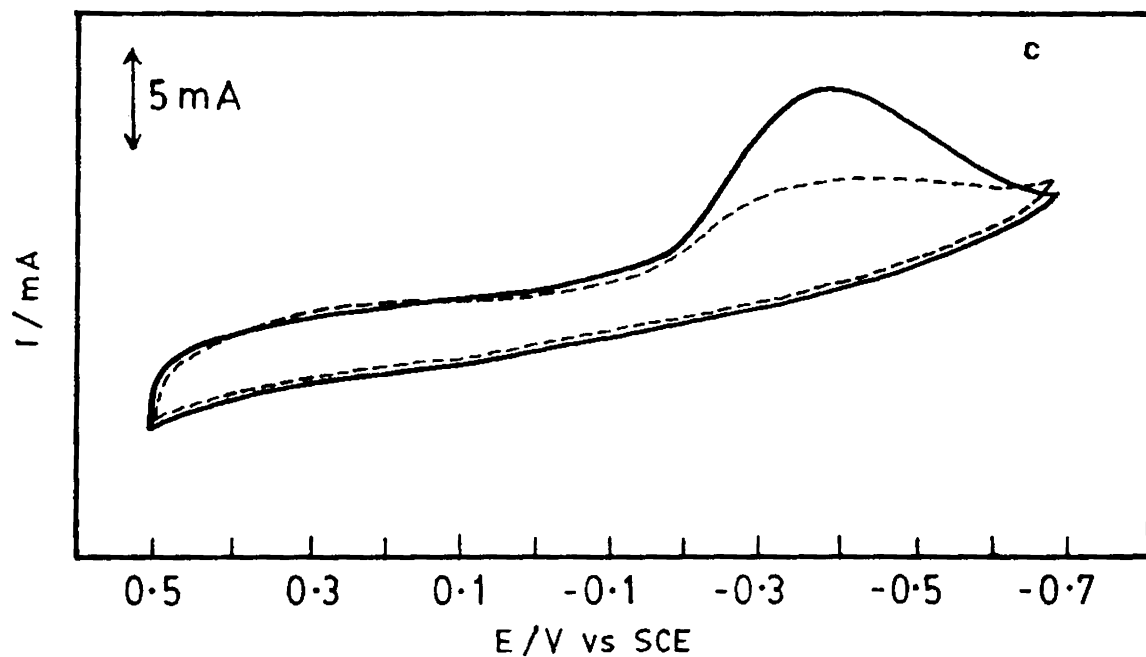


**Fig.3.17** Cyclic voltammetric response of the reduction of  $O_2$  at plasma treated MPc electrodes  
 (a) CoPc (b) FePc (c) ZnPc (d) NiPc  
 (—)  $O_2$  saturated (...)  $N_2$  saturated  
 Supporting electrolyte : 0.1M  $KNO_3$   
 Scan Rate : 100mV/s

**TABLE II****Heterogenous Rate Constant for the Reduction of O<sub>2</sub> at Various Electrodes.**

Electrode	Heterogeneous Rate constant cm sec <sup>-1</sup>	
	Before plasma treatment	After plasma treatment
Platinum	$2.5 \times 10^{-17}$	————
FePc	$3.548 \times 10^{-8}$	$1.61 \times 10^{-7}$
CoPc	$2.042 \times 10^{-12}$	$5.495 \times 10^{-7}$
NiPc	$2.39 \times 10^{-13}$	$1.61 \times 10^{-7}$
ZnPc	$1.312 \times 10^{-13}$	$2.239 \times 10^{-9}$

# CHAPTER IV

## Electrical conductivity of metal phthalocyanines

### 4.1 Introduction

Eley and Vartanyan <sup>170,171</sup> were the first to observe semiconductivity in phthalocyanines (Pc). With intrinsic semiconductivity the current carriers are mobile  $\Pi$ -electrons. The temperature dependence of the conductivity follows the relation

$$\sigma = \sigma_0 \exp (-E_a/kT)$$

where  $\sigma$  = specific conductivity at temperature T in  $\text{Scm}^{-1}$

$\sigma_0$  = specific conductivity at infinite temperature

$E_a$  = activation energy and R = gas constant

The electrical conductivity increases markedly with increasing pressure at constant temperature and with increasing temperature at constant pressure <sup>172</sup>.

Electrons are not excited to the conduction band, but rather they are trapped at impurity centres or crystal imperfection leaving positive holes.

Replacement of the two central hydrogen atoms by a metal atom has little effect upon the energy gap which lies between 1.5 to 1.7 eV and is sensitive to the atmosphere surrounding the sample. The electrical conductivity of single crystals of metal free, copper, nickel and cobalt phthalocyanines were measured in the temperature range 50-390° C. <sup>173</sup>. The weighted mean values of the activation energies obtained were: 1.71 eV for the metal free, 1.60 eV for the cobalt and nickel and 1.64 eV for the copper substituted compounds.

The changes in the crystal habit at  $\alpha - \beta$  phase transformation temperature of phthalocyanine, and appreciable anisotropy effects seriously impair the significance of the data which fail to take these fully into account. <sup>174</sup>

The resistivities of metal phthalocyanines are lower than that of metal free Pc. CuPc shows the highest, and the Mg and Mn Pcs show the lowest resistivity values. The substitution may create a greater overlap between parallelly aligned molecules; the copper atom acts as a bridge between nitrogen atoms on the molecules on the stack.

A considerable drop in resistivity as well as in activation energy is obtained upon changes in the peripheral part of the phthalocyanine ring system. <sup>175</sup>

A study of the effects of high pressure and the combined effects of high pressure and shear deformation on the electrical conductivity of MPcs show a sharp increase in conductivity at a critical pressure which depended on the electrode coating (Zn, Cu, or Ni). This increase is attributed to the onset of carrier injection. Under combined pressure and deformation the increase occurred at lower pressures also.

Electrical conductivity in Pcs is associated with thermal and/or optical excitation of the mobile carriers of the phthalocyanine ring from the valence band containing highest molecular orbital to the conduction band made of lowest empty molecular orbitals.

## Doping in MPcs

The effect of doping on the electrical and photoconductivity of molecular solids is well known. The electrical and photoconductivity of phthalocyanines is also found to be increased by the addition of dopants like *o*-chloranil<sup>177</sup>. Based on the ESR measurements, this change is ascribed to the transfer of electron from Pc to the acceptor molecules in the dark, which produces holes in the Pc layer and converts *o*-chloranil to its anion radicals. When the Pc film is doped with 2,4,7 trinitrofluorenone (TNF)<sup>178</sup> the carrier generation efficiency increases with increase in TNF concentration while its fluorescence is quenched. This is explained as resulting from the singlet exciton diffusion to the surface of the Pc at the dopant site, followed by the exciplex formation and its subsequent dissolution into charge carriers. The electronic process in molecular solids are complicated and their interpretation require molecular level consideration.<sup>179,180</sup> A study of the doping effect on the organic semiconductors gives a clue to the electronic processes such as charge carrier generation upon irradiation, the process being essential in photosynthesis and in solar energy conversion.<sup>181</sup>

The optoelectronic properties of materials can be modified by depositing phthalocyanines on these materials. The photo induced charge injection from metal-free phthalocyanine has been used to photosensitize amorphous selenium in xerographic applications. The low intrinsic conductivity of phthalocyanines limits further exploitation of their optoelectronic properties. However by doping with iodine, the conductivity of phthalocyanines can be markedly increased<sup>184,185</sup>. Because of the high stability of  $I_3^-$  in polar environments, and its ability to accommodate itself into channels in one dimensional lattices, iodine is an advantageous dopant for the oxidation of planar organic molecules. (Oxidation of a divalent metal complex would yield a trivalent metal ion if  $I^-$  were produced, but a nonintegral oxidation state would result if all metal sites in the material were crystallographically equivalent and if only  $I_3^-$  were formed.) The utility of this synthetic approach is applied to phthalocyanines<sup>186</sup>. This results in an extensive new class of highly conducting molecular solids. The oxidation of purified Fe, Co, Ni, Cu, Zn, Pt phthalocyanines and metal-free phthalocyanine by iodine vapour or solutions results in dark colored solids with a range of stoichiometries<sup>187</sup> (equation 1), the exact composition obtained depending on the conditions.



where M = Fe, Co, Ni, Cu, Zn, Pt, H<sub>2</sub>.

A number of chemical methods have been reported on the preparation of iodized metal phthalocyanines. Doping can be done from liquid phase and vapour phase. In the former case a known weight of the Pc is stirred with iodine in CCl<sub>4</sub> for 24-48 hours. Iodine can also be doped by its sublimation and allowing the vapour to diffuse into films of phthalocyanine.

Phthalocyanines of Al, Ga and Cr fluorides were prepared and doped with iodine to give (Pc MFI) complexes [x = 0.012-3.4 (M= Al), 0.048-2.1 (M = Ga) and 0.12-3.3 (M =Cr)]<sup>188</sup>. Thermogravimetric analysis showed that complete loss of iodine occurs at < 250° C leaving a PcMF residue. Iodine doping results in increase in electrical conductivity by factors as high as 10<sup>9</sup> with the highest conductivity 5-Ω-1 cm<sup>-1</sup> being observed for (PcAlFI<sub>3.4</sub>)<sub>n</sub> derived from sublimed ((PcAlF)<sub>n</sub>). An apparent activation energy for conduction of 0.17 eV was observed for (PcAlFI<sub>3.4</sub>)<sub>n</sub>.

Nickel phthalocyanine iodide, NiPcI found earlier to exhibit metal like conductivity at temperatures above ca 50K is shown to be the first molecular crystal that has a high asymptotic low

temperature conductivity  $\sigma \rightarrow$ , 250-1000  $\Omega \text{ cm}^{-1}$  as  $T \rightarrow$  OK, yet contains neither halogen mediated, nor indeed any apparent pathways for strong interactions<sup>189</sup>. This compound is also the first low temperature molecular metal based on a metal organic complex. The complex formed by NiPc can be indicated as  $\text{NiPcI}_x$  where  $x < 3$ . Mossbauer studies on this material suggests that iodine is present only as  $\text{I}_3^-$ ; negligible amount of  $\text{I}_2$  and  $\text{I}^-$  are present<sup>190</sup>. This type of one dimensional conductors are different from simple organic charge transfer complexes. Transition of one electron from donor to acceptor leads to the formation of cation and dianion radical, which stack together in alternating layers. The conductivity of charge transfer complexes are extremely sensitive to impurities. The single crystals of doped NiPc shows metal like conductivity ( $0.7\text{-}0.8 \Omega^{-1} \text{ cm}^{-1}$ )

But at low temperature, e.g. 50K these compounds undergo metal to semiconductor transition. This phenomenon is common to all one dimensional conductors<sup>191</sup>.

$\text{NO}(\text{BF}_4)$  or  $\text{NO}(\text{PF}_6)$  were used to oxidize the stacked, F-bridged metal Pcs ( $\text{PcMF}_x$ ) ( $M = \text{Al}$  or  $\text{Ga}$ ). The oxidized products give pressed pellet conductivities  $< 0.3 \text{ ohm cm}$ . These materials are stable for months in air and only begin to decompose in vacuum at  $> 115\text{-}125^\circ \text{C}$ . No unpaired spins were observed in the neutral polymers but the oxidized products have highly mobile electrons with the spin densities of 0.003-0.3e/anion.

Recently two-channel conductivity and carrier crossover in (phthalocyaninato) nickel iodide and (phthalocyaninato) cobalt iodide is reported<sup>191</sup>. These complexes were shown to be homogeneous solid solutions by EPR and energy-dispersive Xray microprobe analysis. Though the crystals of  $\text{Co}(\text{Pc})\text{I}_x$  ( $x=1$ ) and  $\text{NiPcI}_x$  ( $x=0$ ) are isostructural with metal-over-metal columnar stacks of partially one-third oxidized  $M(\text{Pc})$  units surrounded by chains of  $\text{I}_3^-$  counter ions, the charge transport in these complexes is different. The latter has a high room-temperature conductivity and exhibits metallic behaviour. The conductivity of  $\text{CoPcI}$  at room temperature is about one-tenth that of  $\text{Ni}(\text{Pc})\text{I}$  and is nonmetallic, decreasing continuously on cooling. These differences arise from the difference in the site of partial oxidation<sup>192</sup>. The oxidation of  $\text{CoPc}$  is metal centered and  $\text{CoPcI}$  is metal-spine conductor whose carriers are electrons (negative thermopower) in a less-than-half-filled band associated with the cobalt  $d_{z^2}$  orbitals. In contrast, oxidation of  $\text{NiPc}$  is ligand centred and  $\text{NiPcI}$  is an organic conductor whose carriers are holes (positive thermopower) associated with a band made up of the  $\Pi$  HOMO of the macrocycle. As the percentage of  $\text{CoPcI}$  is increased from  $x=0$  in the alloys,  $\text{Co}_x\text{Ni}_{1-x}(\text{Pc})\text{I}$  there is a smooth change from the highly conducting metallic behaviour of  $\text{NiPcI}$  to the nonmetallic behaviour of  $\text{CoPcI}$  ( $x=1$ ).

#### 4.1 Introduction

Metal phthalocyanines undergo a phase transition ( $\alpha \rightarrow \beta$ ) on heating and this transformation is accompanied by change in its electrical conductivity. The electrical conductivity in MPc can be enhanced by doping. The high electrical conductivity associated with iodine-doped MPc ( $\text{MPcI}$ ) is attributed to the induction of partial oxidation state in the phthalocyanine moiety or the central metal atom.

In this chapter the results of the studies on the temperature dependent electrical conductivity in  $\text{CoPc}$ ,  $\text{FePc}$  and  $\text{ZnPc}$  and their iodine doped forms are discussed. The behaviour of iodine doped MPc modified electrodes with emphasis on their electrocatalytic activity is also discussed. Since  $\text{CoPc}$  has a molecular structure in which the central metal atom or the phthalocyanine moiety can undergo doping induced oxidation. The nature of the transformation occurring in  $\text{CoPc}$  is studied using DSC, IR, EPR and solid state electronic spectra. Investigations were also carried out on the

influence of thermal annealing on the electrical conductivity and electrocatalytic activity of CoPc.

## **4.2 Experimental**

### **4.2.1 Preparation of CoPcI, FePcI and ZnPcI**

The metal phthalocyanines were prepared and characterised as described in section 2.1 Iodine (resublimed), Merck, India was used without further purification.

A sample of finely powder MPc (0.2g.) was stirred with a saturated solution of iodine in dry carbon tetrachloride for 24 h. It was then filtered and washed several times with  $\text{CCl}_4$  till the filtrate was free from iodine. The doped material was dried in a desiccator and stored in stoppered glass bottles.

Doping was also done by exposing the MPc coated electrode to iodine vapour. As a result of doping the MPcs turned dark in colour. The amount of iodine doped was determined from the increase in weight of the sample.

### **4.2.2 Characterisation of MPcI**

#### **(a) Magnetic Susceptibility Measurements**

Static susceptibility was measured using a gouy balance. Mercuric thiocyanate complex was used as calibrant.

#### **(b) Electron Paramagnetic Resonance Measurements**

EPR spectra at 9.5 GHz were obtained on a modified varian E-4 X-band spectrometer at ambient temperature.

#### **(c) Infrared Spectra**

The infrared spectra were recorded using Perkin Elmer PE 983 IR spectrophotometer or polytech FIR-30 Fourier Far IR Spectrometer.

#### **(d) Electronic Spectra**

The electronic spectra was recorded using Hitachi Model 340 UV-vis spectrophotometer.

### **4.2.3 Measurement of Conductivity**

A cell with two electrode configuration was used for measuring electrical conductivity. Powdered samples were pressed at  $750 \text{ kg cm}^{-2}$  to form 12mm dia pellets. Electrical contacts were provided with pressed silver discs and the measurements were made in dynamic air. Temperature of the sample pellet was monitored using a calibrated chromel-alumel thermocouple positioned very close to the sample. Applied voltage was given from a potentiostat. The measuring circuit is shown in Fig. 4.1 The heating rate was controlled at  $10^\circ \text{ C/min}$ .

Measurements were made by maintaining constant potential across the electrodes and continuously recording the current. The conductivity was calculated using the relation  $\sigma = id/AV$

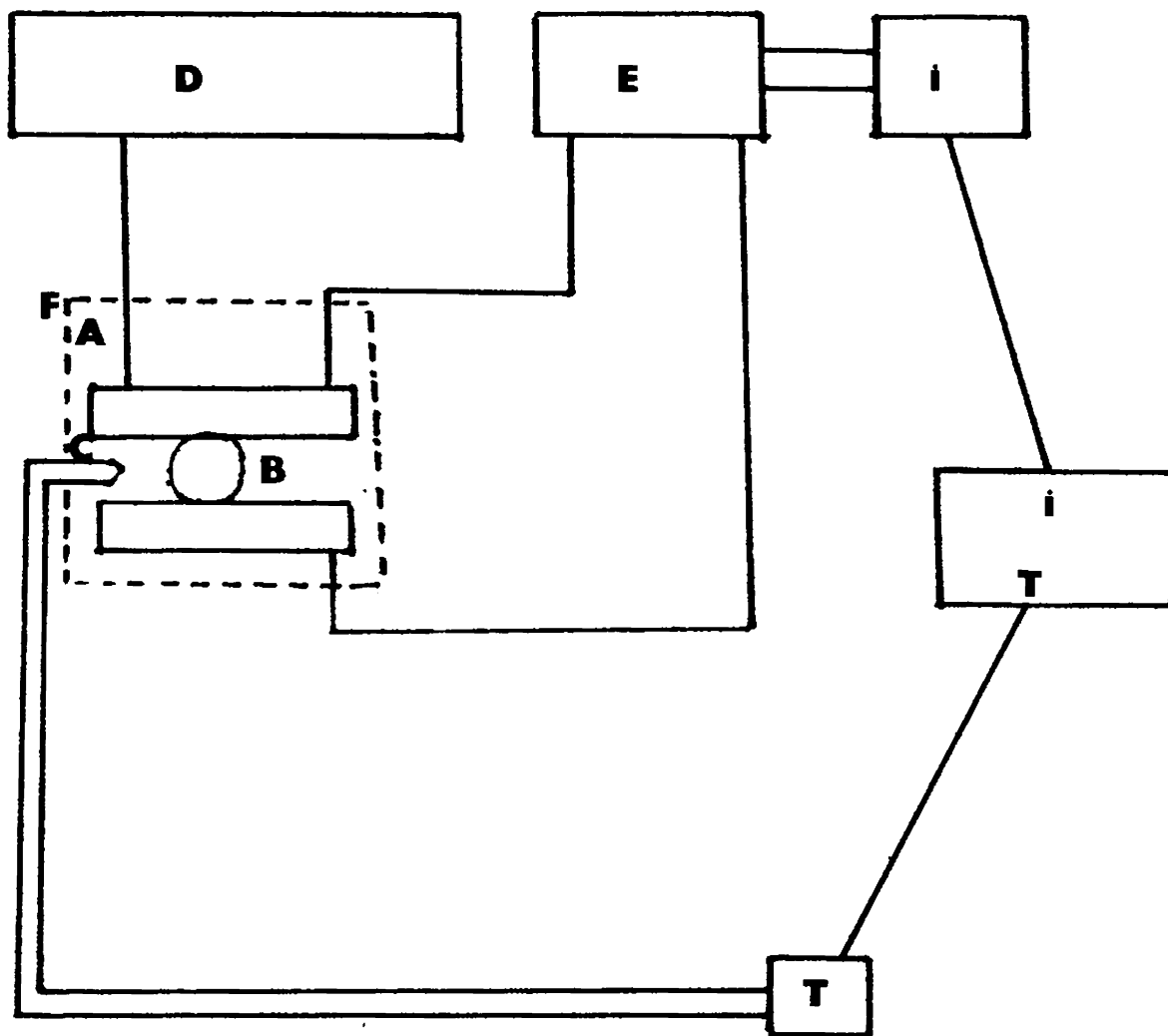


Fig. 4.1 Block diagram showing the measurement of conductivity.

A: conductivity cell B: Sample C: Thermocouple D: Potentiostat E: Electrometer F: Furnace

where  $\sigma$  is the conductivity in  $S\text{ cm}^{-1}$ ,  $i$  is the current in amperes,  $A$  is the area of the pellet in  $\text{cm}^2$  and  $V$  is the applied potential in volts.

#### 4.2.4 Cyclic Voltammetry

The cyclic voltammetric experiment were done in an undivided cell using graphite modified with MPc as the working electrode, platinum foil (10mm X 10mm) as counter electrode. The MPc coated electrodes were prepared by applying a known volume of the MPc solution in DMF on the graphite electrode and slowly evaporating off the solvent. This was repeated a number of times. The investigations were carried out in the supporting electrolytes mentioned in the corresponding sections.

### 4.3 RESULTS AND DISCUSSION

The conductivity increases with increase in the ratio of the dopant and reaches a saturation value at 12% w/w of iodine in MPc. Fig.4.2 gives the concentration dependent of iodine on conductivity of CoPc. After the uptake of about 0.6 equivalents of iodine per mole of CoPc, the conductivity remains steady.

Fig.4.2 shows the plot of  $\log \sigma$  vs  $1/T$  (K) plot for CoPc in air. The conductivity increases as the temperature increases upto  $170^\circ\text{C}$ . The activation energy for the conduction process evaluated from the Arrhenius plot is 1.53 eV. Beyond  $170^\circ\text{C}$  the conductivity decreases. This plot is not retraced in the cooling cycle indicating that the reversal of phase transformation is either very slow or does not takes place.

Fig.4.4 gives the  $\log \sigma - 1/T$  plot for the iodine doped CoPc (CoPcI). The electrical conductivity increases by about seven orders of magnitude. The iodine is not desorbed when exposed to air. In addition to the enhanced electrical conductivity, the transition temperature is lowered by doping, but the shape of the  $\log \sigma$  vs  $1/T$  plot remains the same. The activation energy for conduction process in the temperature range  $50^\circ$  to  $180^\circ\text{C}$  is 0.13 which is lower than the value in undoped sample.

An interesting observation is that CoPc as such is insoluble in acetone, but the iodine doped CoPc is partially soluble in acetone. The acetone soluble portion has a visible spectrum which matches with that of undoped CoPc. This dissolution is similar to the doping and simultaneous dissolution of polymeric semiconductors described by Frammer.<sup>193</sup>

The interaction of iodine with CoPc results in the formation of a CT - complex. The CoPcI so formed consists of partially oxidised CoPc moiety. The conductivity of CoPcI is nonmetallic, decreasing continuously on cooling. The transformation occurring in CoPcI is established using IR, electronic and ESR spectra, magnetic susceptibility and DSC.

#### 4.3.1 Infrared Spectra

The absorption peaks occurring in MPcs at  $1090\text{ cm}^{-1}$ ,  $1300\text{ cm}^{-1}$  and  $1330\text{ cm}^{-1}$  are retained in all the three cases. The low frequency infrared absorption of metal phthalocyanines are shifted to longer wavelength in the case of doped and annealed CoPcI complexes. This indicates a change in nature of metal—ligand bonding in CoPcI and CoPcI annealed. The shift in the infrared absorption band to longer wavelength indicates the presence of stronger charge transfer with the dopant.

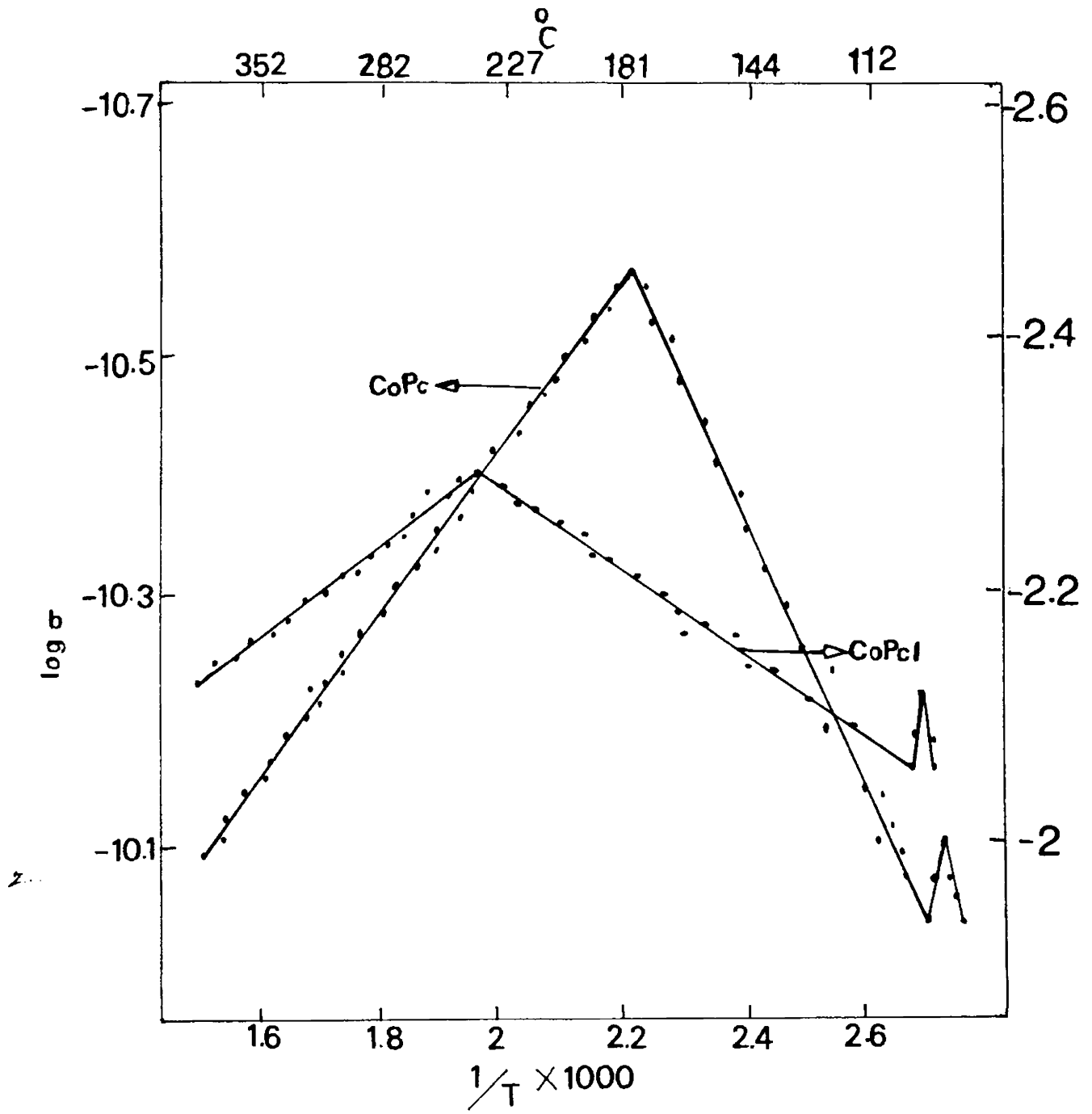


Fig. 4.2 Log  $\sigma$  -  $1/T$  plot for CoPcI pellets

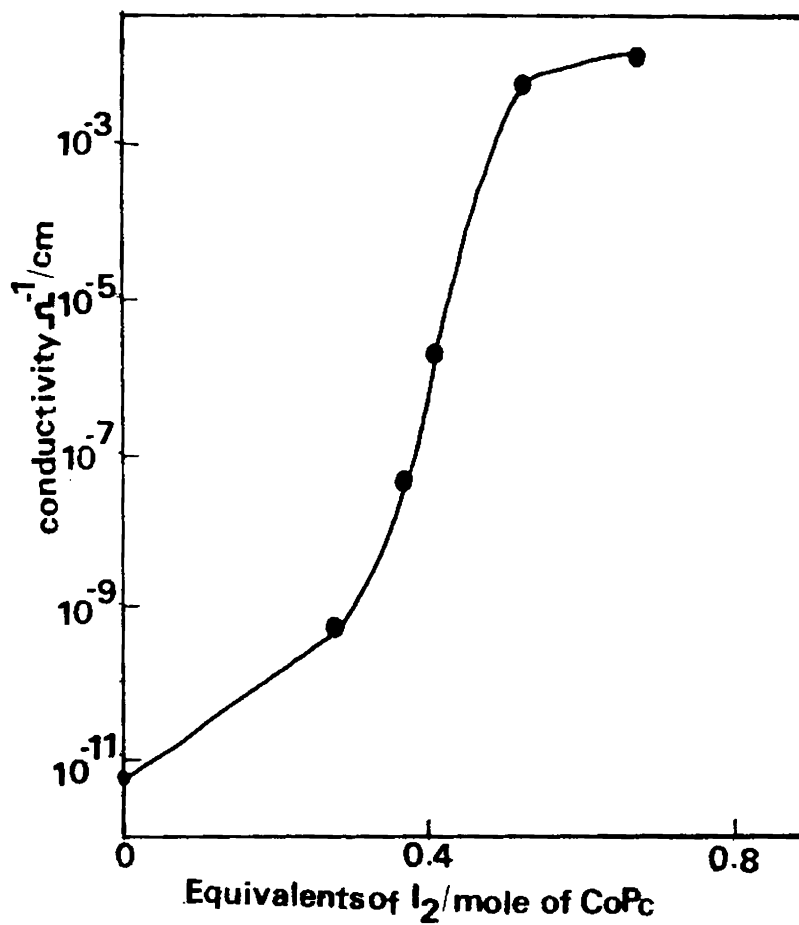


Fig. 4.2.1 Concentration dependant of iodine on the conductivity of CoPc.

### 4.3.2 Electronic Spectra

The peaks at 610 nm and 650 nm observed in the solid state electronic spectrum of CoPc are shifted to 525 nm and 620 nm in CoPcI. In CoPcI annealed in addition to the peaks observed at 525 and 620 nm additional peak emerges at 225 nm and the shoulder at 350 nm disappears. This observation is in agreement with the observation that a blue shift occurs in molecular compounds by charge transfer reaction with iodine. <sup>194</sup>

### 4.3.3 Magnetic Susceptibility

The static magnetic susceptibility of CoPc at room temperature is  $16.55 \times 10^{-4}$  emu/mole. The reduced susceptibility indicates a strong interaction between cobalt atoms and that the site of oxidation is the metal rather than the ring (Co<sup>+3</sup> is diamagnetic) and in annealed CoPcI it is  $5.9 \times 10^{-4}$  emu/mole

### 4.3.4 Differential Scanning Calorimetry

The DSC patterns of the three samples show considerable difference. The thermo gravimetry of CoPc shows that CoPc decomposes at 625° C. The DSC trace of the charge transfer complex formed between iodine and CoPc shows 3 exothermic peaks at 413° C, 328° C, and 130° C. When CoPcI complex is annealed, the endothermic peaks disappear, a new exothermic peak at 148° C appears. The high temperature transformations are not modified.

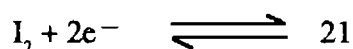
### 4.3.5 Electron Paramagnetic Resonance Spectra

The EPR spectrum of CoPcI and annealed CoPcI give a signal at  $g = 2.04$  and the value is close to that of CoPc ( $g = 2.02$ ). The CoPcI fails to show any feature associated with oxidation of Pc ring system.

The CoPcI is thus shown to form a charge transfer complex. The cobalt metal in CoPc unit gets oxidized and iodine is reduced. Here the charge transfer complex is formed by the charge/transfer interactions within the CoPc-I complex.

### 4.3.6 Electrochemical Studies on CoPcI

The cyclic voltammetric behaviour of the CoPc deposited on graphite electrode in O<sub>2</sub> saturated NaClO<sub>4</sub> medium is shown in Fig.4.4. CoPc deposited graphite electrode gives a peak at 0.57 V characteristic of CoPc and also the catalytic O<sub>2</sub> reduction peak at -0.59V. The peak at -0.59V disappears when sparged with nitrogen. This indicates that the peak at -0.59V is due to the reduction of O<sub>2</sub>. Iodine doped CoPc (CoPcI) gives a cathodic peak at 0.57V and two overlapping anodic peaks at -0.87V and -0.61V. If molecular iodine is present it ought to have given a well defined reduction peak in the potential rang between 0 and 0.3V (vs SCE) which corresponds to



In the cyclic voltammogram of CoPcI the cathodic peak due to I<sub>2</sub> is absent indicating that

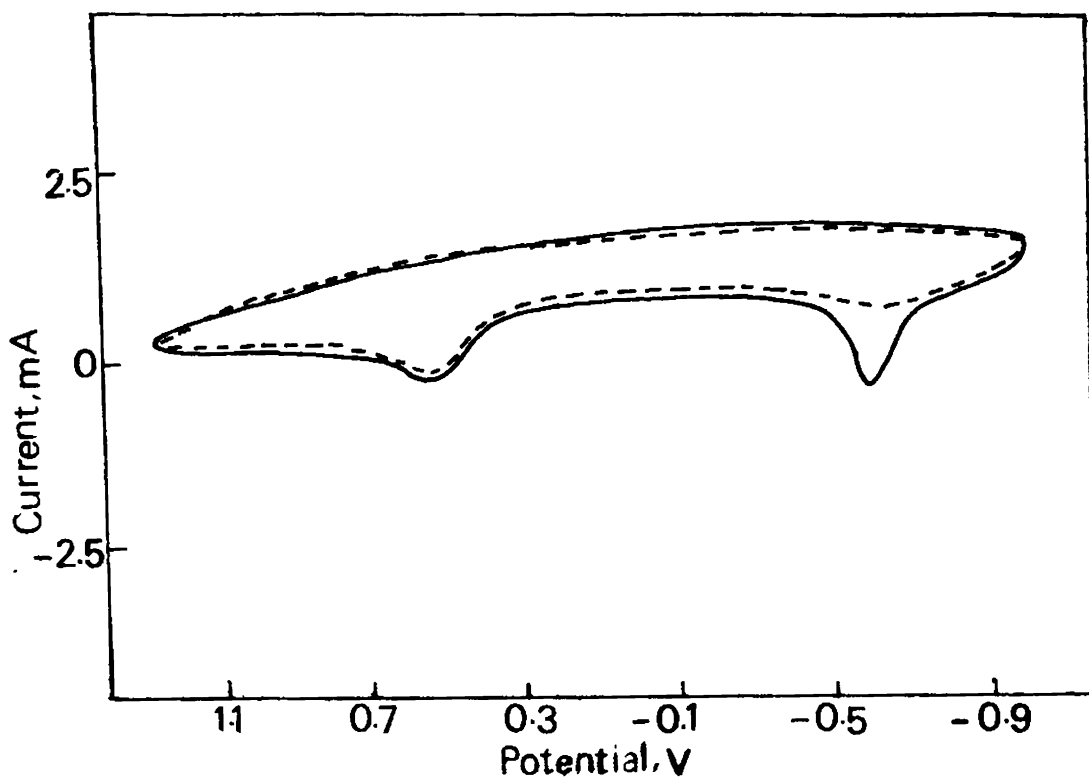


Fig. 4.4 Cyclic voltammogram of the CoPc deposited graphite electrode in 0.1M NaClO<sub>4</sub> solution. (—)O<sub>2</sub> saturated;  
(- -)N<sub>2</sub> saturated  
Scan Rate : 100mV/s

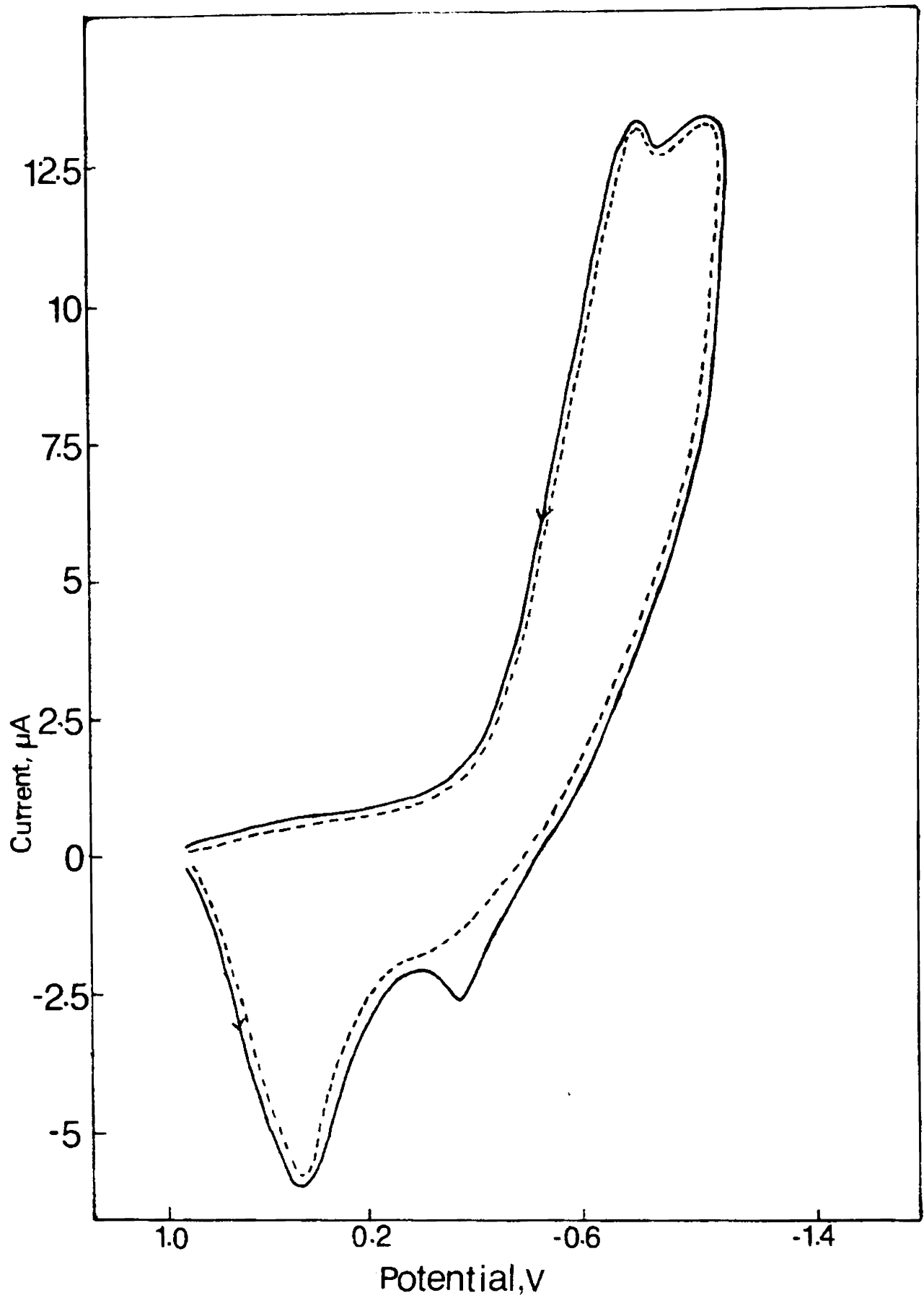


Fig. 4.5 Cyclic voltammogram of the iodine doped CoPc electrode in 0.1M  $\text{NaClO}_4$  solution. (—)  $\text{O}_2$  saturated;  
 (---)  $\text{N}_2$  saturated  
 Scan Rate : 100mV/s

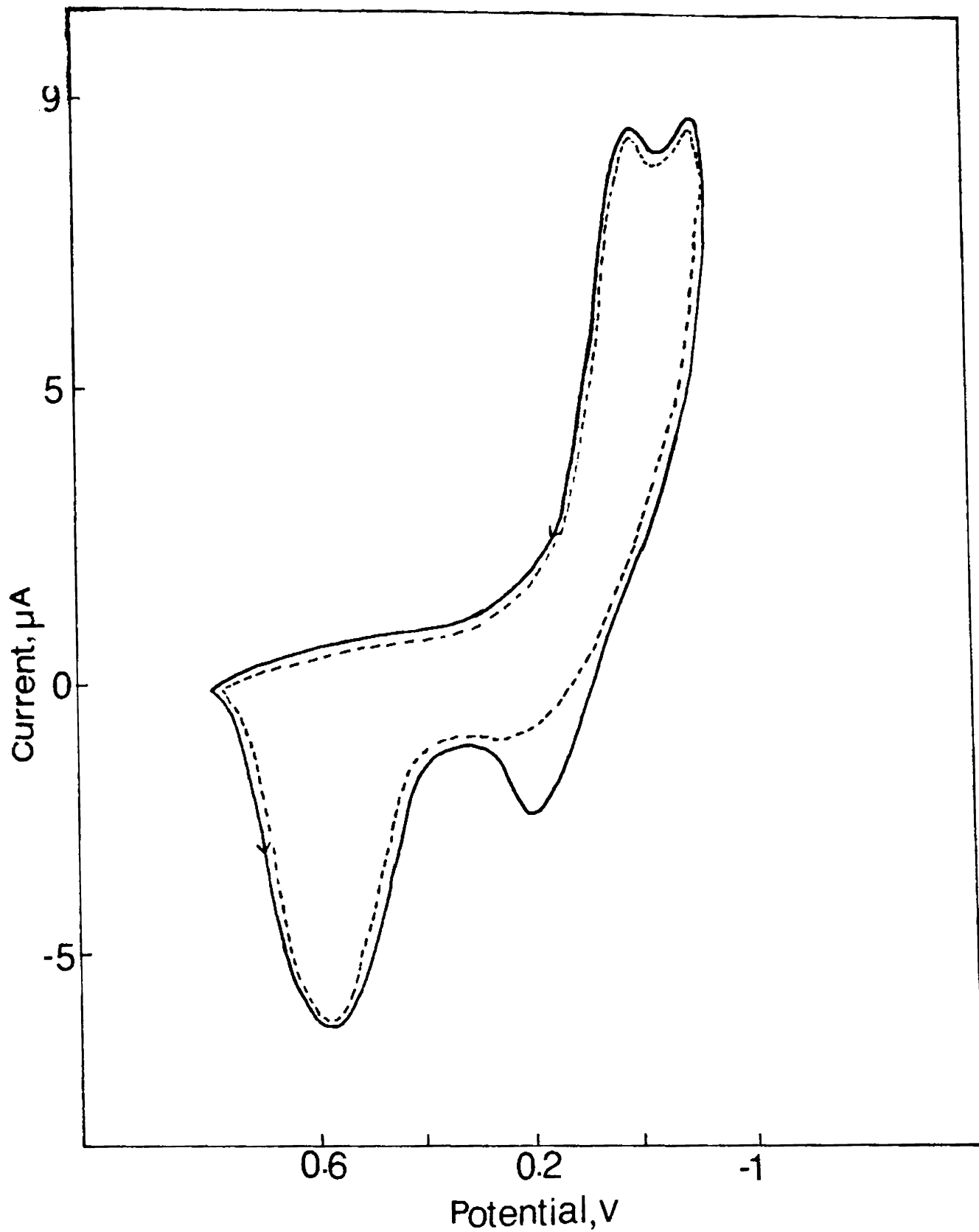


Fig. 4.6 Cyclic voltammetric behaviour of annealed CoPcI electrode.

(—)  $\text{O}_2$  saturated; (---)  $\text{N}_2$  saturated.

Supporting electrolyte : 0.1M  $\text{NaClO}_4$ .

Scan Rate : 100mV/s

I<sup>0</sup> does not exist. The CoPc when exposed to iodine vapour or solution results in the formation of a charge transfer complex having a range of stoichiometries. By interaction with iodine phthalocyanine ring system itself undergoes partial oxidation whereas the oxidation in CoPc is metal centred. The two anodic peaks observed at -0.92 and -1.05V in the CV of annealed CoPcI is probably due to its oxidation. The CoPcI retains the cathodic peak occurring at 0.57 V. As a result of annealing at -210 °C the conductivity increases and simultaneously the cathodic peak at 0.57V shifts to 0.37V. This suggests that the molecule has been further modified by annealing.

#### 4.4 Iron Phthalocyanine

Fig.4.7 shows the  $\log \sigma$  vs  $1/T$  plot for the FePc and FePcI. The FePc shows a transition at 235° C and FePcI at 178° C Fig. 4.8 — 4.10 shows the behaviour of FePc, FePcI and annealed FePcI electrodes in 0.1M NaClO<sub>4</sub> solution saturated with O<sub>2</sub>. At FePc, O is reduced at a potential of 0.62V. At FePcI, the peak potential for the reduction of O<sub>2</sub> shifted by -100 mV and at FePcI annealed, O<sub>2</sub> is reduced at about -0.43V. Here also thermal annealing results in the higher catalytic activity for dioxygen reduction. It is observed that the stability of FePcI in acetone is less than that of CoPcI.

FePcI shows a peak at 0.51V on scanned from 1.1V to -1.0V. On reversing the scan, 3 peaks are observed at -0.85V, -0.56V and 0.14V. This behaviour is similar to that of CoPcI except for the appearance for an additional peak at 0.14V. When FePcI was annealed, it was observed that the peak at 0.51V is shifted to 0.74V and two cathodic peaks at -0.36V and 0.24V are observed. In the case of FePcI, one of the cathodic peaks disappear and the other peak potentials were shifted to positive side.

#### 4.5 Zinc Phthalocyanine

Fig.4.11 shows the  $\log \sigma$  -  $1/T$  plot for ZnPc and iodine doped ZnPc (ZnPcI) samples. The transition temperature for ZnPc is 216° C and for ZnPcI, it is 188° C. The conductivity for ZnPc is of the order of 10<sup>-9</sup> ohm/cm<sup>2</sup> while that of ZnPcI is 10<sup>-4</sup> ohm/cm<sup>2</sup>.

The cyclic voltammetric behaviour of ZnPc, ZnPcI and annealed ZnPcI samples is shown in Fig. 4.11 — 4.13. At ZnPc electrode dioxygen is reduced at -0.64V. In addition to the oxygen reduction peak, a peak is observed at 0.50V which may be due to the reduction of ZnPc.

O<sub>2</sub> is reduced at a lower potential in the case of ZnPcI. In addition to the peaks observed at ZnPc an additional anodic peak appears at -0.35V. The anodic peaks observed at CoPcI or FePcI is absent in this case. When the sample is annealed, it was observed that in addition to the shift of the dioxygen reduction peak, an anodic peak is observed at -0.87V which indicates that as a result of annealing the extent of charge transfer with iodine becomes stronger which is reflected by the emergence of the characteristic anodic peak in CoPcI electrode.

The improvement in the electrochemical activity of thermally annealed samples is associated with the increase in their electrical conductivity which is due to the alteration in the structure of these materials, which facilitates charge transport through hopping or tunnelling, between the aromatised rings. It is also likely that charge carrier intensity is increased by the generation of radical defects during heat treatment. The presence of radical defects have been proved by an increase in magnetic susceptibility value in the case of annealed CoPcI samples.

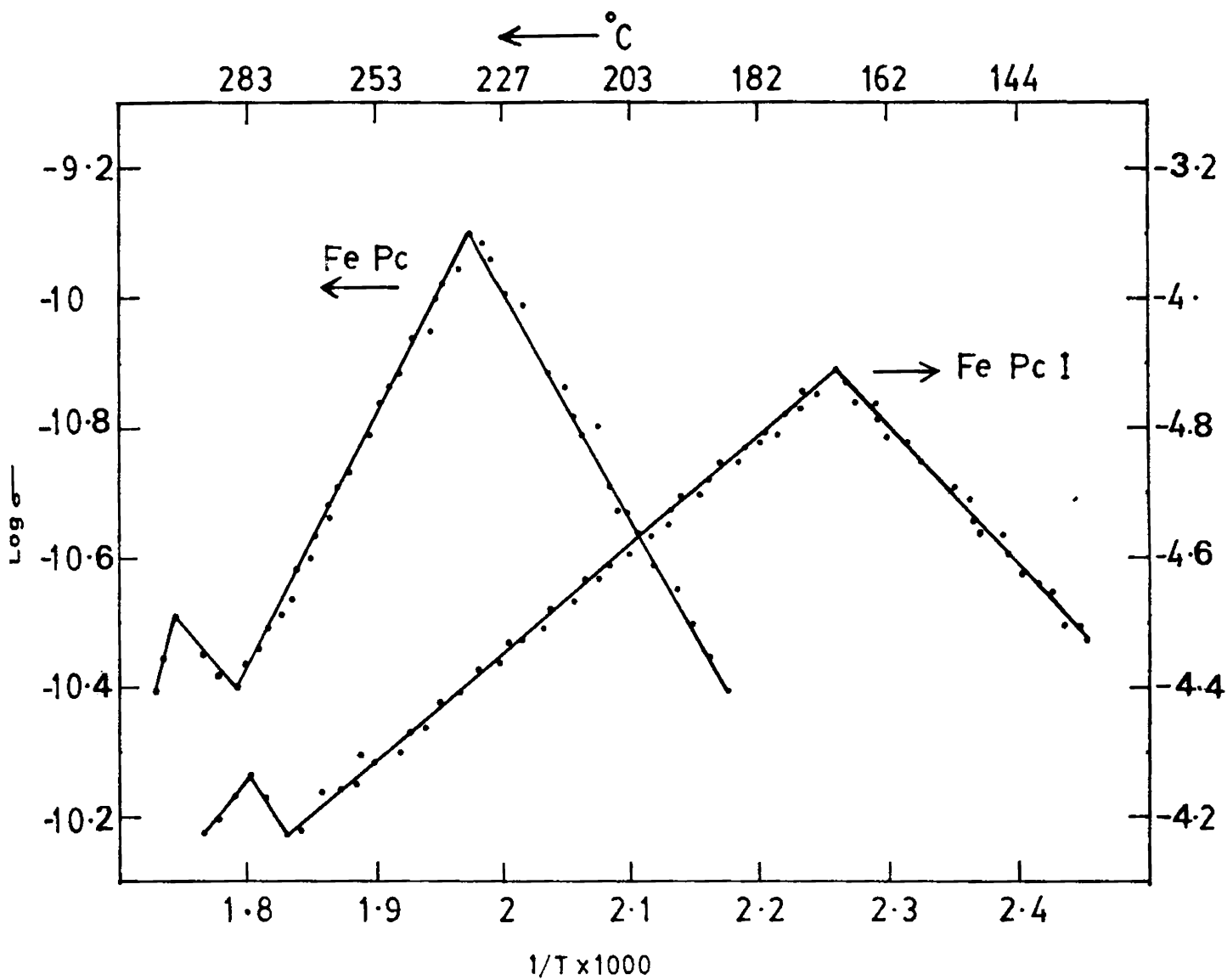


Fig. 4.7  $\text{Log } \sigma - 1/T$  plot for FePc and FePcI pellets.

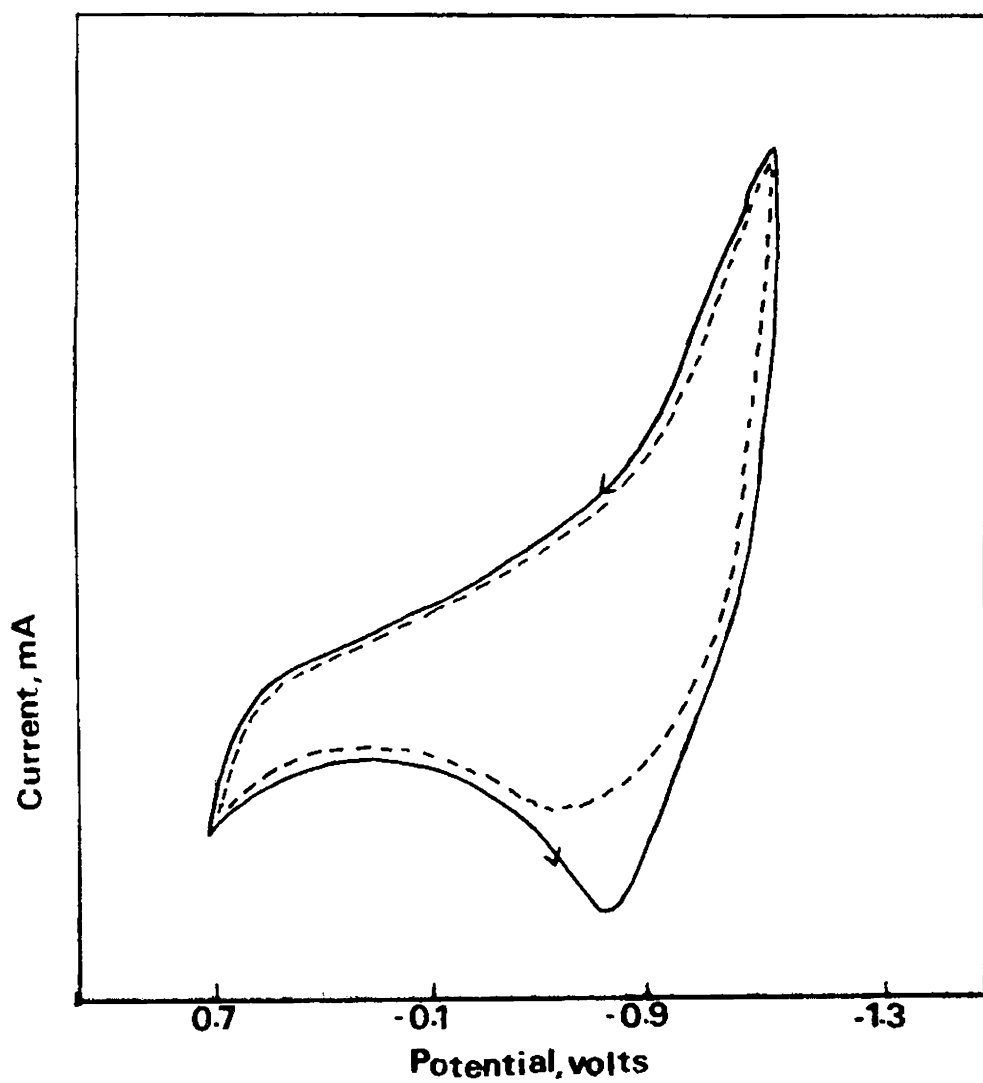


Fig. 4.8 Cyclic voltammogram of the FePc deposited graphite electrode in 0.1M NaClO solution.  
(—) O<sub>2</sub> saturated; (- -) N<sub>2</sub> saturated.  
Scan Rate : 100mV/s

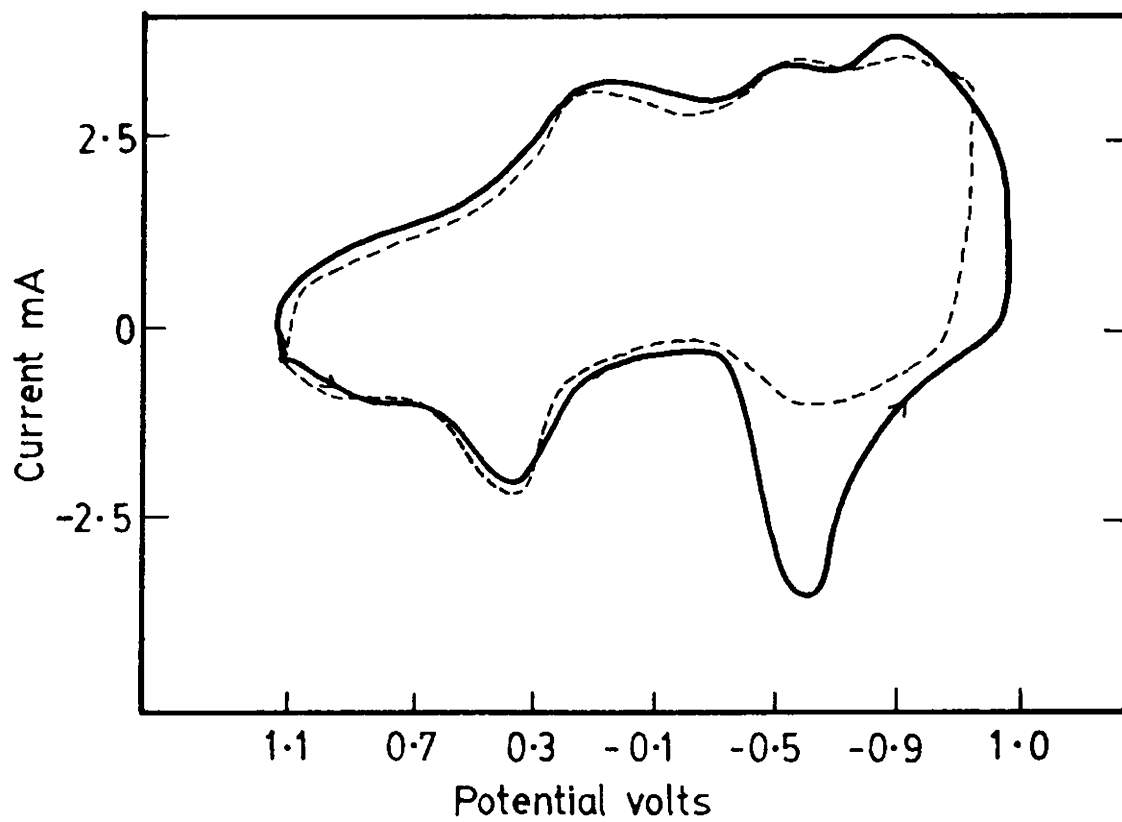


Fig. 4.9 Cyclic voltammogram of the iodine doped FePc electrode in 0.1M NaClO<sub>4</sub> solution.  
(—) O<sub>2</sub> saturated; (- -) N<sub>2</sub> saturated  
Scan Rate : 100mV/s

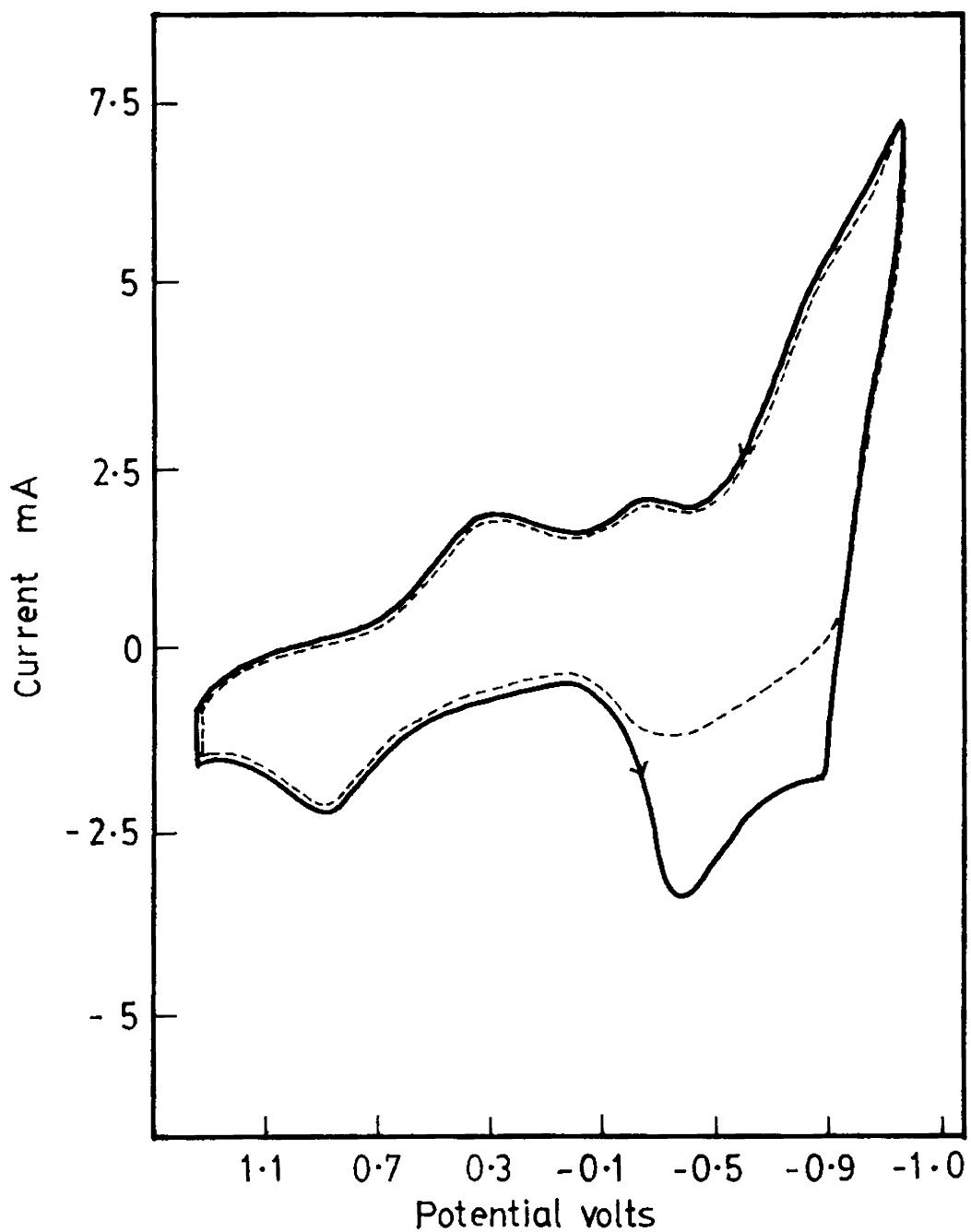


Fig. 4.10 Cyclic voltammetric behaviour of annealed FePcI electrode.  
(—) O<sub>2</sub> saturated; (- -) N<sub>2</sub> saturated.  
Scan Rate 100mV/s

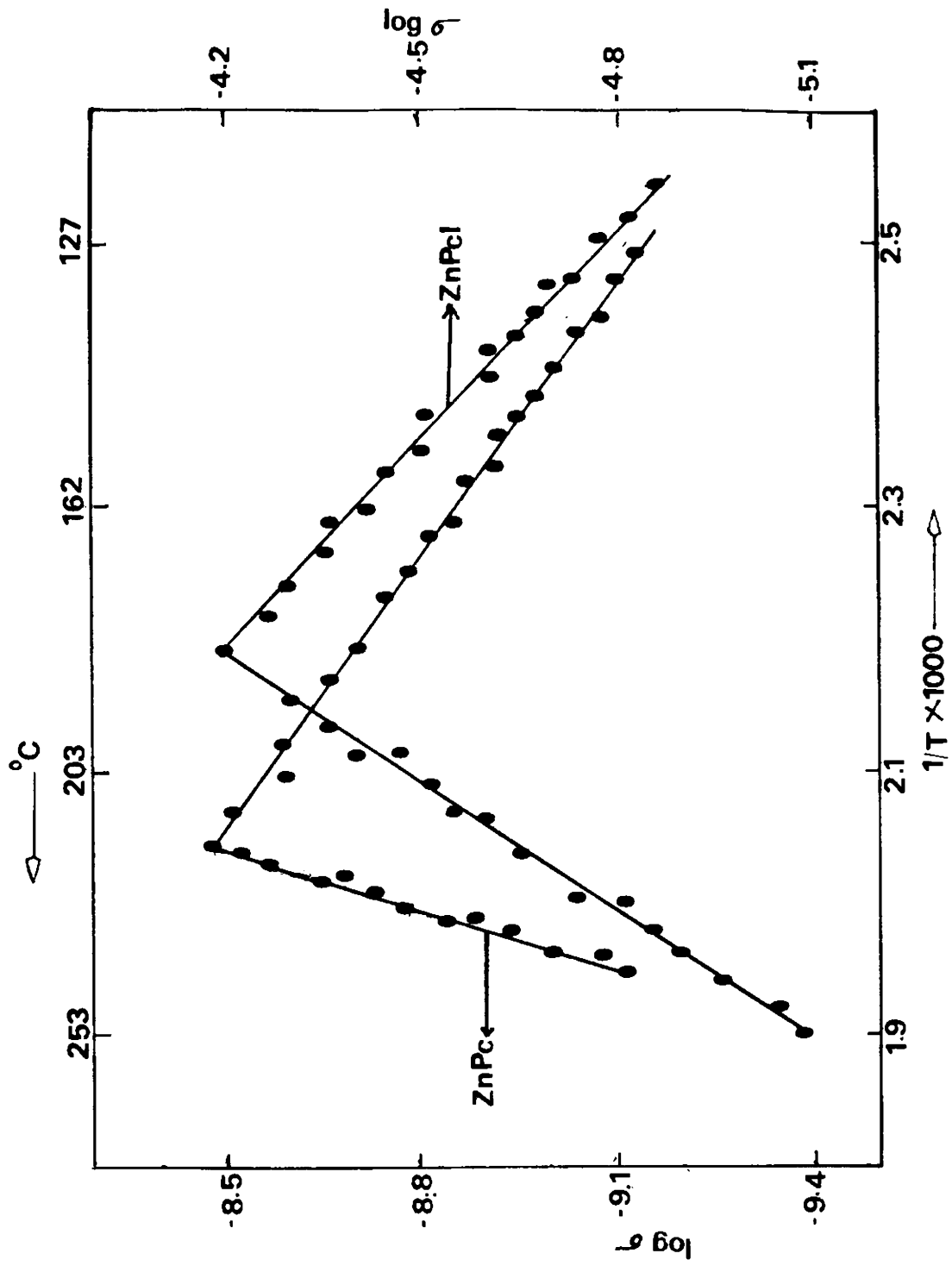


Fig. 4.11  $\log \sigma - 1/T$  for ZnPc and ZnPcI pellets.

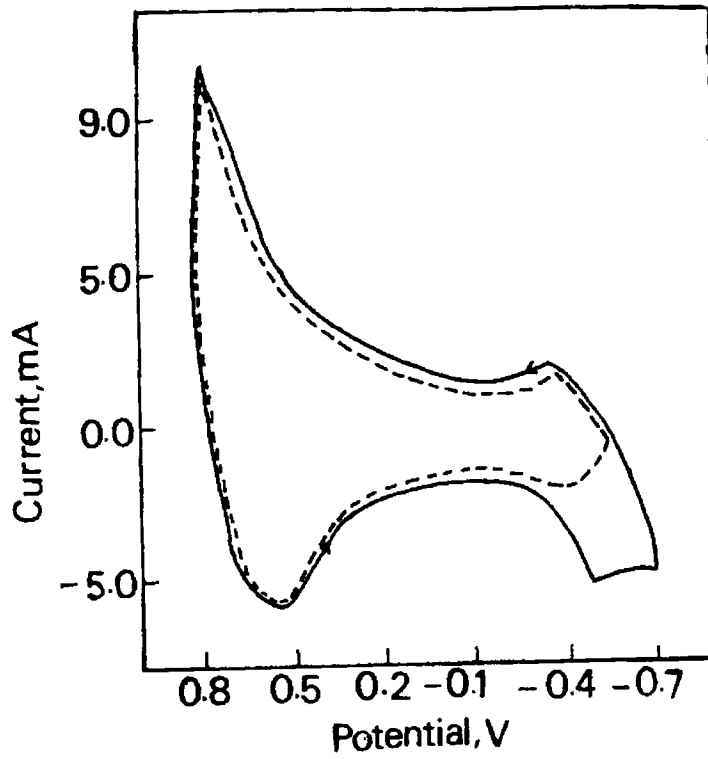


Fig. 4.13 Cyclic voltammogram of the iodine doped ZnPc electrode in 0.1M NaClO<sub>4</sub> solution  
 (—) O<sub>2</sub> saturated; (---) N<sub>2</sub> saturated  
 Scan Rate : 100mV/S

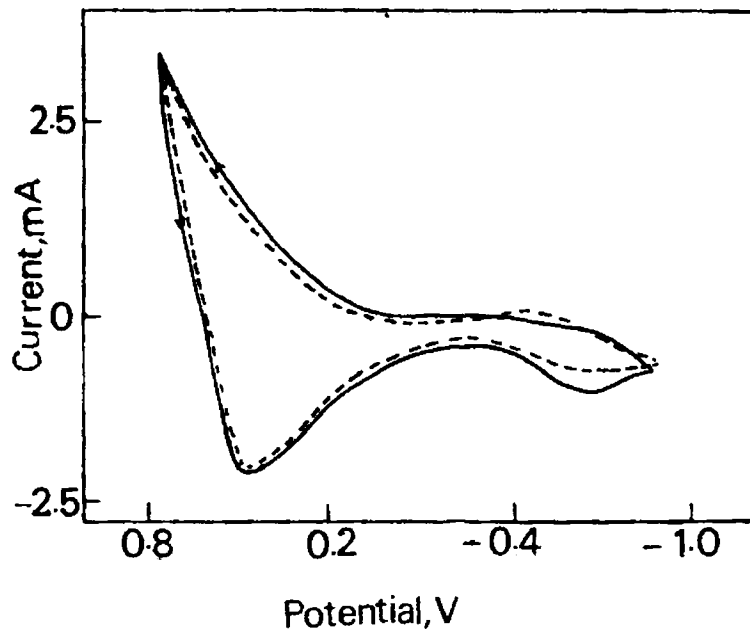


Fig. 4.12 Cyclic voltammogram of ZnPc deposited graphite electrode in 0.1M NaClO<sub>4</sub> solution.  
 (—) O<sub>2</sub> saturated; (---) N<sub>2</sub> saturated.  
 Scan Rate : 100mV/s

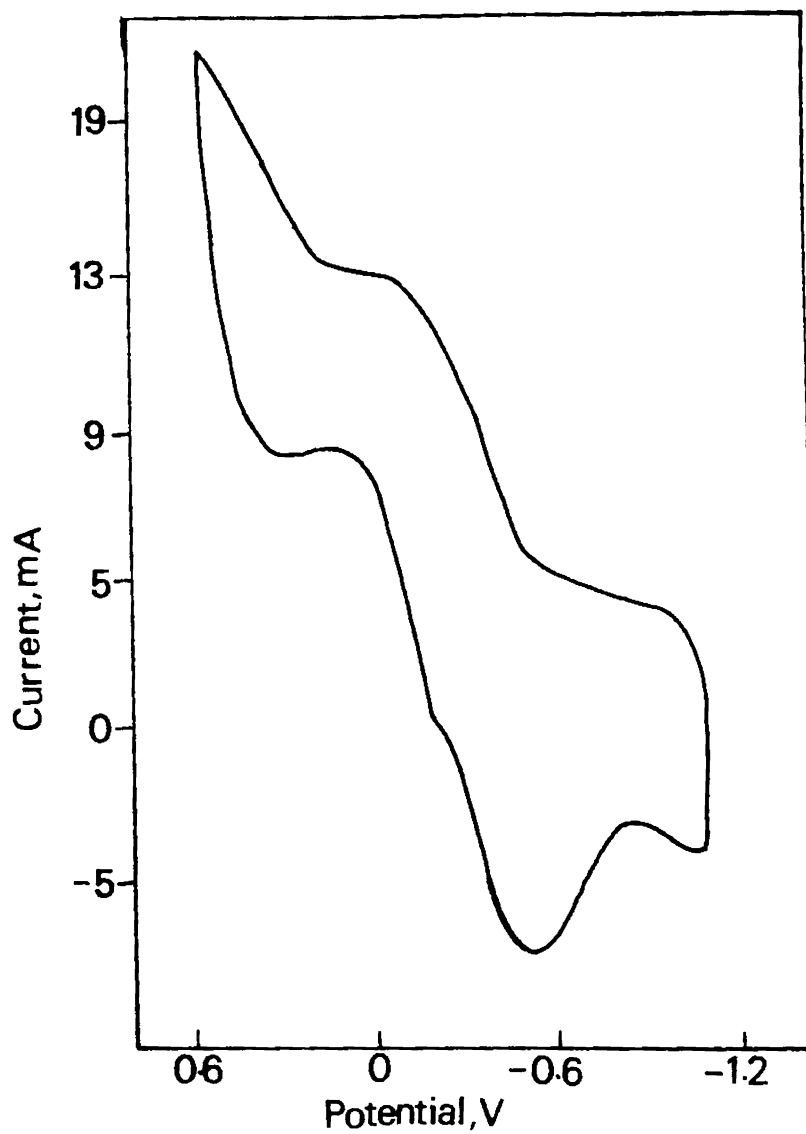


Fig. 4.14 Cyclic voltammetric behaviour of annealed ZnPcI electrode  
 (—) O<sub>2</sub> Saturated; (---) N<sub>2</sub> saturated.  
 Supporting electrolyte : 0.1M NaClO<sub>4</sub>  
 Scan Rate : 100mV/s

# CHAPTER V

## Chemically Modified Electrodes

### 5.1 Introduction

Eventhough electrochemical methods have a wide range of applications in analysis, inorganic and organic synthesis, catalysis, display-devices etc., fouling of the electrode surface by the undesirable precipitation or adsorption of reactants and products and the necessity for applying an overvoltage due to slowness of electron transfer for certain species are some of its major disadvantages. It is anticipated that by attaching chemical reagents to an electrode surface the chemical properties of the attached reagents can be imparted to the surface. If the proper reagent is chosen, desirable properties such as reagent-based control of the rates, selectivity of electrochemical reaction, freedom, from adsorptive and coating effects, and special photochemical features might be obtained. The application of such chemically modified electrodes (CME) has opened up new vistas in the field of electrochemical research. Interest in (CME) has opened up new vistas in the field of electrodes. Interest in CMEs has spread in varied directions, including synthetic design of electrochemically active polymers, basic studies on electrocatalysis, electron transfer kinetics, membrane permeation, electrochromics, photoelectrochemistry, molecular electronics and electroanalysis.<sup>196-200.</sup>

The different methods for the modification of electrode by the immobilization of chemical reagents are:

#### 1. Monomolecular layer formation by the chemisorption of reagent.

- a) On Platinum surface<sup>198</sup>
- b) On carbon surface<sup>201</sup>
- c) On mercury surface<sup>202</sup>
- d) Gold surface<sup>203</sup>

#### 2. Formation of covalent bond formation between electrode and electroactive and electroinactive reagent

- a) At metal oxide surface<sup>204</sup>
- b) At carbon surface<sup>205</sup>
- c) At semiconductors<sup>206</sup>
- d) Of electroinactive, chiral substances<sup>207</sup>

#### 3. Multimolecular layers, polymer film coatings on electrodes

- a) Redox polymers<sup>208</sup>
- b) Ion exchange electrostatically trapped<sup>209</sup>
- c) Electronically conducting polymers<sup>210</sup>
- d) Ionically conducting polymers<sup>211</sup>
- e) Crown ether or complexing agent<sup>212</sup>
- f) Electroinactive chiral polymers<sup>213</sup>

#### 4. Heterogeneous multimolecular layers

- a) Modifying agent mixed with carbon paste<sup>214</sup>
- b) Clay modified<sup>215</sup>
- c) Electroactive particles in electroactive polymer<sup>216</sup>

In the initial phase of development monolayers or submonolayers of electroactive species were irreversibly attached to the electrode surface. Carbon electrodes are especially effective with chemisorbing reagents that have extended  $\Pi$ -bond system. An example is the chemisorption of a dicobalt cofacial porphyrin electrocatalyst ( $\text{CO}_2$  FTF<sub>4</sub>) onto pyrolytic carbon to create an electrode that mediates the 4 electron reduction of dioxygen.

The use of chemical functionalities of electrode surfaces for anchoring reagents has wide range of synthetic diversity and has been extensively developed for attaching monomolecular and multimolecular layers of electroactive substances to metal oxides and carbon semiconductor electrodes.

Electroactive multimolecular layer films of polymers are popular today because they are technically easier to apply to electrodes than are covalently bonded monolayers. They also contain multimolecular layers of electroactive sites, so that their electrochemistry can be more easily observed. Electroactive films can be used as electrocatalysts, as preconcentration media or as transport barrier, where the performance of monolayer films are not reliable. Bare or monolayer-derivatised electrodes permit reduction only in an essentially 2-dimensional zone next to the electrode, whilst homogeneous reactions occur in a 3-dimensional zone, permitting a greater reaction flux. By using thicker modifying films, homogeneous catalysis can take place successfully. Thicker polymeric films are advantageous in corrosion protection by charge transfer blocking and in optical displays by immobilizing redox-state-dependent chromophores.

Electroactive polymer films are intrinsically conductive due to both ions and electrons. There are three kinds: Redox polymers, electronically conducting polymers, and ion exchange polymers. Polymer films with redox sites (localized electronic states), called redox polymers, conduct electricity via electrons hopping between oxidized and reduced sites. The possible use of polypyrrole in electrocatalysis and other related applications has been reviewed by Derronzier et al<sup>217</sup>. This is the case with *o*-quinone, pyrrole, substituted porphyrin and ferrocene polymers. The organic metals or electronically conducting polymers conduct via delocalized, metal-like band structures. Polypyrrole is such a material which can be easily prepared by electrochemical polymerization and can be used to entrap electrocatalysts such as phthalocyanines<sup>218</sup> and enzymes.

Ion exchange polymer films are made electroactive by the exchange of some of their charge-compensating counter ions for electroactive ones. Exchange of  $\text{Fe}(\text{CN})_6^{4-}$  for the  $\text{ClO}_4^-$  counter ion of a protonated polyvinylpyridine film is an example. Ion exchange equilibrium can be slowly reversed when the polymer is used in an electrolyte solution free of electroactive counter ions. The electroactivity sites of ion exchanged polymer is labile compared to those of covalently bound redox polymers. In the ion exchange films, electrons are transported in part by physical diffusion of electroactive ions, which may also undergo self-exchange as part of the transport process.<sup>219</sup> The electrical properties of electroactive polymer films on electrodes and the processes by which they electrocatalytically mediate electron transfers between the electrode and reactive substrates in the contacting solution is a field of active research now. Ionic conductivities of the films have been less fully investigated but need to be better understood, because of electroneutrality a change in the films oxidation state requires movement of charge-compensating counter ions in film.

Heterogeneous films on electrodes can be designed to contain a mixture of constituents with different functions. An example is the addition of constituents such as catalyst monomers and metal complexing agents to carbon paste electrodes.

“The mixed carbon paste electrodes” made from carbon paste which is doped during

preparation with the modifying molecule is marked with the following advantages: simplicity of electrode fabrication procedures, wide flexibility for the attachment of numerous organic and organometallic moieties, convenient control over the modifier concentration and capability for easy renewal of the CME surface.

The electrochemical properties of the polymers can be used for the controlled release of chemicals, especially drugs<sup>220-222</sup>. The basic concept of this application is to bind the drug into a polymer film on an electrode and release the drug as needed by passing a small current through the polymer.

Though catalytic properties of macrocyclic transition metal complexes such as porphyrins and phthalocyanines for an electrochemical oxygen reduction have been recognized and examined extensively by many workers, an active, inexpensive and stable catalyst system has not yet been discovered<sup>223,224</sup>. In this connection special efforts are made to modify the inexpensive materials such as graphite with electroactive substances. Utilization of modified catalytic electrode at monolayer level has not been so successful in that they lack stability and conductivity in a doped state due to the unstable and insulating nature of adsorbed species on the substrate<sup>225,226</sup>.

Electrocatalytic materials have been incorporated into polymer-coated electrodes which is an easy and potential means of fixing a large metal complex as active catalyst on the substrate<sup>227</sup>. Polymer films can be deposited on an electrode by electrooxidative polymerization simultaneously with the incorporation of active materials from the supporting electrolyte. The electrocatalytic activity for oxygen reduction was improved at a glassy carbon electrode modified with polypyrrole/ (tetrasulfonatophthalocyaninato cobalt) electrode<sup>228</sup>. CoTSPc can also be doped into polyaniline<sup>229</sup> and this shows very good catalytic activity and stability for dioxygen reduction.

## 5.2 Polymer Modified Electrodes

### 5.2.1 Electrochemical Characterization

The behaviour of an electrode coated with polymer and its improvements in design and performance and the resulting interface must be characterised fully. Prominent amongst the pieces of information desired are the following<sup>230</sup>.

- a) Polymer Structure : The nature of polymer/electrode bonds (if present), interchain interactions and, particularly for in situ polymerised films, the nature of linkage between repeat units.
- b) Film thickness and the degree of uniformity thereof,
- c) The extent to which monomer properties (E' electron transfer rate constants, optical behaviour, etc) are carried over to the polymer;
- d) the local environment, notably extent of solvation and solution anion/cation incorporation.
- e) the redox composition/potential relation
- f) the presence (or otherwise of electrostatic or other interactions between redox centres and the remainder of the polymer structure and possible resultant structural inhomogeneity.
- g) The rates of electron and ion motion through the film, ie. the conductivity and the mechanism of

charge transport.

## 5.2.2 Thermodynamic Parameters

The principal technique used to determine  $E'_{surf}$  values is cyclic voltammetry. The value of  $E'_{surf}$  may be approximated by the average of the anodic and cathodic peak potential,  $1/2(E_{p,a} + E_{p,c})$  at sufficiently low scan rates ( $\leq 10 \text{ mVs}^{-1}$ ). zero peak separation and linearity of peak current with sweep rate is an important diagnostic criterion for surface attachment.

Cyclic votammtric behaviour for an electrode and for a freely diffusing solution species, both with rapid kinetics		
$E'$	Polymer modified electrode $E'_{surf} = E'_{sol}$	solution redox couple $E'_{soln}$
$i_{p,a}/i_{p,c}$ (a)	1	1
$(\log i_p) / (\log v)$	1	0.5
$\Delta E_p$ (mV)	0	$59/n^{(b)}$
$\Delta E_p/2^{(c)}$ (mV)	90.6	$203/n$
Peak Shape	Symmetric about $E = E'_{surf}$ and $i = 0$	Peak assymetric diffusional 'tailing'
(a) Assuming equal diffusion coefficients		
$b_n$ number of electrons		
(c) Half - peak width		

$|E'_{surf} - E'_{soln}| = 0.1 \text{ V}$ .  $E'_{surf}$  and  $E'_{soln}$  is shown to be equal for  $\text{Fe}(\text{CN})_6^{3-/4-}$ ,  $\text{Ru}(\text{CN})_6^{3-/4-}$ ,  $\text{Mo}(\text{CN})_8^{3-/4-}$  and  $\text{IrCl}_6^{2-/3-}$  electrostatically bound to silylbenzyl and silylpropyl-viologen polymers.

The wave shape of a cyclic voltammogram reflects the potential/composition relation, which governs the extent of 'titration' of mediator centres with potential in mediator charge-transfer-based applications or of chromophore in display applications. The difficulty arises because the same effect may be the result of a variety of causes: Wave broadening in cyclic voltammetry can be caused by repulsive site-site interactions, slow charge transfer/propagation or large uncompensated electrolyte resistance effects. If the kinetics are rapid and equilibrium prevails, the rates of charge transfer of the interface and of charge propagation through the film must be large. This corresponds to large values of  $(D/L^2)/(VF/RT)$ , where the quantity  $(D/L^2)$  represents an effective relaxation rate. Values of this ratio greater than 3 result, for an 'ideal' film, with no interactive effects on (i) symmetrical waves about  $E = E'_{surf}$  and  $i = 0$  (ie.  $E_{p,a} = E_{p,c}$  and  $i_{p,a} = i_{p,c}$ ) (ii) a linear  $i$  versus ' $v$ ' relation and (iii) a peak half-width of 90.6 mV. The result (ii) arises because the charge passed ( $q$ ) is constant

and provides, firstly an important diagnostic test for surface attachment and secondly, a means of determining the total number of electroactive centres ( $\Gamma$  /mol Cm ).

$$\Gamma = q/nFA$$

The presence of interactive effects alters peak half-width and equality of peak currents (although they may still be individually proportional to scan rate if rapid kinetics prevail). Repulsive or attractive interactions result in peak broadening or narrowing respectively.

### Kinetic Parameters

Cyclic voltammetry can be used in two ways to determine kinetic data. In the first, the scan time is sufficiently long for the entire film to have the opportunity to react and one may follow the course of comparatively slow film changes. In the second, one assumes that the film is not involving itself in any way, and uses scan rate as the time domain variable to probe the rate of process associated with redox changes involving the film.

An obvious application of the first type of experiment is as a monitor of electroactive redox centre population during film production/elaboration by redox couple incorporation, ion exchange, silylation or electro-polymerisation. In the latter case, film growth and polymerisation are intimately linked, but the act of cycling the potential is also important in the ion exchange of Ru(bipy)<sub>3</sub><sup>2+</sup> into poly(styrene sulphonate) films. Similarly, the loss of electroactive species has been followed by cyclic voltammetry and also that induced by it, in the case of H<sup>+</sup> reduction within a protonated pyridine iodide system. In most cases the distinction between redox centre loss and isolation, polymer loss, require more direct data for confirmation.

Reaction (rather than loss) of redox centres may be followed by the appearance (and integration of) peaks at different  $E'_{surf}$  or by the loss of reactant peak if the product is electroinactive.

## 5.3 ELECTROCHEMICAL BEHAVIOUR OF COBALT TETRASULPHO — PHTHALOCYANINE ION DOPED INTO POLYANILINE AND POLY (o-TOLUIDINE)

### 5.3.1 Introduction

Polyaniline (PA) is an interesting conducting polymer with a wide range of conductivity including that approach 5 S/cm<sup>231</sup>. Electrochemically formed PA is generally homogeneous, strongly adherent to the electrode surface and chemically stable.<sup>232,233</sup> The electrochemical behaviour of PA depends on its method of preparation<sup>234</sup> and the substrate<sup>235</sup> on which it is formed and also on the temperature<sup>236</sup> of synthesis. The conducting or insulating and electroactive or inactive property of PA depends on the experimental conditions used for its preparation.<sup>238</sup>

Polyaniline can be electrochemically polymerized onto electrodes such as platinum and pyrolytic graphite<sup>239 240</sup> This technique has many advantages like homogeneity strong adherence to electrode surface and chemical stability and the characteristics are reproducible.

PA films have been used as chemical sensors in microelectronic devices, cathode materials in solid state batteries, ion exchangers, display elements in electrochromic devices and as electrocatalysts<sup>241,242</sup>. Polyaniline based devices can be turned 'on' by either a positive or a negative shift of the electrochemical potential, because the films are essentially insulating at sufficiently negative (–0.0V vs SCE) or positive (–0.7V vs SCE) applied potentials. The response of PA based transistors to a

signal thus differs in a significant way from solid-state transistors where the current passing between the source and the drain  $I$  at a given source drain voltage,  $V$ , does not decrease with increasing gate voltage,  $V$ . When a macroscopic electrode is derivatized with a redox polymer and then coated with a porous metal contact, it can show diode-like behaviour<sup>243</sup>.

Platinum microparticles can be electrodeposited as a three dimensional array in a polyaniline film<sup>244</sup>. These electrodes show high activity for hydrogen evolution and methanol oxidation. Metalloporphyrins and phthalocyanine can be incorporated into PA and they show very good catalytic activity and stability for dioxygen reduction.<sup>245</sup>

In this chapter the results of the studies of the electrode process on cobalt tetrasulphophthalocyanine modified polyaniline are reported.

## **5.3.2 EXPERIMENTAL**

### **5.3.3 Chemicals**

Reagent grade aniline (Glaxo Laboratories, Bombay) was vacuum distilled and the middle fraction was used. Other chemicals used were of guaranteed purity.

### **5.3.4 Electrodes, Electrochemical Cells and Instrumentation**

Electrochemical cell and instruments used in this study were the same as those described in section 3.1. Unless otherwise specified experiments were done in deaerated solutions

Spectroscopic grade graphite (Union Carbide, USA), platinum wire or platinum button and carbon paste electrodes were used as the working electrodes.

The graphite electrode of exposed area  $0.8 \text{ cm}^2$  was made by sealing the graphite electrode in a thick walled glass tube with epoxy resin and polishing the surface with fine carborundum powder.

### **5.3.5 Carbon paste electrode**

Dry, chemically formed polyaniline (1-5mg) and carbon powder (5-10 mg) were thoroughly mixed in a mortar and milled with a drop of Nujol until the entire mixture appeared uniformly wetted. A portion of this paste was then introduced into the cavity of a glass tube fitted with a platinum wire connected to a mercury contact. Connections were made through a copper wire immersed in mercury. This electrode gives a very low residual current over the entire range of potential studied.

A saturated calomel electrode was used as the reference electrode.

## **5.4 Preparation and Characterization of Polyaniline Films**

### **Electrochemical preparation**

A variety of electrochemical techniques and conditions are reported for the preparation of polyaniline films.

### 5.4.1 Graphite Electrode

PA film was deposited on graphite from a solution of 0.5M  $H_2SO_4$  /0.1M aniline by cycling the electrode potential between 1.2V and -0.2V vs SCE.

### 5.4.2 Platinum electrode

A platinum wire (length 3mm) or button electrode (area~7mm<sup>2</sup>) was used as the working electrode. Aniline was polymerised onto the electrode as described in section 5.4.1

The polyaniline film formed were characterized by IR spectroscopy.

### 5.4.3 Chemical Preparation of Polyaniline

Aniline (5ml) was dissolved in 50ml of 4M  $H_2SO_4$  and 50 ml of aqueous solution of 40% ammonium persulphate was added. The resulting solution was warmed on a water bath for about 1h. The polymer precipitated out was filtered, washed with distilled water and dried. The PA was characterized by IR spectroscopy.

## 5.5 Results and Discussion

Fig 5.1. 1 shows the polymerisation of aniline at a graphite electrode. The first cycle shows two anodic peaks of aniline which are due to the oxidation of aniline. Subsequent potential cyclings indicate a regular growth of the polymer deposit. The PA film was allowed to grow for about twenty minutes. The electrode was taken out from the solution, washed several times with distilled water and placed in 0.5M  $H_2SO_4$ . This electrode was cycled between -0.2 to 1.2V Fig. 5.2 shows the cyclic voltammetric behaviour of this electrode. The following peaks are observed in the CV:  
Anodic peaks at 0.21V, 0.44V and 0.75V and  
Cathodic peaks at 0.51V, 0.38V and 0.56V.

On repeated potential cycling it was seen that the anodic peak current at 0.75V increases in magnitude. When the anodic limit of the potential scan did not exceed 0.7V a single anodic peak at 0.21V and two shoulder cathodic peaks at -0.16V and 0.0V were only observed. The magnitude of the anodic peak current depends on the pH of the medium. It is also seen that the anodic potential is shifted to more negative values when the concentration of the acid is increased (Fig.5.3)

The same observations were obtained when the film was formed from neutral ( $Na_2HPO_4 / NaH_2PO_4$ ; 0.5M; pH = 7) and from alkaline medium (0.5MKOH)

The cyclic voltammetric behaviour of PA at Pt electrode is shown in Fig.5.4. This shows 2 pairs of distinct redox peaks at -0.7V and -0.1V. Another pair is also observed at -0.5V which is not so prominent.

The electroactivity of aniline depends on the pH of the medium from which it is formed. It is also observed that PA formed from 0.5M  $H_2SO_4$  is active only in pH <3, with an increase in pH, the anodic and cathodic peak potentials shift to more negative values and also the anodic and cathodic peak currents decrease.

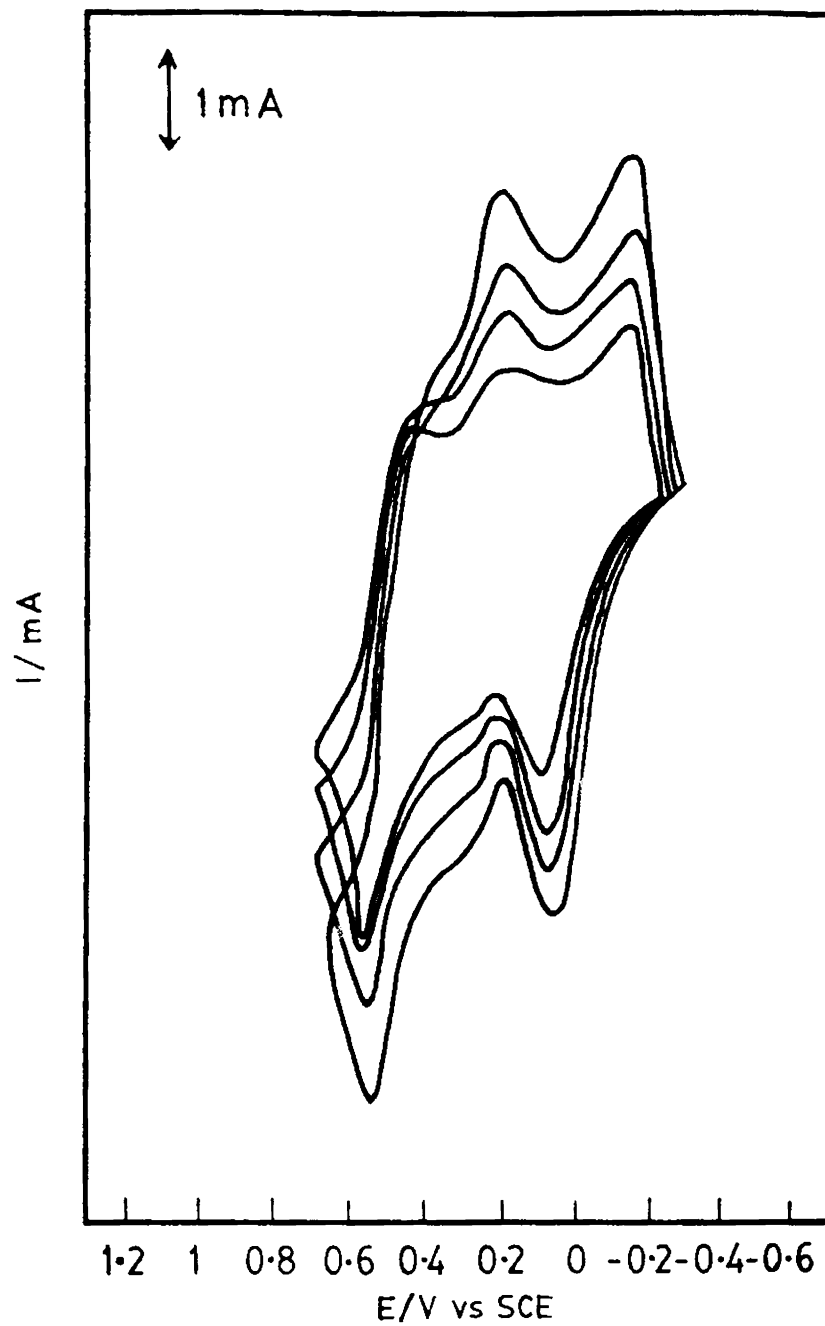


Fig. 5.1 Electrochemical polymerisation of aniline from a solution of 0.1 M aniline at a graphite electrode.

Supporting electrolyte : 0.5M  $H_2SO_4$   
Scan rate : 100mV/s

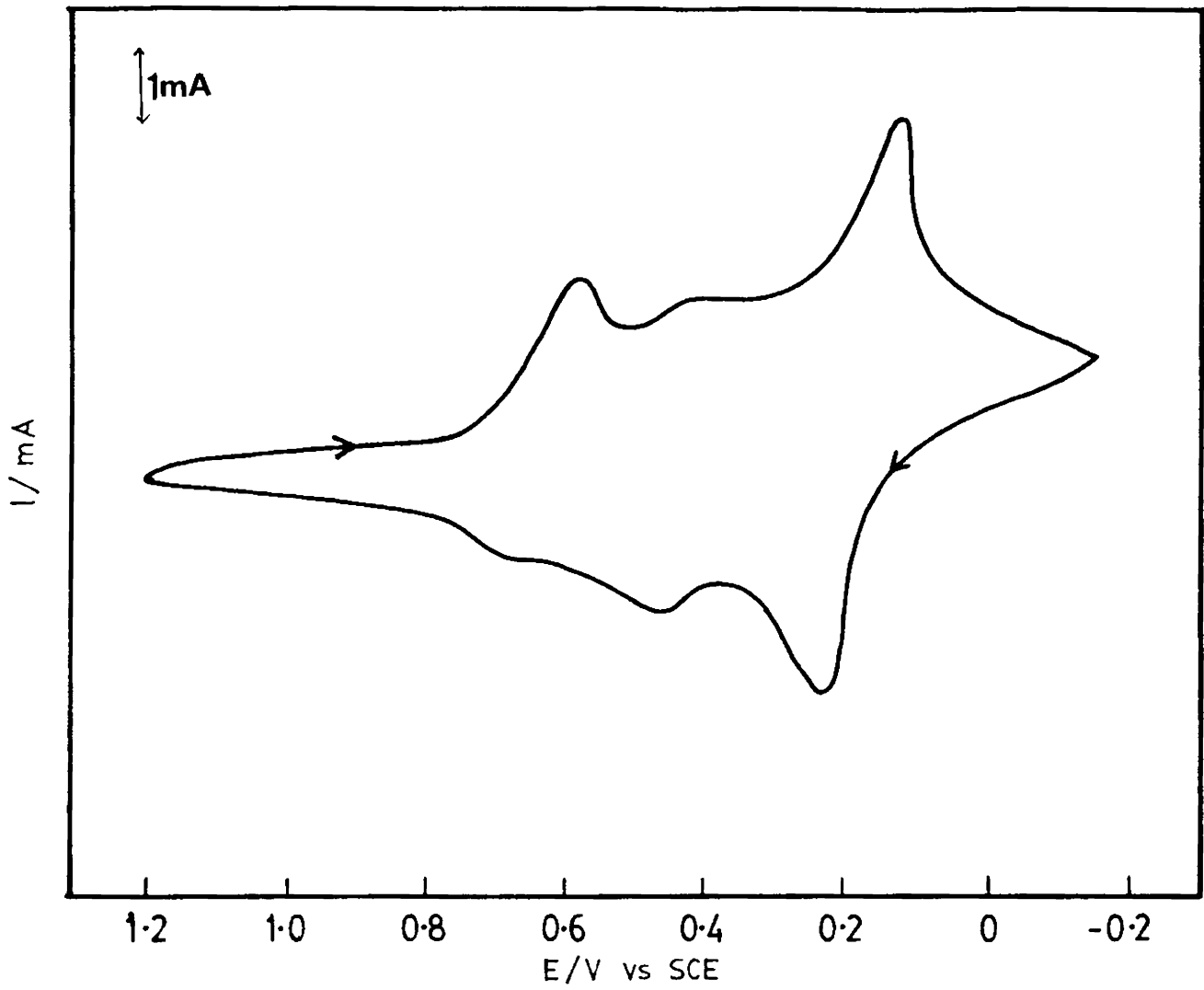


Fig. 5.2 Cyclic voltammetric behaviour of graphite/PA electrode in 0.5M H<sub>2</sub>SO<sub>4</sub>  
Scan rate : 100mV/s

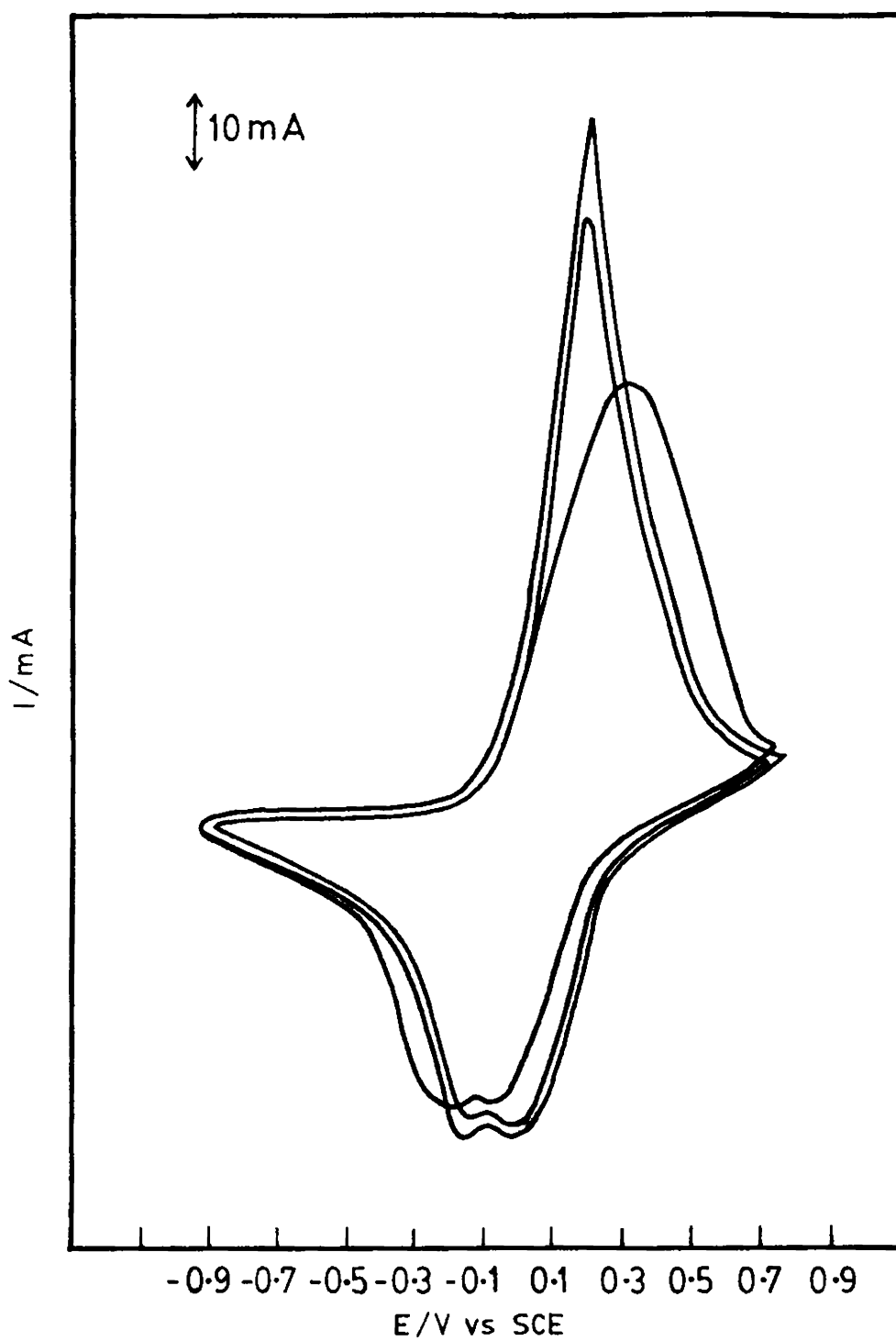


Fig. 5.3 Dependence of acid concentration on the cyclic voltammetric behaviour of graphite/PA electrode.  
Scan Rate : 100mV/s



Fig. 5.4 Cyclic voltammetric behaviour of PA film deposited on platinum electrode.  
Supporting electrolyte : 0.5M  $\text{H}_2\text{SO}_4$

## 5.6 Electrochemical Characterisation of Chemically Prepared Polyaniline.

The finely powdered polyaniline was made into a paste with carbon powder as described in section 3.5 and the potential was cycled in 0.5M H<sub>2</sub>SO<sub>4</sub>. The resultant cyclic voltammogram is shown in Fig.5.5. The CV shows three anodic and three cathodic peaks at the following potentials.

Anodic 0.78V, 0.56V and 0.24V and  
Cathodic 0.64V, 0.35V and 0.02V

The positions of the peaks depend on the sweep rate. The square root of sweep rate is proportional to  $i_p$  (Fig.5.6). The results demonstrate that carbon paste electrochemistry can be conveniently extended to the electrochemical study of chemically prepared PA. The electroactivity of PA/carbon paste electrode is comparable to that of graphite rod and platinum. The advantage of C/PA paste electrode compared to other electrodes are:

the electrode fabrication is simple

PA concentration can be conveniently controlled

electrode surface can be easily renewed and also ease of handling of powder on a larger scale.

## 5.7 Electrochemical Preparation (CoTSP-PA) Electrodes

PA film was doped with CoTSP anion by electrochemically polymerizing aniline in the presence of CoTSP. The CoTSP-PA was prepared in 3 different ways.

i) The graphite electrode was soaked in  $1.0 \times 10^{-3}$  M CoTSP solution for 20 minutes, washed with distilled water and a film of PA was deposited over it by the galvanostatic oxidation of aniline in 0.5M H<sub>2</sub>SO<sub>4</sub> at 2.5mA/cm<sup>2</sup>. This electrode is denoted by C/CoTSP/PA.

ii) A film of PA was galvanostatically deposited over the graphite as described above and then soaked in a solution of  $1.0 \times 10^{-3}$  M CoTSP for 20 min. The electrode was taken out and washed with distilled water. The resultant electrode is indicated by C/PA/CoTSP.

iii) The C/(PA + CoTSP) electrode was prepared as follows: A  $1.0 \times 10^{-3}$  M solution of CoTSP was mixed with 0.5M aniline in 1M H<sub>2</sub>SO<sub>4</sub>. Galvanostatic oxidation of aniline was done at a graphite electrode using this solution at a current of 2.5mA/cm<sup>2</sup>.

A film of CoTSP doped PA was formed at the electrode. This was washed with dil. H<sub>2</sub>SO<sub>4</sub> and then with distilled water. Similarly (Pt/PA/CoTSP) and (Pt/CoTSP + PA) electrodes were also prepared. The CoTSP doped PA carbon paste electrode was prepared by mixing 2 mg. of CoTSP + 10 mg of PA and 50 mg of graphite powder with 2 drops of nujol. This was made into a paste and introduced into the cavity of a glass tube (5 mm i.d) Connections were made as described in section 5.2

## 5.8 Electrochemical Behaviour of CoTSP-PA Electrodes

### 5.8.1 Graphite

When the PA is doped with CoTSP, in all the three cases, it was found that the 3 cathodic peaks are well defined particularly the middle peak which was not resolved in the case of bare PA. (Fig. 5.7) Compared to bare PA, the peak potentials are shifted to more negative values. The peak currents also increase substantially compared to those on PA films.



Fig. 5.5 Cyclic voltammetric behaviour of chemically prepared polyaniline-carbon paste electrode.  
Supporting electrolyte : 0.5M  $\text{H}_2\text{SO}_4$   
Scan rate : 100mV/s

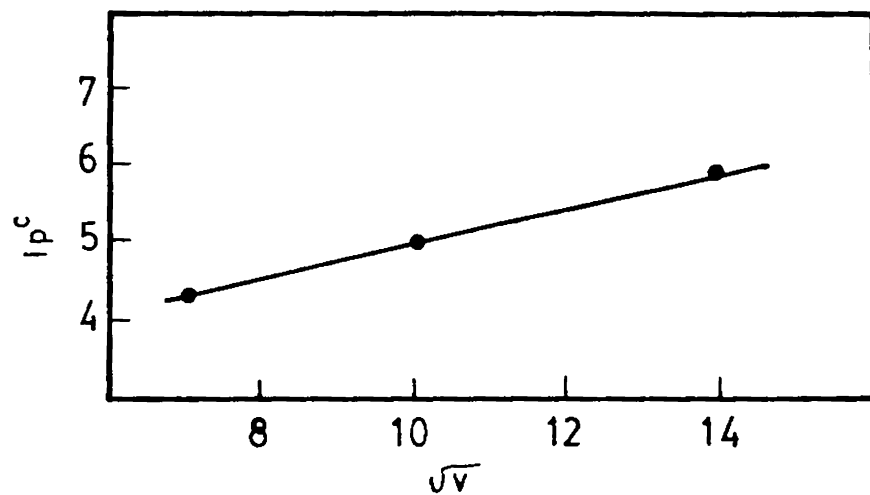
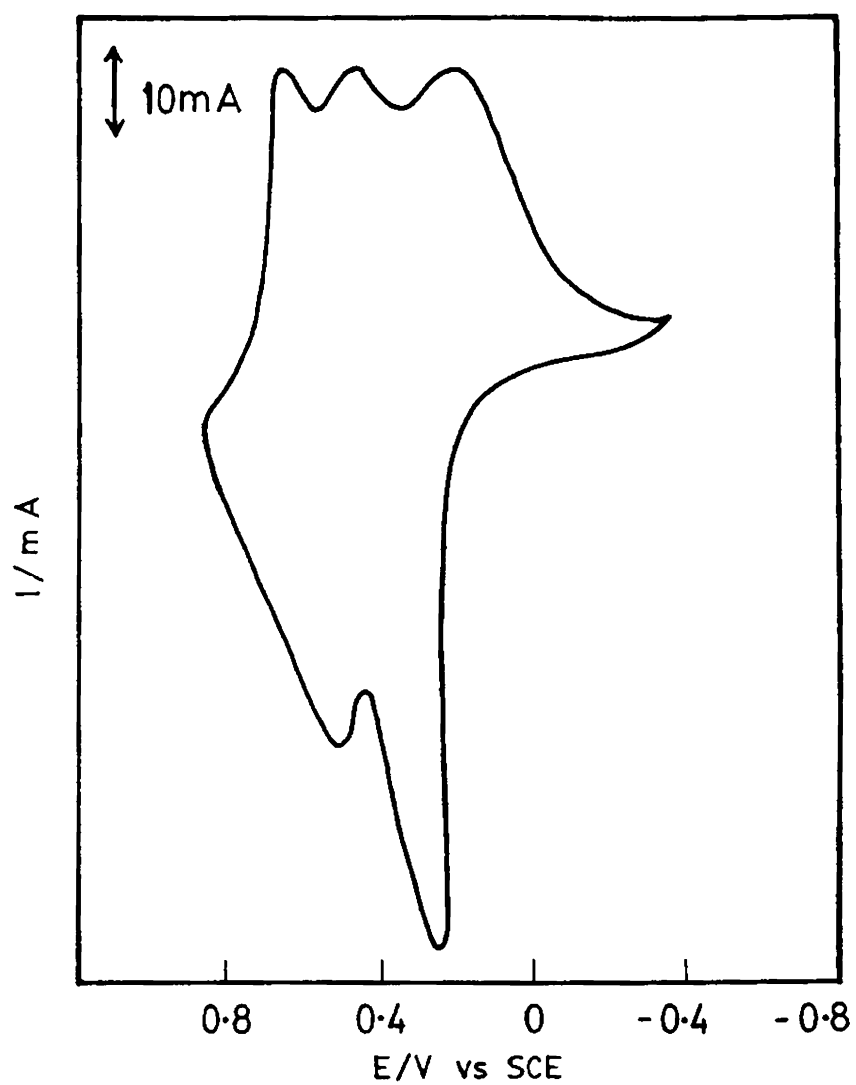


Fig. 5.6 Plot of anodic peak current vs square root of scan rate for the PA/carbon paste electrode



**Fig. 5.7** Cyclic voltammetric behaviour of CoTSP doped PA at graphite electrode  
Supporting electrolyte : 0.5M H<sub>2</sub>SO<sub>4</sub>  
Scan Rate : 100mV/s

## 5.8.2 Platinum

The CoTSP/PA showed the characteristic CV of the PA with a small shift in peak potentials. The cathodic peak observed in PA is absent in this case.

## 5.8.3 Carbon Paste Electrode

When CoTSP-PA/CPE is cycled in 1M H<sub>2</sub>SO<sub>4</sub> two cathodic peaks and a single anodic peak were noticed. The characteristics of all the peaks at different electrodes are given in Tabel I.

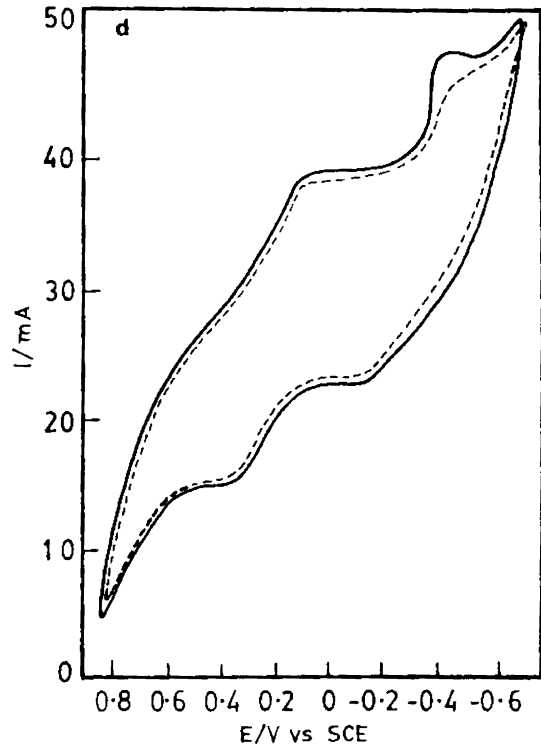
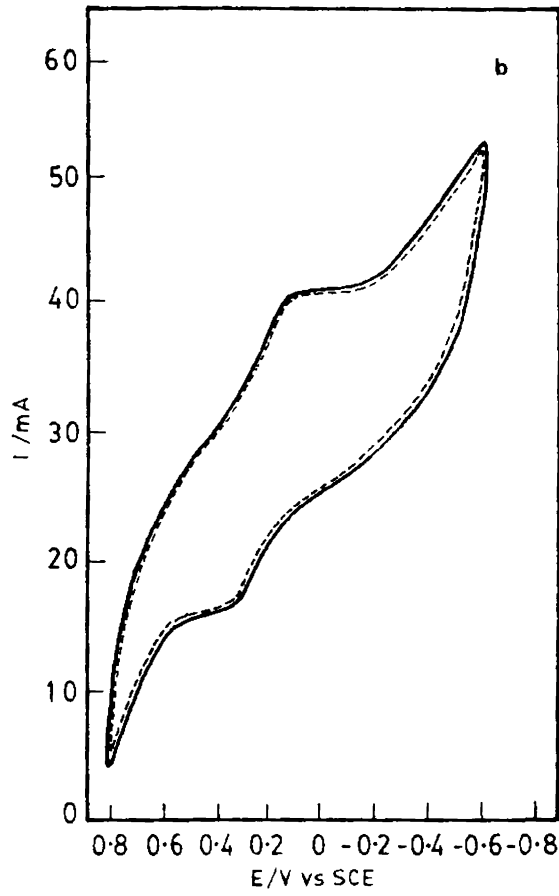
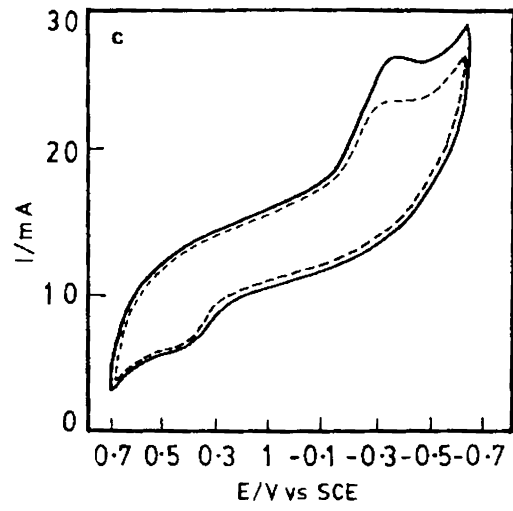
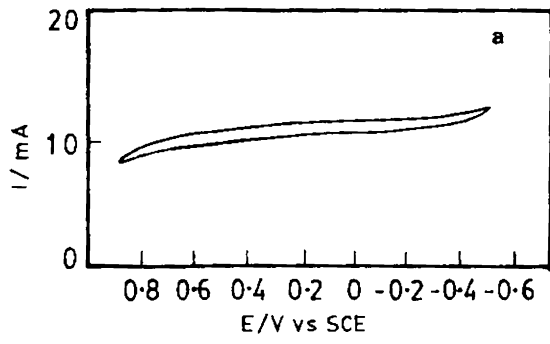
Sample	Epa <sup>I</sup>	Epa <sup>II</sup>	Epa <sup>III</sup>	Epc <sup>I</sup>	Epc <sup>II</sup>	Epc <sup>III</sup>
PA/Graphite	0.75	0.44	0.21	0.56	0.38	0.15
CoTSP PA/Graphite	—	0.45	0.23	0.54	0.33	0.09
PA/Platinum	0.71	0.45	0.17	0.68	0.4	0.06
CoTSP PA/Platinum	0.67	0.44	0.17	0.68	—	0.04
PA/Carbon Paste	0.78	0.56	0.24	0.64	0.35	0.02
CoTSP PA/Carbon Paste	0.62	—	—	—	0.32	0.04

## 5.9 DIOXYGEN REDUCTION

The solution was saturated with O<sub>2</sub> by flushing with O<sub>2</sub> for 10 min. The solution was made O<sub>2</sub> free by flushing with O<sub>2</sub> free nitrogen for about 20 min.

### 5.9.1 Graphite:

Dioxygen is not reduced at a graphite electrode in the applied potential range 1.2 to -0.6V vs SCE. Fig.5.8 shows the cyclic voltammetric behaviour of various graphite electrodes on which the following modifying deposits were formed. C/PA, C/CoTSP, C/PA/CoTSP, C/CoTSP/PA and C/(PA + CoTSP) towards the reduction of dioxygen in 0.5M H<sub>2</sub>SO<sub>4</sub>. At C/PA electrode with and without dissolved O<sub>2</sub>, the same CV is obtained. One cathodic peak at 0.14V and an anodic peak at 0.32V are observed (Fig.5.8b) which are the redox peaks of PA. This shows that C/PA has no catalytic activity for the reduction of O<sub>2</sub>. When CoTSP coated electrode is cycled in 0.5 M H<sub>2</sub>SO<sub>4</sub> O<sub>2</sub> is reduced at a potential of -0.35 V (Fig.9c). The peak is proved to be due to the reduction of O<sub>2</sub> by noticing the increase in the intensity of peak on flushing with N<sub>2</sub>. A cathodic peak at around 0.3V is also observed which may be due to the reduction of CoTSP anion.<sup>248</sup>



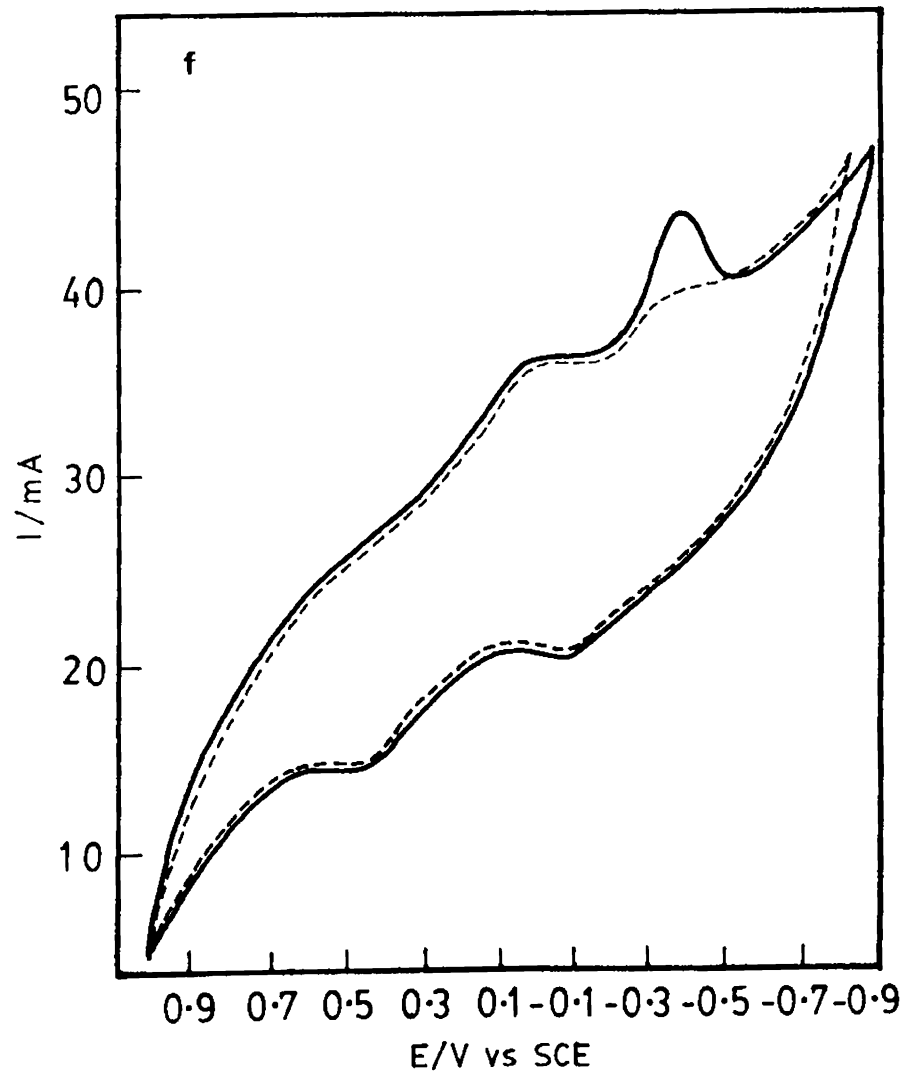
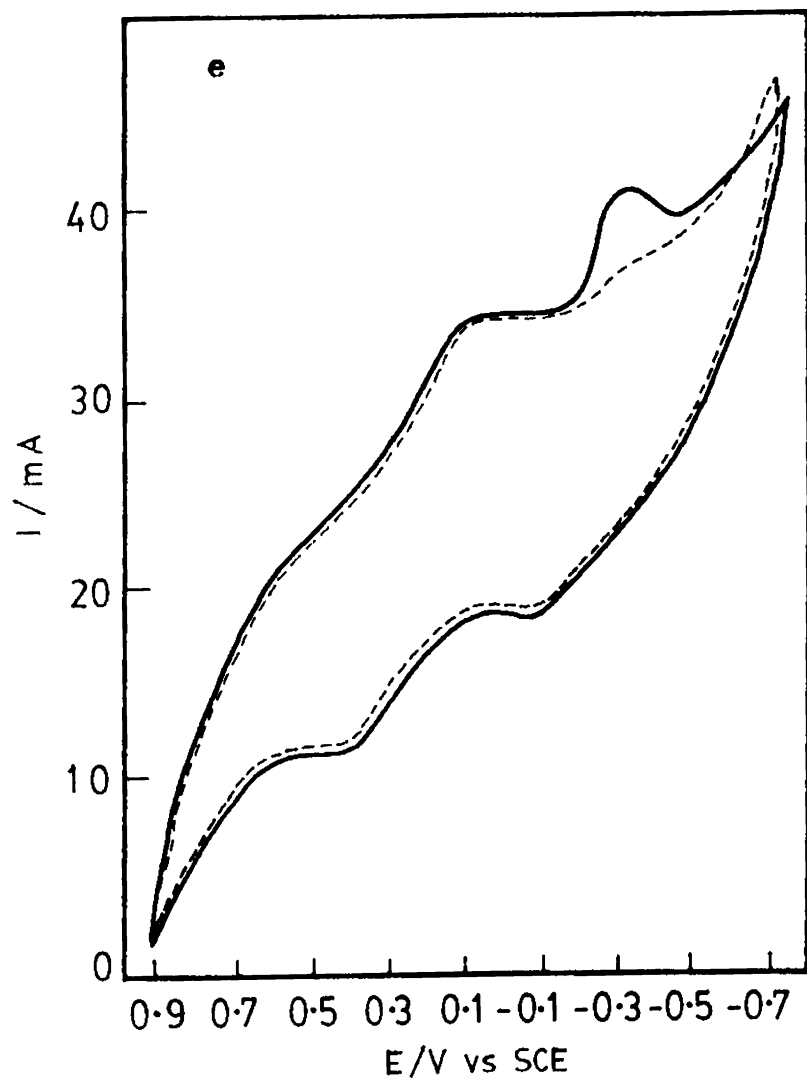


**Fig. 5.8** Cyclic voltammograms at various electrodes in  $O_2$ -saturated (—) and  $N_2$  saturated (- -)  $0.5M H_2SO_4$   
 (a) Bare graphite (b) PA/graphite (c) CoTSP/graphite (d) Graphite/PA/CoTSP (e) Graphite/CoTSP/PA  
 (f) Graphite/(CoTSP + PA)  
 Scan Rate : 100mV/s

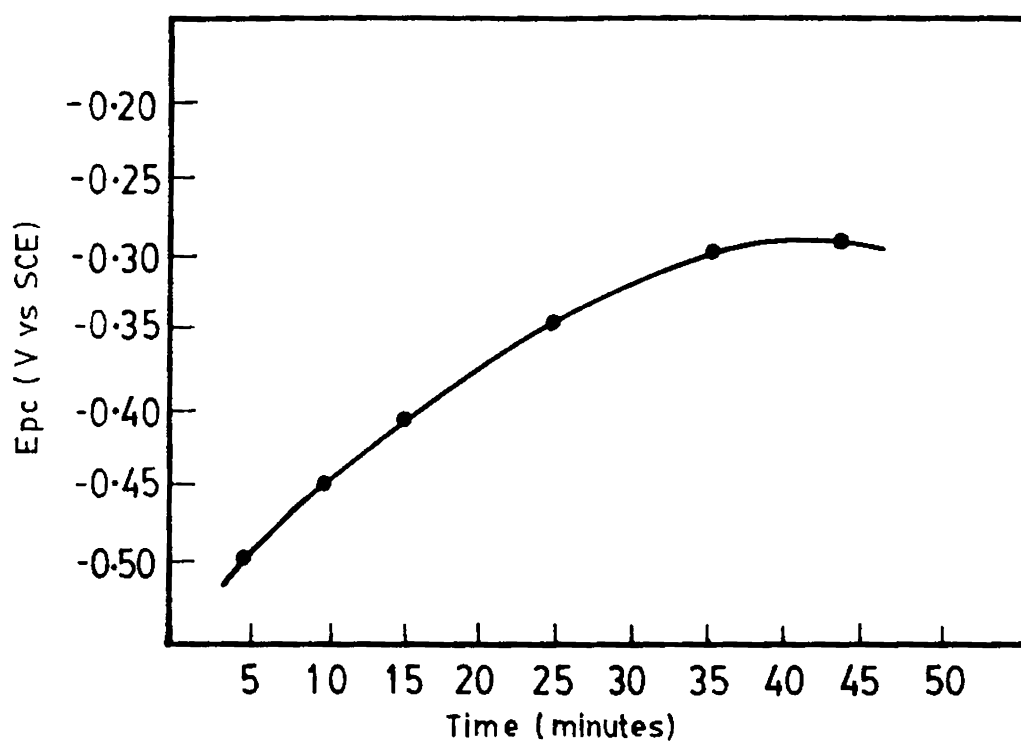
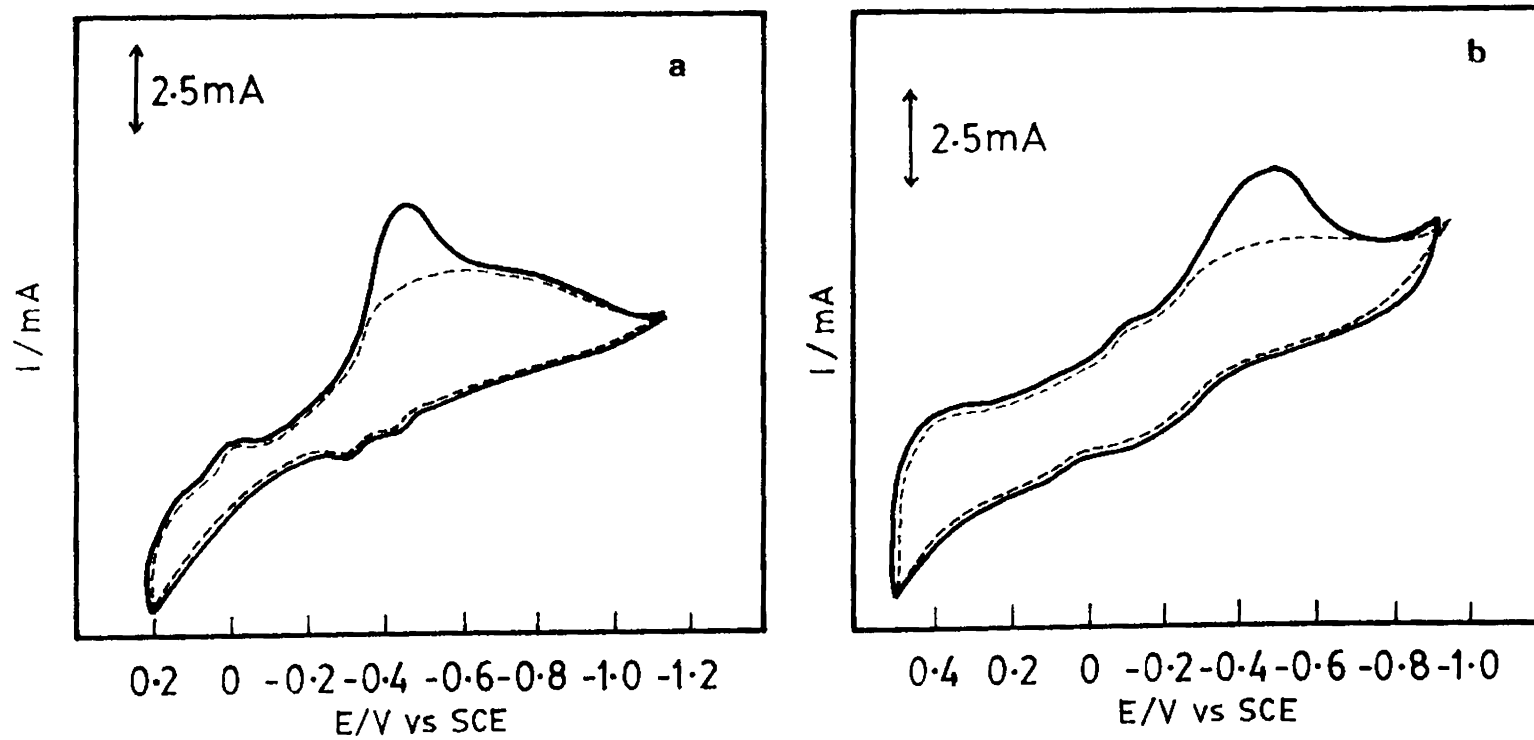


Fig. 5.9 Plot of peak potential vs time of polymerisation for the reduction of dioxygen at graphite/(CoTSP + PA) electrode.  
Supporting electrolyte :  $O_2$  saturated  $0.5M H_2SO_4$   
Scan rate :  $100mV/s$   
(—)  $N_2$  saturated



**Fig. 5.10** Cyclic voltammograms at various electrodes in  $O_2$  saturated  $0.5M H_2SO_4$   
 (a) Pt/(CoTSP + PA) (b) Pt/PA/CoTSP  
 Scan Rate :  $100mV/s$   
 (—)  $N_2$  Saturated  
 (---)  $O_2$  Saturated

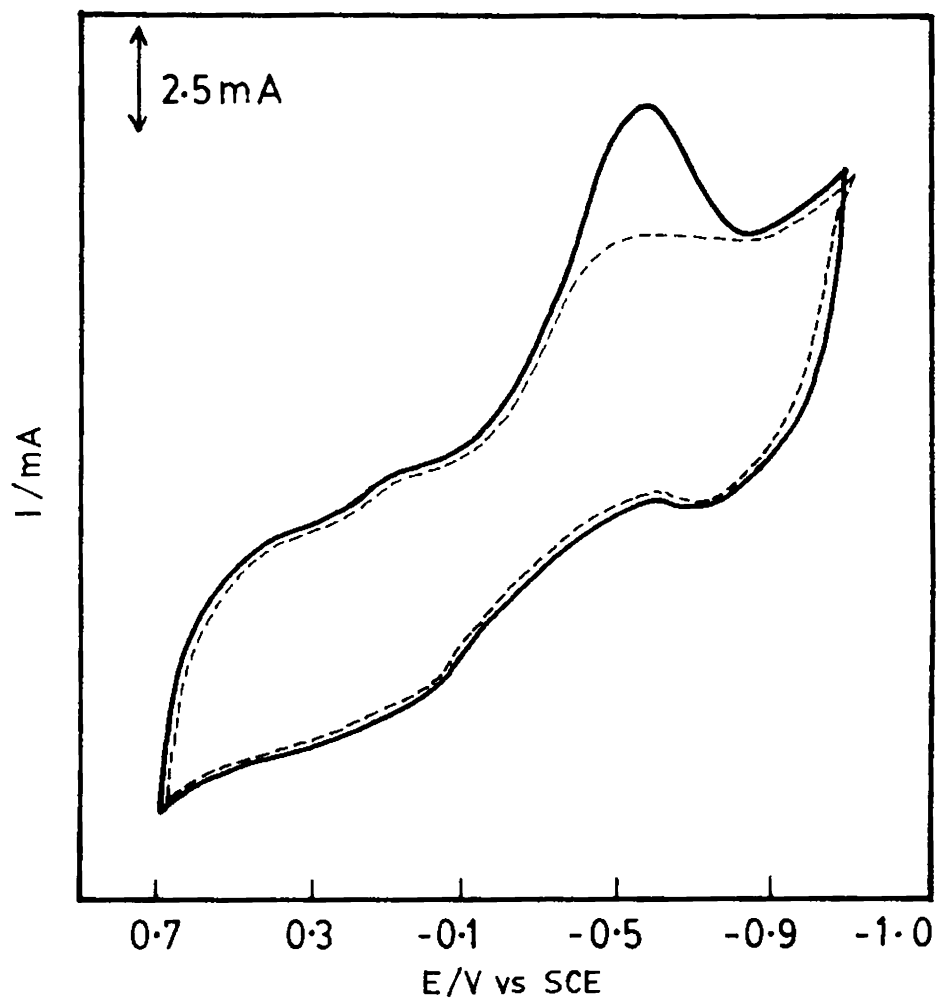


Fig. 5.11 Cyclic voltammetric behaviour of the carbon paste/(PA +CoTSP) electrode in O<sub>2</sub> saturated 0.5M H<sub>2</sub>SO<sub>4</sub>,  
 Scan rate : 100mV/s  
 (—)N<sub>2</sub> Saturated.

also a catalytic wave for  $O_2$  reduction was observed but at a higher negative potential which is perhaps due to the resistance of the PA film for the smooth transfer of electrons. The peak current also decreases substantially. A cathodic peak at  $-0.3V$  is also noticed in the case of CoTSP/PA electrode.  $O_2$  is reduced at a potential of  $-0.43V$  Fig. 5.8e gives the cyclic voltammogram of C/CoTSP/PA. Compared to C/PA/CoTSP, this electrode is more sensitive to  $O_2$  reduction, gives a higher cathodic current at a less negative potential. The electrocatalytic activity is the greatest with C/(PA+CoTSP). In addition to the  $O_2$  reduction peak, a redox peak of PA and an anodic peak of CoTSP are also observed.

The dependence of peak potential for the  $O_2$  reduction on the time given for polymerization of (PA+CoTSP) electrode is shown in Fig.5.9. The electrocatalytic activity increasing with increase in thickness but only upto a certain thickness beyond which the activity is independent of film thickness.

### 5.9.2 At platinum

Dioxygen is reduced (Fig.5.10) at Pt(CoTSP + PA) but at a higher negative potential compared to on graphite/(CoTSP + PA) is required. Pt/PA/(CoTSP) reduces  $O_2$  but the potential shifts to a more negative side i.e.  $-0.49V$ . When a film of PA is deposited on this electrode the  $O_2$  reduction is inhibited. Both Pt/(PA + CoTSP) and Pt/(PA/CoTSP) give the  $O_2$  reduction peak only at  $pH < 3$ .

### 5.9.3 Chemically Prepared CoTSP Doped Polyaniline/Carbon Paste Electrode

Though chemically prepared polyaniline is active in  $pH < 3$ , this electrode does not give any catalytic peak for  $O_2$  reduction. Another interesting aspect is that when the carbon paste electrode is cycled in a solution containing (PA + CoTSP) washed with distilled water and again cycled in 1MKOH, gives a peak for  $O$  reduction with a peak potential of  $-0.52V$  (Fig. 5.11)

## 5.10 Conclusions

The CoTSP anion can be conveniently doped into PA film electrochemically by galvanostatically polymerising aniline in dil.  $H_2SO_4$  medium containing CoTSP. It is seen that the CoTSP doped into the PA film remains in the film even after a number of potential cyclings. Of the different electrodes prepared, C/(CoTSP + PA) showed the highest catalytic activity. The activity for the reduction of  $O_2$  at different electrodes are in the following order.

C/(PA +CoTSP)>C/CoTSP/PA>C/CoTSP>  
 Pt/(PA+CoTSP) = C/PA/ CoTSP>Pt/Pa/CoTSP >  
 C Paste (PA + CoTSP).

The potential for  $O_2$  reduction in the case of C/(PA + CoTSP) is increased with increase in thickness of the PA film. The stability of electroactivity of this electrode is greater than that of C/CoTSP electrode. At (PA +CoTSP) electrode it is likely that the catalytically active centres exist in a multimolecular layer. This is because as the thickness of the PA film increases the availability of active centres for the CoTSP incorporation increases and hence the catalytic activity. Since PA is a moderately conducting polymer, its conductivity in contact with a solution depends on the conditions in the medium.

## 5.11 Mediation of Electron Transfer By (CoTSP) Incorporated Into Poly *o*-Toluidine

The concept of controlling the course of an electrochemical reaction by altering the chemical structure of an electrode surface has been worked out by many researchers since 1973<sup>246-248</sup>. The main attraction of this concept is that the chemical nature of the electrode can be designed in such way as to facilitate the desired electrochemical reduction. The properties and structure of the electrochemically prepared polymer films depend on the experimental conditions such as electrode material pH of the medium, nature of supporting electrolyte, time for polymerization, temperature etc. Desired electrochemical properties can be imparted to such polymers by incorporating other electroactive species into them<sup>249</sup>.

The permeation of electroactive solutes through films of redox polymers and modification of electrode behaviour by the permeated species have been observed<sup>250</sup>. The dynamic behaviour of ionic redox species attached to conducting polymer matrices have been studied in detail<sup>251-253</sup>. The diffusion of ionic redox species into the polymer and the rate of heterogeneous electron transfer reaction on the film depend on the concentration of the incorporated redox species. This phenomenon is believed to play a critical role in the functioning of phospholipid bilayer membranes, corrosion inhibiting films on metals etc. Transport of charge and solutes through the redox polymer film coated on electrodes is important in electrocatalysis and photoelectrochemistry<sup>254-257</sup>.

The ionic polymer films can be used to bind ionic drugs and then its release can be triggered by neutralizing the charge on the polymer<sup>258</sup>. For example a neurotransmitter can be ionically bound to the polymer backbone of a polymeric electrode surface and it remains there until it is released by a pulse of cathodic current<sup>259</sup>.

The redox couples incorporated into polymer and polyelectrolyte coatings on electrodes exhibit a much wider range of effective diffusion coefficients than they do when they are in solution<sup>260-262</sup>. The electron exchange between the oxidized and reduced forms of a redox couple can contribute significantly to, or can even become the predominant mode of controlling the diffusion of redox species into such coatings.

Poly (*o*-toluidine), Poly (*m*-toluidine) and poly(*o*-ethyl aniline) have been recently reported to be synthesized chemically and electrochemically.<sup>263</sup> The properties and structure of the electrochemically prepared polymer films depend on the kind of monomer as well as on the experimental conditions such as electrode material, pH of the medium, nature of supporting electrolyte, time for polymerization etc. The incorporation of electroactive cobalt or iron tetrasulphthalocyanine anion into polypyrrole and polyaniline was reported<sup>264-265</sup>. These films have been used for oxygen reduction catalyzed by anion.

In this section, the behaviour of a (CoTSP) doped poly (*o*-toluidine) (POT) electrode in presence of ferricyanide/ferrocyanide couple in aqueous media is reported. The proposed aim is to bring out the role of ionically bound redox couple on an ionic polymer in its redox behaviour.

## 5.12 EXPERIMENTAL

### 5.12.1 Reagents

*o*-Toluidine was polymerized onto the platinum electrode from 0.01 M solution of *o*-toluidine in 2M HCl by cycling the potential between -0.2V and 0.7V vs SCE at a scan rate of 100 mVs<sup>-1</sup> (Fig. 5.12). The film coated electrode was washed thoroughly with 0.1M HCl. The

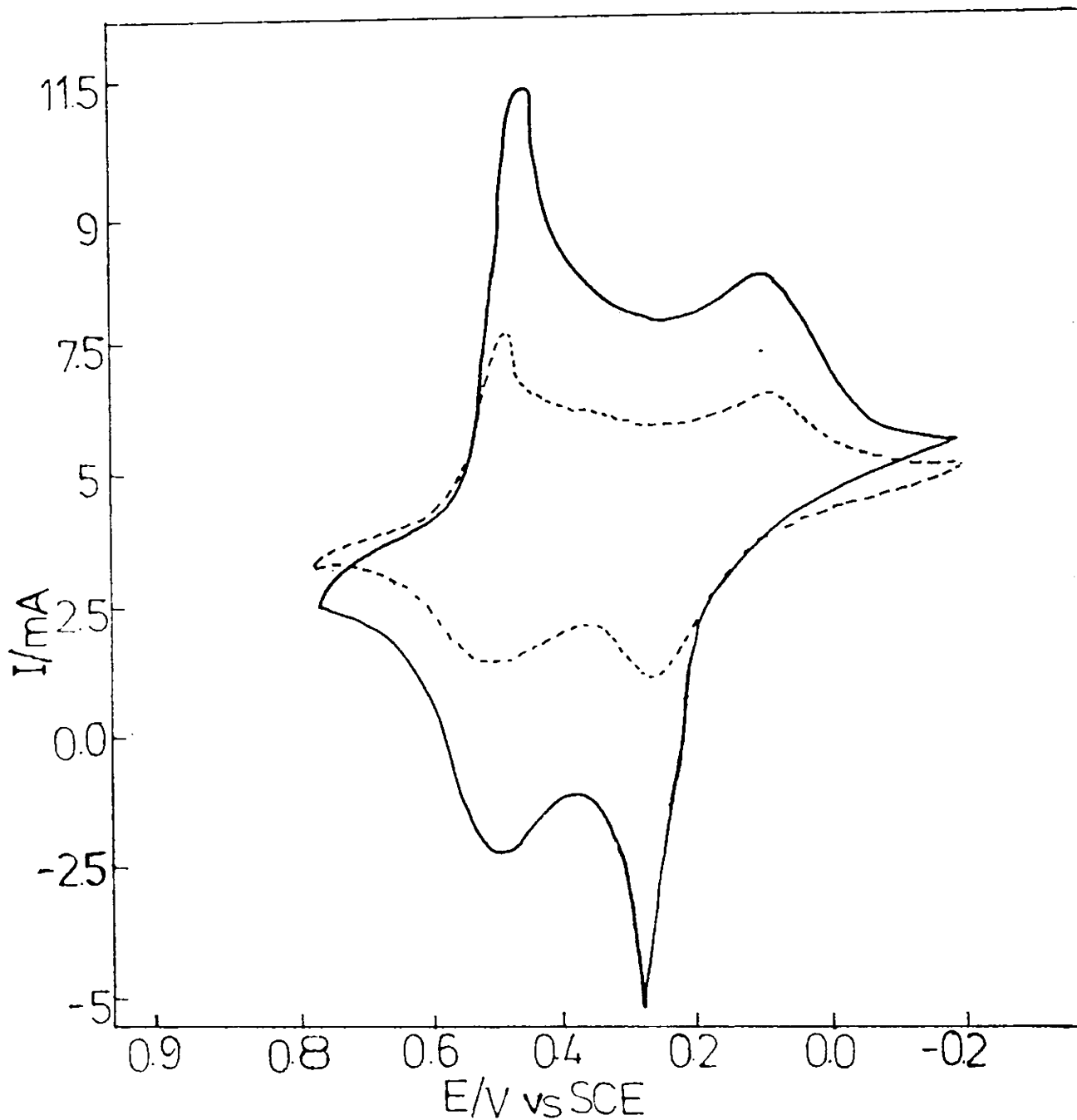


Fig. 5.12 Cyclic voltammograms for the oxidative polymerisation of poly (*o*-toluidine) from a solution containing 0.1M *o*-toluidine in 2M HCl.  
Sweep rate : 100mV/s  
(—) First scan; (---) After 20 cycles.

electrochemical polymerization was repeated using 1M H<sub>2</sub>SO<sub>4</sub> and

1 M HClO<sub>4</sub>

### 5.13 RESULTS AND DISCUSSION

Cyclic voltammograms of the monomer in the supporting electrolytes were recorded before electrochemical polymerization was done. The film formed from 1M H<sub>2</sub>SO<sub>4</sub> is found to peel off easily and from perchloric acid film formation is very slow. The cyclic voltammogram for the formation of POT film in hydrochloric acid medium is shown in Fig. 5.12. It is found that POT film formed in HCl medium is best studies for electrochemical studies. The cyclic voltammogram of a washed film run in 1M HCl is shown in Fig.5.13.

### 5.14 Incorporation of CoTSP into POT Film

CoTSP was incorporated into POT film by the procedure outlined above but from a medium containing 0.1M *o*-toluidine in 2M HCl and 1.0X10<sup>-2</sup> M CoTSP and by cycling the potential between -0.3V to 0.7V vs SCE or by galvanostating oxidation at a current density of 5mA/cm<sup>2</sup>. After uptake equilibrium was attained by multiple scanning the electrode was thoroughly washed with distilled water.

Ferrocyanide ion was incorporated into the (CoTSP + POT) film by exposing it to a solution of potassium ferrocyanide in 1M KNO<sub>3</sub> and by cycling the electrode between - 0.2 and 0.7 vs SCE. After uptake equilibrium was attained by multiple scanning (~ 2h) the film coated electrode was thoroughly washed with distilled water.

Mediation of faradaic reaction by the polymer modified electrode was evaluated by recording cyclic voltammograms of Fe(CN)<sub>6</sub><sup>4-</sup> in 1M KNO<sub>3</sub> solution. In neutral KNO<sub>3</sub> solution in the range of potential studied POT does not give any voltammetric peak. Hence under this condition the peak obtained is solely due to the Fe(CN)<sub>6</sub><sup>4-</sup> ion. Ferrocyanide ion gives a redox peak on poly (*o*-toluidine) but the peak currents are small and also the peaks are slightly distorted (Fig.5.14b). Continued contact of the film with ferrocyanide did not improve this behaviour. The incorporation of Fe(CN)<sub>6</sub><sup>4-</sup> into POT film was tried by cycling the electrode potential between 0.5V to -0.3V vs SCE for 1h in 1M KNO<sub>3</sub> containing 4.0 X 10<sup>-3</sup> M Fe(CN)<sub>6</sub><sup>4-</sup>. The electrode was washed thoroughly with distilled water and subsequent scanning in KNO<sub>3</sub> did not show any faradaic process indicating that Fe(CN)<sub>6</sub><sup>4-</sup> was not incorporated into the polymer film.

The pattern generated by cycling the electrode potential between 0.5 and -0.3V in 4.0 X 10<sup>-3</sup> M K<sub>4</sub>Fe (CN)<sub>6</sub> in 1M KNO<sub>3</sub> at (CoTSP +POT) electrode is given in Fig.5.14c. It is a typical cyclic voltammogram due to Fe (CN)<sub>6</sub><sup>3-/4-</sup> couple. After repeated cycling of the CoTSP/POT electrode in ferrocyanide solution, the electrode was taken out and washed with distilled water to remove any adhering solution. This electrode was scanned in 1M KNO<sub>3</sub> and the resulting cyclic voltammogram is given in Fig.5.14d.

The emergence of redox peaks for Fe(CN)<sub>6</sub><sup>3-/4-</sup> on a CoTSP modified POT film can be accounted for as follows. The redox peaks observed for Fe(CN)<sub>6</sub><sup>3-/4-</sup> on a CoTSP/POT electrode are not separated on the potential axis. This is strikingly similar to that obtained for redox ions incorporated into a cationic polymer domain by the electrostatic interactions between the cationic sites in the polymer and anionic redox species. During repeated potential cycling the peak height decreases during initial scans and then remains constant (Fig.5.15).

When *o*-toluidine is polymerized in presence of CoTSP, The CoTSP anion is incorporated

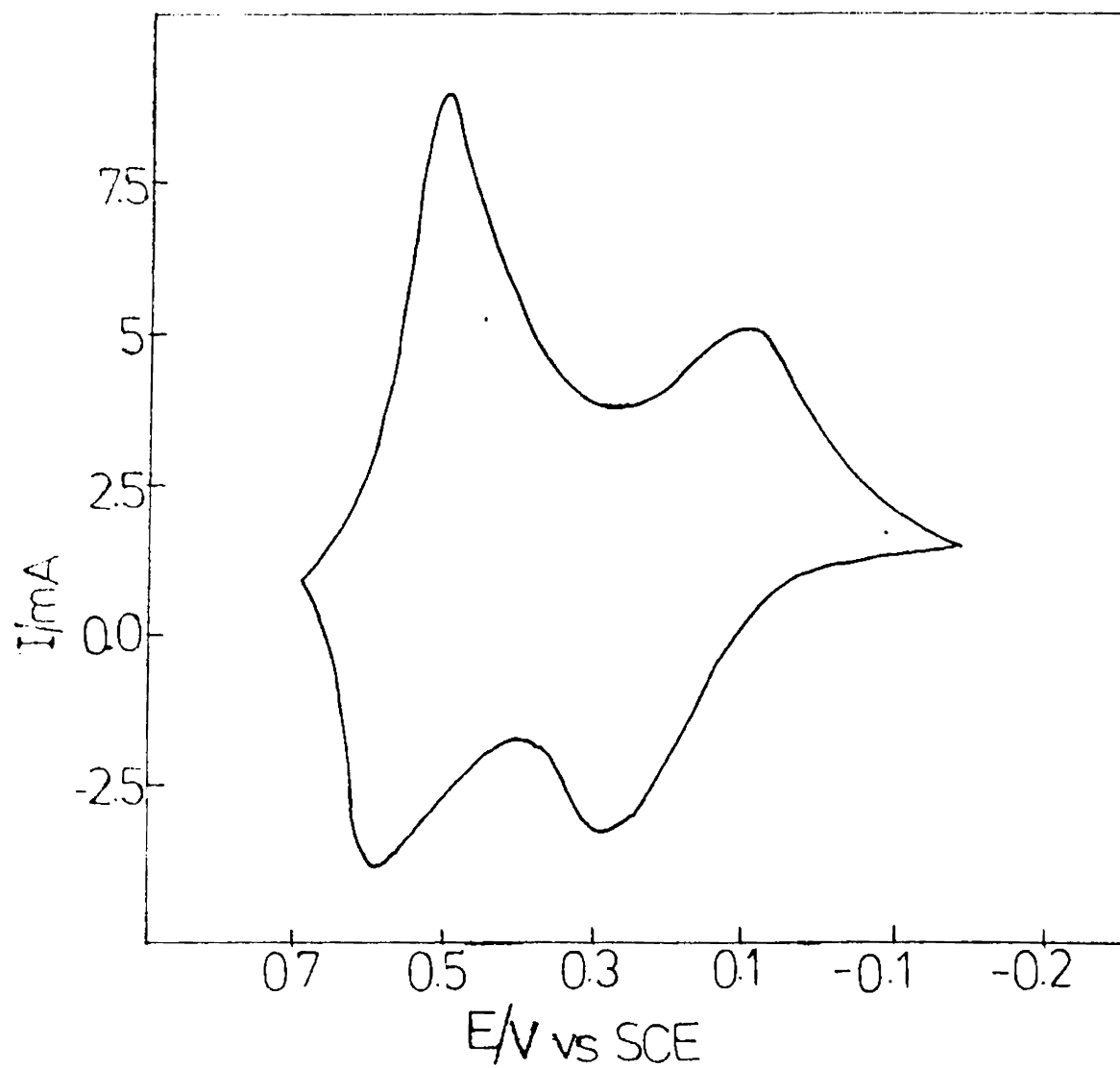


Fig. 5.13 Cyclic voltammogram of the resulting polymeric film described in Fig. 5. 12, which was cycled in 2M HCl.  
Scan rate : 100mV/s

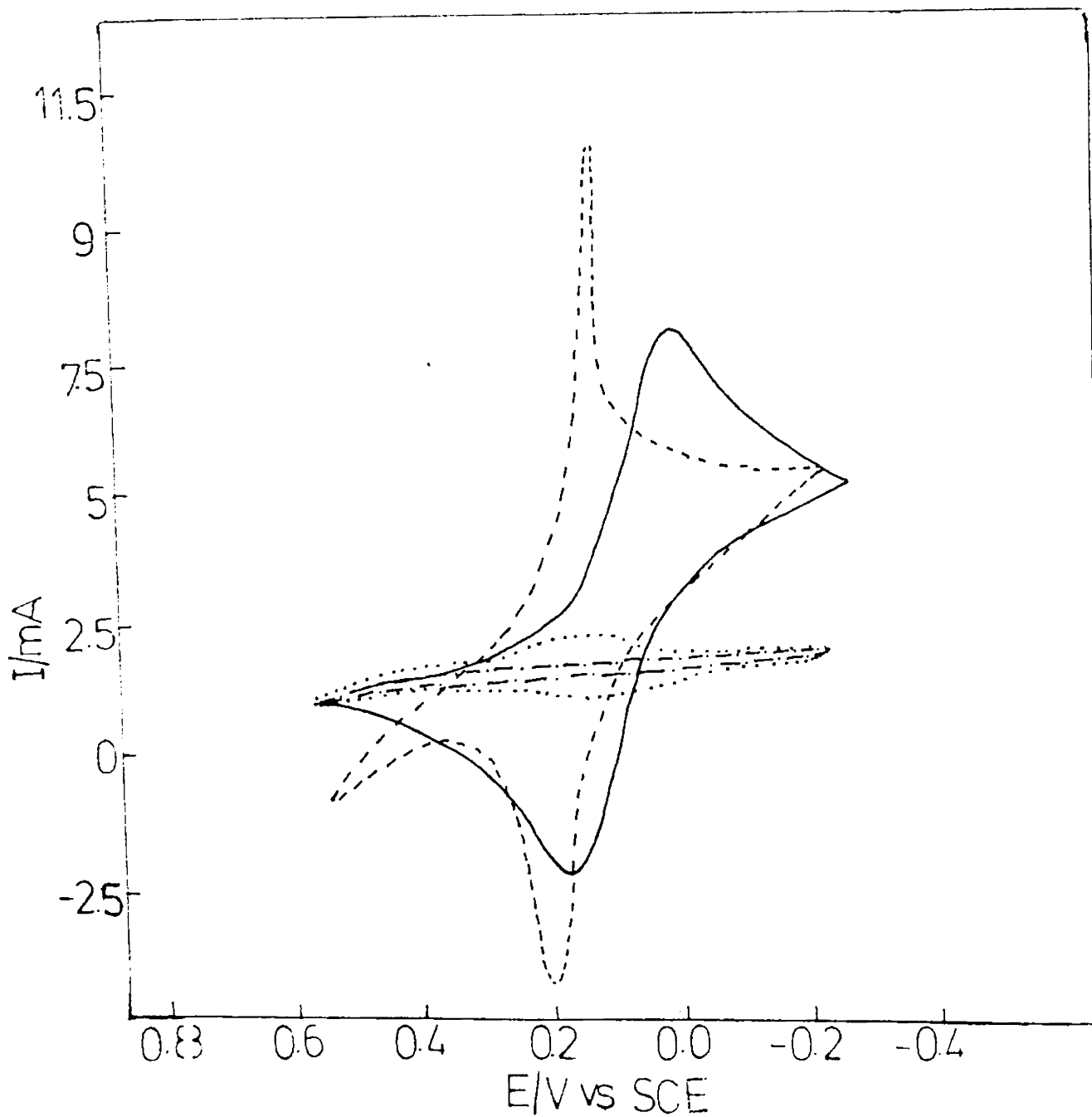


Fig. 5.14 Cyclic voltammogram of poly (*o*-toluidine) film on Pt electrode.

(a) 1M  $\text{KNO}_3$  (—●—) (b)  $4 \times 10^{-3}$  M  $\text{K}_4\text{Fe}(\text{CN})_6/1\text{M KNO}_3$  (- -) (c)  $4 \times 10^{-3}$  M  $\text{K}_4\text{Fe}(\text{CN})_6/1\text{M KNO}_3$  on poly (*o*-toluidine) modified with CoTSP (—) (d) Electrode used in (c) washed with distilled water and scanned in 1M  $\text{KNO}_3$  (- -).

Scan rate : 100mV/s

Note : (CoTSP + POT) does not give any peak in this region of potential.

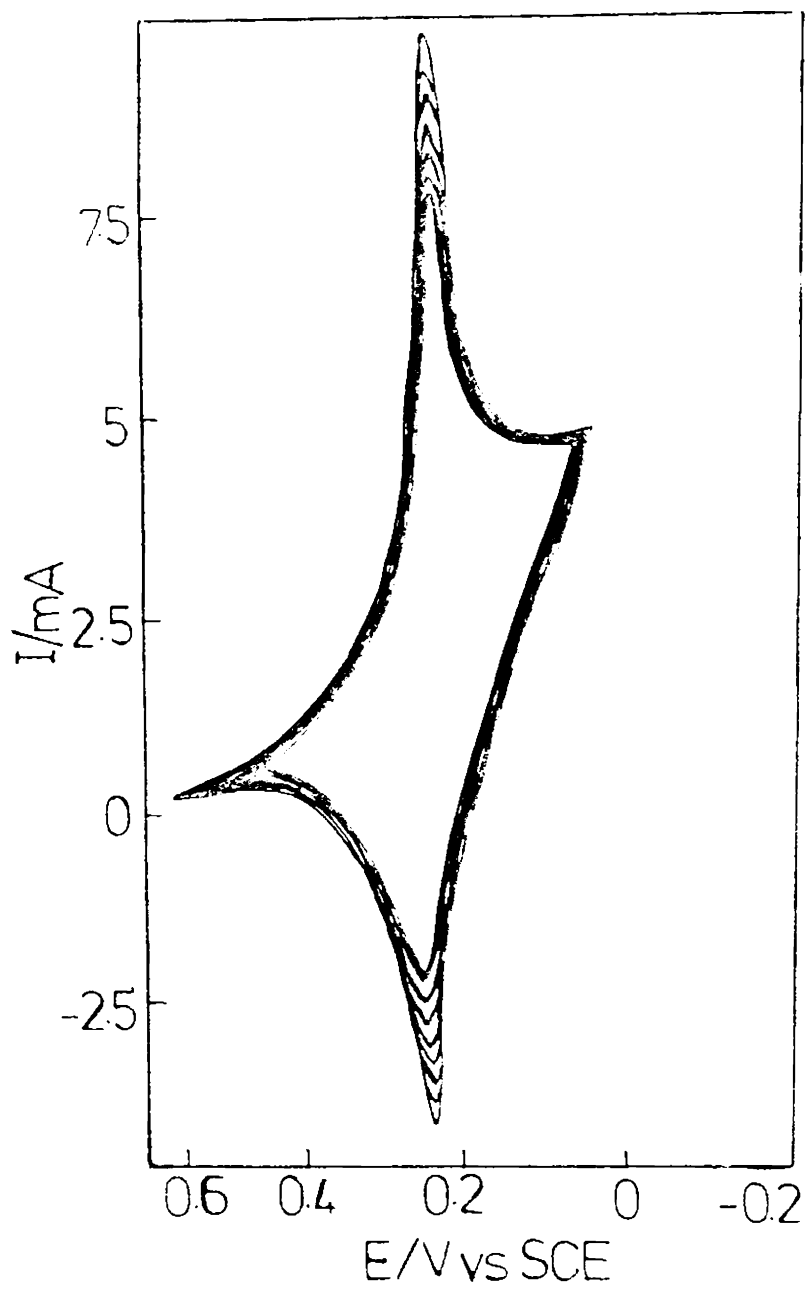


Fig. 5.15 Multiple scan cyclic voltammogram of  $\text{Fe}(\text{CN})_6^{4-}$  ion incorporated into (CoTSP + POT) film in 1M  $\text{KNO}_3$ .  
Scan rate : 100m V/s

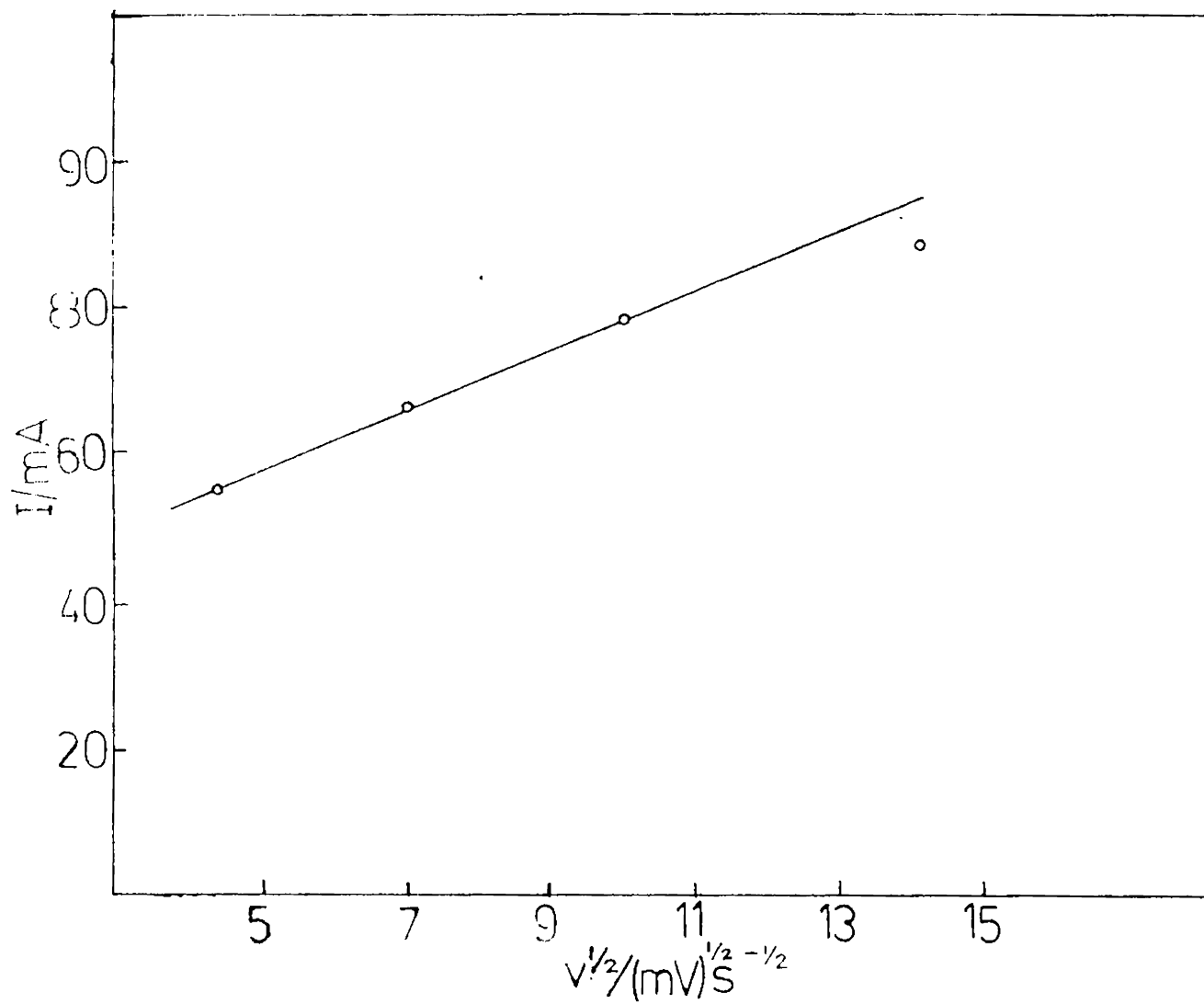


Fig. 5.17 The dependence of the cathodic peak current on square root of scan rate for the oxidation reduction of  $Fe(CN)_6^{3-/4-}$  redox couple on a (CoTSP + POT) electrode.

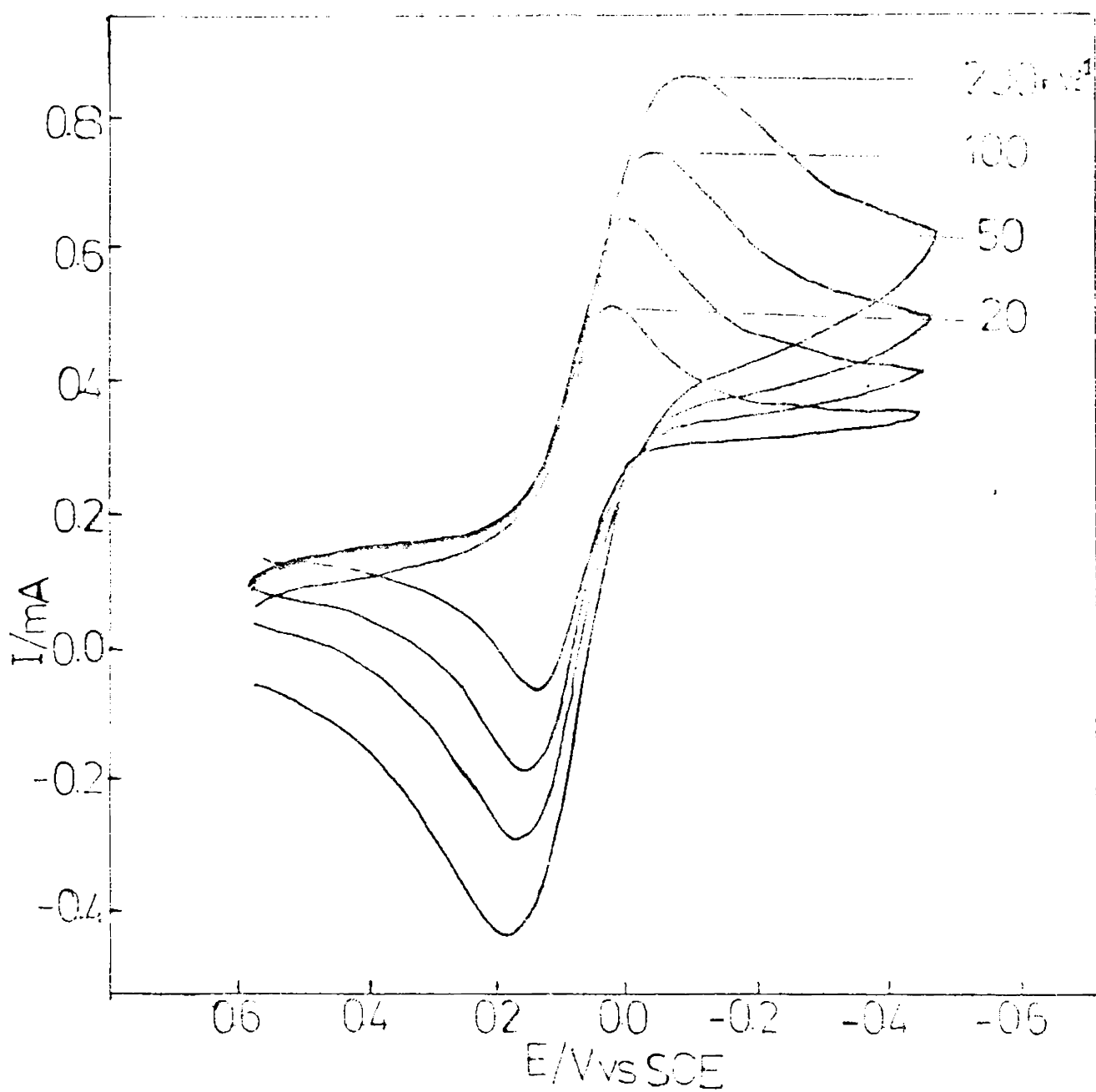


Fig. 5.16 Cyclic voltammogram for  $\text{Fe}(\text{CN})_6^{3-/4-}$  recorded at different scan rates on a (CoTSP + POT film deposited on Pt electrode in a 1M  $\text{KNO}_3$  solution containing  $4.0 \times 10^{-3}$  M  $\text{K}_4\text{Fe}(\text{CN})_6$

onto the poly *o*-toluidine as a counter ion to the cationic (protonated) polymer matrix. The same process takes place when the poly *o*-toluidine film is scanned in a solution of CoTSP. In this case the ion exchange is between the CoTSP<sup>-</sup> anion and supporting electrolyte anion (Cl<sup>-</sup> in this case) initially present in the film. When an electrode of this kind is scanned in a solution containing Fe(CN)<sub>6</sub><sup>3-4-</sup> species, two possibilities arise:

i) After incorporation of CoTSP anion, there may still exist vacant exchange sites in the poly *o*-toluidine skeleton. Ferrocyanide ion may get incorporated at these sites by a similar exchange of ions and

ii) When the CoTSP/POT film is subjected to potential cycling in K<sub>4</sub>Fe(CN)<sub>6</sub> solution, some of the loosely bound CoTSP ions are displaced from the film by Fe(CN)<sub>6</sub><sup>3-4-</sup> ions. The UV-Vis absorption spectrum of such a solution gives characteristic absorption profile of CoTSP. Under identical conditions CoTSP is not liberated into solution if potential cycling is not done indicating that desorption of CoTSP does not occur as a simple physical process.

### 5.15 Role Of CoTSP On The Cyclic Voltammetric Behaviour Of Fe(CN)<sub>6</sub><sup>3-4-</sup> Couple

When the CoTSP modified poly (*o*-toluidine) film is subjected to potential cycling between 0.5V to -0.3V vs SCE at a scan rate of 100mV/s for 1h in K<sub>4</sub>Fe(CN)<sub>6</sub> solution, some of the CoTSP is lost from the electrode giving rise to vacant sites where the Fe(CN)<sub>6</sub><sup>3-4-</sup> ions will be incorporated. After repeated cycling saturation of Fe(CN)<sub>6</sub><sup>3-4-</sup> uptake into the film takes place. This behaviour is substantiated by the following observations. When the (CoTSP + POT) electrode is scanned in Fe(CN)<sub>6</sub><sup>3-4-</sup> solution, during the initial cycles  $i_p$  is proportional to  $v$  (where ' $v$ ' is potential scan rate in mVs<sup>-1</sup>) which indicates that the process is diffusion controlled at this stage<sup>266</sup> (Fig.5.16 and 5.17). The same electrode when washed with distilled water and cycled in 1M KNO<sub>3</sub>, the cyclic voltammogram obtained is shown in Fig.5.14. The retention of CV peaks characteristic of ferrocyanide and zero potential separation for anodic and cathodic peaks and the direct dependence of peak current of scan rate suggest that the redox couple is entrapped in the matrix<sup>266-269</sup>

The linear dependence of on peak current on sweep rate when Fe(CN)<sub>6</sub><sup>3-4-</sup> is entrapped in (CoTSP + POT) film can be explained in the following manner. Unlike the solution case, simultaneous oxidation or reduction of the entire reservoir of redox centre take place. That is the amount of charge to be passed is fixed. Hence decrease in the time taken (increase in scan rate) must be accompanied by proportionate increase in current to maintain the current-time integral constant.

The amount of ferrocyanide incorporated into the polymer can be calculated from a measurement of the area of the cyclic voltammogram (for the oxidation-reduction reactions of Fe(CN)<sub>6</sub><sup>3-4-</sup> obtained at slow potential scan rates. Assuming that the surface redox couple obeys the Nernst equation, the peak current for the voltammogram is given by

$$i_p = n_2 F_2 T n / 4RT$$

Where 'T' is the total surface concentration of the adsorbed complex in moles/cm<sup>2</sup>, ' $v$ ' is the potential scan rate and  $n$  is the number of electrons per adsorbed molecule. The charge under the peak is equal to  $Q = nFT$ .

The quantity (T) of Fe(CN)<sub>6</sub><sup>3-4-</sup> incorporated into the (CoTSP + POT) film was estimated by measuring the area of the cyclic voltammograms for the oxidation of ferrocyanide obtained at

slow scan rate.

T value was calculated from the relation

$$\begin{aligned} T &= i_p \times 4RT / n^2F^2 \\ &= i_p \times 4RT / nF \text{ coulombs} \end{aligned}$$

The quantity of  $\text{Fe}(\text{CN})_6^{4-}$  incorporated was found to be  $2.98 \times 10^{-2}$  m moles/cm<sup>2</sup>

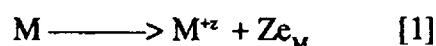
# CHAPTER VI

## Metal Tetrasulphophthalocyanine As Corrosion Inhibitors

### 6.1 Introduction

Corrosion is the deterioration of metals by electrochemical or direct chemical reactions and in that sense it is an industry in reverse<sup>271</sup>. Corrosion rate is influenced by factors such as nature of the metal, the corrodent, nature of the corrosion product temperature, electrical potential between two metals and the relative velocity of the corrodent with respect to the metal. The relationship among these factors determines the type of corrosion.

All metals except gold are thermodynamically unstable with respect to their oxides. Corrosion represents the tendency of pure metals and alloys to return to thermodynamically stable compounds. The fundamental process of corrosion is the anodic dissolution of the metal to form its ions.



The ions may be carried away into the bulk of the solution in contact with the metal or may form insoluble compounds which adhere on the metal surface. A layer of oxide or hydroxide may be formed on the surface and this is sometimes further converted to a higher oxide. Such layers may be porous allowing further corrosion (as with iron), or they may be compact and nonporous, forming a protective layer blocking further corrosion (as with aluminium).

When an isolated piece of metal is communicating with a corrosive medium the corrosion reaction represented by equation (1) cannot proceed unless another process takes place at the same rate to carry away the electrons accumulated in the metal. In most cases, spontaneous corrosion is accompanied by hydrogen evolution or oxygen reduction, although other cathodic reactions may serve the same purpose of consuming the electrons released in the anodic dissolution of the metal.<sup>272</sup>

Corrosion will be either accelerated or retarded by an applied electric potential by changing the chemical activity of metals relative to each other and to hydrogen. In general, if an applied potential lowers the activity of metal below to each other and to hydrogen, corrosion is retarded or stopped and the metal is said to be cathodically protected. Cathodic protection can also be secured by using an external electrode that is more active than the metal being protected.

Active metals such as aluminium, titanium and high chromium (stainless) steel owe their good corrosion resistance under oxidising conditions to surface oxide film that is adherent and impervious, though of non oxidizing conditions. When this passive layer is not formed these metals may corrode quite rapidly. The acidity of the corroding medium and whether or not it is aerated also can affect the formation of passive layer.

In the case of spontaneous corrosion, when steady state is reached, the metal attains a constant potential,  $E_{\text{corr}}$  which is termed the *mixed potential or corrosion potential*. At this potential there is an anodic overpotential,

$$\eta_a = E_{\text{corr}} - E_{r,a}$$

driving the metal dissolution process, and a cathodic overpotential  $\eta_c = E_{\text{corr}} - E_{r,c}$  driving the

cathodic process.

The value of these overpotentials and hence the corrosion potential  $E_{\text{corr}}$  are determined by the condition that the anodic and cathodic process must occur at exactly the same rate.  $E_{\text{corr}}$  is determined by the reversible potentials of the two processes taking place as well as their exchange-current densities and the Tafel slopes, i.e. by both thermodynamic and kinetic factors.

When the corroding metal is connected to a source of current or potential and polarized anodically or cathodically with respect to its  $E_{\text{corr}}$  and if the anodic and cathodic processes are assumed to be linear in the Tafel region of  $E_{\text{corr}}$

$$\begin{aligned} i_{\text{corr}} &= i_{0,a} \exp (E_{\text{corr}} - E_{r,a}) / ba \\ &= \exp (- E_{\text{corr}} - E_{r,c}) / bc \end{aligned} \quad [2]$$

Where the subscripts a and c refer to the anodic and cathodic process respectively. The current which flows is given by

$$i = i_{0,a} \exp (E_{r,a} / b'a) - i_{0,c} \exp (-E - E_{r,c} / b'c) \quad [3]$$

When eq. [2] & [3] are combined

$$i = i_{\text{corr}} [\exp(E - E_{\text{corr}} / ba) - \exp(- E - E_{\text{corr}} / bc)]$$

The equation permits the electrochemical determination of the corrosion rate  $i_{\text{corr}}$  by extrapolation of the  $E$  vs  $\log i$  plot from high values of  $E - E_{\text{corr}}$  on either the anodic or cathodic side to the corrosion potential, or by measuring  $i$  as a function of  $E$  in the vicinity of  $E_{\text{corr}}$

The anodic and the cathodic reactions occur on different parts of the metal, which may be termed anodic and cathodic areas. These are determined by the structure and composition of the metal, mechanical strain (highly strained areas tend to be more anodic) partial contact with the corrosive medium (through fault coating), variation in the composition of the medium etc. Under steady state corrosion, the total anodic and cathodic currents must be equal, while the current densities may differ substantially depending on the relative magnitude of the anodic and cathodic areas.

## CORROSION PREVENTION

The methods of corrosion prevention are many and varied. Cathodic protection, anodic protection and inhibition are the electrochemical methods generally applied to prevent corrosion.

### 6.1.2 Protective films

During corrosion reactions, thicker films may also be formed on metals. However, the corroding condition determines whether these films are protective or not. In petroleum refineries ferrous sulfide corrosion will be protective if organic foulants are co-deposited as they are formed; whereas when formed alone, under clean conditions, it may turn to be non-protective.

The electronic conductor transports electrons released by anodic dissolution from the corroding surface to the cathodic surface where the electrons reduce the corroding agent. In aqueous

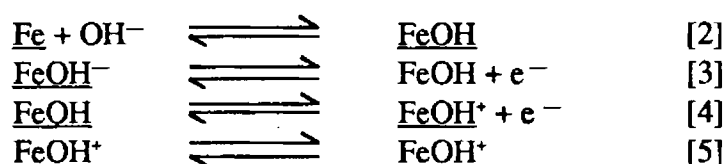
solutions the electron acceptor is usually dissolved  $O_2$ . Ionic conduction through the medium completes the circuit to the corroding surface. Because such a corrosion cell is a closed circuit, the overall rate of corrosion is limited to that of its slowest step, which may occur at the anode, or at the cathode.

### 6.1.3 At the Anode

For metal atoms to undergo anodic dissolution from bulk metallic phase to mobile ion, a thorough transformation is necessary. An atom, for example an iron atom must leave its tiny body-centred cubic form, pick up six coordinating ligands and lose two electrons.



The net reaction involves more steps in between. The most significant aspects of this anodic dissolution are adsorption, desorption and electron transfer as shown below



underlining in these equations indicates species that are adsorbed on the metal surface.

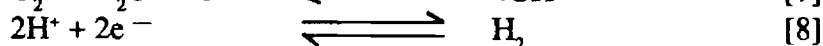
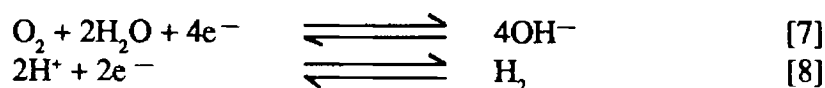
The adsorption-desorption steps (2) and (5) are obviously susceptible to environmental influences and thus to inhibition. Competitive adsorption from electrolyte constituents, such as chloride and benzoate or even neutral molecules, can either retard corrosion by repression step (2) or accelerate it by promoting step (5).

In anodic control of corrosion, passivation which is by far the most important phenomenon, and inhibitors can greatly broaden the range over which passivity can be obtained.

Anodic protection can be used successfully only in certain well defined cases which occur commonly in the chemical industry and in the storage of certain corrosive chemicals. The structure to be protected is made the anode, and its potential is set in the passive region.

### 6.1.4 At the Cathode

A cathodic process of corrosive reduction is the necessary complement of every anodic reaction. Only one of the two corrosives is involved in a great majority of practical corrosion problems dissolved dioxygen or hydrogen ion. The overall reactions for the cathodic reduction of these two are:



In the case of oxygen caused corrosion, the mass transfer of oxygen is usually rate-determining due to its low solubility.

In an acid-caused corrosion, when a hydrogen ion arrives at the cathodic interface it is adsorbed and reduced to adsorbed atomic hydrogen, as;



At this point, two alternative paths appear to be well established. Either hydrogen gas is formed by the combination of adsorbed hydrogen atoms,



or hydrogen gas is formed by reaction between an adsorbed hydrogen atom and a hydrogen ion plus an electron



In either case, desorption of the hydrogen molecule completes the process.



In the case of cathodic protection an external net cathodic current is allowed to pass through the metal so that the corrosion rate can be brought to the desired level. An active metal, generally zinc is used as a "sacrificial" anode in contact with the corrodable metal, and no external power source is required. The zinc serves as the anode and is slowly dissolved while the other metal is cathodically protected by the current passed.

### 6.1.5 Corrosion Inhibitors

Any electrochemical poison which retards either the cathodic or the anodic reaction involved in the spontaneous corrosion process, can retard the process itself. The corrosion inhibitors can be broadly classified into three groups viz., corrosive deactivators, adsorptive inhibitors and passivators, and corrosion product-barrier formers.<sup>274</sup>

### 6.1.6 Corrosive Deactivators

This approach is used to combat corrosion in boilers through removal of oxygen by chemical reaction with sulfite, or possibly with hydrazine. In a similar manner, acid corrosion can be stopped by neutralization with ammonia or other bases. This approach represents a direct frontal assault on the corrosion process; removes the corrodent and stops corrosion.

### 6.1.7 Adsorptive Inhibitors

In deaerated aqueous solutions, the corrosion is controlled mainly by the cathodic hydrogen evolution reaction. Since the rate limiting steps in cathodic reduction of hydrogen ion occur on the cathode surface, the adsorption characteristics of this surface determine the overall cathodic reaction rate to a large degree. Chemical factors affecting adsorption are (1) the inherent properties of the cathode material (2) the presence or absence of competing species.

Many compounds which are known to poison cathodic hydrogen evolution reaction (e.g.  $\text{As}_2\text{O}_3$ , pyridine, piperidine, some nitrogen-containing alkaloids) are found to be effective corrosion inhibitors. The action of such inhibitors is two fold. They are adsorbed on the surface of the metal (upto a monolayer or less) and physically block the sites on the surface at which hydrogen is evolved. The structure of the double layer is altered by adsorbing the inhibitor. Thus the specific electron

transfer rate constants for both the anodic and cathodic reactions may be changed even on sites which are not directly blocked by the adsorbed inhibitor.

### 6.1.8 Passive and corrosion product barrier formers

These act to varying degrees on both the anodic and cathodic reactions. In anodic reactions, the effects of these inhibitors are of a suppressing nature, whereas on cathodic reaction their effects are opposite. Thus, a passivator may increase potential cathodic-current density to exceed the critical anodic current density for spontaneous passivation, whereas a corrosion-product barrier may limit the cathodic reaction.

### Applications

Corrosion by strong acids (HCl and H<sub>2</sub>SO<sub>4</sub>) are usually inhibited by adsorption type inhibitors. With concentrated solutions, combinations of acetylenic alcohols and polar nitrogen compounds are most commonly used. Weak acids (H<sub>2</sub>S and CO<sub>2</sub>) can usually be effectively inhibited by nonacetylenic, adsorption type inhibitors.

### 6.1.9 Some general considerations

1. Effect of inhibitor on corrosion rate : minimum concentration exists below which it is not effective
2. Relation to surface area of metal : initial consumption in coating surface or reaction with existing scale.
3. Effectiveness as a function of time.
4. Tendency to be consumed by a reaction with ingredients of the medium.
5. Effectiveness under varied conditions, such as temperature, concentration of corrodent etc..
6. Effectiveness on already corroded metal.
7. Adverse effects on quality of product from the process.
8. Adverse effects on process, as for example, emulsification, impaired heat transfer etc..
9. Effect on other metals or on bimetallic couples that may be present.

## 6.2 INHIBITION OF CORROSION OF ALUMINIUM IN HYDROCHLORIC ACID BY METAL TETRASULPHOPHTHALOCYANINES

Metal phthalocyanines (MPcs) have a variety of electrochemical and surface adsorption properties by virtue of their molecular structure<sup>275-277</sup> The phthalocyanine moiety is planar and the electronegative groups are located at the centre. They have a strong tendency to be adsorbed on metal surface. The favourable characteristics of MPcs can be exploited for inhibiting corrosion if they are rendered soluble in aqueous medium.

Metal tetrasulphophthalocyanines (MTSP) form a class of unique water soluble pigments stable in acid and alkaline media. MTSPs withstand optical radiations and are not degraded by dioxygen even in strong alkali. The stability of MTSPs in a wide variety of environments and their electrochemical and adsorptive properties make them potential corrosion inhibitors.

In an uninhibited media the following electron transfer reactions which lead to the corrosion of aluminium take place;



This reaction can be further enhanced by the presence of species which break the protective oxide layer on aluminium. CoTSP is known to catalyse dioxygen reduction and has a tendency to be adsorbed on metal surface, whereas CuTSP is isostructural but its catalytic activity towards  $O_2$  reduction is less. Which one of these conflicting properties dominates can be ascertained by evaluating the corrosion inhibition efficiency of these two MTSPs. Advantageous solubility characteristics are found in MTSP and it is worthwhile to investigate the effect of metal phthalocyanines on the inhibition of aluminium dissolution in HCl medium. Inhibition activity has been measured by weight loss, thermometry, gas evolution and polarization methods and the thermodynamic parameters are reported.

## 6.2.2 EXPERIMENTAL

Aluminium strips (Indal 2S of the constitution, Si-0.3%, Fe - 0.5%, Ti -0.01%, B -0.05%, Ga - 0.02% and the rest Al) were used for the studies. The test pieces were polished with 4/0 grade emery paper degreased with alkaline solution (15g/l  $Na_2CO_3$  + 15g/l  $Na_3PO_4$ ) and washed with a copious amount of distilled water. They were washed with reagent grade acetone and dried by pressing between filter paper folds. A fresh test piece was used for each measurement. CoTSP and CuTSP were prepared and purified by the procedure of Weber and Busch<sup>278</sup>. Solutions of different concentrations were prepared from a  $10^{-2}$  M stock solution in water.

## 6.2.3 THERMOMETRIC METHOD

The test pieces of aluminium were bent to U shape and put in a reaction vessel which was insulated with foamed polystyrene to prevent heat loss. The temperature of the system was measured using a sensitive mercury thermometer, lower end of which rested on the dome of the metal specimen.

The dissolution of aluminium in hydrochloric acid is considerable at concentrations  $> 1.5M$ . Hence 2M HCl containing varying amounts of CoTSP was used as the medium.

## 6.2.4 WEIGHT LOSS METHOD

The test pieces were prepared as above, weighed, and immersed in 50 ml of test solution at room temperature for a period of 15 minutes. They were then washed with distilled water, dried and weighed.

## 6.2.5 GASOMETRIC METHOD

The dissolution of aluminium in 2M HCl with and without the inhibitor was studied by the hydrogen evolution method in the temperature range  $25^\circ$  to  $45^\circ$  C. The test pieces were prepared as above. A gasometric reaction vessel of the type shown in fig. 6.1 described by Hassan et al<sup>280</sup> was used. Temperature was controlled at  $\pm 0.1^\circ$  C by circulating thermostated water around the reaction vessel.

## 6.2.6 POLARIZATION STUDIES

Aluminium sheet of size 50X25X0.5 mm was used as the electrode. This was polished cleaned and dried as described above. A coating of wax was applied on the specimen using a mask, thus exposing only a defined area ( $2\text{ cm}^2$ ) to the medium. A platinum sheet was used as auxiliary electrode and saturated calomel was used as the reference electrode. Measurements were done in

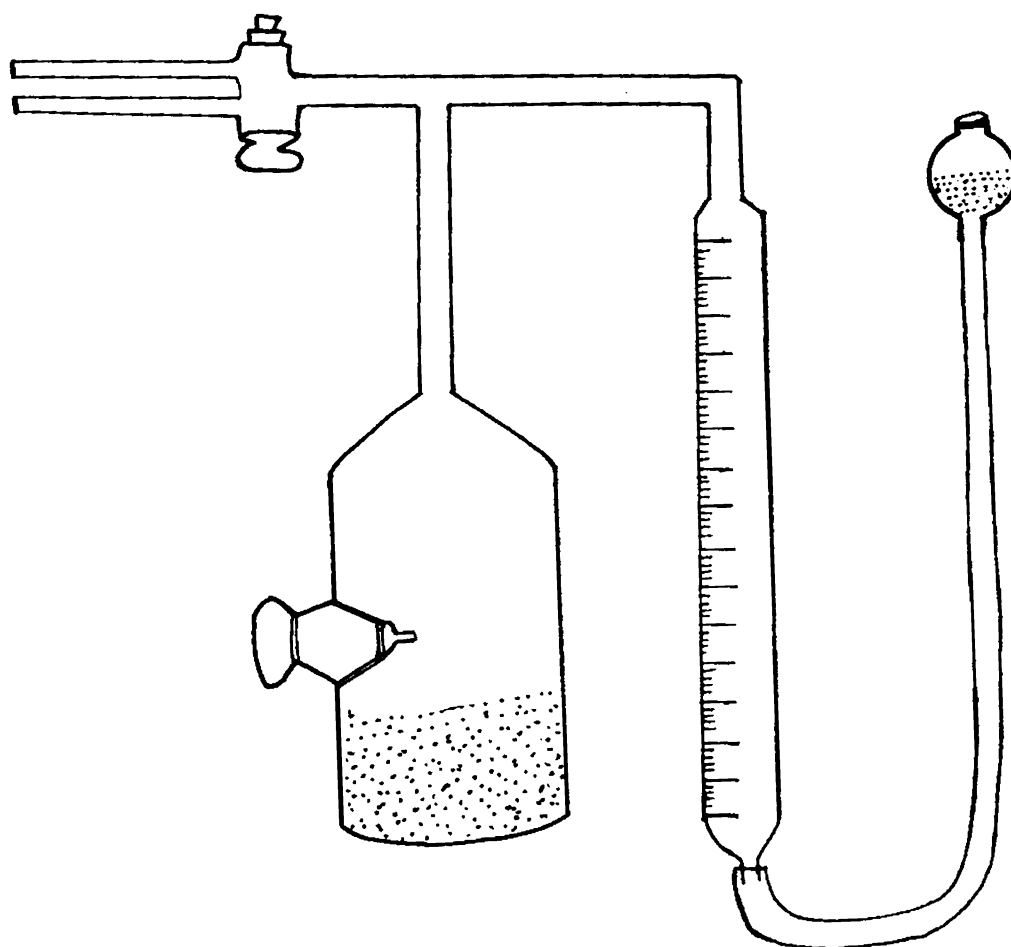


Fig. 6.1: Gasometric Reaction Vessel

the test solution (75 ml.) in an undivided cell. A scanning potentiostat/galvanostat (EG & G PAR Model 362) was used for the polarization studies. The test solutions were flushed with nitrogen for 30 minutes. Both anodic and cathodic polarization measurements were made.

### 6.3.3 RESULTS AND DISCUSSION

The inhibitor efficiency, I, is calculated from the weight loss method using the relation,

$$\%I = [\text{Wt. loss}_{\text{pure}} - \text{Wt. loss}_{\text{inh}} / \text{Wt. loss}_{\text{inh}}] \times 100$$

Fig.6.2 & 6.10 shows that the weight loss-time relationship for different concentrations of CoTSP and CuTSP also in their absence. The dissolution is markedly inhibited by the presence of MTSPs. The induction period is enhanced in presence of MTSP. This may be due to the protection of the oxide layer against dissolution by MTSP molecules adsorbed on the surface.

Thermometric method was used to evaluate the reaction number and percentage inhibition<sup>279,280</sup>. The reaction number is defined as

$$\text{RN} = [T_m - T_i / t] \text{ } ^\circ\text{C min}^{-1}$$

where,  $T_m$  &  $T_i$  are the maximum and initial temperatures respectively in  $^\circ\text{C}$  and 't' is the time in minutes taken to reach  $T_m$ . The percentage inhibition is calculated from the relation;

$$\%I = [\text{RN}_{\text{pure}} - \text{RN}_{\text{inh}} / \text{RN}_{\text{pure}}] \times 100$$

In Fig. 6.3 & 6.11 the variation of temperature with time for different concentrations of MTSP is shown. It is seen that the effectiveness of CoTSP and CuTSP inhibitors is distinct only in concentration exceeding  $10^{-5}$  M. Below this concentration, the inhibition efficiency sharply falls. The reaction number vs log C plot (Fig.6.4 & 6.2) also shows that RN is low upto  $10^{-5}$  M CoTSP.

At concentrations below this RN increases rapidly (Table II). This is in agreement with the temperature - time plot and the gravimetric results.

The inhibition efficiency is expressed by the percentage reduction in reaction rate as measured by gasometry according to the relation,

$$\% \text{ reduction in RR} = [R_{\text{free}} - R_{\text{inh}} / R_{\text{free}}] \times 100$$

where  $R_{\text{free}}$  and  $R_{\text{inh}}$  are rates of aluminium dissolution in the absence and in the presence of the added reagent respectively, both being measured for the same reaction time.

The rate of hydrogen evolution was determined at 25, 35,40 and 45° C at different concentrations of MTSP in 2M HCl. Typical results are given in Fig.6.5 and 6.13.

The plot of volume of hydrogen evolved vs time at different temperatures shows that the rate increases slowly during the initial period. Thermometric method also shows an incubation period for dissolution. This incubation corresponds to the breakdown of the oxide film present on the metal surface<sup>281</sup> by its dissolution in acid which does not involve hydrogen evolution. The post-incubation reaction of aluminium is linearly related to reaction time and this behaviour is characteristic of zero order reaction may be written in the form,  $x = kt$  where x is the fraction of aluminium converted into

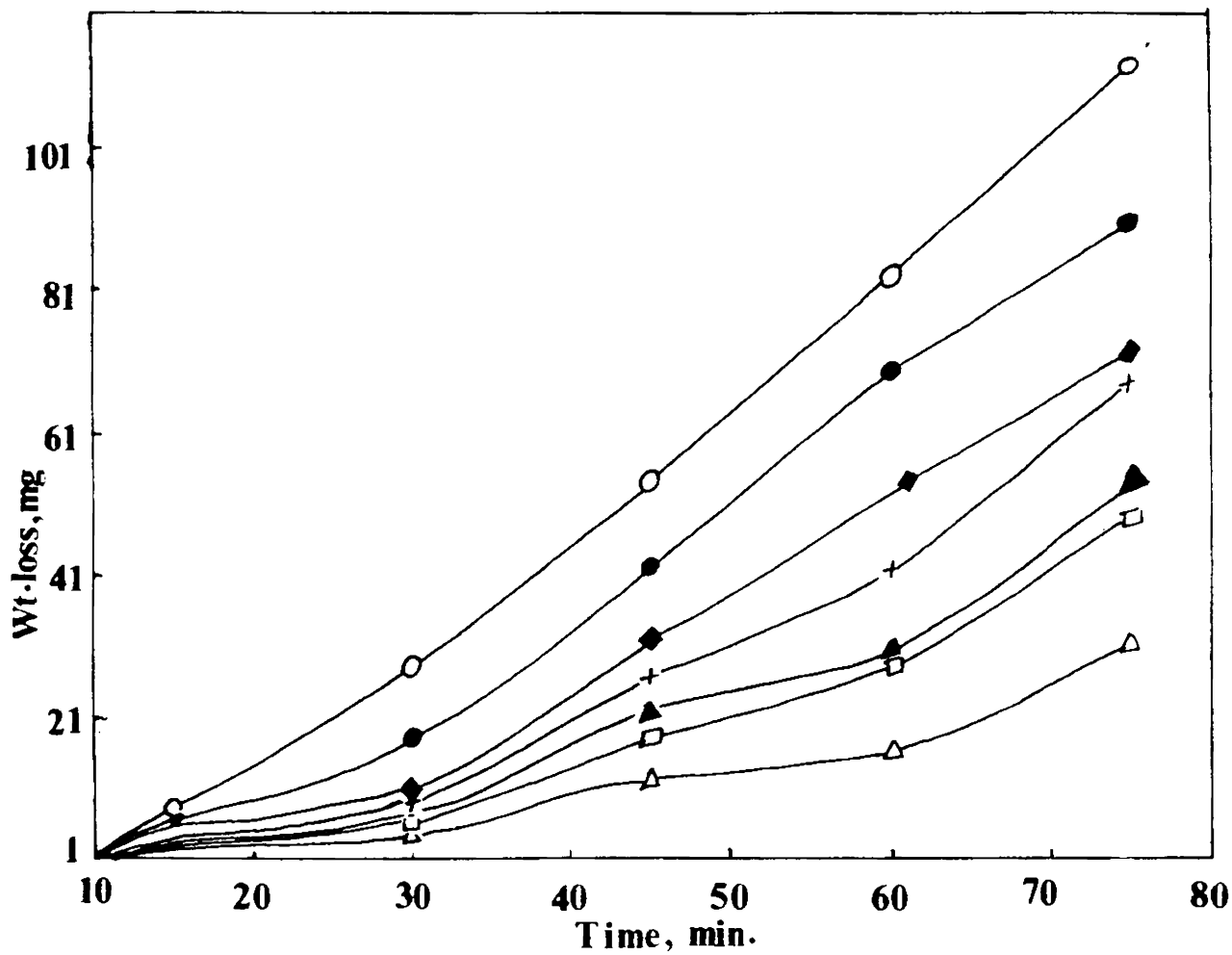


Fig. 6.2: Weight loss-time plot for the dissolution of aluminium in presence and absence of CoTSP; medium 2M HCl.  
 ○ HCl ; ●  $10^{-8}$  M; □  $10^{-7}$  M; ×  $10^{-6}$  M; ▽  $10^{-4}$  M; ▲  $2 \times 10^{-4}$  M

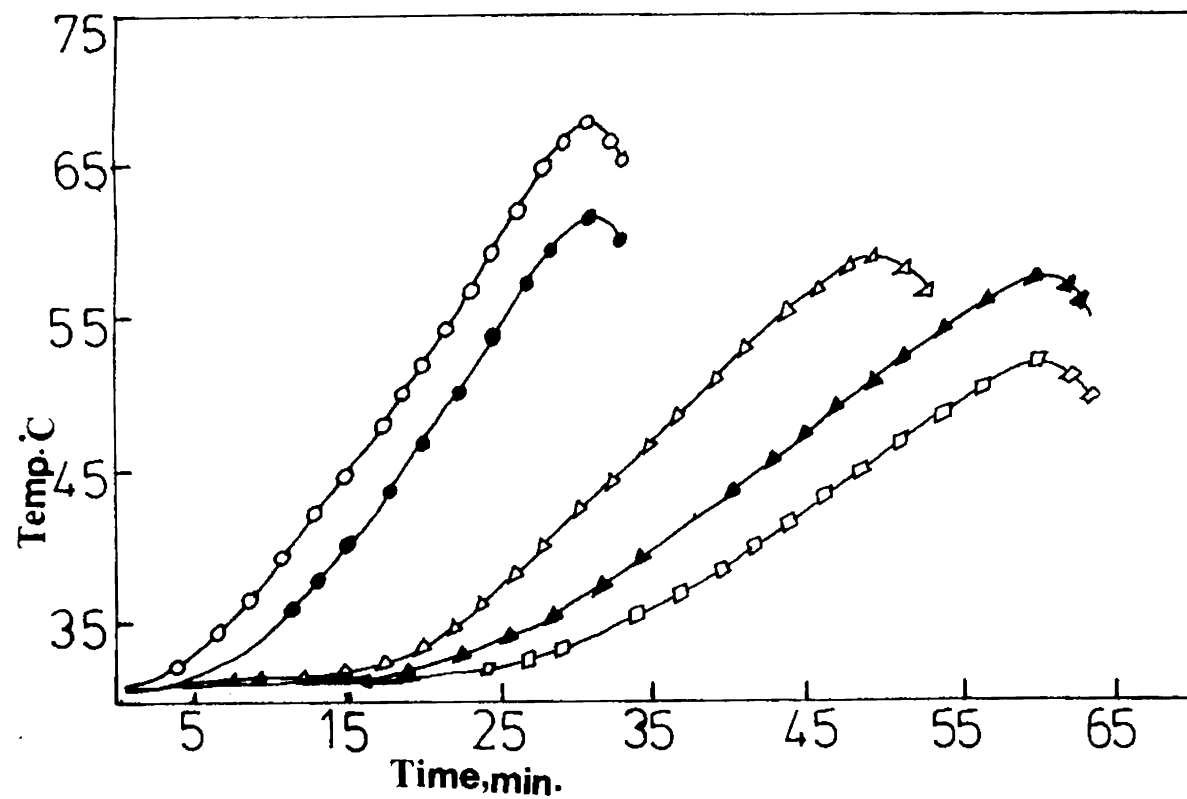


Fig. 6.3: Temperature- time plots for the dissolution of aluminium at different concentrations of CoTSP in 2M HCl  
 ○ HCl; ●  $10^{-7}M$ ; △  $10^{-6}M$ ; ▲  $10^{-5}M$ ; □  $2 \times 10^{-4}M$

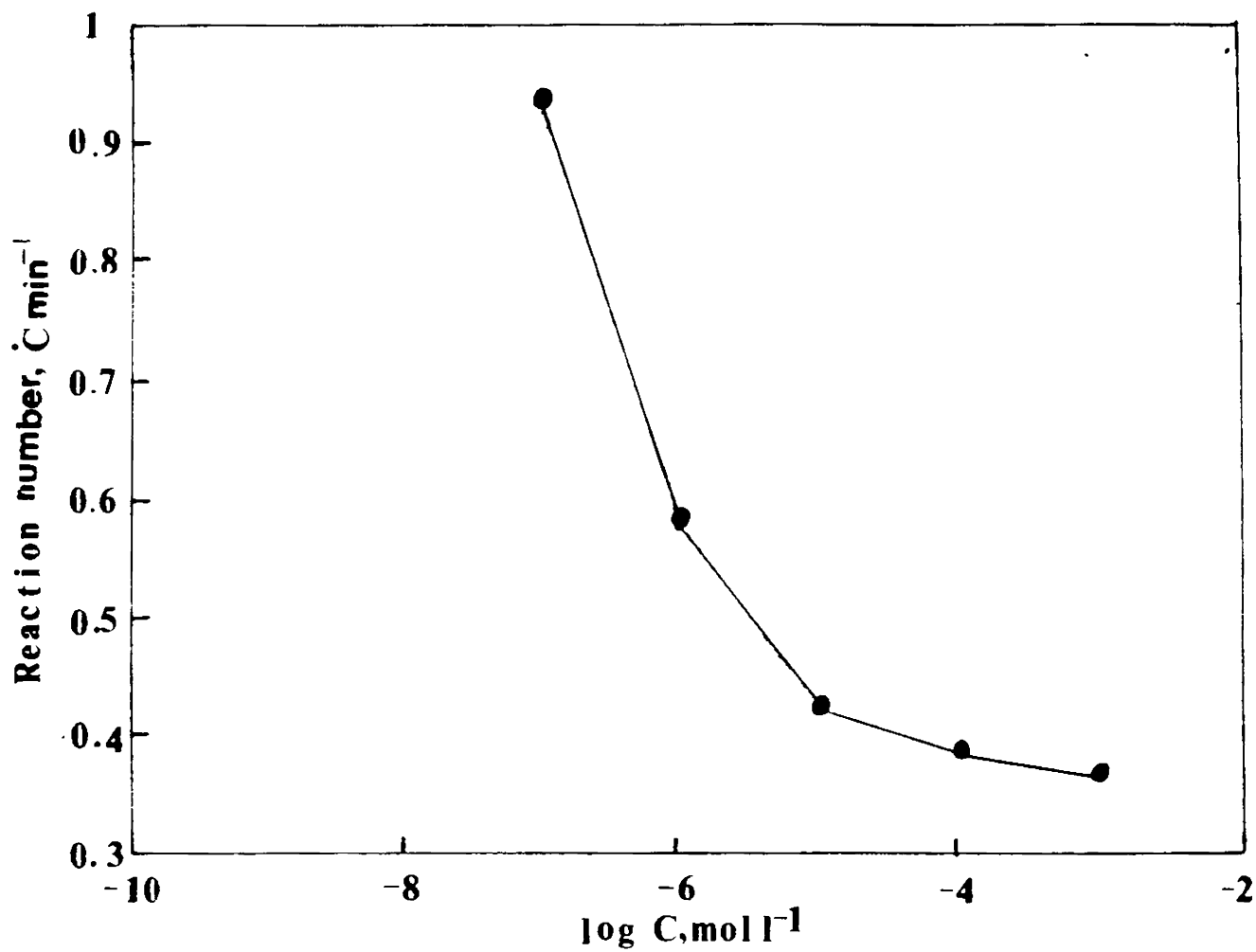


Fig. 6.4: Plot of  $\log C_{\text{CoTSP}}$  versus reaction number for the dissolution of aluminium in 2M HCl

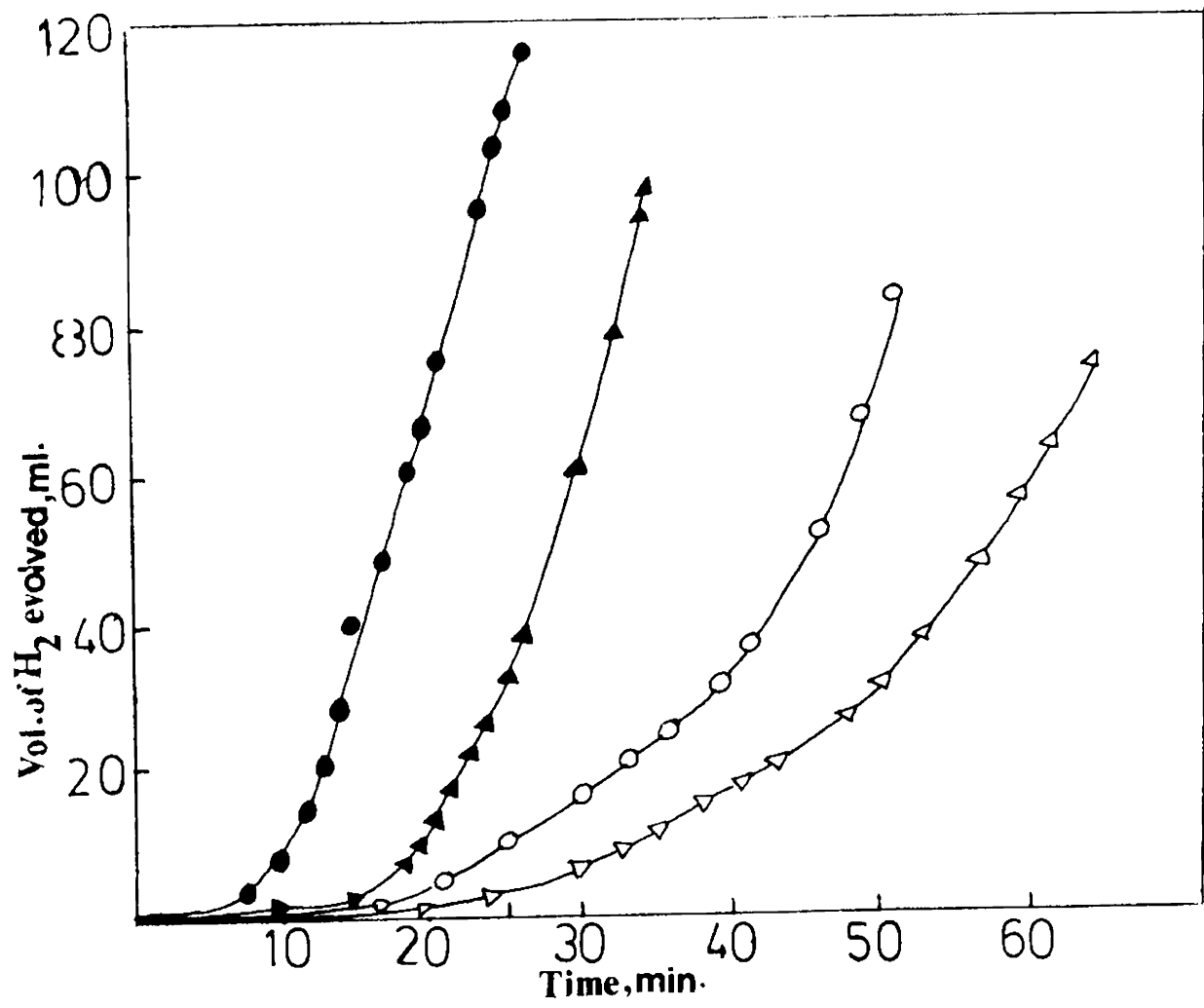


Fig. 6.5: Volume of hydrogen evolved- time curves obtained at various temperatures in 2M HCl Only.  
 ● 45°C;    ▲ 40°C;    ○ 35°C;    △ 25°C

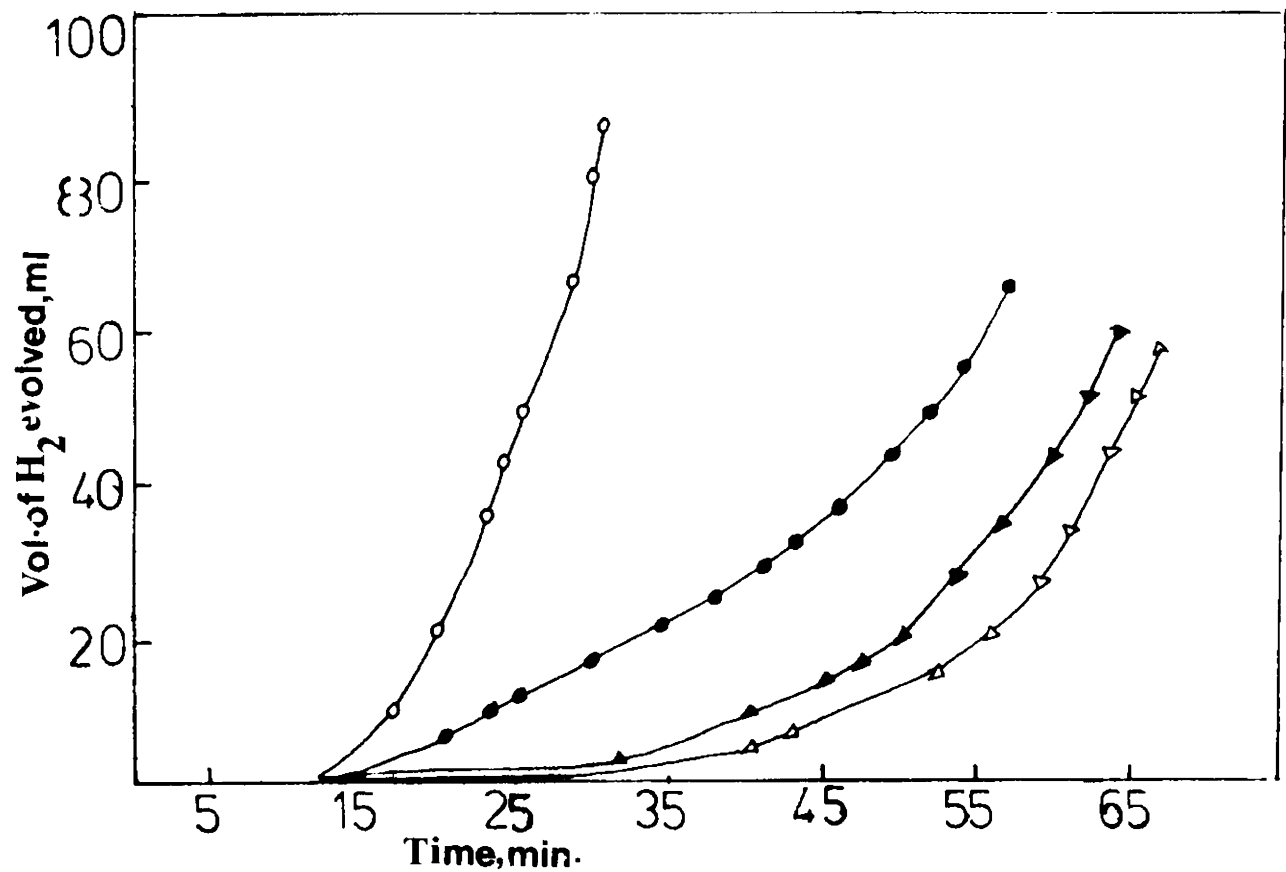


Fig. 6.6: Volume of hydrogen evolved-time curves obtained at various temperatures in the presence of  $2 \times 10^{-4}$  M CoTSP. Medium 2M HCl.  
 o 45°C;      ● 40°C;      ▲ 35°C;      △ 25°C

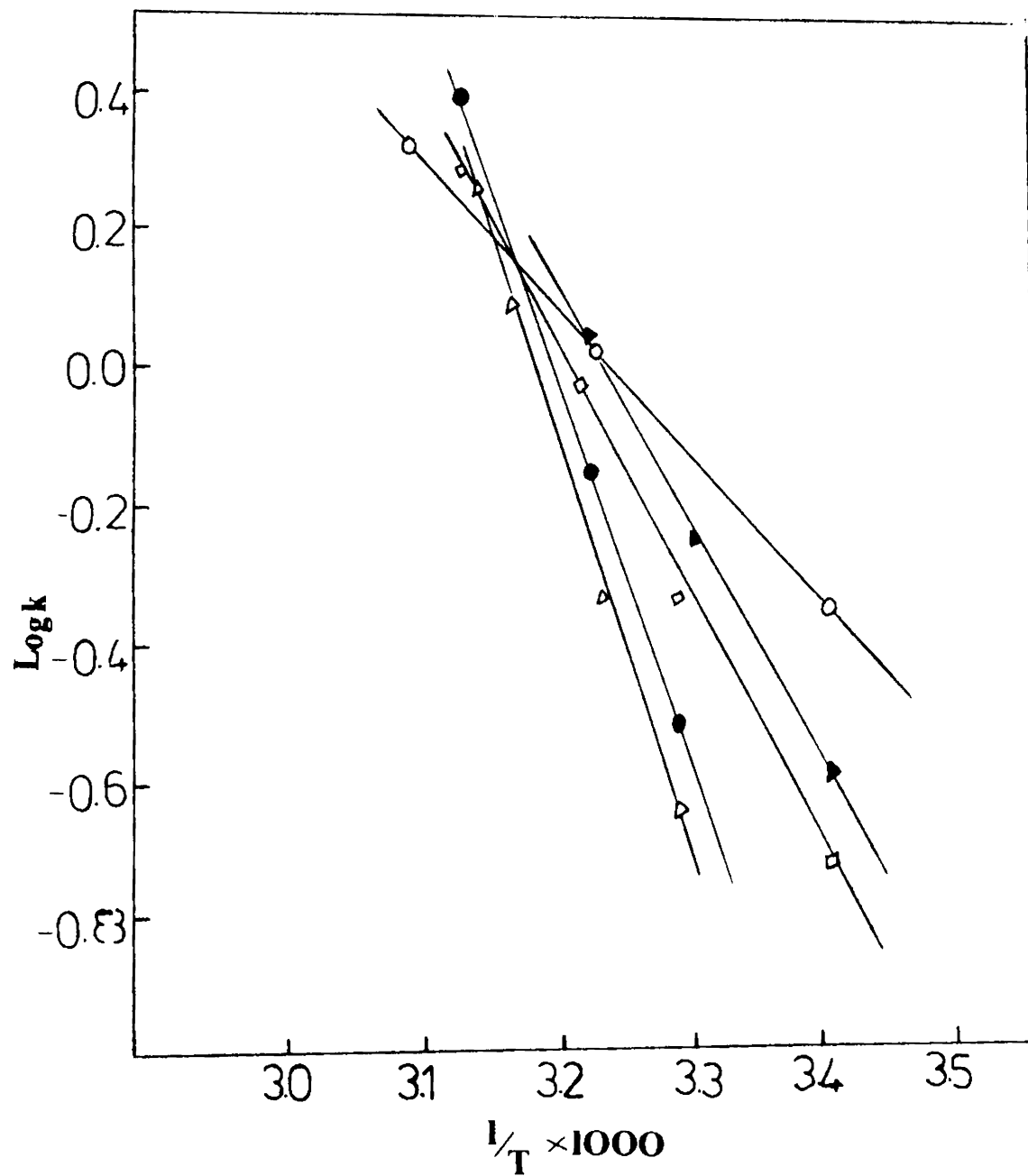


Fig. 6.7: Log k-1/T plot at different concentrations of CoTSP.

○ HCl;

△ 10<sup>-7</sup>M;

□ 10<sup>-6</sup>M;

● 10<sup>-5</sup>M;

▲ 2 x 10<sup>-4</sup>M

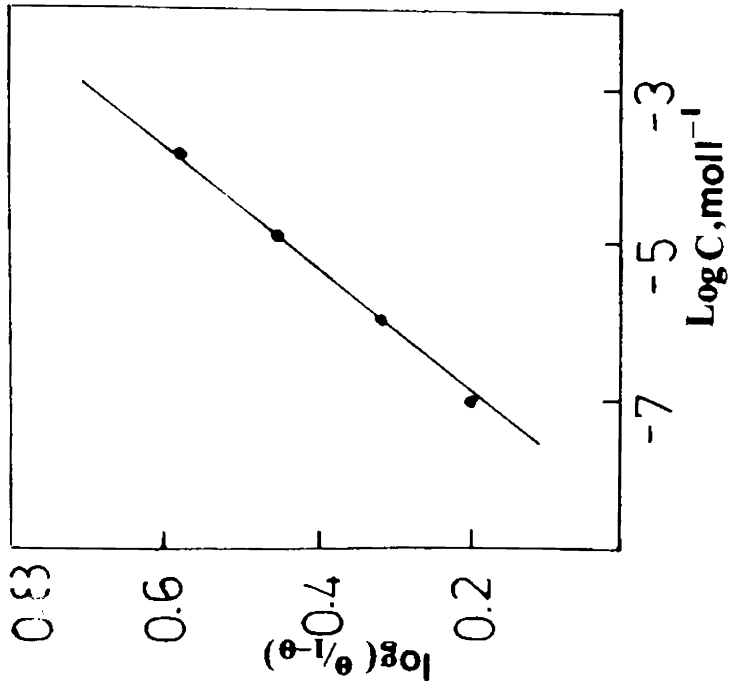


Fig. 6.8: Dependence of  $\log(\theta/1 - \theta)$  on the concentration of CoTSP.

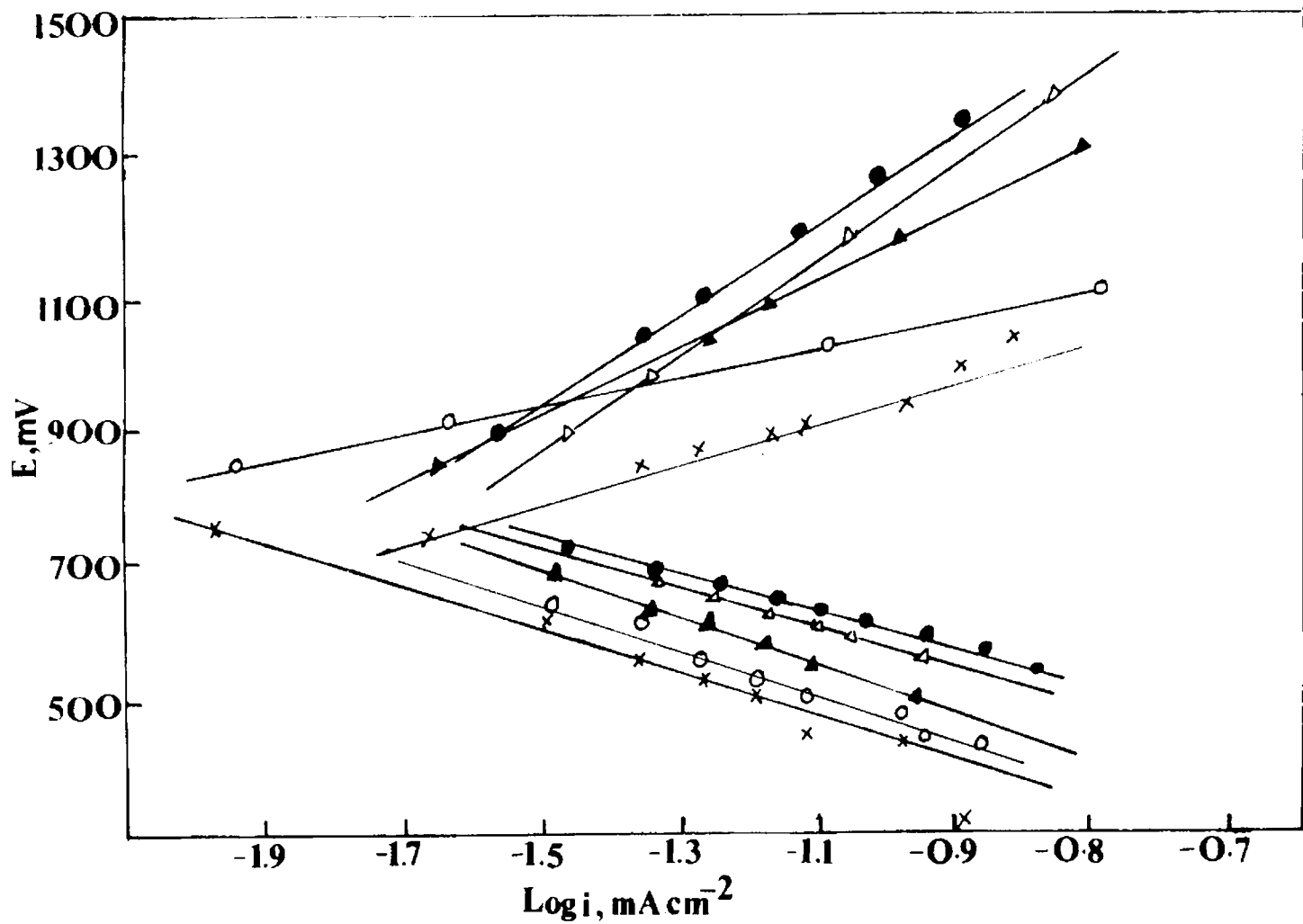


Fig. 6.9: Polarization curves obtained at different concentrations of CoTSP. Medium 2HCl.  
 $\circ$  HCl;  $\triangle$   $10^{-7}\text{M}$ ;  $\blacktriangle$   $10^{-6}\text{M}$ ;  $\circ$   $10^{-5}\text{M}$ ;  $\times$   $2 \times 10^{-4}\text{M}$

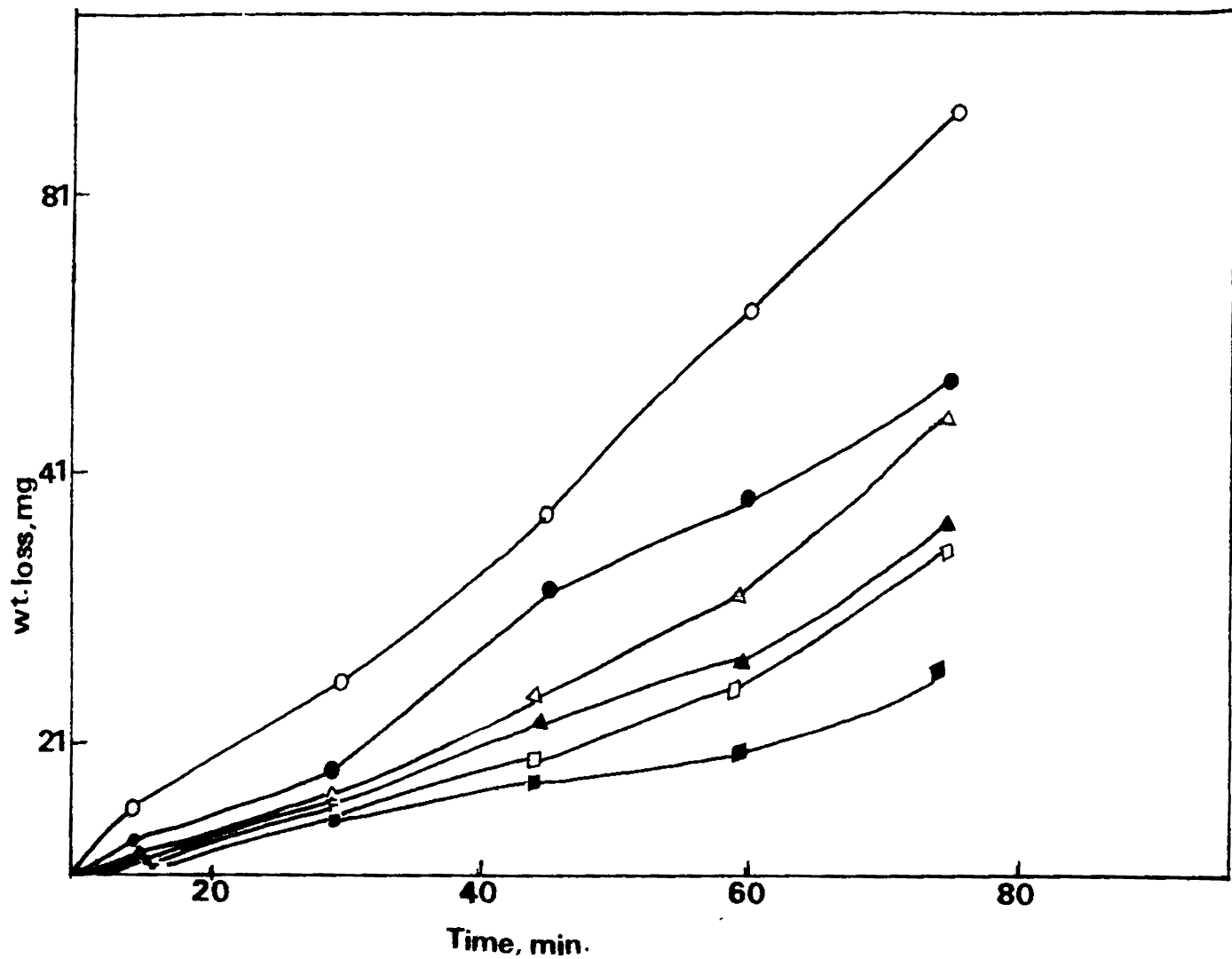


Fig. 6.10: Weight loss-time plot for the dissolution of aluminium in presence and absence of CuTSP; medium 2M HCl.  
 10<sup>-8</sup> M; ● 10<sup>-7</sup>M; △ 10<sup>-6</sup> M; □ 10<sup>-4</sup>M; ■ 2 x 10<sup>-4</sup>M

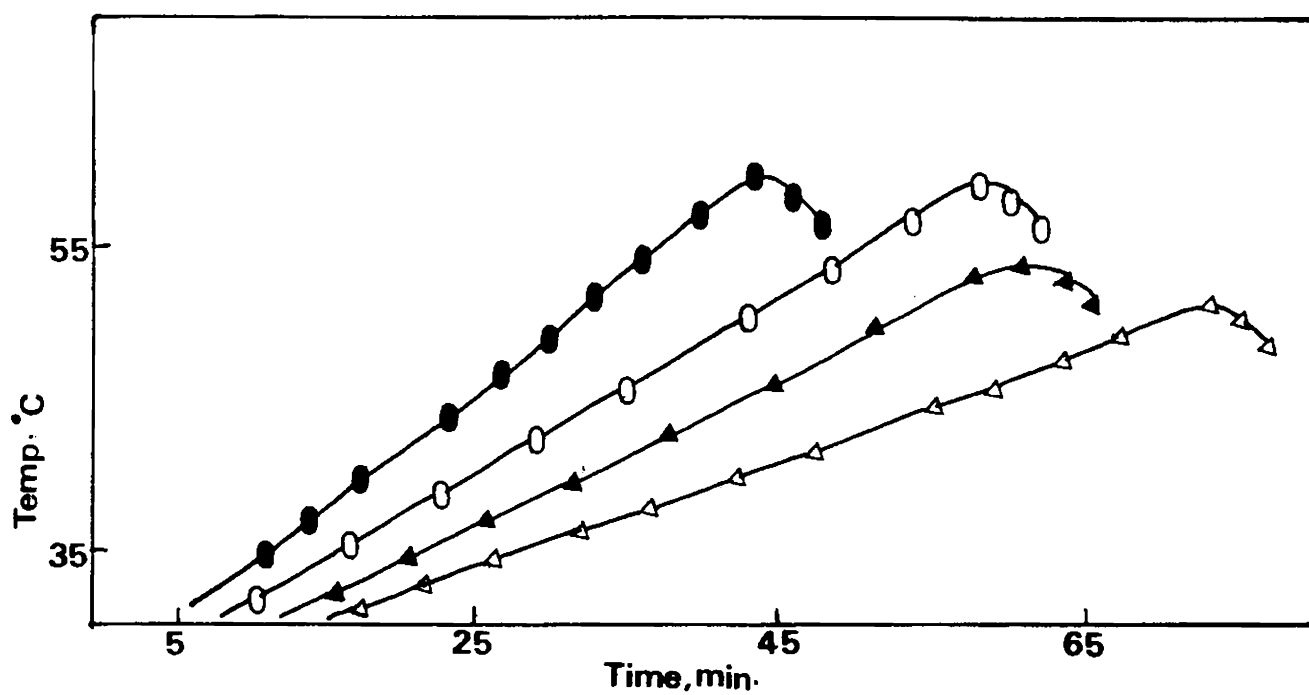


Fig: 6.11: Temperature - time plots for the dissolution of aluminium at different concentrations of CuTSP in 2M HCl.  
 ●  $10^{-6}M$ ; ○  $10^{-3}M$ ; △  $2 \times 10^{-4}M$  ▲  $10^{-4}M$

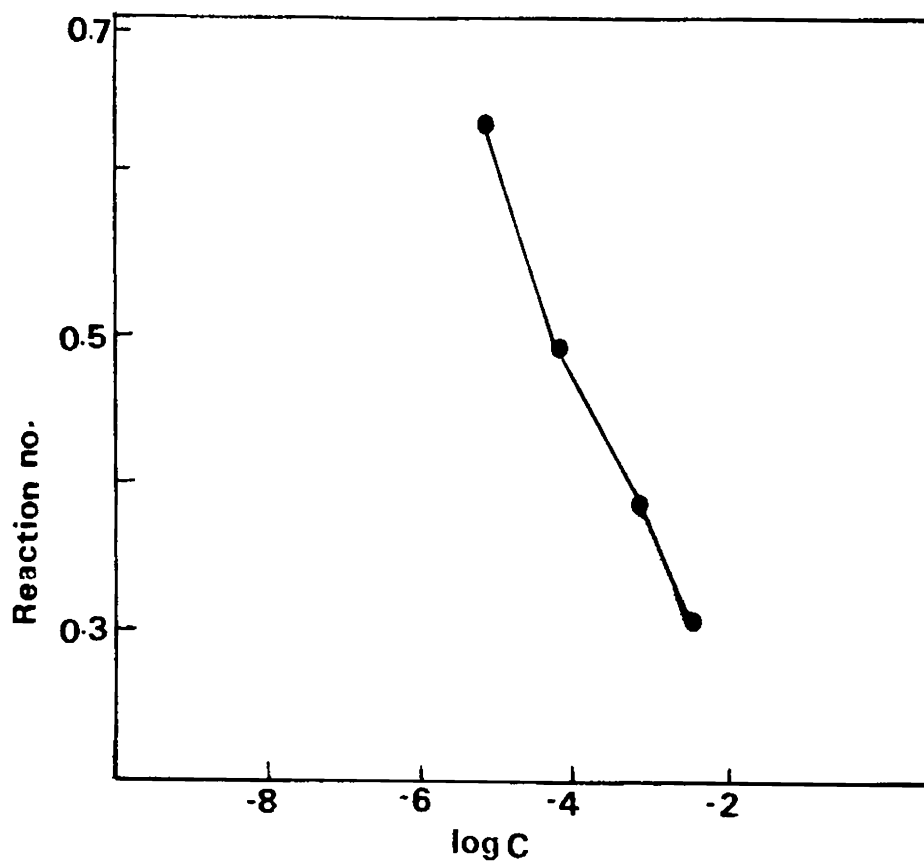


Fig. 6.12: Plot of  $\log C_{CuTSP}$  versus reaction number for the dissolution of aluminium CuI

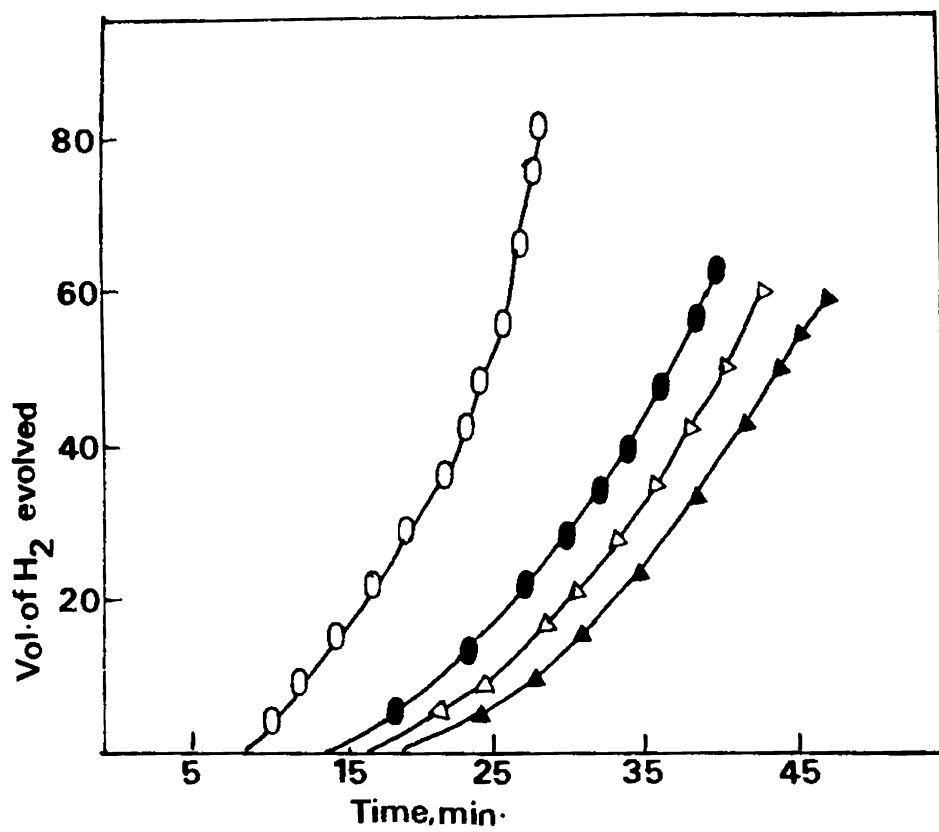


Fig. 6.13: Volume of hydrogen evolved vs time curves obtained at various temperatures in the presence of  $2 \times 10^{-4}$  M CuTSP. Medium 2M HCl  
 ○ 45°C; ● 40°C; △ 35°C; ▲ 25°C

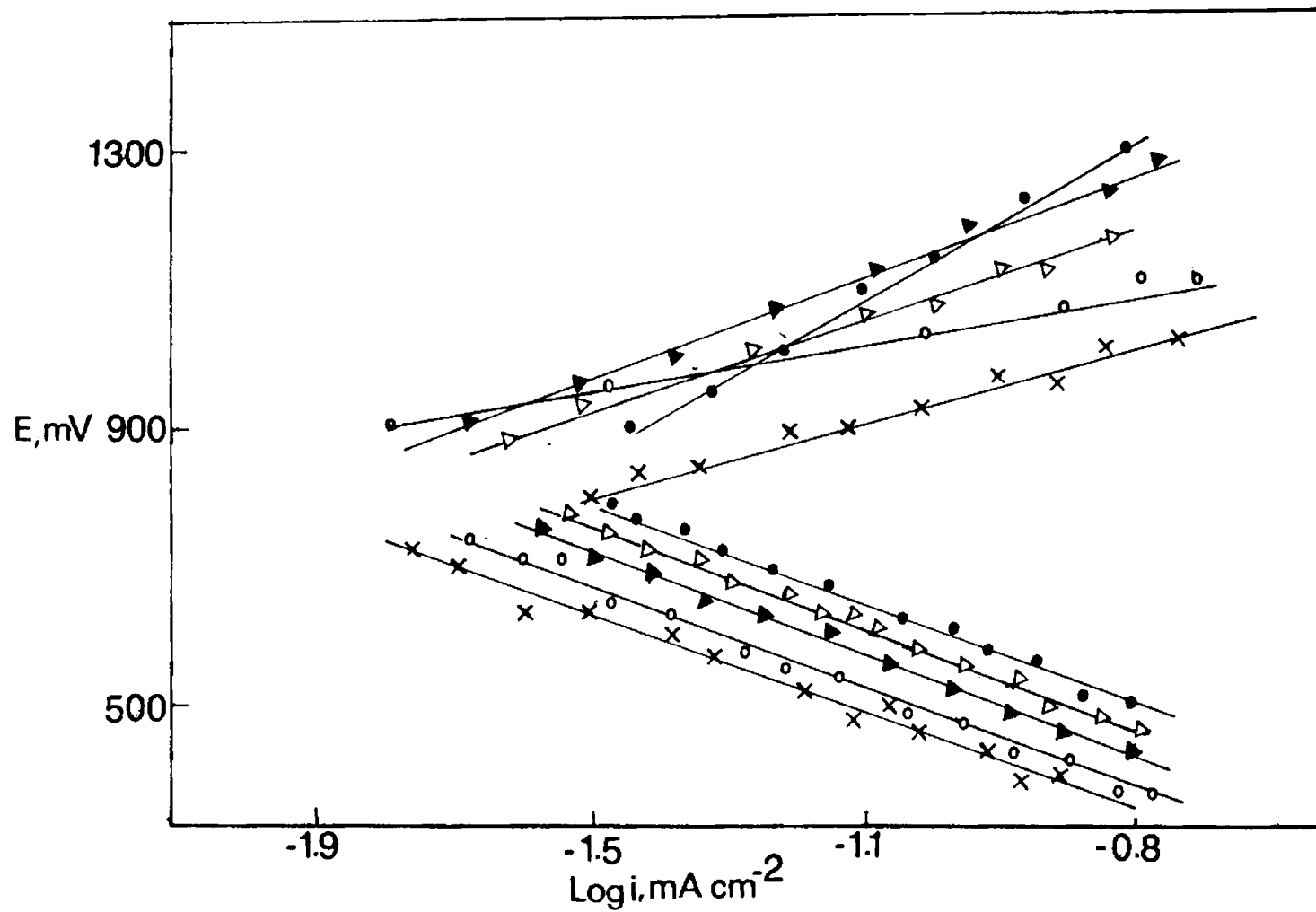


Fig. 6.14: Polarization curves obtained at different concentrations of CuTSP Medium 2M HCl.

● HCl;    △  $10^{-7}M$ ;    ▲  $10^{-6}M$ ;    ○  $10^{-5}M$ ;    ×  $10^{-4}M$ ;    ×  $2 \times 10^{-4}M$

products at time 't', which in turn is directly proportional to volume of hydrogen evolved at time 't' and k is the rate constant of the reaction. The value of k can be calculated from x-t curve at any given temperature (table 4). The value of k increases with increase in temperature and decreases with increase in inhibitor concentration.

The activation energy  $E_a$  is calculated from Arrhenius relationship,  $k = Ae^{-E_a / RT}$  where k is the rate constant and A is the pre-exponential factor. From the plot of  $\log k$  vs  $1/T$  (Fig.6.7) the value of  $E_a$  is evaluated and given in Table 5.

The activation energy for aluminium dissolution increases with increasing inhibitor concentration. Increase in activation energy is due to increased adsorption of the inhibitor on the metal surface.

Surface coverage  $\theta$  of the inhibitor on the metal surface was determined using the relation,

$$\theta = 1 - U_i / U$$

where  $U_i$  and  $U$  are the corrosion rates in solution with and without inhibitor respectively  
<sup>279</sup> The isothermal variation of  $\theta$  with concentration confirmed to the Langmuir adsorption isotherm which may be written in the form,

$$\log \theta / 1 - \theta = \log BC - [G / 2.303] RT$$

Where B is the adsorption equilibrium constant and G is the free energy of adsorption. Fig.6.8 is the plot of  $\log \theta / 1 - \theta$  vs  $\log C$ . The slope of this straight line is free energy of adsorption  $\Delta G_{ads}^\circ$  and is found to be  $-38.9 \text{ kJ mol}^{-1}$  for CoTSP. This is in agreement with the fact that stronger the adsorption greater will be the free energy of adsorption and the inhibition efficiency. The negative value indicate the spontaneous absorption of the inhibitors on aluminium.

The effect of inhibitor on the anodic and cathodic reactions can be determined using the relation,

$$\begin{aligned} I_a &= 1 - [i_a / i_{corr}^0] \\ I_c &= 1 - [i_c / i_{corr}^0] \end{aligned}$$

Where  $I_a$  and  $I_c$  are the efficiency of anodic and cathodic reactions,  $i_{corr}^0$  is the corrosion current density without inhibitor,  $i_a$  and  $i_c$  were obtained from the log (current density) vs potential plot. The polarization curves clearly indicate that the inhibitor shows down the hydrogen evolution. Table 5 gives the tafel slope and percentage inhibition from polarization data.

It is seen that catalysing effect of CoTSP for dioxygen reduction does not interfere with its corrosion inhibition efficiency. The nonconducting aluminium oxide layer on which CoTSP is absorbed inhibits the CoTSP-mediated electron transfer from aluminium to dioxygen. CuTSP is also effective but to a lesser extent.

The inhibition efficiency of CoTSP and CuTSP in HCl medium is superior to that of  $\beta$ -diketo compounds and phenyl azo derivatives. The surface coverage of CoTSP on aluminium surface is 0.85 and for CuTSP it is 0.76 which are much higher than the values for similar inhibitors. The activation energy for corrosion is also high. CoTSP exhibits its inhibiting property in concentrations as low as  $1.0 \times 10^{-7} \text{ M}$  and the inhibition efficiency reaches saturation at concentrations exceeding

about  $2.0 \times 10^{-4}$  M. In the case of CuTSP of lowest concentration at which it displays corrosion efficiency is  $1.0 \times 10^{-6}$  M. Even at lower concentrations it does not accelerate corrosion. Moreover phthalocyanines are non-toxic and well tolerated in living systems<sup>282</sup>.

**Table 1****INHIBITOR EFFICIENCY FOR THE DISSOLUTION OF ALUMINIUM 2S IN 2M HCl AT VARIOUS CONCENTRATIONS OF CoTSP AND CuTSP**

Conc./ M	% Inhibition after 30 min
<b>CoTSP</b>	
2.0 x 10 <sup>-4</sup>	84.6
1.0 x 10 <sup>-4</sup>	78.6
1.0 x 10 <sup>-5</sup>	73.6
1.0 x 10 <sup>-6</sup>	67.9
1.0 x 10 <sup>-7</sup>	60.7
1.0 x 10 <sup>-8</sup>	35.7
<b>CuTSP</b>	
2.0 x 10 <sup>-4</sup>	71.78
1.0 x 10 <sup>-4</sup>	68.57
1.0 x 10 <sup>-5</sup>	63.57
1.0 x 10 <sup>-6</sup>	57.50

**Table 2****DEPENDENCE OF REACTION NUMBER AND PERCENTAGE INHIBITION ON THE CONCENTRATION OF CoTSP & CuTSP; MEDIUM 2M HCl**

Conc. MTSP	Tinitial/ °C	Tmax/ °C	Time/minute	RN	%I
2M HCl	31.0	68.3	31	1.19	—
<b>CoTSP</b>					
2.0 X 10 <sup>-4</sup> M	31.0	50.4	78	0.25	79
1.0 X 10 <sup>-4</sup> M	31.0	53.8	60	0.38	68
1.0 X 10 <sup>-5</sup> M	31.0	58.6	65	0.41	60
1.0 X 10 <sup>-6</sup> M	31.0	59.2	48	0.58	51
1.0 X 10 <sup>-7</sup> M	31.0	63.1	35	0.93	23
<b>CuTSP</b>					
2.0 X 10 <sup>-4</sup> M	31.0	51.2	74	0.30	67.22
1.0 X 10 <sup>-4</sup> M	31.0	54.6	62	0.38	68.02
1.0 X 10 <sup>-5</sup> M	31.0	59.3	59	0.48	56.36
1.0 X 10 <sup>-6</sup> M	31.0	60.4	44	0.67	44.45

Table 3

**PERCENTAGE REDUCTION IN RR AT VARIOUS CONCENTRATIONS OF MTSP;  
MEDIUM 2M HCl**

Temp °C	Time/Min	% Reduction in RR Concentration of MTSP/M			
		$2.0 \times 10^{-4}$	$1.0 \times 10^{-5}$	$1.0 \times 10^{-6}$	$1.0 \times 10^{-7}$
<b>CoTSP</b>					
25.0	40	75.8	62.4	57.0	41.8
35.0	40	68.3	57.8	40.3	26.1
40.0	25	65.4	47.3	29.8	16.2
45.0	25	54.7	46.0	29.9	15.6
<b>CuTSP</b>					
25.0	40	70.30	69.02	55.87	58.5
35.0	40	62.42	55.22	45.07	52.0
40.0	25	55.75	43.28	26.66	22.42
45.0	25	47.27	40.67	22.85	22.10

TABLE 4

**RATE CONSTANT, SURFACE COVERAGE, ACTIVATION ENERGY AND HEAT OF  
ADSORPTION FOR THE DISSOLUTION OF ALUMINIUM IN 2M HCl AT  
DIFFERENT CONCENTRATIONS OF MTSP**

Conc. of MTSP	25°C	Rate Constant, k				Surface Coverage	Activation Energy, E <sub>a</sub> kJ mol <sup>-1</sup>	Heat of Adsorption kJ mol <sup>-1</sup>
		35°C	40°C	45°C				
Nil	0.42	0.67	1.25	4.23	—	17.9	—	
<b>CoTSP</b>								
$2.0 \times 10^{-4}$ M	0.1	0.21	0.44	1.88	0.85	69.3	12.9	
$1.0 \times 10^{-5}$ M	0.16	0.28	0.66	2.28	0.79	62.7	21.3	
$1.0 \times 10^{-6}$ M	0.18	0.42	0.88	2.82	0.68	37.7	30.4	
$1.0 \times 10^{-7}$ M	0.24	0.49	1.56	3.56	0.61	34.7	29.10	
<b>CuTSP</b>								
$2.0 \times 10^{-4}$ M	0.12	0.21	0.56	1.99	0.76	61.8	14.5	
$1.0 \times 10^{-4}$ M	0.16	0.30	0.69	2.39	0.72	56.4	24.3	
$1.0 \times 10^{-5}$ M	0.18	0.38	0.92	3.28	0.69	35.2	32.7	
$1.0 \times 10^{-6}$ M	0.22	0.37	0.97	3.29	0.64	34.0	28.3	

**TABLE 5:****PERCENTAGE INHIBITION AND TAFEL SLOPES AT VARIOUS  
CONCENTRATIONS OF MTSP IN 2M HCl**

<b>Conc. of MTSP/M</b>	<b><math>i_c</math>, mA cm<sup>2</sup></b>	<b>TAFEL Slope/mV</b>	<b>%Inhibition</b>
<b>CoTSP</b> Nil	18.0 = $i_0$	353	—
2 X 10 <sup>-4</sup>	0.36	313	98
1.0 X 10 <sup>-5</sup>	0.45	301	97
1.0 X 10 <sup>-6</sup>	0.66	314	95
1.0 X 10 <sup>-7</sup>	5.3	352	70
<b>CuTSP</b> 2 X 10 <sup>-4</sup>	0.58	318	96.7
1.0 X 10 <sup>-5</sup>	0.94	321	94.7
1.0 X 10 <sup>-6</sup>	3.31	325	81.6
1.0 X 10 <sup>-7</sup>	6.8	334	62.22

# CHAPTER VII

## SUMMARY AND CONCLUSION

The salient features of the results obtained in this work were discussed in detail in the foregoing sections and are summarised here.

One of the formidable obstacles encountered in phthalocyanine chemistry is the separation of singular species for physicochemical studies. Polymorphic forms and molecular aggregates formed by association have varied optical, electrical and electrochemical properties. They show time dependent variation in properties in solution as well as in the solid phase. In addition the elemental analysis is often plagued by deviations which are larger than normal. For the studies reported here, the samples were purified by vacuum sublimation and chromatography which give samples with reproducible properties.

Iron phthalocyanine (Fe Pc) and cobalt phthalocyanine (CoPc) catalyse dioxygen reduction and they find application as electrocatalyst in oxygen or air cathode fuel cells. Plasma treatment leads to improved material properties in plasma treatment leads to polymers, surface coatings and catalysts. Effect of low energy plasma treatment on the electroactivity of Co, Fe, Zn and Ni phthalocyanines are reported. Plasma modified materials showed enhanced activity in terms of the lower potential required for the reaction and the higher peak currents observed for cyclic voltammograms. The electrocatalytic activity is further established by comparing the behaviour of standard redox systems like Fe - EDTA, Fe(*o*-phenanthroline),  $\text{Fe}(\text{CN})_6^{4-}$ , and hydroquinone on modified and unmodified film electrodes. The facile faradaic activity at MPc modified electrode can be explained in terms of the modification of the flat band potentials associated with these. The heterogeneous rate constants for the electrode reaction on the modified electrodes are many orders of magnitude larger than those for unmodified electrodes.

MPcs are p-type semiconductors and the activation energy of the conduction process can be evaluated from the Arrhenius plot of the electrical conductivity versus temperature. Since most of the Pcs undergo polymorphic transitions the method cannot be applied beyond the first phase transition. Doping of MPc with iodine leads to enhanced electrical conductivity. Some authors have reported that doping is very similar to a chemisorption and the iodine can be removed by prolonged evacuation. This question has been investigated in detail in this work with reference to CoPc. CoPc was chosen for the study since it has a metal with variable oxidation state at the centre. The magnetic susceptibility, EPR, IR, and the electronic spectra were used to probe the change taking place on the metal ion. The results reveal a change taking place for the central metal atom. DSC was used to see whether iodine is reversibly lost during the heating cycle and to confirm whether it modifies the polymorphic transition. It is seen that  $\text{I}_2$  doped CoPc when subjected to thermal annealing undergoes an irreversible transition and a corresponding exothermic peak is seen in the DSC.

Cyclic voltammograms for the iodine doped and thermally annealed sample in an inert supporting electrolyte give an additional peak which is attributed to the newly generated oxidized form of CoPc. Of the thermally annealed metal phthalocyanines CoPc shows maximum activity which is evidenced by the electrode process for dioxygen reduction. FePc and ZnPc also give similar results but the activity is much less in these cases.

The study of chemically modified electrodes gives an insight into the mechanism of charge transport through surface species to molecules in solution. The behaviour of cobalt tetrasulphophthalocyanine modified polyaniline and poly(*o*-toluidine) electrodes were studied. The

polyaniline (PA) modified electrode surface was prepared by five different methods and are designated: (i) PA (ii) C/CoTSP/PA (iii) C/PA/CoTSP and Pt/PA/CoTSP (iv) C/(PA + CoTSP) and (v) carbon paste/PA and carbon paste/PA/CoTSP electrodes. These electrodes were electrochemically characterised in acid and alkaline supporting electrolytes by cyclic voltammetry. Of the different electrodes prepared graphite/ (PA + CoTSP) showed the highest activity for the catalytic reduction of dioxygen. Other electrodes also mediate O<sub>2</sub> reduction but the reduction occurs only at higher negative potentials. Though the carbon paste/PA and C/PA/CoTSP paste electrodes show electrochemical activity at pH < 3, they do not show any catalytic activity.

The mediation of electron transfer by cobalt tetrasulphophthalocyanine ion (CoTSP) incorporated into poly (*o*-toluidine) POT) was also studied by the same techniques. The CoTSP ion was incorporated into (POT) electrochemically. The mediation of reversible electron transfer by this film was studied. Multiply charged anionic species like ferrocyanide was exchanged on (CoTSP + POT) electrode and are not displaced even after repeated potential cycling.

Tetrasulpho derivatives of MPcs are among the easily prepared water soluble phthalocyanine derivatives. These are also easily adsorbed on surfaces. Cobalt tetrasulphophthalocyanine (CoTSP) catalyses certain reactions including O<sub>2</sub> reduction in solution. The influence of the dual properties, namely, catalysis of O<sub>2</sub> reduction and adsorption on surfaces on the corrosion of metals is interesting and this was studied. A comparison is made with CuTSP which is noncatalysing.

Aluminium undergoes very fast corrosion especially in chloride medium. The corrosion is accelerated in acid medium and is fast enough in hydrochloric acid solutions to be pursued by standard techniques. Both CoTSP and CuTSP act as cathodic inhibitors on Indal 2S aluminium samples CoTSP has a larger surface coverage and activation energy for corrosion, than CuTSP when used in identical concentrations CoTSP is effective in corrosion inhibition in concentration exceeding  $1.0 \times 10^{-7}$  M and it reaches a maximum at  $\sim 1.0 \times 10^{-4}$  M. These limits are slightly altered for CuTSP. Parameters like percentage inhibition, RN and heat of adsorption also indicate the same trend. This conclusively proves that CoTSP and CuTSP are useful as corrosion inhibitors for Al in chloride medium.

A part of the results of these studies has been published in journals or presented in conferences in the following forms:

1. Cyclic Voltammetric Studies on Plasma Treated Cobalt Phthalocyanine. P.S. Harikumar, P. Narayanan and V.N. Sivasankara Pillai, Bulletin of Electrochemistry, 1988 4(3), 233.
2. Doping Enhanced Electrical Conductivity and Electrocatalytic Activity in Cobalt Phthalocyanine. P.S Harikumar and V.N. Sivasankara Pillai, Journal of Material Science Letters, 1989, 8(8), 969.
3. Mediation of Electron Transfer by Cobalt Tetrasulphophthalocyanine ion Incorporated into Poly (*o*-toluidine) P.S. Harikumar and V.N. Sivasankarapillai, Communicated to 'Polymer' (UK)
4. Inhibition of Corrosion of Aluminium in Hydrochloric Acid by Cobalt Tetrasulphophthalocyanine P.S. Harikumar and V.N. Sivasankara Pillai Communicated to 'Corrosion Science' (UK).

5. **Electrical Conductivity and Electrochemical Behaviour of Iodine Doped Iron and Zinc Phthalocyanines.** P.S. Harikumar and V.N. Sivasankara Pillai.(to be communicated)
- 6 **Cyclic Voltammetric Studies by Plasma Treated Cobalt Phthalocyanines.** First National Conference on Electrocatalysis Jan. 28 & 29, 1987, Baroda.
7. **Fabrication of a Rotated Disk Electrode Using Locally Available Components and its Performance.** National Seminar on Instrumentation, 7-9 November, 1989, Cochin.
8. **Oxidative Transformation in Iodine Doped Thermally Annealed Cobalt Phthalocyanine.** Solid State Physics Symposium, December, 1989, Madras.
9. **Electrode Process on Cobalt Tetrasulpho Phthalocyanine Modified Polyaniline.** To be presented in National Symposium on Polymer Chemistry, February 9-11, Anandh Gujarat.

## REFERENCES

1. Moser, F.H. and Thomas, A.L. "Phthalocyanine Compounds", Reinhold Publishing Corporation, New York, 1963, p.8.
2. Barret, P.A.; Dent, C.E. and Linstead, R.P. *J.Chem. Soc.* 1936, 1719.
3. Kroenke, W.J. and Kenney, M.E. *J.Inorg. Chem.* 1964, 3, 25
4. Barret, P.A.; Frye, D.A. and Linstead, R.P. *J.Chem. Soc.* 1938, 1157.
5. Frigerio, N.A. and Coley, F.R. *J.Inorg. Nucl. Chem.* 1963, 25, 1111.
6. Shinabe, M. et al *NSK, JP 842/54; CA.* 1955, 49, 11019
7. Owen, J.E. and Kenney, M.E. *Inorg. Chem.* 1962, 1, 331.
8. Coaitis, D. *Bull. Soc. Chim. France* 1962, p.23.
9. Joyner, R.D. and Kenney, M.E. *Inorg. Chem.* 1962, 1, 236.
10. Lowery, M.K.; Starschak, A.J.; Esposito, J.N.; Krueger, P.C and Kenney, M.E *Inorg. Chem.* 1965, 4, 128.
11. Joyner, R.D. and Kenny, M.E. *Inorg. Chem.* 1964, 3, 251.
12. Rutter, H.A. and Mcqueen, J.D. *J.Inorg. Nucl. Chem.* 1960, 12, 361.
13. Barret, P.A.; Dent, C.E. and Linstead, R.P. *J. Chem. Soc.* 1936, 1719.
14. Toubé, R. *Z. Chem.*, 1963, 3, 194.
15. Block, B.P. and Meloni, E.G. *Inorg. Chem.* 1965, 4, 11.
16. Plyushchev, V.E.; Shkloner, L.P. and Rozdin, I.A. *Zh. Neorgan Khim* 1964, 9, 125. *CA* 1964, 60, 8879
17. Assour, J.M.; Goldmacher, J. and Harrison, S.E. *J.Chem. Phys.* 1965, 43, 159
18. Buslaev, Y.A.; Kuznetsova, A.A. and Gonyachova, L.F. *Izv. Akad Nauk SSSR, Neorg. Mater.* 1967, 31, 170.
19. Meloni, E.; Ocone, L.R. and Block, B.P. *Inorg. Chem.* 1967, 6, 424
20. Elvidge, J.A. and Lever, A.B.P. *J.Chem. Soc.* 1961, p. 1257.
21. Hill, H.A.O. and Norgett, M.M. *J.Chem. Soc.* 1966, p.1476.
22. Elvidge, J.A. and Lever, A.B.P. *Proc. Chem. Soc.* 1959, 195.

22. (a) Przywarska, H - Boniccka, **Roczniki Chem.** 1966, 40, 1627. CA - 1967, 66, 7200 k.
23. Krueger, P.C. and Kenney, M.E. **J. Inorg. Nucl. Chem.** 1963, 25, 303.
24. Berezin, B.D. and Sosnikova, N.I. **Dokl. Akad. Nauk SSSR.** 1962. CA 1963, 58, 13410.
25. Berezin, B.D. **Dokl. Akad. Nauk. SSSR.** 1963, 150, 1039. CA 1963, 59, 7148.
26. Berezin, B.D. and Sennikova, G.V. **Dokl. Akad. Nauk SSSR.** 1964, 59, 117. CA 1965, 62, 3637.
27. Ebert, N.A. and Gottlieb, H.O.J. **Am. Chem. Soc.** 1952, 74, 2806.
28. Mac Craugh, A and Koski, W.S. **J. Am. Chem. Soc.** 1965, 87, 2497.
29. Gurevich, M.G. and Solovev, K.N. **Dokl. Akad. Nauk Belorussk, SSSR.** 1961, 5, 291. CA 1962, 57, 15948.
30. Kirin, I.S.; Moskalev, P.N. and Makashev, Y.A. **Zh. Neorg. Khim.** 1965, 10, 1951, CA 1965, 63, 13449.
31. Wolf, L and John, H.J. **J. Prakt. Chem.** 1955, 4 (1) 257.
32. Frigerio, N.A. and U.S. Atomic Energy Commission, UPS 3, 027, 319.
33. Bloor, J.E.; Schlabitiz, J.; Walden, C.C. and Demerdache, A. **Can. J. Chem.** 1964, 42, 2201.
34. Kirin, S.; Moskalev, P.N. and Mishin, V.Y. **Zh. Obshch. Khim.** 1967, 37, 280.
35. Englelsma, G.; Yamamoto, A.; Markham, E. and Calvin, M. **J. Phys. Chem.** 1962, 66, 2517.
36. Kirin, I.S.; Moskalev, P.N. and Makashev, Yu. A. **Russ. J. Inorg. Chem.** 1967, 369.
37. Kirin, I.S.; Moskalev, P.N. and Makashev, Yu. A. **Russ. J. Inorg. Chem.** 1967, 369.
38. Sadak, M.M.; Roncali, J. and Garner, F.J. **Electroanal. Chem.** 1985, 189, 99
39. Frigerio, N.A. and Coley, F.R. **J. Inorg. Nucl. Chem.** 1963, 25, 1111
40. Kobyshev, G.I.; Lyalin, G.N. and Terenin, A.N. **Dokl. Akad. Nauk. SSSR** 1963, 148, 1053.
41. Bloor, J.E.; Schlabitiz, J. and Walden, C.C. **Can. J. Chem.** 1964, 42, 2201.
42. Keen, I.M. and Malerbi, B.W. **J. Inorg. Nucl. Chem.** 1965, 27, 1311.
43. Boas, J.F.; Fielding, P.E. and Mckay, A.G. **Aust. J. Chem.** 1974, 27, 7.
44. Clare, P and Glocking, F, **Inorg. Chem. Acta.** 1975, 14, 112.
45. Binert, B. and Holzach, K (to General AnilineWorks, Inc. U.S. Patent 2, 125, 633 (Nov. 8, 1938). CA 1987, 106, 157971.

46. Weber, H. and Busch, D.H. *Inorg. Chem.* 1965, **4**, 469.
47. Akira, M.; Mastomo, K.; Nob whito, W.; Jpn Kokai, Tokkyo CA 1987, 106, 157971.
48. Ercolani, C.; Gardini, M.; Minacelli, F.; Pennesi, G. and Rossi, G. *Inorg. Chem.* 1983, **22**, 2854.
49. Tanaka, A.A.; Fierro, C.; Scherron, D and Yeager, C.B. *J. Phys. Chem.* 1987, **91**, 3799.
50. Bottomley, L.A.; Gosec, J.N.; Goedken, V.L. and Ercolani, C. *Inorg. Chem.* 1985, **24**, 3733
51. Ercolani, C.; Rossi, G. and Monacelli, F. *Inorg. Chim. Acta.* 1980, **44**, 215.
52. Hiroyoshi, S.; Kenji, H.; Fakuzawa, T. CA 1988, 109, 137524
53. Seichiro, I.; Osamu, O.; Kunichiro, I. CA 1988, 109, 137527.
54. Harima, Y and Yamashita, K.J. *Phys. Chem.* 1989, **93**,4184.
55. Harima, Y.; Yamashita, K.; Saji, T. *Appl. Phys. Lett.* 1988; **52**, 1542.
56. Dent, C.E.; Linstead, R.P. *J. Chem. Soc.* 1934, 1027.
57. Fan, Fu-Ren Frank 'Rectifying Properties, Photovoltaic Effects and Electrochemical Studies of Phthalocyanine Films. (Ph. D. Thesis, University of Illinois at Urbana-Champaign 1978).
58. Kirin, I.S.; Moskalev, P.N. and Makashev, Yu. A. *Russ. J. Inorg. Chem.* 1967, **12**, 369.
59. Kirin, I.S.; Moskalev, P.N. and Makashev, Yu. A. *Russ. J. Inorg. Chem.* 1965, **10**, 1065.
60. Walton, D.; Ely, B and Elliott, G.J. *Electrochem. Soc. Solid-state Science and Technology*, 1981, **128**, 2479.
61. Linstead, R.P. and Robertson, J.M. *J. Chem. Soc.* 1936, 1736.
62. Robertson, J.M. and Woodward, I.J. *Chem. Soc.* 1940, 336.
63. Tsutsumi, K.; Hayase, A and Seroad, M.J. *Phys. Soc. Jpn*, 1957, **12**, 793.
64. Shigemitsu, M. *Bull. Chem. Soc Jpn*. 1959, **32**, 502
65. Kendall, D.N. *Anal. Chem.* 1953, **25**, 382.
66. Beynon, J.H. and Himphries, A.R. *Trans, Faraday Soc.* 1955, **51**, 1065.
67. Easter, J.W. (to American Cynamid Co.) US Patent 2, 770. 629 (Nov. 13, 1956).
68. Badische, Anilin and Soda Fabrik Akt. Ges. Brit. 783, 634, Sept. 25, 1957. CA. 1957. **51**, 7722i.
69. Kuhn, H. *J. Chem. Phys.* 1949, **17**, 1198.
70. Kuhn, H.Z. *Electrochem.* 1949, **55**, 165.

71. Elvidge, J.A. and Lever, A.B.P. **J. Chem. Soc.** 1961, 1257.
72. Vartanyan, A.T. **Zhur Fiz. Khim.** 1956, **30**, 1028.
73. Ebert, Jr., A.A. and Gottlieb, H.B. **J. Am. Chem. Soc.** 1952, **74**, 2806.
74. Sidorov, A.N. and Terenin, A.N. **Doklady Akad. Nauk. SSSR** 1955, **104**, 575
75. Lawton, E.A. **J. Phys. Chem.** 1958, **62**, 384.
76. Klemm, L and Klem, W.W. **J. Prakt. Chem.** 1935, **143**, 82.
77. Sheppard, S.E. and Gedder, A.L. **J. Am. Chem. Soc.** 1944, **66**, 1995
78. Kobayashi, H.; Torri, Y and Fakuda, N. **J. Chem. Soc. (Japan)** 1960, **81**, 694
79. Schelly, Z.A.; Farina, R.D. and Eyring, E.A. **J. Phys. Chem.** 1970, **74**, 617.
80. Boyd, P.D.W. and Smith, T.D. **J. Chem. Soc. (Dalton Trans)** 1972, 839.
81. Snow, A.W. and Jarvis, N.L. **J. Am. Chem. Soc.** 1984, **106**, 4706.
82. Reynolds, W.L. and Kolstad, J.J. **J. Inorg. Nucl. Chem.** 1976, **38**, 1835.
83. Sigel, H.; Waldmeir, P and Prijs, B. **Inorg. Nucl. Chem. Lett.** 1971, **7**, 161
84. Tanner, H.G. (to E.I.) du Pont de Numours & Co) U.S. Patent 2, 163, 768 June 27, 1939.
85. Ciba Ltd., British Patent 685, 582 (Jan. 7, 21953).
86. Colwell, R.E. and Platzer, N (to Monsanto Chemical Co.) U.S. Patent 2,857, 341 (Oct. 21, 1958).
87. Walker, E.E.; Shaw, M.P. and Fisher, V.W.F. (to British Celanese Ltd.) U.S. Patent 2, 825, 655 (Mar. 4, 1958).
88. Taul, H and Indest, H (Vereinigte Glanzstoff-Fabriken A.G. ) US Patent 2,997,450 (Aug. 22, 1961).
89. Sander, A. **Die Chemie** 1942, **55**, 255.
90. Gopala Rao, and Sastri, T.P. **Z Anal. Chem.** 160, 109.
91. Calvin, M; Cockbain, E.G. and Polyani, M. **Trans. Faraday Soc.** 1936, **32**, 1443.
92. Polyani, M. **Trans. Faraday Soc.** 1938, **34**, 1191.
93. Paquot, C. **Bull. Soc. Chim.** 1941, **8**, 695.
94. Paquot, C. **Compt. rend.** 1942, 214, 173.

95. Paquot, C. **Bull. Soc. Chim.** 1945, **12**, 450.
96. Uri, N. **Nature**, 1956, **177**, 1177.
97. Brouwer, W.M.; Traa, D.A.M., De. W.; Piet, W. **Angew Makromol. Chem.** 1984, **128**, 133.
98. Santos, L.M. and Baldwin, **Anal. Chem.** 1986, **58**, 848.
99. Moser, F.H. and Thomas, A.L. "The Phthalocyanines" CRC Press, Boca Ration, F.L. 1983, Vol.I.
100. Behret, H.; Binder, H.; Sandstete, G.; Scherer, G.G. **J. Electroanal. Chem.** 1981, **29**, 117.
101. Zagel, J.; Sen, R.K.; Yeager, E. **J. Electroanal. Chem.** 1977, **83**, 207.
102. Kuwana, T.; Fujihira, M.; Sunakawa, K.; Osa, T. **J. Electroanal. Chem.** 1978, **88**, 299.
103. Randin, J.P. **Electrochim Acta**, 1974, **19**, 83.
104. Zagal, J.; Bindra, P. and Yeager, E.J. **Electrochem. Soc.** 1980, **127**, 1506.
105. Kobayashi, N. and Nishiyama, Y.J. **Phys. Chem.** 1985, **89**, 1167.
106. Osaka, T.T.; Naol, K.; Hirabayashi, T. and Nakamura, S. **Bull. Chem. Soc. Jpn.** 1986, **59**, 2717.
107. Elzing, A.; Vander Putten, A.; Visscher, W. and Barendrecht, E.J. **J. Electroanal. Chem.** 1987, **233**, 113.
108. Blomquist, J.; Helgeson, U.; Mobery, L.C.; Johnson, L. Y.; Larson, R. **Electrochem. Acta.** 1982, **27**, 1445
109. Toshiba Corp. Jpn. Kokai Tokkyo Koho Jp. Appl. 81/41, 673, 24 March 1981, CA. **1985**, **102**, 754174.
110. Savy, M.; Anddro, P. and Bernard, C. **Electrochim Acta**, 1974, **19**, 403.
111. Alfernov, G.A. and Sevast'yenov. **Electrochimiya** 1975, **11**, 827.
112. Meshitsuka, M. and Tamaru, K.J. **Chem. Soc. Faraday Trans.** 1977, **73**, 236.
113. Linkous, C.; Klofta, T.; Armstrong, N.R. **J. Electrochem. Soc.** 1983, **130**, 1050.
114. Halbert, M.K. and Baldwin, R.P. **Anal. Chem.** 1985, **57**, 591.
115. Korfhage, K.M.; Ravichandran, K. and Baldwin, R.P. **Anal. Chem.** 1984, **57**, 1514.
116. Tachikawa, H. and Faulkner, L.R. **J. Am. Chem. Soc.** 1978, **100**, 4379.
117. Fu Ren Fan and Faulkner, L.R. **J. Am. Chem. Soc.** 1979, **101**, 4779.

118. Meshitsuka, S and Tamar, K. **J. Chem. Soc Faraday Trans.** 1977, 1, 73, 23.
119. Grammatica, S and Mort. **J. Appl. Physics Lett.** 1981, 38, 445.
120. Kakuta, A., Mori, Y.; Takano, S. Sawada, M and Shibuya, I. **J. Imag, Technol.** 1985, 11, 7.
121. Ghosh, A.K.; Morel, D.L.; Feng, T.; Shaw, R.F. and Rowe, C.A. **J. Appl. Phys.** 1974, 45, 230.
122. Shimura, M. and Toyoda, A. **Jpn. J. Appl. Phys.** 184, 23, 1462.
123. Loutfy, R.O. and McIntyne, L.F. **Energy Mater.** 1982, 6, 467.
124. Sobczynski, A and White, J.M.J. **Mol. Catal.** 1985, 29, 379.
125. Magloiozzo, R.S. and Krasana, A.I. **Photochem. Photobiol.** 1983, 38, 15.
126. Moskalev, P.N. and Alimova, N.I. **Russ. J. Inorg. Chem.** 1967, 41, 251.
127. Moskalev, P.N. and Kirin, I.S. **Russ. J. Phys. Chem.** 1972, 46, 1019.
128. La Mar, G.N.; Jefferey, S.R.; Smith, K.M. and Langry, K.C. **J. Am. Chem. Soc.** 1980, 102, 4835.
129. Collins, G.C.S. and Schiffrin, D.J. **J. Electrochem. Soc.** 1985, 132, 1835
130. Toshiba Corp. Jpn. Kokai Tokkyo, Koho J.P. 57, 157, 468 (82, 157, 468) 1982 CA. 1983, 75417.
131. Doddapaneni, N. Eur. Pat. Appl. E.P 57, 986, 1982. CA 1983, 19510m.
132. Miasik, J.J.; Hooper, A and Tofield, B.C. **J. Chem. Soc. Faraday Trans.** 1986. 82, 1117
133. Sawa Seikosha Co., Ltd. Jpn. Kokai Tokkyo Koho JP 57, 108, 652, 1982. CA 1983, 46165j.
134. Royo Ink Mfg. Ltd. Jpn. Kokai, Tokkyo Koho JP 59, 116, 754. 1982. CA 1985, 123055d.
135. Section, J.A.; Sherif, F.G. and Audrieth, L.F. **J. Inorg. Nucl. Chem.** 1959, 9, 222
136. Weber, J.H. and Busch, D.H. **J. Inorg. Chem.** 1967, 4, 469.
137. Linstead, R.P. **J. Chem. Soc.** 1934, 1016.
138. Schoniger, W. **Mikrochim. Acta.** 1956, 869.
139. Lever, A.B.P. **Adv. Inorg. Radiochem.** 1965, 7, 84.
140. Rollman, L.D. and Iwamoto, R.T.J. **Am. Chem. Soc.** 1968, 90, 1455.
141. Moser, S.H. and Thomas, A.L. 'Phthalocyanine Compounds' Reinhold Publishing Company, New York, 1963, p.35.

142. Lever A.B.P. **Adv. Inorg. Chem. Radiochem.** 1965, **7**, p.87.
143. Dyer, J.R. 'Application of Absorption Spectroscopy of Organic Compounds. Prentice-Hall of India, New Delhi, 1984, p. 37 and 38.
144. Jasinski, R. **Nature (London)**, 1964, **201**, 1212.
145. Jasinski, R.J. **Electrochem. Soc.** 1965, **112**, 526.
146. Savy, M.; Andro, P.; Bernard, C and Manager, J. **Electrochim. Acta.** 1973, **18**, 191.
147. Appleby, A.J. and Savy, M. **Electrochim. Acta.** 1976, **21**, 567.
148. McCorthey, R.C. **J.Chem. Phys.** 1984, **22**, 1360.
149. Kaufman, F.J. **Chem. Phys.** 1984, **22**, 1360.
150. Kaufman, F.J. **Chem. Phys.** 1960, **32**, 301.
151. Suhr, H and Schucker, U. **Synthesis**, 1970, 431.
152. Thara, T.; Ito, S and Kiboku, M. **Chem. Letts.** 1986, 675.
153. Kissinger, T., and Heineman, W.R. 'Laboratory Techniques in Electroanalytical Chemistry', Marcel/ Dekker Inc. New York, 1984.
154. Nicholson, R.S. and Shain, I. **Anal. Chem.** 1964, **36**, 706.
155. Evan, D.H. **Acc. Chem. Res.** 1977, **10**, 313.
156. Delahay, P. 'Ney Instrumental Methods in Electrochemistry', Interscience, New York, 1954, Chapter III.
157. Nicholson, R.S. and Shain, I. **Anal. Chem.** 1965, **37**, 190.
158. Adams, R.N. 'Electrochemistry at Solid Electrodes' Marcel Dekker, New York 1969, p.144.
159. Gileadi, E. Kirowa-Eisner and Penciner, J. 'Interfacial Electrochemistry- An Experimental Approach' Addison-Wesley, London, 1975, p.370.
160. Greef, R.; Peat, R.; Peter, L.M.; Pletcher, D and Robinson, J. 'Instrumental Methods in Electrochemistry' Ellis Horwood Ltd. England 1985, 178.
161. Matsuda, H. and Ayabe, Y.Z. **Electrochem.** 1955, **59**, 494.
162. 'Polymer modified electrodes: Preparation and characterisation' Hillman, R.A. in 'Electrochemical Science and Technology of Polymers', Linford, R.G.ed. Elsevier Applied Science Publishers Ltd. London, 1987, P.182.

163. Murray, R.W. 'Chemically Modified Electrodes' in *Electroanalytical Chemistry*, ed. Bard, A.J. Marcel Dekker, Inc. New York, 1966, 13, p. 200.
164. Adams, R.N. 'electrochemistry at solid surfaces', Marcel Dekker, Inc. New York, 1969, p.207.
165. EG & G PARC, Model 362, Scanning Potentiostat Operating and Service Manual, p.IV-II.
166. Tachikawa, H and Faulkner, L.R.J. *Am. Chem. Soc.* 1978, **100**, 4379.
167. Narayanan, P. and Sivasankara Pillai, V.N., Unpublished results.
168. Harrison, S.E. and Ludewig, K.H.J. *Chem. Phys.* 1966, **45**, 343.
169. Kohl, P.A, and Bard, A.J. *J. Am. Chem. Soc.* 1977, **99**, 7531.
170. Hoare, J.P. in 'Advances in Electrochemistry and Electrochemical Engineering, Delahay, P. ed. Interscience Publishers, New York, 1966, p.249.
171. Eley, *Nature*, 1948, **162**, 819.
172. Vartanyan, A.S. *J. Phys. Chem. (USSR)* 1946,**20**,1065
173. Bradley, R.S.; Grace, J.D. and Munro, D.C. *Trans. Faraday Soc.* 1962, **58**, 776.
174. Fielding, P.E. and Gutman, F.J. *Chem. Phys.* 1957, **26(2)** 411.
175. Gutman, F. and Lyons, L.E. 'Organic Semiconductors', John Wiley & Sons, New York, 1967, p.457.
176. Harrison, S.C. and Assour, J.M. *J. Chem. Phys.* 1964, **40**, 365.
177. Berlin Yu. A.; Beshenko, S.J.; Danielyn, N.G., Zhorin, V.A.; Enikolopyan, N.S. *Klim. Fiz.* 1983 (C.A. 1984, **100**, 113170g)
178. Tollin, G., Kearns, D.R. and Calvin, M.J. *Chem. Phys.* 1960, **32**, 1013.
179. Loutfy, R.O. and Menzel, E.R. *J. Am. Chem. Soc.* 1980, **102**, 4967.
180. Hoegl, H.J. *Phys. Chem.* 1965, **69**, 755
181. Chaiken, R.F. and Kearns, D.R. *J. Chem. Phys.* 1970, **45**, 3966.
182. Harima, T., Yamamoto, K.; Takeda, K and Yamashita, K. *Bull. Chem. Soc. Jpn.* 1989, **62**, 1458.
183. Flynn, B.W.; Owen, A.E. and Major, J.J. *Phys. Chem.* 1977, **10**, 4051.
184. Ghosh, A.D.; Morel, D.L.; Feng, T.; Shaw, R.S. and Rowe Jr. *J. Appl. Phys.* 1974, **1**, 230.
185. Gleizes, T.; Marks T.J. and Ibers, J.A. *J. Am. Chem. Soc.* 1975, **97**, 3545.

186. Aoyagi, Y.; Manida, K. and Namba, S.J. *Phys. Soc. Jpn.* 1971, **31**, 524.
187. Pelletier, S.W. and Mody, N.U. *J. Am. Chem. Soc.* 1977, **99**(1), 286.
188. Taube, R. *Pure Appl. Chem.* 1974, **38**, 427.
189. Wynne, J.; Nohr and Ronald, S. *Mol. Cryst. Liq. Cryst.* 1982, **81**, 243.
190. Martinsen, J.; Greene, R.L.; Palmer, Petersen, J.L.; Marks, T.J. *J. Am. Chem. Soc.* 1977, **99**, 286.
191. Brant, P.; Nohr, R.S.; Wynne, K.J. and Webber, D.C. *Mol. Cryst. Liq. Cryst.* 1982, **81**, 255.
192. Martinsen, J.; Santan, J.L.; Greene, R.L.; Tanaka, J and Hoffman, B.M. *J. Am. Chem. Soc.* 1985, **107**, 6915.
193. Frammer, J.E. *Acc. Chem. Res.* 1986, **19**, 2.
194. Drago, S.R. *Physical Methods in Chemistry* W.B. Saunders Company, London, 119.
195. Kolthoff, I.M. and Jordan, J.J. *J. Am. Chem. Soc.* 1953, **75**, 1571.
196. Murray, R.W.; Ewing, A.G. and Durst, R.A. *Anal. Chem.* 1987, **59**, 379.
197. Murray, R.W. in 'Electroanalytical Chemistry' Bard, A.J. ed. Marcel Dekker, New York, 1984, Vol. 13, 191-368.
198. Lane, R.F.; Hubbard, A.T. *J. Phys. Chem.* 1973, **77**, 1401.
199. Bard, A.J. *Chem. Educ.* 1983, **60**, 302.
200. Chidsay, C.E.D.; Murray, R.W. *Science*, 1986, **231**, 25.
201. Collman, J.P.; Denisevich, P.; Konai, Y.; Morrocco, M.; Koval, C and Anson, F.C. *J. Am. Chem. Soc.* 1980, **102**, 6027.
202. Tomi, T.T.; Liu, H.Y. and Weaver, M.J. *J. Am. Chem. Soc.* 1984, **106**, 1233
203. Albery, J.W.; Eddowes, M.J.; Hill, H.A.O. and Hillman, A.R. *J. Am. Chem. Soc.* 1981, **103**, 3904.
204. Lenbard, J.R.; Rocklin, R.; Abruna, H.; William, K.; Kuo, K.; Nowak, R. and Murray, R.W. *J. Am. Chem. Soc.* 1978, **100**, 7870.
205. Tse, D.S.C. and Kuwana, T. *Anal. Chem.* 1978, **50**, 1315.
206. Wrigton, M.S. in 'Catalysis and Electrocatalysis', Miller, J.S., Ed. ACS Symposium Series 192, Washington, D.C., 1982, p. 99.
207. Watkins, B.J.; Bebling, J.R.; Kariv, F and Miller, L.L. *J. Am. Chem. Soc.* 1975, **97**, 3549.

208. Lau, A.N.K. and Miller, L.L. *J. Am. Chem. Soc.* 1983, **105**, 5271.
209. Anson, F.C.; Ohsaka, T and Saveant, J.M. *J. Am. Chem. Soc.* 1983, **105**, 4883.
210. Kanozawa, K.K.; Diaz, A.F.; Yiess, R.H.; Gill, W.D.; Kauk, J.F.; Logan, I.A.; Rabolt, J.F. and Street, G.B. *J. Chem. Soc. Chem. Commun.* 1979, 854.
211. Reed, R.A.; Geng, L. and Murray, R.W.J. *Electroanal. Chem.* 1985, **188**, 85.
212. Guadalupe, A.R. and Abruna, H.S. *Anal. Chem.* 1985, **57**, 142.
213. Komori, T. and Nonaka, T.J. *Am. Chem. Soc.* 1983, **105**, 5690.
214. Baldwin, R.P.; Chrisenesen, J.K. and Krygger, L. *Anal. Chem.* 1986, **58**, 1790.
215. Ghosh, P.K. and Bard, A.J. *J. Am. Chem. Soc.* 1983, **105**, 5691.
216. Bull, R.A.; fan, F.R.; Bard, A.J. *J. Electrochem. Soc.* 1984, **131**, 687.
217. Deronzier, A. and Moutel, J.C. *Acc. Chem. Res.* 1989, **22**, 249.
218. Bull, R.A.; Fan, F.R. and Bard, A.J. *J. Electrochem. Soc.* 1984, **131**, 687.
219. Buttry, D.A. and Anson, F.C. *J. Am. Chem. Soc.* 1982, **104**, 4824.
220. Zinger, B and Miller, L.L. *J. Am. Chem. Soc.* 1984, **106**, 6861.
221. Blankespoor, R. and Miller, L.L. *Chem. Commun.* 1985, 90.
222. Miller, L.L.; Zinger, B and Zhou, X-Q. *J. Am. Chem. Soc.* 1987, **109**, 2267.
223. Zagal, J.; Bindra, P. and Layer, J. *Electrochem. Soc.* 1980, **127**, 1506.
224. Bull, R.A.; Fan, F.R. and Bard, A.J. *J. Electrochem. Soc.* 1982, **129**, 1009.
225. Bettelheim, A.; Parash, R. and Ozet, D.J. *Electrochem. Soc.* 1982, **129**, 2247.
226. Collman, J.P.; Denisevich, P.; Konai, Y.; Marro, M.; Koval, C. and And Anson, F.C. *J. Am. Chem. Soc.* 1980, **102**, 6027.
227. Okabayashi, K.; Ikeda, O and Tamura, H.J. *Chem. Soc. Chem. Commun.* 1983, 684.
228. Osaka, T.; Naol, K.; Hirabayashi, T. and Nakamura, S. *Bull. Chem. Soc. Jpn.* 1986, **59**, 2717.
229. Jiang, R. and Dong, S.J. *Electroanal. Chem.* 1988, **246**, 101.
230. Hillman, R.A. in *Polymer Modified Electrodes: Preparation and Characterisation*", Linford, R.G., ed. Elsevier Applied Science Publishers Ltd. London, 1987, p.181.
231. Chiang, J.C. and Mac Diarmid, A. *Synth. Met.* 1986, **13**, 193.

232. Haung, W.S.; Humphrey, B.D. and Mac Diarmid, A.G. **J. Chem. Soc. Faraday Trans. I**, 1986, **82**, 2385.
233. Genies, E.M. and Tsintavis, C.J. **Electroanal. Chem.** 1985, **195**, 109.
234. Ohnuki, Y.; Ohsaka, T.; Matsuda, H and Oyama, N. **J. Electroanal. Chem.** 1983, **158**, 55.
235. Ohsaka, T.; Ohnuki, Y.; Oyama, N.; Katagiri, G. and Kamisaka, K.J. **Electroanal. Chem.** 1984, **161**, 399.
236. Gholamian, M. and Contractor, A.Q. **J. Electroanal. Chem.** 1988, 252.
237. Diaz, A.F. and Logan, J.A. **J. Electroanal. Chem.** 1980, **111**, 111.
238. Noufi, R.; Nazik, A.J.; White, J. and Warren, L.F. **J. Electrochem. Soc.** 1982, **129**, 2261.
239. Bull, R.A.; Fan, F.R. and Bard, A.J.J., **Electrochem. Soc.** 1983, **130**, 1636.
240. Jiang, R. and Dong, S.J. **Electroanal. Chem.** 1988, **246**, 101.
241. Volkov, A.; Tourillon, G.; Lacaze, P.C. and Dubois, J.E. **J. Electroanal. Chem.** 1980, **115**, 279.
242. Ohsaka, T.; Ohnuki, Y.; Oyama, N.; Katagiri, G. and Kamisaka, K.J. **Electroanal. Chem.** 1984, **161**, 399.
243. Pickup, P.G.; Murray, R.W., **J. Electrochem. Soc.** 1984, **131**, 833.
244. Kost, K.M.; Bartak, D.E.; Kazet, B. and Kuwana, T. **Anal. Chem.** 1988, **60**, 2379.
245. Bull, R.A.; Fan, F.R. and Bard, A.J., **J. Electrochem. Soc.** 1983, **130**, 1636.
246. Lane, R.F. and Hubbard, A.T.J. **Phys. Chem** 1973, **77**, 1401.
247. Zinger, B. and Miller, L.L., **J. Am. Chem. Soc.** 1984, **106**, 6861.
248. Blankespoor, R. and Miller, L.L. **Chem. Commun.** 1985, 90.
249. Bull, R.A.; Fan, F.R. and Bard, A.J., **J. Electrochem. Soc.** 1984, **131**, 687.
250. Ikeda, T.; Schmehl, R.; Denisvevich, P.; William, K. and Murray, R.W., **J. Am. Chem. Soc.** 1982, **194**, 2683.
251. Andrieux, C.P.; Saveant, J.M. **J. Electroanal Chem.** 1978, **93**, 163.
252. Anson, F.C.; Saveant, J.M. and Shigehara, K., **J. Phys. Chem.** 1983, **87**, 214.
253. Oyama, N.; Ohsaka, T. and Ushirogouchi, T.J. **Phys. Chem.** 1984, **88**, 5274.
254. Oyama, N. and Anson, F.C. **Anal. Chem.** 1980, **52**, 1192.

255. Peere, P.J. and Bard, A.J., **J. Electroanal. Chem.** 1980, **112**, 97.
256. Kaufman, F.B.; Schroeder, A.H.; Engler, E.M.; Kramer, S.R. and Chambers, J.O., **J. Am. Chem. Soc.** 1980, **102**, 483.
257. Bookbinder, D.C.; Lewis, N.S.; Bradley, M.G.; Bocarsly, A.B. and Wrighton, M.S. **J. Am. Chem. Soc.** 1979, **101**, 1378.
258. Miller, L.L.; Zinger, B. and Quin-Vin zhou, **J. Am. Chem. Soc.** 1987, **109**, 2267.
259. Zinger, B. and Miller, L.L. **J. Am. Chem. Soc.** 1984, **106**, 6861
260. Daum, P.; Lenbard, J.R.; Rolison, D.; Murray, R.W. **J. Am. Chem. Soc.** 1980, **102**, 4649.
261. Facci, J.; Schmel, R.H. and Murray, R.W. **J. Am. Chem. Soc.** 1982, **104**, 4959.
262. Kuo, K. and Murray, R.W., **J. Electroanal. Chem.** 1982, **131**, 37
263. Yen Wei.; Walter, W.F.; Gary, E.W.; Anjan Ray and Mac Diarmid, A.G. **J. Phys. Chem.** 1989, **93**, 495.
264. Bull, R.A.; Fan, F.R. and Bard, A.J., **J. Electrochem. Soc.** 1984, **131**, 687.
265. Jiang, R. and Dong, S.J. **Electronal. Chem.** 1988, **246**, 101.
266. Laviron, E.J. **Electroanal. Chem.** 1980, **112**, 1.
267. Jiang, R. and Dong, S.J. **Electroanal. Chem.** 1988, **246**, 101
268. Laviron, E.J. **Electronal. Chem.** 1972, **39**, 1.
269. Oyama, N.; Ohsaka, T. and Shimuzu, T. **Anal. Chem.** 1985, **57**, 1526.
270. Oyama, N.; Ohsaka, T. and Ushuroguchi, T., **J. Phys. Chem.** 1984, **88**, 5274.
271. Evan Ulick, 'The Corrosion and Oxidation of metals: Scientific Principles and Practical Applications Edwood Arnold, London, 1960.
272. Shrier, L.L., 'Corrosion' Vol.1 and 2 Newnes and Butterworths, London, 1976.
273. Uhlig, H'Corrosion and Corrosion Control', An Introduction to Corrosion Science: John Wiley & Sons, New York, 1971.
274. Glordano Trabanelli in 'Corrosion Mechanism' ed. Florian Mansfield, Marcel Dekker, Inc. New York, 1987.
275. McLendon, G. and Martell, A.E. **Inorg. Chem.** 1977, **16**, 181.
276. Rollman, L.D. and Iwamoto, R.T. **J. Am. Chem. Soc.** 1968, **90**, 1455.

277. Nikolic, B.Z.; Adzic, R.R. and Yeager, E.B., **J. Electroanal. Chem.** 1979, **103**, 281.
278. Weber, J.H. and Busch, D.H. **Inorg. Chem.** 1965, **4**, 469.
279. Fouda, A.; Moussa Nader, H.A.M.; Moussa, M.N.D. and Shehata, I **Bull. Chem Soc. Jpn.** 1988, **61**, 4411.
280. Hassan, S.M.; Moussa, M.N.H.; Taha, F.I.M. and Fouda, A.S. **Corros. Sci.** 1981, **21**, 439.
281. Desai, M.N.; Patel, R.R. and Shah, D.K. **J. Indian Chem. Soc.** 1973, **50**, 341.
282. Moser, F-H. and Thomas, A.L. 'Phthalocyanine Compounds' Reinhold Publishing Corporation, New York, 1963, p.302.